



Universiteit
Leiden
The Netherlands

Wiles and wanderings: immune-evasive maneuvers of skin-penetrating parasites

Winkel, B.M.F.

Citation

Winkel, B. M. F. (2021, October 5). *Wiles and wanderings: immune-evasive maneuvers of skin-penetrating parasites*. Retrieved from <https://hdl.handle.net/1887/3214576>

Version: Publisher's Version

License: [Licence agreement concerning inclusion of doctoral thesis in the Institutional Repository of the University of Leiden](#)

Downloaded from: <https://hdl.handle.net/1887/3214576>

Note: To cite this publication please use the final published version (if applicable).

WILES AND WANDERINGS

Immune-evasive maneuvers of
skin-penetrating parasites

BÉATRICE M.F. WINKEL

WILES AND WANDERINGS

**Immune-evasive maneuvers of
skin-penetrating parasites**

BÉATRICE M.F. WINKEL

COLOPHON

Cover design: James Jardine | www.jamesjardine.nl
Layout: James Jardine | www.jamesjardine.nl
Print: Ridderprint | www.ridderprint.nl
ISBN: 978-94-6416-106-9

Copyright © 2021 by Béatrice Marguérite Françoise Winkel. All rights reserved. Any unauthorized reprint or use of this material is prohibited. No part of this thesis may be reproduced, stored or transmitted in any form or by any means, without written permission of the author or, when appropriate, of the publishers of the publications.

Immune-evasive maneuvers of skin-penetrating parasites

P R O E F S C H R I F T

ter verkrijging van
de graad van doctor aan de Universiteit Leiden
op gezag van rector magnificus prof.dr.ir. H. Bijl,
volgens besluit van het college voor promoties
te verdedigen op dinsdag 5 oktober 2021
klokke 15:00 uur

door
Béatrice Marguérite Françoise Winkel
geboren te Willemstad, Curaçao
in 1985

Promotor:

Prof. dr. M. Roestenberg

Co-promotores:

Prof. dr. F.W.B. van Leeuwen

Dr. B. Franke-Fayard

Leden promotiecommissie:

Prof. dr. T.W.J. Huizinga

Prof. dr. S.H van den Burg

Prof. dr. E.C. de Jong (Universiteit van Amsterdam, AMC-UvA, Amsterdam)

Prof. dr. S.M. van Ham (Universiteit van Amsterdam, Amsterdam)

In memoriam Carlos Alberto Winkel

TABLE OF CONTENTS

| | | |
|------------------|---|---|
| Chapter 1 | General introduction and thesis outline | 9 |
|------------------|---|---|

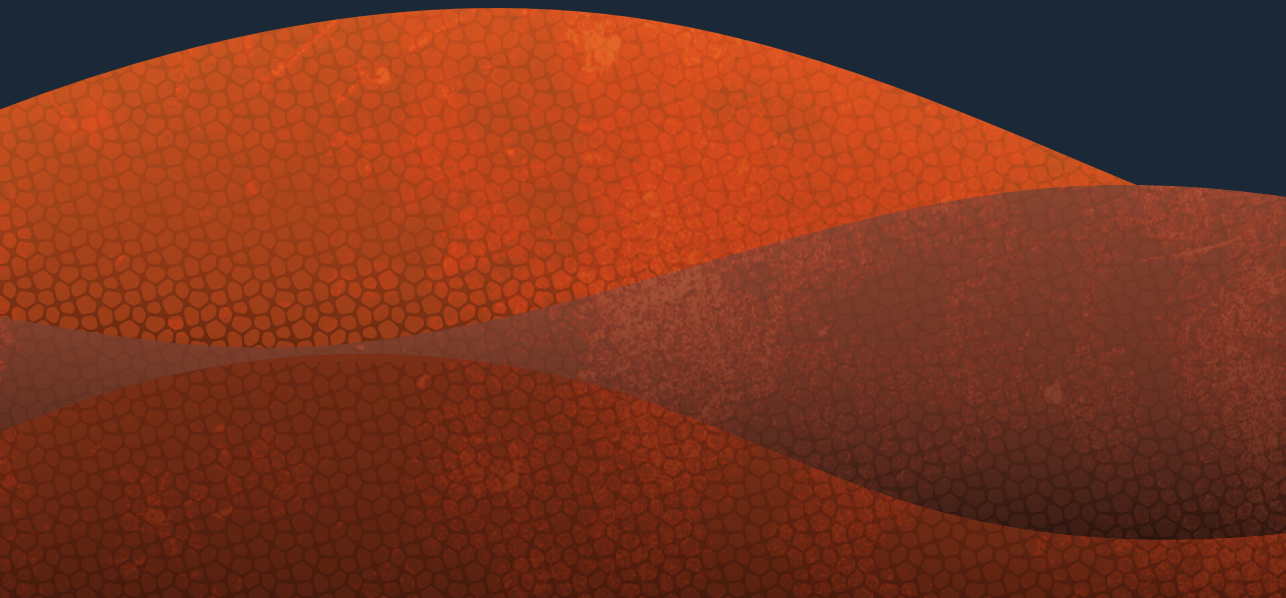
Part 1: Wiles

| | | |
|------------------|---|----|
| Chapter 2 | Plasmodium sporozoites induce regulatory macrophages <i>PLOS pathogens 2020</i> | 25 |
| Chapter 3 | Human dermal APC responses to needle- and mosquito bite- injected Plasmodium falciparum sporozoites <i>Manuscript in preparation</i> | 63 |
| Chapter 4 | Early induction of human regulatory dermal antigen presenting cells by skin-penetrating Schistosoma mansoni cercariae <i>Frontiers in Immunology 2018</i> | 87 |

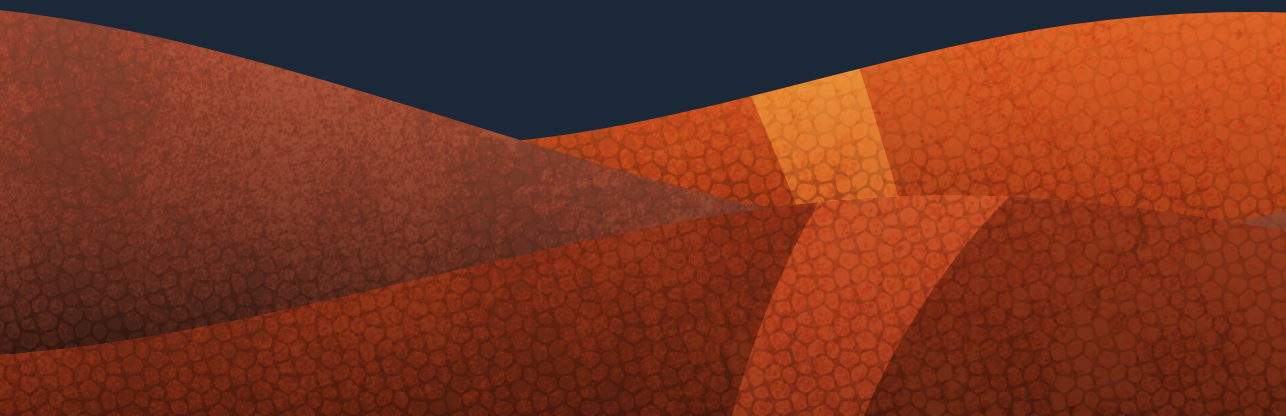
Part 2: Wanderings

| | | |
|------------------|---|-----|
| Chapter 5 | Quantification of wild-type and radiation attenuated Plasmodium falciparum sporozoite motility in human skin <i>Scientific Reports 2019</i> | 117 |
| Chapter 6 | A tracer-based method enables tracking of Plasmodium falciparum malaria parasites during human skin infection <i>Theranostics 2019</i> | 145 |
| Chapter 7 | Summarizing discussion | 175 |
| Appendix | English summary | 195 |
| | Nederlandse samenvatting | 197 |
| | Resúmen na papiamentu | 199 |
| | Curriculum Vitae | 201 |
| | List of abbreviations | 203 |
| | List of publications | 205 |
| | Acknowledgements | 207 |

1



General introduction and thesis outline



GENERAL INTRODUCTION

Skin-penetrating parasites such as those causing malaria and schistosomiasis infect hundreds of millions of people annually. Over half of the world's population is at risk for malaria, and in 2017 alone, an estimated 216 million people were infected, eventually leading to the death of 435 thousand individuals, 61% of whom were children under the age of five¹. Schistosomiasis is a less deadly disease yet causes substantial morbidity worldwide as patients suffer from chronic illness. Over 240 million people are infected worldwide and several million suffer from severe morbidity. It is estimated that around 200 thousand patients die yearly due to the disease and it is still thought that the burden of disease due to schistosomiasis is underestimated as it often goes unrecognized². Given the global burden of these diseases, the need for an effective vaccine is evident^{1,2}. Yet to date, no such vaccine exists for any parasitic disease. Naturally acquired protection following parasite exposure is a slow process that may take years or decades to develop and does not result in sterile immunity³. Currently, the most promising vaccine candidates are live-attenuated parasites, either yielding sterile immunity (in the case of malaria)^{4,5} or decreasing parasite burden after subsequent infection (in the case of *Schistosoma*)⁶⁻⁸.

Migration and kinetics

Malaria infection starts when the skin-penetrating form of the parasite, motile protozoans called sporozoites, are injected into the dermal stroma via the bite of infected mosquitoes while they search for blood⁹. Although the majority of parasites remain in the skin, within a matter of hours approximately 15% make their way through the dermis to reach the hosts vasculature which transports them to the liver, where they continue development intracellularly in hepatocytes¹⁰⁻¹². *Schistosoma cercariae*, on the other hand, are released from freshwater snails and are aquatic multicellular organisms that bore their way into skin tissue upon contact. Subsequently, the tail detaches and the head of the cercaria continues as a schistosome; slowly making its way out of the skin in the span of days before gaining entry to the vascular space by entering venules or lymphatic vessels. Eventually, the schistosomes mature in the hepatic portal vein¹³⁻¹⁵. The dermal stage of both malaria and schistosomiasis is clinically silent, although the initial skin penetration is accompanied by a mosquito bite or a cercarial rash¹⁶, showing that at least a mild form of immune activation at the site of parasite entry does exist.

Immunity to malaria and schistosomiasis

Immunity to malaria is complex and parasite-stage specific. When natural acquired immunity develops, it is primarily against blood-stage and does not appear to protect

against re-infection¹⁷. Vaccines against malaria are aimed to mediate protection at the pre-erythrocytic stage of disease, as up to this stage the disease is symptom free, parasites numbers are still low, parasites are located extracellularly making them vulnerable to antibody attack and blood-stage malaria does not yet activate immunoregulatory effects. RTS,S is currently the only licensed malaria vaccine and yields only approximately 30% protection over the course of the study period¹⁸⁻²⁰. It is based on the circumsporozoite protein (CSP) which coats sporozoites and aims to increase anti-CSP antibodies in order to prevent migration of parasites from the skin to the liver. However, failure in blocking just one sporozoite from migrating into the vasculature would already render the vaccine inadequate as RTS,S initiates only modest T cell immunity.

The rationale for developing a live-attenuated parasite vaccine which confers sterile protection stems from findings by Nussenzweig and colleagues in the 1960's. They were the first to prove complete protection against pre-erythrocytic stages of malaria in mice vaccinated with radiation-attenuated sporozoites (RAS) that terminate development in the liver²¹. In the 70's it was then shown that exposure to over one thousand attenuated-parasite infected mosquitoes could indeed also protect human volunteers^{22,23}. Currently, controlled human malaria infection studies using intravenously injected RAS show protective efficacy of up to 100%^{24,25}. The immunological basis of protection by RAS has been characterized in murine malaria models. In mice, RAS vaccination results in antibody generation, which block migration of sporozoites during subsequent infections, and CD8⁺ T cell activation, which eliminate infected hepatocytes²⁶⁻²⁸. Although antibodies significantly contribute to protection, CD8⁺ T cells alone are capable of conferring sterile protection in mice^{29,30}. In addition, more recently important roles for $\gamma\delta$ -T cells as well as tissue resident memory (T(RM)) cells were suggested^{5,31}. Overall, antibodies appear to play a role in sporozoite stage (anti-CSP antibodies) and blood-stage infection³², and T cells have a dominant role in liver stage immunity, when parasites are localized intracellularly.

In the case of schistosomiasis, mouse studies have characterized immune responses to the various parasite stages. In the first 5 weeks of infection Th1 responses develop which are primarily associated with IFN- γ production. Subsequently starting at 6 weeks post infection, Th2 responses are initiated when parasites mature and start to generate eggs. Lastly, later stages of disease are characterized by immunomodulatory responses such as activation of alternatively-activated (M2) macrophages and regulatory T cells (Tregs), as well as IL-10 production as a regulatory feedback to proinflammatory immune activation³³⁻³⁵. Nonetheless, exposure to wild-type cercariae does not result in protective immunity. This has been suggested to result from the early increase in dermal

immunoregulatory mechanisms in the first few days post infection³⁶. However, in the early 1960's mice were immunized using irradiated cercariae resulting in a reduction of worm burden post challenge³⁷. Although immune responses to these diseases are slowly unraveled, none of the vaccination approaches have thus far resulted in long-term sterile protection to either parasitic disease.

Why the skin matters

The common ground for all skin-penetrating parasites is the route they must navigate from their site of entry through a densely packed immune organ: the skin³⁸. The skin is the largest organ in the human body, and it is a specialized barrier to the outside world, both by forming a physiological barrier as well as functioning as an important immunological organ. Its most important function is to maintain the immunological balance between tolerance to commensal microbes and inflammation in response to pathogens. Within the skin reside a wide variety of immune cells such as dermal T cells, Natural Killer cells, innate lymphoid cells and mast cells. Importantly, the human dermis contains antigen presenting cells (APCs), dendritic cells (DCs) and macrophages (MΦ), that sample the surroundings and present antigens to the adaptive immune system³⁹⁻⁴². These cells coordinate the following adaptive immune responses by polarizing lymphocytes towards regulation or inflammation depending on the type of antigen encountered⁴². In addition, the dermis is rich in blood and lymphatic vessels which allow quick access to blood-derived immune cells such as neutrophils, monocytes, monocyte-derived macrophages and additional lymphocytes. Antigens are transferred continuously from the skin to the skin-draining lymph nodes either actively by migrating APCs, or passively through lymphatic vessels. It is here, in the skin draining lymph node, that an adaptive response is launched. For skin-penetrating parasites, the skin is the first site of interaction with the host's immune response.

In the case of malaria, the importance of the skin stage in vaccine development against parasitic infections is demonstrated by the importance of the route of administration of live-attenuated parasite vaccines on the protectivity of the response. In vaccination protocols against a variety of diseases dose reduction can be achieved by administering the vaccine not subcutaneously or intramuscularly, but directly into the skin⁴³⁻⁴⁵. In contrast, early clinical studies show that inoculation with malaria sporozoites results in a strong protective immune response when delivered by the bite of an infected mosquito or after intravenous administration of purified parasites⁴. However, the intradermal route of administration, often preferred due to practicalities, results in inferior protective immunity in both rodent and human models of malaria^{46,47}. In addition to this, the skin may well be an important effector site for antibody responses against pre-erythrocytic

stages of malaria. Blocking dermal parasite migration retains sporozoites in the skin, preventing them from reaching the liver and initiating infection^{48,49}. For schistosomiasis it was shown that irradiated cercariae could induce an APC-mediated IFN- γ response in the skin draining lymph node (sdLN) of mice. Additionally, non-attenuated larvae were demonstrated to induce the production of IL-10 in mouse skin⁶. These findings suggest that the skin stage of disease may be critical to the initiation of tolerance for both malaria and *Schistosoma*.

Could pathogens hijack existing immune pathways to avoid clearance?

Some pathogens, such as viruses and bacteria but also parasites, are capable of exploiting APC mechanisms for regulation in order to evade degradation by the immune system⁵⁰⁻⁵⁵. To convey a signal to the adaptive immune system, APCs present antigens in a context of co-stimulation and cytokine signals⁴². The human body contains a variety of mechanisms to down-modulate immune responses, in order to prevent continuous inflammation and subsequent tissue destruction. This can be achieved for example by secretion of regulatory cytokines such as interleukin 10 (IL-10)⁵⁶ or by co-stimulatory signaling through immune checkpoint molecules such as the PD-1/PD-L1 pathway^{57,58}. Although immune modulation by parasites has widely been described during the blood stadia of these diseases⁵⁹⁻⁶¹, early immunoregulatory responses to skin stage parasites have not been investigated in the human host to date. Some murine models have begun to look into the skin-stage of skin-penetrating parasitic disease, nonetheless human responses have remained wholly uncharacterized. As murine skin differs drastically from human skin, both anatomically as well as functionally, looking into the human counterpart of the skin stage could prove critical in order to investigate some of the pitfalls in vaccine-induced immunity. In this thesis we aimed to test human responses to both malaria and *Schistosoma*, by characterizing responses of human monocyte-derived APCs as well as primary dermal APCs freshly isolated from human skin. In addition, we use a human skin explant model in order to expose skin to parasites in its natural three-dimensional state.

Parasite motility, prerequisite for immune responses

A critical feature in both parasite infectivity and subsequent responses is their motility. For malaria, parasites deficient in motility proteins do not establish an infection. In the case of *Schistosoma* parasite motility equally plays an important role; irradiated cercariae have been shown to persist in the skin much longer than their non-irradiated counterparts, increasing their time in the dermis from a few days up to a week^{62,63}. In addition, over-irradiation of cercariae led to a much decreased number of parasites in the hepatic veins and a reduction of protective immunity³⁷. Although the significance

of parasite movement has been widely accepted, motility analysis of live-attenuated sporozoite vaccines is routinely performed *in vitro*⁶⁴, and in-host motility of *Schistosoma* parasites has not been characterized at all. However, *in vitro* modelling passes over the consequential effect of the tissue environment on motility^{65,66}. Therefore visualization and quantification of parasite motility in the three-dimensional setting may prove a crucial factor in the detailed comprehension of parasite-skin interactions. We dedicated the second part of this thesis to the development and implementation of (molecular) imaging techniques in the characterization of dermal parasite movement.

Understanding the details of dermal immune regulation by skin-penetrating parasites could significantly aid in the development and optimization of live-attenuated parasite vaccines. Bypassing or counteracting the regulatory effects of these parasites on dermal immune cells may optimize their protective effect. This thesis aims to unravel the pivotal role of the skin stage of skin-penetrating parasites in the potential polarization towards immune tolerance, both by investigating the kinetics of parasite migration, as well as the immune responses after exposure.

THESIS OUTLINE

The first part of this thesis describes the host immune-regulatory mechanisms that are exploited by two different skin-penetrating parasites immediately after their entry into the skin. In **chapter 2** we investigated APC responses to whole *Plasmodium falciparum* (*Pf*) sporozoite stimulation and show that malaria sporozoites induce regulatory MΦs that can suppress subsequent adaptive T cell responses. **Chapter 3** investigates the effect of the route of administration of whole sporozoites on their ability to skew towards dermal immune regulation. In **chapter 4** we show that a different skin-penetrating parasite, *Schistosoma mansoni*, is similarly capable of inducing regulatory immune responses in human skin and that its ability to do so is decreased upon radiation attenuation, the most commonly used mode of attenuation in parasite vaccines.

The second part of this thesis focusses on the motility behavior of malaria parasites in the human dermis. In **chapter 5**, we show that radiation attenuation impairs sporozoite movement in the human skin and reverts sporozoite motility back to “default”, non-directional movement. **Chapter 6** describes a novel method for targeted molecular imaging of genetically wild-type *Pf* sporozoites, allowing for imaging and subsequent motility analysis of non-GMO *Pf* sporozoites in human skin tissue.

Finally, in **chapter 7** the results are summarized and discussed in the broader context of the current literature and regarding potential new lines of research necessary for

refinement and development of novel vaccines. We draw parallels between the two species of skin-penetrating parasites investigated and discuss the effect of radiation attenuation of parasites.

REFERENCES

- 1 [Internet] WHO: Geneva Switzerland. 19 November 2018, World Malaria report 2018. <https://www.who.int/malaria/media/world-malaria-report-2018/en/>.
- 2 [Internet] WHO: Geneva Switzerland. 17 April 2019, Schistosomiasis fact sheet. <https://www.who.int/news-room/fact-sheets/detail/schistosomiasis> (2019).
- 3 Doolan, D. L., Dobano, C. & Baird, J. K. Acquired immunity to malaria. *Clin Microbiol Rev* 22, 13-36, Table of Contents, doi:10.1128/CMR.00025-08 (2009).
- 4 Seder, R. A. et al. Protection against malaria by intravenous immunization with a nonreplicating sporozoite vaccine. *Science* 341, 1359-1365, doi:10.1126/science.1241800 (2013).
- 5 Ishizuka, A. S. et al. Protection against malaria at 1 year and immune correlates following PfSPZ vaccination. *Nat Med* 22, 614-623, doi:10.1038/nm.4110 (2016).
- 6 Hogg, K. G., Kumkate, S., Anderson, S. & Mountford, A. P. Interleukin-12 p40 secretion by cutaneous CD11c+ and F4/80+ cells is a major feature of the innate immune response in mice that develop Th1-mediated protective immunity to *Schistosoma mansoni*. *Infect Immun* 71, 3563-3571 (2003).
- 7 Hogg, K. G., Kumkate, S. & Mountford, A. P. IL-10 regulates early IL-12-mediated immune responses induced by the radiation-attenuated schistosome vaccine. *Int Immunol* 15, 1451-1459 (2003).
- 8 Hewitson, J. P., Hamblin, P. A. & Mountford, A. P. Immunity induced by the radiation-attenuated schistosome vaccine. *Parasite Immunol* 27, 271-280, doi:10.1111/j.1365-3024.2005.00764.x (2005).
- 9 Menard, R. et al. Looking under the skin: the first steps in malarial infection and immunity. *Nat Rev Microbiol* 11, 701-712, doi:10.1038/nrmicro3111 (2013).
- 10 Amino, R. et al. Quantitative imaging of *Plasmodium* transmission from mosquito to mammal. *Nat Med* 12, 220-224, doi:10.1038/nm1350 (2006).
- 11 Amino, R. et al. Imaging malaria sporozoites in the dermis of the mammalian host. *Nat Protoc* 2, 1705-1712, doi:10.1038/nprot.2007.120 (2007).
- 12 Yamauchi, L. M., Coppi, A., Snounou, G. & Sinnis, P. *Plasmodium* sporozoites trickle out of the injection site. *Cell Microbiol* 9, 1215-1222, doi:10.1111/j.1462-5822.2006.00861.x (2007).
- 13 Wheeler, P. R. & Wilson, R. A. *Schistosoma mansoni*: a histological study of migration in the laboratory mouse. *Parasitology* 79, 49-62 (1979).
- 14 Mangold, B. L. & Dean, D. A. Autoradiographic analysis of *Schistosoma mansoni* migration from skin to lungs in naive mice. Evidence that most attrition occurs after the skin phase. *Am J Trop Med Hyg* 32, 785-789 (1983).
- 15 Wilson, R. A., Coulson, P. S., Sturrock, R. F. & Reid, G. D. Schistosome migration in primates: a study in the olive baboon (*Papio anubis*). *Trans R Soc Trop Med Hyg* 84, 80-83 (1990).
- 16 Gray, D. J., Ross, A. G., Li, Y. S. & McManus, D. P. Diagnosis and management of schistosomiasis. *BMJ* 342, d2651, doi:10.1136/bmj.d2651 (2011).
- 17 Tran, T. M. et al. An intensive longitudinal cohort study of Malian children and adults reveals no evidence of acquired immunity to *Plasmodium falciparum* infection. *Clin Infect Dis* 57, 40-47, doi:10.1093/cid/cit174 (2013).
- 18 Rts, S. C. T. P. Efficacy and safety of the RTS,S/AS01 malaria vaccine during 18 months after vaccination: a phase 3 randomized, controlled trial in children and young infants at 11 African sites. *PLoS Med* 11, e1001685, doi:10.1371/journal.pmed.1001685 (2014).
- 19 Rts, S. C. T. P. et al. A phase 3 trial of RTS,S/AS01 malaria vaccine in African infants. *N*

- Engl J Med 367, 2284-2295, doi:10.1056/NEJMoa1208394 (2012).
- 20 Rts, S. C. T. P. Efficacy and safety of RTS,S/AS01 malaria vaccine with or without a booster dose in infants and children in Africa: final results of a phase 3, individually randomised, controlled trial. *Lancet* 386, 31-45, doi:10.1016/S0140-6736(15)60721-8 (2015).
- 21 Nussenzweig, R. S., Vanderberg, J., Most, H. & Orton, C. Protective immunity produced by the injection of x-irradiated sporozoites of *Plasmodium berghei*. *Nature* 216, 160-162, doi:10.1038/216160a0 (1967).
- 22 Clyde, D. F. Immunization of man against falciparum and vivax malaria by use of attenuated sporozoites. *Am J Trop Med Hyg* 24, 397-401, doi:10.4269/ajtmh.1975.24.397 (1975).
- 23 Luke, T. C. & Hoffman, S. L. Rationale and plans for developing a non-replicating, metabolically active, radiation-attenuated *Plasmodium falciparum* sporozoite vaccine. *J Exp Biol* 206, 3803-3808, doi:10.1242/jeb.00644 (2003).
- 24 Roestenberg, M. et al. Protection against a malaria challenge by sporozoite inoculation. *N Engl J Med* 361, 468-477, doi:10.1056/NEJMoa0805832 (2009).
- 25 Mordmuller, B. et al. Sterile protection against human malaria by chemo attenuated PfSPZ vaccine. *Nature* 542, 445-449, doi:10.1038/nature21060 (2017).
- 26 Chakravarty, S. et al. CD8+ T lymphocytes protective against malaria liver stages are primed in skin-draining lymph nodes. *Nat Med* 13, 1035-1041, doi:10.1038/nm1628 (2007).
- 27 Schofield, L. et al. Gamma interferon, CD8+ T cells and antibodies required for immunity to malaria sporozoites. *Nature* 330, 664-666, doi:10.1038/330664a0 (1987).
- 28 Rodrigues, M., Nussenzweig, R. S. & Zavala, F. The relative contribution of antibodies, CD4+ and CD8+ T cells to sporozoite-induced protection against malaria. *Immunology* 80, 1-5 (1993).
- 29 Cockburn, I. A., Tse, S. W. & Zavala, F. CD8+ T cells eliminate liver-stage *Plasmodium berghei* parasites without detectable bystander effect. *Infect Immun* 82, 1460-1464, doi:10.1128/IAI.01500-13 (2014).
- 30 Van Braeckel-Budimir, N. & Harty, J. T. CD8 T-cell-mediated protection against liver-stage malaria: lessons from a mouse model. *Front Microbiol* 5, 272, doi:10.3389/fmicb.2014.00272 (2014).
- 31 Lyke, K. E. et al. Attenuated PfSPZ Vaccine induces strain-transcending T cells and durable protection against heterologous controlled human malaria infection. *Proc Natl Acad Sci U S A* 114, 2711-2716, doi:10.1073/pnas.1615324114 (2017).
- 32 Teo, A., Feng, G., Brown, G. V., Beeson, J. G. & Rogerson, S. J. Functional Antibodies and Protection against Blood-stage Malaria. *Trends Parasitol* 32, 887-898, doi:10.1016/j.pt.2016.07.003 (2016).
- 33 Dunne, D. W. & Cooke, A. A worm's eye view of the immune system: consequences for evolution of human autoimmune disease. *Nat Rev Immunol* 5, 420-426, doi:10.1038/nri1601 (2005).
- 34 Colley, D. G. & Secor, W. E. Immunology of human schistosomiasis. *Parasite Immunol* 36, 347-357, doi:10.1111/pim.12087 (2014).
- 35 Grogan, J. L., Kreamsner, P. G., Deelder, A. M. & Yazdanbakhsh, M. The effect of anti-IL-10 on proliferation and cytokine production in human schistosomiasis: fresh versus cryopreserved cells. *Parasite Immunol* 20, 345-349, doi:10.1046/j.1365-3024.1998.00157.x (1998).
- 36 Mountford, A. P. & Trottein, F. Schistosomes in the skin: a balance between immune priming and regulation. *Trends Parasitol* 20, 221-226, doi:10.1016/j.pt.2004.03.003 (2004).
- 37 Vilella, J. B., Gomberg, H. J. & Gould, S. E. Immunization to *Schistosoma mansoni* in mice inoculated with radiated cercariae.

- Science 134, 1073-1075, doi:10.1126/science.134.3485.1073 (1961).
- 38 Di Meglio, P., Perera, G. K. & Nestle, F. O. The multitasking organ: recent insights into skin immune function. *Immunity* 35, 857-869, doi:10.1016/j.immuni.2011.12.003 (2011).
- 39 Tay, S. S., Roediger, B., Tong, P. L., Tikoo, S. & Weninger, W. The Skin-Resident Immune Network. *Curr Dermatol Rep* 3, 13-22, doi:10.1007/s13671-013-0063-9 (2014).
- 40 Wang, X. N. et al. A three-dimensional atlas of human dermal leukocytes, lymphatics, and blood vessels. *J Invest Dermatol* 134, 965-974, doi:10.1038/jid.2013.481 (2014).
- 41 Richmond, J. M. & Harris, J. E. Immunology and skin in health and disease. *Cold Spring Harb Perspect Med* 4, a015339, doi:10.1101/cshperspect.a015339 (2014).
- 42 de Jong, E. C., Smits, H. H. & Kapsenberg, M. L. Dendritic cell-mediated T cell polarization. *Springer Semin Immunopathol* 26, 289-307, doi:10.1007/s00281-004-0167-1 (2005).
- 43 Denis, M. et al. An overview of the immunogenicity and effectiveness of current human rabies vaccines administered by intradermal route. *Vaccine* 37 Suppl 1, A99-A106, doi:10.1016/j.vaccine.2018.11.072 (2019).
- 44 Kenney, R. T., Frech, S. A., Muenz, L. R., Villar, C. P. & Glenn, G. M. Dose sparing with intradermal injection of influenza vaccine. *N Engl J Med* 351, 2295-2301, doi:10.1056/NEJMoa043540 (2004).
- 45 Okayasu, H. et al. Intradermal Administration of Fractional Doses of Inactivated Poliovirus Vaccine: A Dose-Sparing Option for Polio Immunization. *J Infect Dis* 216, S161-S167, doi:10.1093/infdis/jix038 (2017).
- 46 Epstein, J. E. et al. Live attenuated malaria vaccine designed to protect through hepatic CD8(+) T cell immunity. *Science* 334, 475-480, doi:10.1126/science.1211548 (2011).
- 47 Haeberlein, S. et al. Protective immunity differs between routes of administration of attenuated malaria parasites independent of parasite liver load. *Sci Rep* 7, 10372, doi:10.1038/s41598-017-10480-1 (2017).
- 48 Vanderberg, J. P. & Frevert, U. Intravital microscopy demonstrating antibody-mediated immobilisation of *Plasmodium berghei* sporozoites injected into skin by mosquitoes. *Int J Parasitol* 34, 991-996, doi:10.1016/j.ijpara.2004.05.005 (2004).
- 49 Stewart, M. J., Nawrot, R. J., Schulman, S. & Vanderberg, J. P. *Plasmodium berghei* sporozoite invasion is blocked in vitro by sporozoite-immobilizing antibodies. *Infect Immun* 51, 859-864 (1986).
- 50 Horne-Debets, J. M. et al. PD-1 dependent exhaustion of CD8+ T cells drives chronic malaria. *Cell Rep* 5, 1204-1213, doi:10.1016/j.celrep.2013.11.002 (2013).
- 51 Huang, X. et al. PD-1 expression by macrophages plays a pathologic role in altering microbial clearance and the innate inflammatory response to sepsis. *Proc Natl Acad Sci U S A* 106, 6303-6308, doi:10.1073/pnas.0809422106 (2009).
- 52 Illingworth, J. et al. Chronic exposure to *Plasmodium falciparum* is associated with phenotypic evidence of B and T cell exhaustion. *J Immunol* 190, 1038-1047, doi:10.4049/jimmunol.1202438 (2013).
- 53 Narasimhan, P. B. et al. Similarities and differences between helminth parasites and cancer cell lines in shaping human monocytes: Insights into parallel mechanisms of immune evasion. *PLoS Negl Trop Dis* 12, e0006404, doi:10.1371/journal.pntd.0006404 (2018).
- 54 Winkel, B. M. F. et al. Early Induction of Human Regulatory Dermal Antigen Presenting Cells by Skin-Penetrating *Schistosoma Mansoni* Cercariae. *Front Immunol* 9, 2510, doi:10.3389/fimmu.2018.02510 (2018).
- 55 Xiao, J., Li, Y., Yolken, R. H. & Viscidi, R. P. PD-1 immune checkpoint blockade promotes brain leukocyte infiltration and diminishes cyst burden in a mouse model of *Toxoplasma* infection. *J Neuroimmunol* 319, 55-62, doi:10.1016/j.jneuroim.2018.03.013 (2018).

- 56 Couper, K. N., Blount, D. G. & Riley, E. M. IL-10: the master regulator of immunity to infection. *J Immunol* 180, 5771-5777, doi:10.4049/jimmunol.180.9.5771 (2008).
- 57 Riella, L. V., Paterson, A. M., Sharpe, A. H. & Chandraker, A. Role of the PD-1 pathway in the immune response. *Am J Transplant* 12, 2575-2587, doi:10.1111/j.1600-6143.2012.04224.x (2012).
- 58 Francisco, L. M., Sage, P. T. & Sharpe, A. H. The PD-1 pathway in tolerance and autoimmunity. *Immunol Rev* 236, 219-242, doi:10.1111/j.1600-065X.2010.00923.x (2010).
- 59 Ocana-Morgner, C., Mota, M. M. & Rodriguez, A. Malaria blood stage suppression of liver stage immunity by dendritic cells. *J Exp Med* 197, 143-151, doi:10.1084/jem.20021072 (2003).
- 60 Coban, C., Ishii, K. J., Horii, T. & Akira, S. Manipulation of host innate immune responses by the malaria parasite. *Trends Microbiol* 15, 271-278, doi:10.1016/j.tim.2007.04.003 (2007).
- 61 Maizels, R. M., Smits, H. H. & McSorley, H. J. Modulation of Host Immunity by Helminths: The Expanding Repertoire of Parasite Effector Molecules. *Immunity* 49, 801-818, doi:10.1016/j.immuni.2018.10.016 (2018).
- 62 Wilson, R. A., Coulson, P. S. & Dixon, B. Migration of the schistosomula of *Schistosoma mansoni* in mice vaccinated with radiation-attenuated cercariae, and normal mice: an attempt to identify the timing and site of parasite death. *Parasitology* 92 (Pt 1), 101-116, doi:10.1017/s0031182000063484 (1986).
- 63 Richter, D., Harn, D. A. & Matuschka, F. R. The irradiated cercariae vaccine model: looking on the bright side of radiation. *Parasitol Today* 11, 288-293, doi:10.1016/0169-4758(95)80041-7 (1995).
- 64 Prinz, H. L., Sattler, J. M. & Frischknecht, F. Plasmodium Sporozoite Motility on Flat Substrates. *Bio-protocol* 7, e2395, doi:10.21769/BioProtoc.2395. (2017).
- 65 Battista, A., Frischknecht, F. & Schwarz, U. S. Geometrical model for malaria parasite migration in structured environments. *Phys Rev E Stat Nonlin Soft Matter Phys* 90, 042720, doi:10.1103/PhysRevE.90.042720 (2014).
- 66 Hellmann, J. K. et al. Environmental constraints guide migration of malaria parasites during transmission. *PLoS Pathog* 7, e1002080, doi:10.1371/journal.ppat.1002080 (2011).

Part 1

Wiles *noun*

◀ /wɪɪlz/

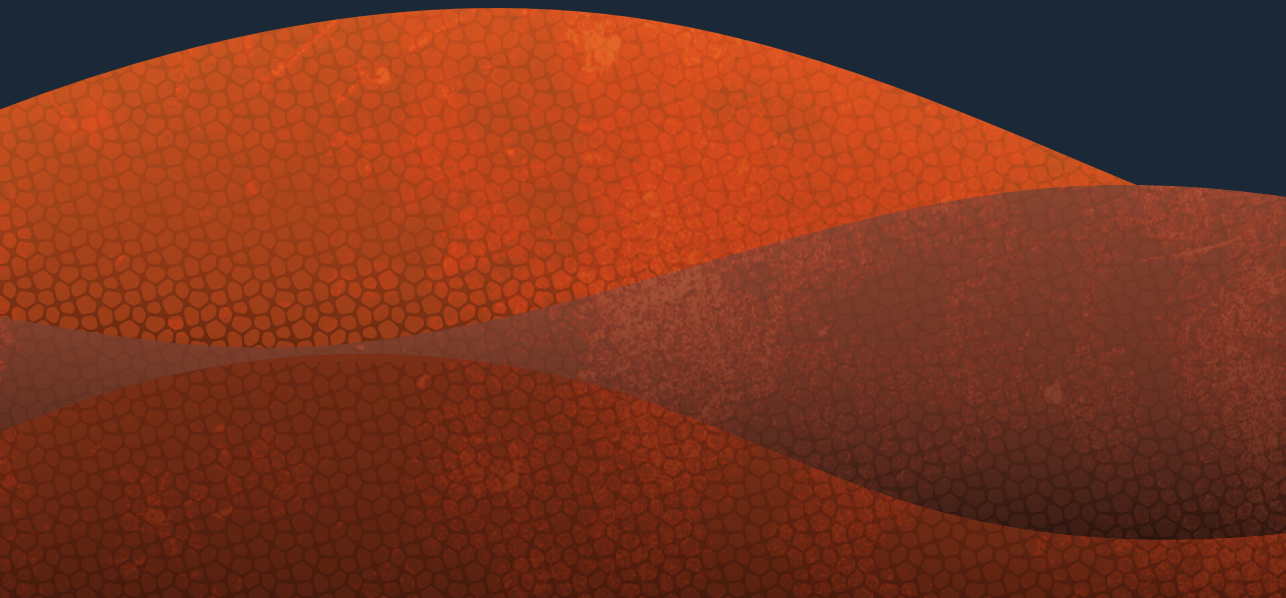
Devious or cunning stratagems
employed in manipulating or persuading
someone to do what one wants

— **Oxford Dictionary**

“

Parasites employ a variety of wiles to induce immune regulation by dermal antigen presenting cells

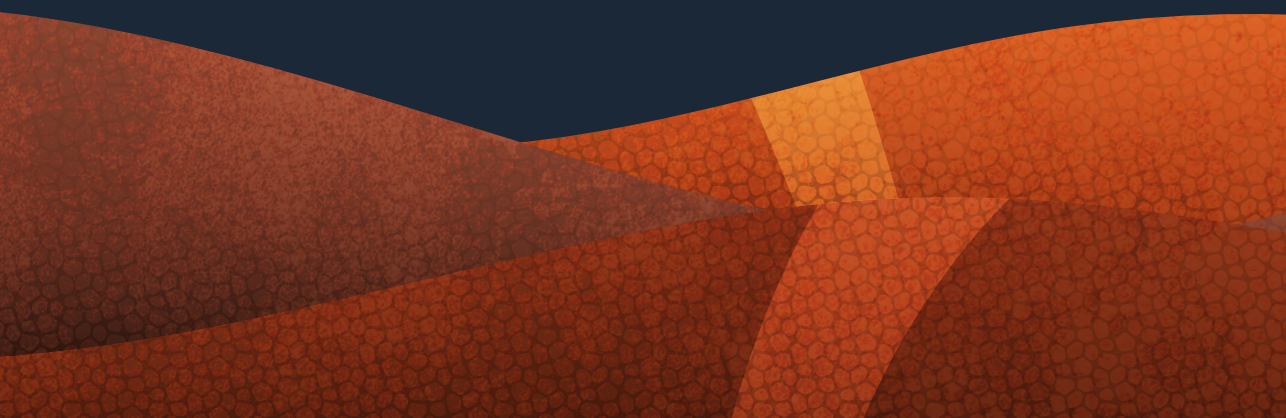
2



Plasmodium sporozoites induce regulatory macrophages

Béatrice M.F. Winkel, Leonard R. Pelgrom, Roos van Schuijlenburg, Els Baalbergen, Munisha S. Ganesh, Heleen Gerritsma, Clarize M. de Korne, Nikolas Duszenko, Marijke C.C. Langenberg, Séverine C. Chevalley-Maurel, Hermelijn H. Smits, Esther C. de Jong, Bart Everts, Blandine Franke-Fayard, Meta Roestenberg

PLOS Pathogens 2020. DOI: [10.1371/journal.ppat.1008799](https://doi.org/10.1371/journal.ppat.1008799)



ABSTRACT

Professional antigen-presenting cells (APCs), like macrophages (Mφs) and dendritic cells (DCs), are central players in the induction of natural and vaccine-induced immunity to malaria, yet very little is known about the interaction of SPZ with human APCs. Intradermal delivery of whole-sporozoite vaccines reduces their effectivity, possibly due to dermal immunoregulatory effects. Therefore, understanding these interactions could prove pivotal to malaria vaccination. We investigated human APC responses to recombinant circumsporozoite protein (recCSP), SPZ and anti-CSP opsonized SPZ both in monocyte derived MoDCs and MoMφs. Both MoDCs and MoMφs readily took up recCSP but did not change phenotype or function upon doing so. SPZ are preferentially phagocytosed by MoMφs instead of DCs and phagocytosis greatly increased after opsonization. Subsequently MoMφs show increased surface marker expression of activation markers as well as tolerogenic markers such as Programmed Death-Ligand 1 (PD-L1). Additionally, they show reduced motility, produce interleukin 10 and suppressed interferon gamma (IFNγ) production by antigen specific CD8⁺ T cells. Importantly, we investigated phenotypic responses to SPZ in primary dermal APCs isolated from human skin explants, which respond similarly to their monocyte-derived counterparts. These findings are a first step in enhancing our understanding of pre-erythrocytic natural immunity and the pitfalls of intradermal vaccination-induced immunity.

AUTHOR SUMMARY

Malaria continues to be the deadliest parasitic disease worldwide, and an effective vaccine yielding sterile immunity does not yet exist. Attenuated parasites can induce sterile protection in both human and rodent models for malaria, but these vaccines need to be administered directly into the bloodstream in order to convey protection; administration via the skin results in a much-reduced efficacy. We hypothesized this is caused by an early immune regulation initiated at the first site of contact with the immune system: the skin. However, the human skin stage of malaria has not been investigated to date. We used human antigen presenting cells as well as whole human skin explants to investigate (dermal) immune responses and found that *Plasmodium* sporozoites are able to suppress immune responses by inducing regulatory macrophages. Our study provides new insights in the mechanism of early immune regulation exploited by *Plasmodium* parasites and can help to explain why intradermal vaccination using whole attenuated sporozoites results in reduced protection.

INTRODUCTION

Despite decades of research into the world's most deadly parasite, over 200 million individuals develop malaria after the bite of an infected *Anopheles* mosquito yearly¹. Unfortunately, natural immunity to malaria mounts only very slowly and requires sustained exposure to repeated infections². The only currently licensed malaria vaccine, RTS,S, is based on circumsporozoite protein (CSP), the most abundant and immunodominant protein on the surface of malaria sporozoites (SPZ), and yields only limited protection^{3,4}. Therefore, the development of highly effective vaccines remains of vital importance. Attenuated malaria sporozoites that arrest development in the liver are promising vaccine candidates because they yield sterile protection against homologous parasite challenge in malaria naïve individuals^{5,6}. The protection of these attenuated SPZ vaccines is thought to be mediated through interferon gamma (IFN γ)-producing CD8⁺ effector T cells which target infected hepatocytes^{7,8}, as well as antibodies which target the migrating extracellular sporozoite on its way to the liver⁹⁻¹¹. Large numbers of sporozoites seem to be required to induce sufficient protective immune responses in attenuated SPZ vaccination, whereby there is a remarkable difference between intradermal (ID), intravenous (IV) or mosquito bite administration^{5,12-14}. Given the inferiority of ID administration, the immune interaction between attenuated SPZ and skin immune cells might downmodulate the ensuing immune responses. Evidence for this hypothesis was found in mice, where lower levels of protection after ID vaccination were associated with an increase in immune regulatory interleukin (IL)-10 producing

lymphocytes in the skin draining lymph node (sdLN)¹². Understanding the interplay between SPZ and the immune system is important to overcome malaria tolerogenic responses and potentially enhance the potency of attenuated SPZ to allow for skin-administered vaccines.

It was previously thought that SPZ rapidly leave the skin, outrunning host immune cells due to their high migratory velocity¹⁵. However, recent research has shown that only a minority of injected SPZ succeed in finding a blood vessel to transport them to the liver, and that the majority of injected parasites remains in the skin¹⁶⁻¹⁸. There, SPZ interact with antigen-presenting cells (APCs) such as dermally-residing dendritic cells (DCs) and macrophages (Mφs)¹⁹, which orchestrate immune responses by providing processed antigens, co-stimulatory molecules and cytokines to T lymphocytes²⁰⁻²⁴. Ultimately, SPZ were shown able to affect skin regulatory T cell (Treg) activity in mice²⁵. How malaria SPZ initiate these responses has not been investigated to date. We hypothesize that SPZ enhance their chance of survival by inducing a regulatory immune environment through exploitation of the signaling mechanisms of APCs.

Plausible candidate targets for exploitation of APC pathways are immune checkpoints. Checkpoint molecules such as Programmed Death-1 (PD-1) and its ligand (PD-1/PD-L1) are regulators of immune activation and have initially been described in the context of tumor immunology²⁶⁻²⁹. PD-L1 is expressed on APCs and, after ligation with PD-1 on T cells, can lead to T cell anergy^{26,30,31} and the induction of immunological tolerance²⁷⁻²⁹. Many pathogens such as viruses³², bacteria³³ as well as parasites³⁴⁻³⁸ have been demonstrated to use immune checkpoints to their advantage. Blood stage malaria parasites were shown to reduce T cell immunity through induction of the PD-L1 pathway³⁹. Whether SPZ are able to similarly skew dermal APC responses to induce tolerance at the pre-erythrocytic stage of disease is still unknown.

To date, studies investigating the malaria skin stage have focused on rodent models. However, using rodent parasites in rodent skin in lieu of human parasites in human skin poses obstacles for extrapolating the findings to humans. Mouse skin is both anatomically⁴⁰ as well as immunologically^{21,41,42} different from human skin. In addition, some rodent malaria parasites are able to invade and develop inside skin cells⁴³, whereas for human parasites this is still unclear. Therefore, we set out to investigate the interaction of *Plasmodium falciparum* (Pf) SPZ with human (skin) APCs (Figure 1) and analyze their effect on the ensuing adaptive immune response.

MATERIALS AND METHODS

Parasite culture

Plasmodium berghei (*Pb*) SPZ were obtained from a transgenic rodent malaria species that expresses fluorescent and luminescent reporter proteins: *Pb* line 1868c11 expressing mCherry and luciferase under the constitutive HSP70 and *eef1a* promoters respectively⁴⁴ (RMgm-1320, www.pberghei.eu) and *Pb* line Bergreen⁴⁵, expressing green fluorescent protein (GFP) under the constitutive HSP70 promoter (RMgm-757, www.pberghei.eu). Mosquitoes were infected with *Pb* by feeding on infected mice as described previously⁴⁶. We used female OF1 mice (6-7 weeks old; Charles River, Leiden, The Netherlands). In addition, SPZ were obtained from the human parasite *Plasmodium falciparum* (*Pf*; NF54⁴⁷; WT or mCherry-expressing under the Sui1 promoter). Mosquitoes were infected with *Pf* by standard membrane feeding as previously described⁴⁸. Salivary glands of infected and uninfected mosquitoes were manually dissected at day 21-28 (*Pb*) or day 14-21 (*Pf*) post infection. Salivary glands were kept on ice until use within 1 hour. Immediately prior to their use, glands were homogenized to extract parasites. Parasites were counted using a Bürker chamber.

Opsonization of parasites

Opsonization of parasites was performed by incubating parasite sporozoites with anti-CSP antibody (For *Pf* SPZ: 2A10; IgG2 α ; 10 μ g/ml; MR4, BEI resources, for *Pb* SPZ: 3D11; 70ug/ml; kindly provided by Prof. M. Prudêncio) for 30 minutes at room temperature before stimulation.

Monocyte-derived dendritic cells (MoDCs) and macrophages (MoM ϕ) culture

Monocytes were isolated from venous whole blood of healthy volunteers using CD14⁺ MACS isolation (Miltenyi Biotec, Bergisch Gladbach, Germany) and differentiated into MoDCs as described previously⁴⁹. Alternatively, monocytes were differentiated into M0 MoM ϕ using Macrophage Colony Stimulating Factor (M-CSF; 20ng/ml; Biolegend, San Diego, CA, USA)⁵⁰. On Day 6, MoDCs and M0 MoM ϕ were harvested, counted and re-cultured at 10⁵ cells/24-well NUNC plate with Nunclon delta surface coating in RPMI containing 10% FCS supplemented with Penicillin/streptomycin and rested for 24 hours. For recCSP and SPZ uptake assays the cells were re-cultured at 10⁴ cells/96-well.

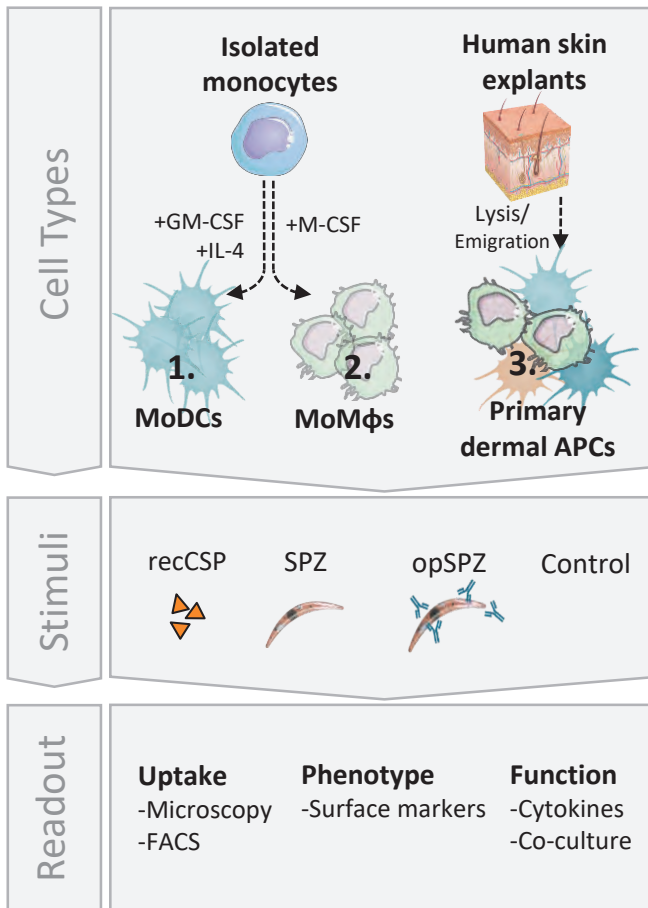


Figure 1. Experimental setup. MoDCs and MoMφs were differentiated in vitro from freshly isolated monocytes. Additionally, fresh human skin explants containing primary dermal APCs were lysed to form a single cell suspension. All cell types were stimulated in vitro with recombinant SPZ surface antigen, circumsporozoite protein (recCSP) or whole sporozoites (untreated: SPZ or opsonized: SPZ aCSP). Uptake of recCSP and (a)SPZ was determined by confocal microscopy and flow cytometry. Subsequently, cells were analyzed for their phenotype and function.

Sporozoite and recCSP uptake analysis by flow cytometry

For uptake experiments, rested MoDCs and MoMφs were stimulated for 1 hour with recCSP in the concentrations described or a 1:1 sporozoite:cell number of (opsonized) fluorescent *Pb* parasites. Opsonization of parasites was performed as described above. Alternatively, SPZ were fixed for 15 minutes at room temperature using 4% formaldehyde, which was followed by three washes with phosphate buffered saline

(PBS). RecCSP had been fluorescently labelled using a commercial antibody labeling kit (ALEXA Fluor 660 antibody labeling kit, Thermo Fisher Scientific, Waltham, MA, USA) according to their protocol. After 1 hour of stimulation, cells were harvested, stained with 7-aminoactinomycin D (7-AAD) live/dead dye (Invitrogen, Waltham, MA, USA) and analyzed by Flow Cytometry using a BD LSR Fortessa (BD Biosciences, San Jose, CA, USA) and analyzed in FlowJo version 9.9.6 (FlowJo LLC, Ashland, OR, USA).

Confocal microscopy uptake analysis of Pf SPZ

Four-quadrant glass bottom confocal dishes (ø14mm cover slip; MatTek Corporation) were coated overnight with Poly-D-Lysine (PDL) at 37°C. 10⁴ MoDCs and MoMacs were plated into each quadrant and allowed to adhere for 6 hours. (Opsonized) mCherry expressing *Pf* SPZ were added in a 1:1 ratio and fixed after 1 hour using 15 minute incubation with 3.7% formalin (Sigma Aldrich, St Louis, MO, USA) at room temperature. Opsonization of parasites was performed as described above. Dishes were imaged in 3-dimensional Z-stacks using the 40x objective on a SP8X WLL (white light laser) microscope (Leica Microsystems, Wetzlar, Germany; 4 donors, 12-16 fields of view per donor per condition; on average 1150 MoMacs and 550 MoDCs per donor per condition). The nuclei of the cells were stained with Hoechst prior to the imaging. mCherry was excited at 587 nm and the emission was collected between 600-650 nm. Hoechst was excited at 405 nm and emission was collected between 420-470 nm. Cell membranes were identified either on the basis of brightfield or after 10 minute incubation with CellBrite Green (Biotium, Hayward, CA, USA). CellBrite Green was excited at 488 nm and emission collected between 500-530 nm. Cells were analyzed manually for intracellular SPZ using LASX software (Leica Microsystems).

Confocal video microscopy of whole SPZ phagocytosis

Glass bottom confocal dishes (ø14mm cover slip; MatTek Corporation) were coated overnight with Poly-D-Lysine (PDL) at 37°C. 10⁴ MoDCs and MoMacs were plated onto dishes and allowed to adhere for 6 hours. The nuclei of the cells were stained with Hoechst prior to the imaging. Opsonized mCherry expressing *Pb* or *Pf* SPZ added in a 1:1 ratio and dishes were imaged directly using the 40x objective on a SP8X WLL (white light laser) microscope (Leica Microsystems, Wetzlar, Germany) with climate control at 37°C, 5% CO₂ for the duration of 1 hour. mCherry was excited at 587 nm and the emission was collected between 600-650 nm. Hoechst was excited at 405 nm and emission was collected between 420-470 nm.

Sporozoite and recCSP stimulation

On day 7, rested immature MoDCs and M0 MoMφ were exposed for 24 hours to recombinant *pf* circumsporozoite protein (recCSP; Alpha Diagnostics, San Antonio, TX, USA catalognr: CSPF17-R-10), 20.000 *Plasmodium falciparum* (*Pf*) SPZ, a matched volume of salivary gland extract (SGE) of uninfected control mosquitoes or medium as a true negative control and ultrapure lipopolysaccharide (LPS; 100ng/ml; *Escherichia coli* 0111 B4 strain, InvivoGen, San Diego, CA, USA) as an inflammatory control. When different well sizes were used, the same 1:5 sporozoite:cell ratio was maintained. Importantly, SGE was used as a matched control as SPZ preparations do contain traces of salivary gland material. After 24 hour, cells were harvested, stained with 7-aminoactinomycin D (7AAD) live/dead dye (Invitrogen, Waltham, MA, USA), and antibodies against CD80 (L307.4; BD Biosciences), CD86 (N331 FUN-1; BD Biosciences), CD25 (2A3; BD Biosciences), CD197 (3D12; BD Biosciences), CD206 (15-2; Biolegend), CD209 (DCN46; BD Biosciences), PD-L1 (MIH1; BD Biosciences), PD-L2 (MIH18; eBioscience) and Immunoglobulin-like transcript 3 (ILT3; zm4.1; Biolegend) and analyzed by Flow Cytometry using a BD LSR Fortessa (BD Biosciences, San Jose, CA, USA) and analyzed in FlowJo version 9.9.6 (FlowJo LLC, Ashland, OR, USA).

Naïve CD4+ T cell co-culture

For analysis of T cell polarization, 5×10^3 LPS-matured, *Pf* SPZ or control antigen-stimulated MoDCs were co-cultured with 2×10^4 allogeneic naïve CD4+ T cells isolated from buffy coat (Sanquin, Amsterdam, The Netherlands). Co-cultures were performed in the presence of staphylococcal enterotoxin B (10pg/ml)⁴⁹. On days 6 and 8, recombinant human IL2 (10U/ml; R&D Systems) was added and the T cells were expanded until day 11. Intracellular cytokine production was analyzed after polyclonal restimulation with 100ng/ml phorbol myristate acetate (PMA; Sigma Aldrich) and 1ug/ml ionomycin (Sigma Aldrich) for 6 hours. Brefaldin A (10ug/ml; Sigma Aldrich) was added for the last 4 hours of restimulation. Cells were fixed in 3.7% paraformaldehyde (Sigma Aldrich), permeabilized with permeabilization buffer (Affymetrix, Santa Clara, CA, USA), stained with antibodies against IL-4 and IFN γ (BD biosciences) and analyzed with flow cytometry using a FACScanto (BD Biosciences) with FlowJo version 9.9.6 (FlowJo LLC). In addition, 10^5 expanded CD4 T cells were restimulated with antibodies against CD3 and CD28 (Biolegend) for 24 hours in a 96-wells plate. Supernatants were harvested and analyzed for IL-10 secretion using standard ELISA (Sanquin, Amsterdam, The Netherlands).

Cytokine measurement

MoDC and MoM ϕ supernatants were harvested after 24 hour stimulation with *Pf* SPZ, SPZ antigens or controls. Supernatants (IL-10, IL-1 β and IL6) were analyzed by standard ELISA (Sanquin, The Netherlands)

Wound closing assay

MoM ϕ s were plated in a monolayer in a 96 wells flat bottom plate and allowed to adhere for 24 hours. *Pf* SPZ (1:1 ratio), matched equivalent of SGE or Cytochalasin D⁵¹ (10 μ M) was added, and plates were spun down at a low centrifugal speed (1000rpm) in order to sediment SPZ. Using a pipet tip a scratch was made in one fluent motion in the monolayer. Plates were incubated at 37°C, 5% CO₂ and imaged after 1 hour and 40 hours using a SP8 inverted confocal microscope (Leica Microsystems, Wetzlar). Images were analyzed using ImageJ 1.48v public domain software (NIH, USA) using the following protocol: Process-> Find edges, process->Sharpen, Image-> Adjust threshold (set threshold manually to reduce background noise), process->Find edges, analyze particles->plot profile. Profile data of scratch area of the image was then loaded into Microsoft Excel and plotted using GraphPad Prism (La Jolla, CA, USA) version 7. The scratch area was located a gray value below 700. In addition, we plotted the difference between the mean gray value over a representative section of the full scratch area per donor comparing T40 with T1.

CSP specific CD8 T cell co-culture

A CSP specific CD8⁺T cell clone⁵² was expanded in co-culture with irradiated PBMC feeder cells from anonymous HLA-matched donors (3000 rad; 10:1 (feeder:CD8 cells)) and irradiated Epstein-Barr virus immortalized B cells (3000 rad; 2:1 (EBV to CD8 cells); mix of three, AKO, Boleth and JY cells) in RPMI containing 10% heat inactivated human serum, β -mercaptoethanol (50 μ ; Sigma-Aldrich, St Louis, MO, USA), phytohemagglutinin (1 μ g/ml; Thermo Fischer Scientific, Waltham, MA, USA) and recombinant human IL-2 (100U/ml; R&D systems, Minneapolis, MI, USA) in a 96 wells round bottom plate. After 10 days, cells were harvested, counted and expanded further by co-culture of 2x10⁴ CD8 cells with 5x10⁴ irradiated feeder PBMCs, human recombinant IL-15 (5ng/ml), human recombinant IL-7 (5ng/ml), CD3/28 Dynabeads (Thermo Fisher Scientific) in RPMI 10% human serum. After two days, human recombinant IL-2 was added (100U/ml), cells were used 10 days after expansion.

T cells were cultured together with peptide-stimulated MoDCs overnight in the presence or absence of *Pf* SPZ or control antigen-stimulated MoMφs (40.000 T cells, 10.000 MoDCs and 10.000 MoMφs) in a 96 wells round bottom. For blocking of the IL10 and PD-1 pathway, antibodies against IL-10 (Biolegend, clone JES3-19F1) and IL10 receptor (CD210, Biolegend clone 3F9) or PD-1 (pembrolizumab) were added during the incubation in a concentration of 10ug/ml. After 4 hours, Brefaldin A (10ug/ml; Sigma Aldrich) was added. Cells were harvested, stained with Aqua fixable live/dead dye (Thermo Fischer Scientific) and fixed in 3.7% paraformaldehyde (Sigma Aldrich). After permeabilization with permeabilization buffer (Affymetrix, Santa Clara, CA, USA) cells were stained intracellularly for CD3 (UCHT1; eBioscience, Santa Clara, CA, USA), IFN γ (B27; BD Biosciences), CD137 (4B4-1; Biolegend), Granzyme A (CB9; Biolegend), Granzyme B (GB11; Biolegend) and Perforin (dG9; Invitrogen) and analyzed by Flow Cytometry using a FACSCanto II (BD bioscience).

Suppression assay

MoDCs were generated and stimulated as described above. Next we analyzed suppression of proliferation of bystander T cells by test T cells after interaction with *Pf* SPZ-stimulated MoDCs. SPZ stimulated, LPS-matured MoDCs were co-cultured with naïve CD4⁺ T cells for 6 days in a 24 wells plate in a 1:10 ratio (Test T cells). Next, mature test T cells were harvested, irradiated (30Gy) to prevent proliferation, and co-cultured with carboxyfluorescein succinimidyl ester (CFSE) stained CD4⁺ memory T cells of the same T cell donor in a 1:2 ratio (25.000 and 50.000 respectively) in the presence of 1000 LPS matured MoDCs.

Vitamin D treated MoDCs were used as a regulatory T cell-inducing control. After 6 days of co-culture, bystander (target) T cells were harvested and stained with CD45RO, CD4, CD25 and Aqua live dead stain (Invitrogen). Samples were analyzed with flow cytometry using a FACScanto II (BD Biosciences) with FlowJo version 9.9.6 (FlowJo LLC). Cell proliferation was calculated by measuring the CFSE peaks using the Proliferation Tool by FlowJo. Data was analyzed in Graphpad Prism version 7.

Skin explants

Human skin explants were obtained from collaborating hospitals immediately after abdominal or breast skin reduction surgery (IRB B18.009) and kept at 4°C until use (within 6 hours). Six biopsies, each 6mm in diameter, were taken using punch biopsies. Biopsies were either cultured for 72 hours, floating in medium supplemented with 10% FCS after which biopsies were discarded and supernatant was spun down to collect spontaneously emigrated cells (dermal APCs; used for confocal quantification of *Pf* SPZ

uptake), or enzymatically digested overnight using the A and D enzymes of the human Whole Skin Dissociation Kit with associated C-tubes and GentleMACS tissue dissociator (all Miltenyi Biotec, Bergisch Gladbach, Germany) for immunological assays.

Confocal microscopy Pf SPZ uptake by dermal APCs

Emigrated dermal APCs were subsequently frozen and stored in liquid nitrogen. For confocal uptake experiments, thawed cells were plated in with Poly-D-Lysine coated glass bottom confocal dishes (ø14mm cover slip; MatTek Corporation) and allowed to adhere for 6 hours. Cells were stimulated with (opsonized) *Pf* SPZ (1:1 SPZ:cell ratio) or SGE control and fixed after 1 hour using 15 minute 3.7% formalin (Sigma Aldrich, St Louis, MO, USA) incubation at room temperature. Cell membranes were stained using 10 minute incubation with CellBrite Green (Biotium). Nucleic dye Hoechst was added prior to imaging. Dishes were imaged in 3 dimensional Z-stacks using the 40x objective on a SP8X WLL (white light laser) microscope (Leica Microsystems; 3 donors, 20 fields of view per donor per condition). mCherry was excited at 587 nm and the emission was collected between 600-650 nm, CellBrite Green was excited at 488 nm and emission collected between 500-530 nm and Hoechst was excited at 405 nm and emission collected between 420-470 nm. Cells were analyzed for intracellular SPZ manually using LASX software (Leica Microsystems).

Phenotypic analysis of dermal APCs after SPZ uptake

Lysed single cell skin suspensions were counted and plated out in 48 well plates at 2×10^5 cells per well. Cells were stimulated with mCherry expressing *Pb* or Wild-type *Pf* SPZ for 1 hour (*Pb* uptake experiments) or 24 hours (*Pb* and *Pf* stimulated dermal APC phenotyping). Cells were stained with 7AAD live/dead dye (uptake) or with Aqua fixable live/dead dye (Thermo Fischer Scientific; phenotyping), CD45 (HI30; Biolegend), HLA-DR (L243; eBioscience), CD11c (Bu15, Biolegend), PD-L1 (MIH1; BD Biosciences), CD80 (L307.4; BD Biosciences) and analyzed by Flow Cytometry using an LSRFortessa (BD Biosciences). Data was analyzed in FlowJo version 9.9.6 (FlowJo LLC). Gates were set using 'fluorescence minus one' (FMO) stained control samples.

Statistical analysis

Data was analyzed using GraphPad Prism (La Jolla, CA, USA) version 7 or 8. Comparisons between two or more independent data groups were made by Student's T test (parametric data)/ Wilcoxon test (nonparametric data) or analysis of variance test (ANOVA) respectively. $P < 0.05$ was considered statistically significant.

RESULTS

Uptake of RecCSP and SPZ by APCs

We first determined which APC types take up CSP and/or whole SPZ. We found that fluorescently labeled, recombinant CSP (recCSP) was taken up readily by both monocyte-derived dendritic cells (MoDCs) as well as M0 monocyte-derived macrophages (MoMφs) *in vitro* in a concentration dependent manner (Figure 2A). In contrast, *Plasmodium berghei* (Pb) SPZ were preferentially phagocytized by MoMφs. Whereas only about one percent (mean 0.86%; range 0.62-1.36) of MoDCs phagocytized mCherry-expressing Pb SPZ, on average four percent (range 0.78-10.2%) of MoMφs took up whole SPZ *in vitro* (Figure 2B, Movie S1). Opsonization of SPZ using an anti-CSP antibody increased their uptake by MoMφs five-fold (mean 20%; range 9.5-37.5), whereas uptake by MoDCs was unaffected. Flow cytometric analysis of *Plasmodium falciparum* (Pf) uptake was not feasible due to the low fluorescent signal of the transgenic Pf lines used in comparison to the high autofluorescence of human APCs (Supplementary figure S1). Therefore, we quantified Pf uptake by confocal microscopy. Similarly, Pf SPZ were phagocytized by MoMφs, but not MoDCs (Figure 2C; MoMφs: mean 3.2%, range 0-9.7%; MoDCs: mean 0.76%, range 0-5.1%; Movie S1 and Movie S2) and uptake by MoMφ, but not MoDCs, increased 3.6 fold after parasite opsonization (mean 11.6%, range 2-29.5%). SPZ were clearly identified on their morphology and fluorescence and membrane staining of APCs allowed us to determine their intracellular location (Figure 2D). In addition, video microscopy revealed that uptake of SPZ by MoMφs is an active phagocytic process and not the result of SPZ invasion of the cells (Movie S1). Furthermore, formaldehyde fixation of non-opsonized SPZ, which renders SPZ immobile and incapable of invading, did not decrease uptake of SPZ by MoMφs, suggesting that increased uptake of opsonized-SPZ by MoMφs is not due to immobilization or a result of active APC invasion.

MoDCs and MoMφs do not respond to recCSP stimulation

Having shown that MoDCs readily take up recombinant Pf CSP (recCSP), but almost no SPZ, we next investigated their phenotypic and functional response to the most abundant surface protein of SPZ: CSP (the main component of RTS,S vaccine, which is excreted upon SPZ migration). We measured no changes in the surface expression of activation markers CD80, CD86 and CD25; the endocytic receptors CD206 (Mannose receptor) and CD209 (DC-SIGN) or the regulatory markers CD200R, PD-L1 and Immunoglobulin-like transcript 3 (ILT3; Figure 3A) at a recCSP dose of 250ng/ml. Increasing the dosage of recCSP had no effect (2.5-2500 ng/ml; Supplementary figure S2A) nor did recCSP modulate LPS-induced activation of MoDCs (Supplementary figure S2B). In line with this, co-culturing of LPS-matured, recCSP-stimulated MoDCs with

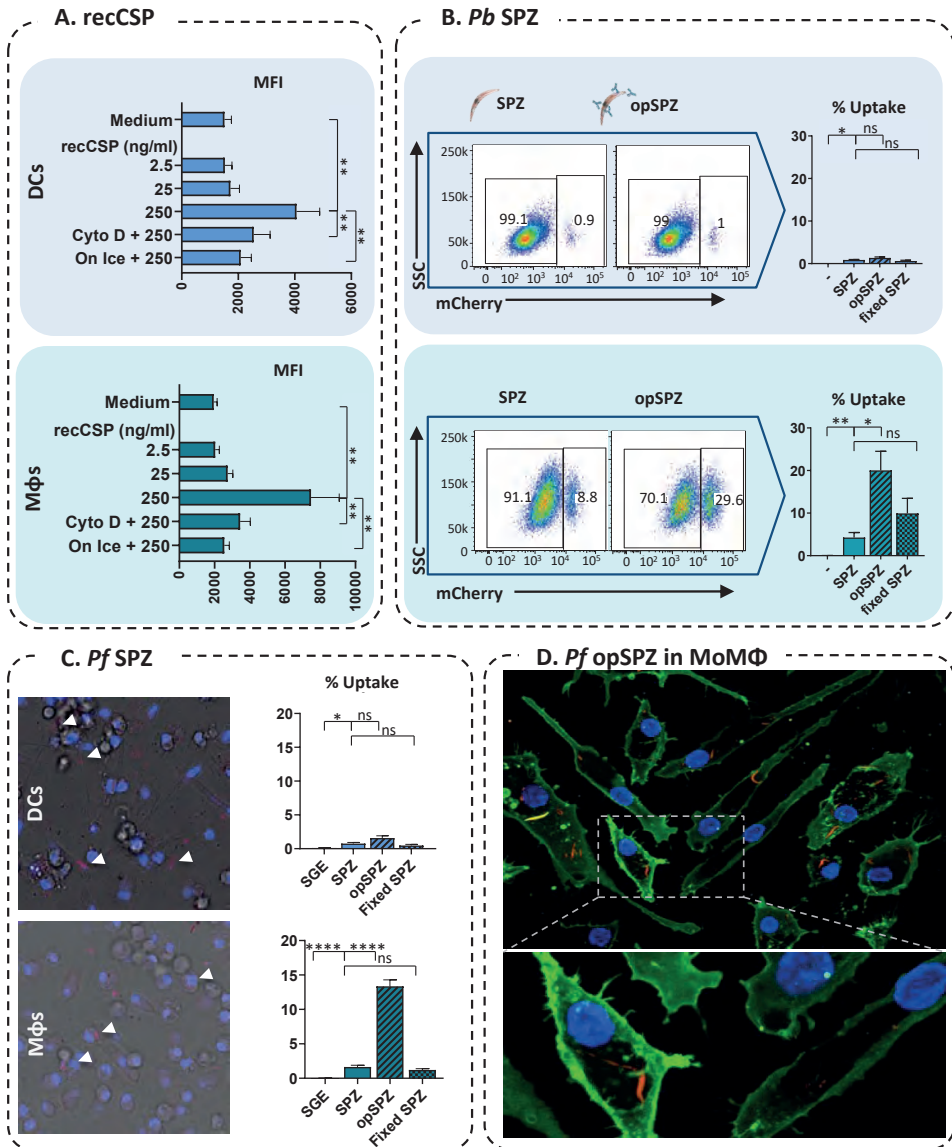


Figure 2. Uptake of recCSP and whole SPZ by MoDCs and MoMφs. **A.** Quantification of fluorescent recCSP uptake (ng/ml) in MoDCs (top) and MoMφs (bottom); MFI: median fluorescence intensity. N=2, 4 donors. **B.** Uptake of whole *Pb* sporozoites by MoDCs and MoMφs. Representative flow cytometry plots showing mCherry expression in MoDCs (top) and MoMφs (bottom) after stimulation with SPZ or opsonized SPZ using an anti-CSP antibody (opSPZ). Quantification of SPZ uptake (% of mCherry⁺ APCs) by flow cytometry. N=3, 9 donors (fixed SPZ: 4 donors). **C.** Uptake of whole *Pf* sporozoites by MoDCs and MoMφs quantified by confocal microscopy. N=2, 4 donors, on average 1150 MoMacs and 550 MoDCs per donor per condition. **D.** Confocal microscopy image of *Pf*SPZ uptake by MoMφs.

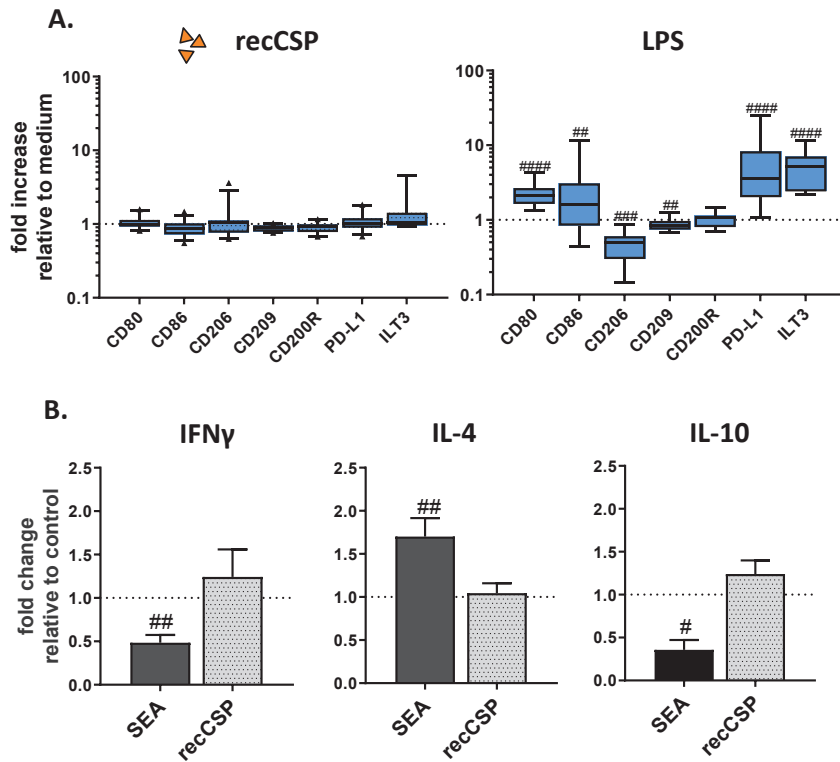


Figure 3. MoDC responses to recCSP. **A.** RecCSP stimulation (250 ng/ml) does not alter MoDC surface markers. Responses to control LPS are shown on the right. Data shown as fold changes compared to medium stimulated control. N=8, 10-19 donors per marker. **B.** CD4⁺ T cell polarization after recCSP stimulation. RecCSP stimulation of LPS-matured MoDCs does not polarize naïve T cells towards a Th1 (IFN γ), Th2 (IL-4; both measured by intracellular staining, N=2, 6 donors) or Treg (IL-10; measured by ELISA after CD3/28 restimulation, N=2, 4 donors) response. Soluble Schistosome Egg Antigen (SEA) used as a Th2 inducing control. Data shown relative to LPS-matured MoDC control. A and B: # indicates comparison to control. #: P<0.05, ##: P<0.005, ###: P<0.0005 and ####: P<0.0001

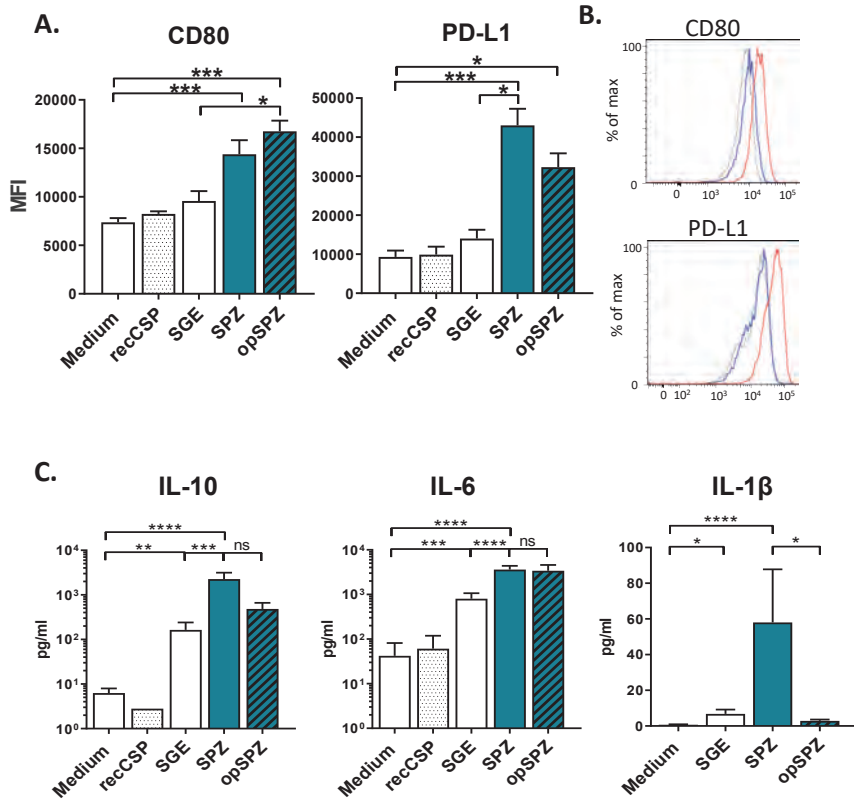


Figure 4. MoMφ responses to (opsonized) Pf SPZ. A. SPZ and opSPZ upregulate activation marker CD80 as well as regulatory marker PD-L1. Analysis using one way ANOVA. N=9, at least 10 donors per marker. **B.** Representative histograms of CD80 and PD-L1 surface marker expression. Medium stimulated MoMφs in grey, SGE stimulated MoMφs in blue and SPZ stimulated MoMφs in red. **C.** MoMφs produce IL-10, IL-6 and IL1β in response to (op)SPZ stimulation. Analysis using one way ANOVA on log transformed data. *: P<0.05, **: P<0.005, ***: P<0.0005 and ****: P<0.0001, ns= not significant. IL-10: N=8, 25 donors; IL-6: N=5, 17 donors; IL1β: N=3, 7 donors

naïve CD4⁺ T cells did not result in polarization of T cells to a Th1 (IFN γ), Th2 (IL-4) or regulatory (IL-10) response (Figure 3B). Similarly, to the MoDCs, MoM ϕ s did not change their phenotype upon recCSP stimulation (Figure 4; Supplementary figure S4). Overall, these data show that MoDCs and MoM ϕ s do not respond phenotypically to recCSP stimulation and uptake.

Uptake of *Pf* sporozoites activates MoM ϕ s *in vitro*

Next, we tested APC responses to whole *Pf* SPZ stimulation. SPZ stimulation of MoDCs did not result in upregulation of surface activation markers and did not alter their capacity to prime effector CD4⁺ T cells or regulatory T cells (Supplementary figure S3), indicating that SPZ stimulation of MoDCs has no effect on their phenotype or function.

In contrast, SPZ stimulation of MoM ϕ s resulted in an increased surface expression of activation markers (CD80 and CD25) as well as regulatory markers (PD-L1 and ILT3), which was not seen with uninfected salivary gland extract (SGE) alone (Figure 4A; Supplementary figure S4). This phenotype of mixed pro- and anti-inflammatory surface marker expression was mirrored in cytokine production, where we saw approximately 5-fold increases of pro-inflammatory IL-6 and IL-1 β , together with a more pronounced 12-fold increase in hallmark regulatory cytokine IL-10 upon stimulation with SPZ. This enhanced production was not seen in MoM ϕ s stimulated with recCSP and was much lower with SGE alone (Figure 4B; Supplementary figure S5). Opsonization of SPZ did not significantly influence their surface marker responses, although there was a trend towards increased activation and a concomitant decrease in regulatory markers (Figure 4A). Interestingly, opsonization of SPZ abrogated IL-1 β production by MoM ϕ s (Figure 4B), although titers of IL-1 β were significantly lower than those of IL-6 and IL-10. Overall, these data show MoM ϕ s are activated by *Pf* sporozoite stimulation, resulting in a mixed pro- and anti-inflammatory phenotype.

MoM ϕ s display decreased motility after SPZ stimulation

The combined increased surface expression of activation markers as well as regulatory markers on macrophages has been described previously in tumor immunology, where they are referred to as regulatory macrophages, or Mregs. Tumor-associated macrophages have been shown to exhibit decreased motility upon exposure to cancer cell products⁵³. To investigate whether SPZ have a similar effect on MoM ϕ s, we performed a wound closing assay in which MoM ϕ s were allowed to migrate for 40 hours after disturbance of their monolayer in a cell culture plate (“wounding” by scratch). As a control we used Cytochalasin D (Cyto D), which blocks migration by inhibition of actin polymerization⁵¹. MoM ϕ s stimulated with SPZ displayed reduced wound closure at 40

hours compared to MoMφs stimulated with SGE alone (Figure 5B and C; $p < 0.0001$; Supplementary figure S6). Therefore, SPZ stimulated MoMφs seem to share multiple characteristics with tumor Mregs, including the molecules they express on the surface and their motility.

SPZ-stimulated MoMφs decrease IFN γ production during DC-mediated CD8 $^+$ T cell priming

Next, we explored whether the regulatory phenotype of SPZ-stimulated MoMφs allows them to suppress CD8 $^+$ T cell responses. MoMφs stimulated with SPZ, SGE alone or LPS were co-cultured with an antigen-specific CD8 $^+$ T cell clone in the presence of antigen-loaded MoDCs (Figure 6A). Intracellular cytokine analysis revealed that fewer CD8 $^+$ T cells produced IFN γ in the presence of MoMφs stimulated with SPZ (mean reduction 21% compared to SGE; $P < 0.05$) and produced less perforin (Figure 6B and Supplementary figure S7; mean reduction 9% compared to SGE; $p = 0.01$). Opsonized SPZ were not as effective in reducing IFN γ production by CD8 $^+$ T cells as compared to un-opsonized SPZ (Figure 6B and Supplementary figure S7; mean reduction 6% IFN γ compared to SGE) but were equally capable of reducing perforin responses. We found no changes in granzyme A and B production by the T cell clone in the presence of MoMφs stimulated with SPZ (Supplementary figure S7). Together, these data confirm a modest functional regulatory potential of SPZ-stimulated MoMφs.

Next we investigated whether IL-10 or PD-L1 play a role in the induction of the immunosuppressive capacity of SPZ stimulated MoMφs by blocking the IL-10 or PD/PD-L1 pathway using antibodies against IL-10 and IL-10 receptor (IL10R) or PD-1 respectively. Blocking of the IL-10 or PD-L1 pathway did not restore the percentage of CD8 T cells producing IFN γ (Figure 7A). However, blocking IL-10 and IL-10R, but not PD-1, restored the mean fluorescence intensity (MFI) of IFN γ -producing CD8 $^+$ T cells, indicating that the suppression of CD8 $^+$ T cell responses by MoMφs is at least partially IL-10 dependent (Figure 7B).

Human dermal APCs responses to SPZ mimic MoMφ responses.

To confirm that human skin APCs respond in a similar fashion as their monocyte-derived counterparts, we stimulated primary dermal APCs obtained from human skin explants with *Pb* and *Pf* SPZ or SGE *in vitro*. Approximately 6% (range 1.4-10.7) of primary HLA-DR $^+$, CD11c $^+$ total dermal APCs (this population contains both dermal Mφ and DC populations as surface marker plasticity impairs distinguishing dermal Mφ from dermal DCs) took up *Pb* SPZ. When SPZ were opsonized, the uptake increased five-fold to 33%

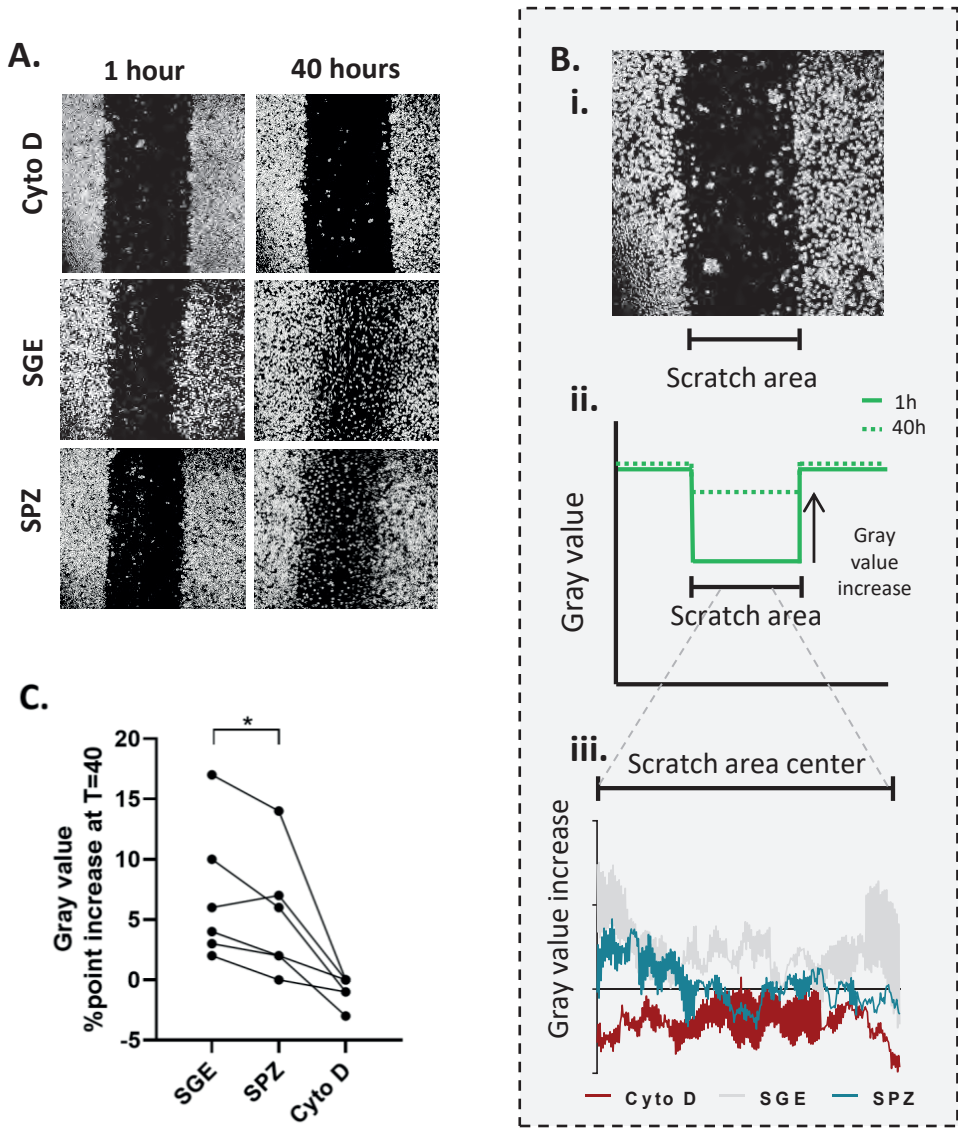


Figure 5. MoMφ migration upon Pf SPZ stimulation. **A.** Representative examples of wound closing assay. The images show wells containing MoMφs (grey) with a central “wound” (black), where MoMφs have been scratched away. After 40 hours, blurring of the scratch indicates migrated MoMφs. Cytochalasin D (Cyto D) blocks all cell migration as control. **B.** i. example of a scratch with indication of scratch area to be analysed. ii. Schematic of a surface plot of entire microscopic image. An increase in the gray value is seen over the scratch area over time, as cells fill up the wound. iii. Difference in gray value between T=40 and T=1 over the scratch area center, where an increased difference reflects higher migration. Lines indicate the mean of three independent experiments including six donors.

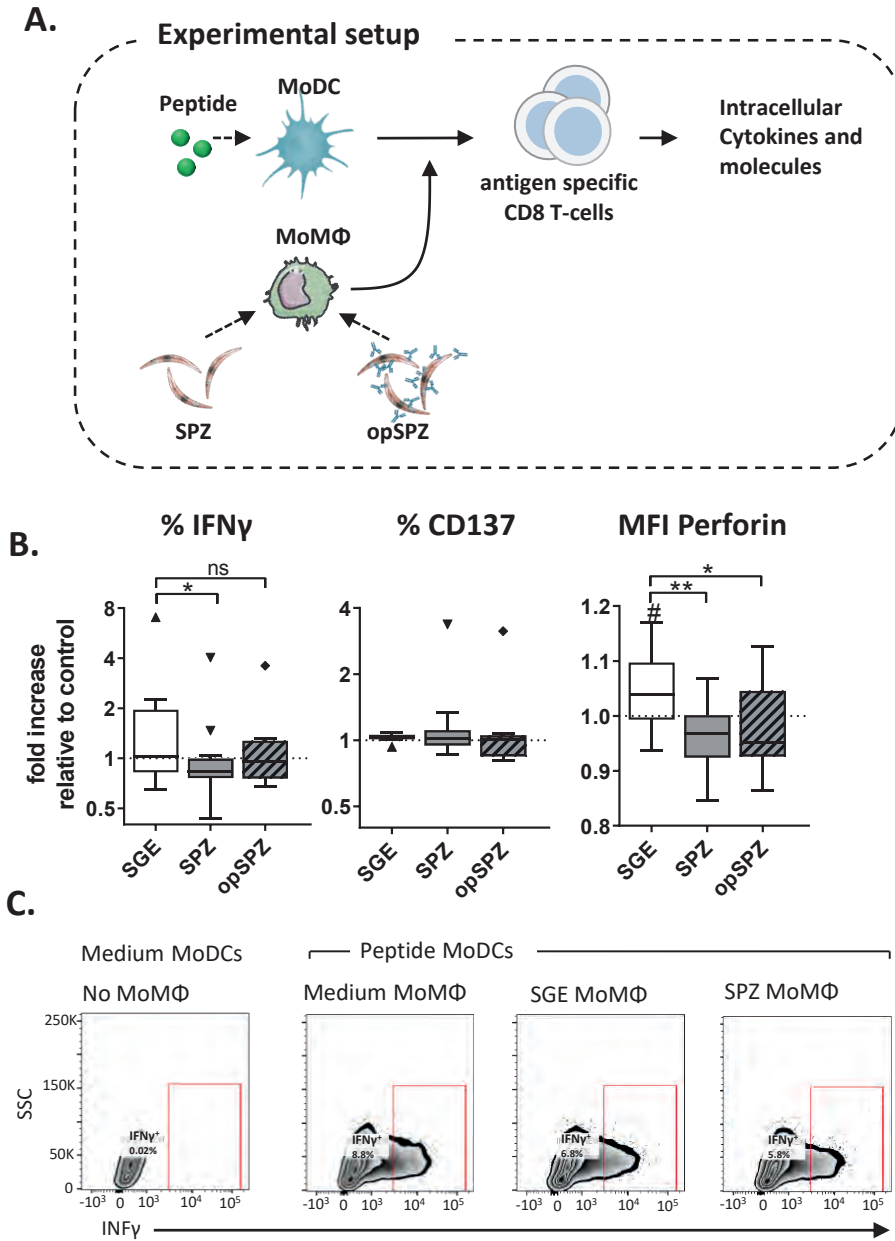


Figure 6. Immune suppression by Pf SPZ stimulated macrophages. **A.** Experimental setup. Peptide stimulated MoDCs are co-cultured with a peptide specific CD8+ T cell clone in the presence or absence of parasite or control stimulated MoM Φ s (information in materials and methods). **B.** CD8+ cell phenotype after overnight co-culture with MoDCs and MoM Φ s. Intracellular IFN γ , activation marker CD137 and Perforin expression. Analysis using Wilcoxon test, N=4, at least 6 donors. #: P<0.05 compared to medium control. *: P<0.05, **: P<0.005. **C.** Representative cytometry plots showing percentage of IFN γ + CD8+ T cells.

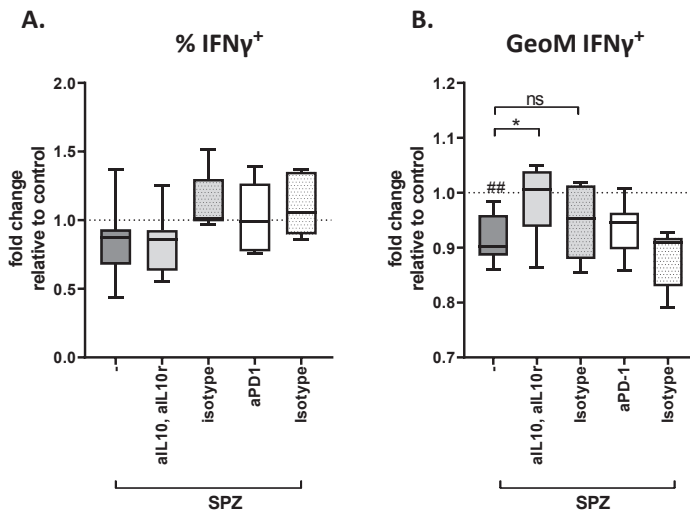


Figure 7. Blocking the IL10 pathway partially restores IFN γ production in IFN γ ⁺ CD8⁺ T cells. **A. Blocking IL-10 and its receptor, or PD-1 does not restore the percentage of IFN γ producing CD8 T cells. Data shows % of IFN γ ⁺ antigen specific CD8⁺ T cells after co-culture with antigen pulsed MoDCs in the presence of macrophages stimulated with Pf SPZ alone (-) or Pf SPZ and anti IL-10(R) or PD-1 antibodies or their isotype controls. **B.** Blocking IL-10 and its receptor, but not PD-1 restores the levels of IFN γ produced by IFN γ ⁺ CD8 T cells (data shown in Mean Fluorescent intensity compared to medium control). # indicates comparison to control (standardized to 1). ##: $p < 0.01$, *: $p < 0.05$**

(range 11.4-61.7), mimicking MoM ϕ s responses to SPZ opsonization (Figure 8A i). In line with this, confocal quantification of *Pf* SPZ uptake in dermal APCs showed 0.7% uptake of *Pf* SPZ on average. This increased to 15% after opsonization of SPZ (Figure 8Bi).

In addition, corroborating MoM ϕ responses, phenotypic responses of dermal APCs after uptake of *Pb* SPZ was characterized by gating on SPZ⁺ cells and revealed increased surface PD-L1 as well as CD80 expression upon phagocytosis of *Pb* parasites (Figure 8A ii). Total dermal APC surface PD-L1 and CD80 did not show significant differences between SGE and *Pf* SPZ stimulation (Supplementary figure S8). Flow cytometric detection of SPZ uptake was not technically feasible with *Pf*, therefore we analyzed the supernatant of these cells for IL-10 and IL-1 β production. Paralleling MoM ϕ responses, IL-10 and IL-1 β production increased upon *Pf* SPZ stimulation of dermal APCs.

Collectively, these data indicate that dermal primary APC responses resemble MoM ϕ responses to SPZ and indicate a regulatory role upon encounter with SPZ.

DISCUSSION

Here we show that malaria SPZ induce M ϕ s which express PD-L1, produce IL-10 and show reduced motility. In addition, these M ϕ s suppress IFN γ and perforin production by memory CD8⁺T cells. This early-onset suppression of host defenses by SPZ at the skin stage may help explain why immunity to sporozoites is difficult to induce and can be highly relevant for improving next generation CSP-based or attenuated SPZ vaccines.

Interestingly, these M ϕ s retained their ability to produce IL-6 and express CD80. The production of regulatory IL-10 and the expression of inhibitory PD-L1 and/or PD-L2⁵⁴, despite their retained ability to produce proinflammatory cytokines and express high levels of co-stimulatory molecules⁵⁵ is characteristic of regulatory M ϕ s (Mregs). Mregs have primarily been described in the physiological context of tissue repair⁵⁴ and pathological context of cancer⁵⁶, where they promote wound healing and tumor outgrowth respectively. However, in chronic parasitic diseases such as leishmania⁵⁷ and trypanosoma⁵⁸ as well as helminths^{37,59,60} these monocytes/macrophages have also been suggested to play a role in immune evasion. With regard to helminths, we have previously shown that *Schistosoma mansoni*, the causative agent of Schistosomiasis and also a skin-penetrating parasite, induces a similar early dermal induction of immune regulation, characterized by PD-L1 expressing and IL-10 producing dermal APCs³⁵. The finding that Mregs could play a role in immune evasion by malaria in addition to other parasitic diseases provides compelling support for the evaluation of checkpoint inhibitors in these chronic infections⁶¹.

Our data did not show any phenotypic changes of both MoDCs and MoM ϕ s in response to recCSP. CSP is the most abundant SPZ antigen in the pre-erythrocytic stage of malaria and has been shown to be sufficient for inducing proliferation of CSP-specific CD8⁺T cells *in vitro*⁶².

We used a commercially available recCSP which contains a large part of the repeat region (B-cell epitopes), the full C terminal containing the majority of known T cell epitopes and the glycosylphosphatidylinositol (GPI) anchor sequence^{63,64}, similar to the CSP protein sequence used in the CSP-based malaria vaccine RTS,S. These recombinant CSPs lack the native parasite GPI anchor which is a known Toll-like receptor (TLR)-2/4 activating pathogen-associated molecular pattern (PAMP) in protozoa⁶⁵ and plays a role in blood stage malaria⁶⁶. We conclude that despite containing the B and T cell epitope regions and the GPI anchor sequence, recCSP alone is not sufficient to trigger an innate immune response. This may explain why strong adjuvants such as GlaxoSmithsKline's Adjuvant System are needed to induce sufficient antibody levels in the CSP-based

malaria vaccine RTS,S⁶⁷. In the setting of natural infection, danger associated molecular patterns (DAMPs) introduced via cell damage by mosquito probing and/or parasite migration through the skin could provide necessary stimulation of APCs to induce activation. Alternatively, the low immunogenic potential of the antigen alone may be critical to the survival of the parasite as it would initiate T cell anergy in the absence of co-stimulation, or the induction of regulatory T cells.

In addition to antibody responses, CD8⁺ T cells play a central role in the protection against pre-erythrocytic stages of malaria^{8,68,69}. Clinical trials have shown that sterile protection largely correlates with total numbers of IFN γ producing CD8⁺ T cells⁷. Next to IFN γ , other cytotoxic molecules produced by CD8⁺ T cells such as perforin and granzymes have also been associated with protection⁷⁰. We show that SPZ-stimulated MoM ϕ s can suppress IFN γ and perforin, but not granzyme production by MoDC-activated CD8⁺ T cells, underlining the potentially detrimental effect of regulatory M ϕ s on immune responses in the context of attenuated SPZ vaccines. Because blocking IL-10 and its receptor only partially restored IFN γ production, additional interactions between macrophages, dendritic cells and CD8⁺ T cells are likely to add to the observed immune-suppressive effect.

In order to translate our findings to the human skin setting, we used primary human dermal APCs alongside monocyte-derived APCs and showed that the primary cells exhibit a similar phenotype compared to MoM ϕ s. Where the priming of CD8⁺ T cells subsequently takes place after attenuated SPZ vaccination is an ongoing matter of debate^{71,72}. Given the nature of macrophages and a further reduced motility, it seems unlikely that SPZ-induced regulatory macrophages migrate to regional lymph nodes. Potentially, regulation could be established directly in peripheral tissues, by affecting dermal-resident T cells or T cells recruited to the site of infection. Alternatively, regulatory signals may be conveyed to dermal DCs⁷³, thereby influencing the priming of CD8⁺ T cells. Lastly, SPZ have been shown to migrate out of the skin site to local lymph nodes, where they could induce a similar tolerogenic response by LN-resident macrophages⁷⁴; similar mechanisms could potentially be exploited in liver tissue via liver-resident macrophages, Kupffer cells⁷⁵. A translation to *in vivo* models, such as controlled human infections^{76,77}, or the use of primate models for malaria (with skin more comparable to that of humans) will allow for a more detailed dissection of the site of immune cell interaction and cell types involved.

We revealed a dual effect of SPZ antibodies on APC responses: As non-opsonized SPZ induced a regulatory phenotype in APCs, boosting the efficiency of SPZ phagocytosis could result in an increased number of Mregs. However, phenotypic analysis showed

a trend towards decreased regulatory markers when SPZ were pre-incubated with a monoclonal anti-CSP antibody and opsonization also restored CD8⁺ T cell IFN γ production. These findings are in line with previous reports that Fc gamma receptor (Fc γ R) stimulation promotes proinflammatory responses^{78,79}. Whether similar effects would occur in the presence of polyclonal anti-SPZ antibodies remains to be investigated. How this would ultimately translate to the *in vivo* situation is unclear, as factors such as reduced SPZ motility play an important role in the local tissue density of M ϕ s that have interacted with SPZ⁸⁰, as well as the local immune (regulatory) environment. Understanding the interplay between antibodies and ensuing immune responses has important implications for vaccine development. For example, pre-existing anti-CSP antibodies^{81,82} in endemic populations may neutralize vaccine SPZ through opsonization and increased phagocytosis. However, anti-CSP antibodies can be used as a surrogate of protection in vaccine studies involving RTS/S^{83,84}. Taken together, this underlines the need to fully appreciate the net effect of natural and vaccine boosting in pre-erythrocytic vaccine strategies.

To date, dermal immune responses to malaria and vaccine candidates are wholly uncharacterized in humans, yet the development of an effective live pre-erythrocytic malaria vaccine arguably is crucially dependent on our understanding of these initial parasite-host interactions. Whether the relatively minor differences in CD8 T cell function have an impact on overall immunity to malaria during natural infection, where SPZ concentration in the skin is much lower than in our *in vitro* assays, remains to be determined. With this study, we aimed to elucidate the critical initial steps of human skin stage malaria. Such insights into the immune regulatory properties of SPZ are a pivotal first step in broadening our understanding of pre-erythrocytic natural immunity and the pitfalls of intradermal vaccination-induced immunity.

SUPPLEMENTARY NOTES

Author Contributions Statement: The methodology was developed by BW, LP, BE, BF, EJ and MR. Experiments were performed and interpreted by BW, LP, RS, EB, MG, HG, ND, CK, ML, SC, BF and MR and supervised by HS, BE, BF and MR. BW and MR drafted the manuscript.

Acknowledgments: The authors would like to thank G.J. van Gemert of Radboud UMC, Nijmegen for supplying us with the *Plasmodium falciparum* infected mosquitoes, and Prof. G. Corradin of the university of Lausanne, Switzerland for supplying us with the antigen-specific CD8 T cell line. We would also like to thank Krista van Meijgaarden of the LUMC department of infectious diseases Leiden, for her help with establishing the CD8 co-culture assay, Toni van Capel of the AMC, Amsterdam for assisting with the human skin assays as well as Jai Ramesar and Chris Janse of the LUMC department of parasitology for their technical support.

Ethics statement: All animal experiments of this study were granted with a license by Competent Authority after an advice on the ethical evaluation by the Animal Experiments Committee Leiden (AVD1160020173304-01). All experiments were performed in accordance with the Experiments on Animals Act (Wod, 2014), the applicable legislation in the Netherlands and the European guidelines (EU directive no. 2010/63/EU) regarding the protection of animals used for scientific purposes. All experiments were executed in a licensed establishment for use of experimental animals (LUMC).

The use of human skin explants (obtained as waste material after abdominal reduction surgery) for this research was approved by the Commission Medical Ethics (CME) of the LUMC, Leiden. Approval number CME: B18-009.

Conflict of Interest Statement: The authors declare no conflict of interest.

REFERENCES

- 1 [Internet] WHO: Geneva Switzerland. 19 November 2018, World Malaria report 2018. <https://www.who.int/malaria/media/world-malaria-report-2018/en/>.
- 2 Doolan, D. L., Dobano, C. & Baird, J. K. Acquired immunity to malaria. *Clin Microbiol Rev* **22**, 13-36, Table of Contents, doi:10.1128/CMR.00025-08 (2009).
- 3 Graves, P. & Gelband, H. Vaccines for preventing malaria (pre-erythrocytic). *Cochrane Database Syst Rev*, CD006198, doi:10.1002/14651858.CD006198 (2006).
- 4 Rts, S. C. T. P. *et al.* A phase 3 trial of RTS,S/AS01 malaria vaccine in African infants. *N Engl J Med* **367**, 2284-2295, doi:10.1056/NEJMoa1208394 (2012).
- 5 Seder, R. A. *et al.* Protection against malaria by intravenous immunization with a nonreplicating sporozoite vaccine. *Science* **341**, 1359-1365, doi:10.1126/science.1241800 (2013).
- 6 Ishizuka, A. S. *et al.* Protection against malaria at 1 year and immune correlates following PfSPZ vaccination. *Nat Med* **22**, 614-623, doi:10.1038/nm.4110 (2016).
- 7 Epstein, J. E. *et al.* Live attenuated malaria vaccine designed to protect through hepatic CD8(+) T cell immunity. *Science* **334**, 475-480, doi:10.1126/science.1211548 (2011).
- 8 Weiss, W. R. & Jiang, C. G. Protective CD8+ T lymphocytes in primates immunized with malaria sporozoites. *PLoS One* **7**, e31247, doi:10.1371/journal.pone.0031247 (2012).
- 9 Vanderberg, J. P. & Frevert, U. Intravital microscopy demonstrating antibody-mediated immobilisation of Plasmodium berghei sporozoites injected into skin by mosquitoes. *Int J Parasitol* **34**, 991-996, doi:10.1016/j.ijpara.2004.05.005 (2004).
- 10 Flores-Garcia, Y. *et al.* Antibody-Mediated Protection against Plasmodium Sporozoites Begins at the Dermal Inoculation Site. *mBio* **9**, doi:10.1128/mBio.02194-18 (2018).
- 11 Aliprandini, E. *et al.* Cytotoxic anti-circumsporozoite antibodies target malaria sporozoites in the host skin. *Nat Microbiol* **3**, 1224-1233, doi:10.1038/s41564-018-0254-z (2018).
- 12 Haeberlein, S. *et al.* Protective immunity differs between routes of administration of attenuated malaria parasites independent of parasite liver load. *Sci Rep* **7**, 10372, doi:10.1038/s41598-017-10480-1 (2017).
- 13 Epstein, J. E. *et al.* Protection against Plasmodium falciparum malaria by PfSPZ Vaccine. *JCI Insight* **2**, e89154, doi:10.1172/jci.insight.89154 (2017).
- 14 Bastiaens, G. J. *et al.* Safety, Immunogenicity, and Protective Efficacy of Intradermal Immunization with Aseptic, Purified, Cryopreserved Plasmodium falciparum Sporozoites in Volunteers Under Chloroquine Prophylaxis: A Randomized Controlled Trial. *Am J Trop Med Hyg* **94**, 663-673, doi:10.4269/ajtmh.15-0621 (2016).
- 15 Amino, R. *et al.* Host cell traversal is important for progression of the malaria parasite through the dermis to the liver. *Cell Host Microbe* **3**, 88-96, doi:10.1016/j.chom.2007.12.007 (2008).
- 16 Amino, R. *et al.* Quantitative imaging of Plasmodium transmission from mosquito to mammal. *Nat Med* **12**, 220-224, doi:10.1038/nm1350 (2006).
- 17 Yamauchi, L. M., Coppi, A., Snounou, G. & Sinnis, P. Plasmodium sporozoites trickle out of the injection site. *Cell Microbiol* **9**, 1215-1222, doi:10.1111/j.1462-5822.2006.00861.x (2007).
- 18 Hopp, C. S. *et al.* Longitudinal analysis of Plasmodium sporozoite motility in the dermis reveals component of blood vessel recognition. *Elife* **4**, doi:10.7554/eLife.07789 (2015).
- 19 Mac-Daniel, L. *et al.* Local immune response to injection of Plasmodium sporozoites into the

- skin. *J Immunol* **193**, 1246-1257, doi:10.4049/jimmunol.1302669 (2014).
- 20 Levin, C., Perrin, H. & Combadiere, B. Tailored immunity by skin antigen-presenting cells. *Hum Vaccin Immunother* **11**, 27-36, doi:10.4161/hv.34299 (2015).
- 21 Kashem, S. W., Haniffa, M. & Kaplan, D. H. Antigen-Presenting Cells in the Skin. *Annu Rev Immunol* **35**, 469-499, doi:10.1146/annurev-immunol-051116-052215 (2017).
- 22 Di Meglio, P., Perera, G. K. & Nestle, F. O. The multitasking organ: recent insights into skin immune function. *Immunity* **35**, 857-869, doi:10.1016/j.immuni.2011.12.003 (2011).
- 23 Seneschal, J., Clark, R. A., Gehad, A., Baecher-Allan, C. M. & Kupper, T. S. Human epidermal Langerhans cells maintain immune homeostasis in skin by activating skin resident regulatory T cells. *Immunity* **36**, 873-884, doi:10.1016/j.immuni.2012.03.018 (2012).
- 24 Buckwalter, M. R. & Albert, M. L. Orchestration of the immune response by dendritic cells. *Curr Biol* **19**, R355-361, doi:10.1016/j.cub.2009.03.012 (2009).
- 25 da Silva, H. B. *et al.* Early skin immunological disturbance after Plasmodium-infected mosquito bites. *Cell Immunol* **277**, 22-32, doi:10.1016/j.cellimm.2012.06.003 (2012).
- 26 Keir, M. E., Butte, M. J., Freeman, G. J. & Sharpe, A. H. PD-1 and its ligands in tolerance and immunity. *Annu Rev Immunol* **26**, 677-704, doi:10.1146/annurev-immunol.26.021607.090331 (2008).
- 27 Keir, M. E. *et al.* Tissue expression of PD-L1 mediates peripheral T cell tolerance. *J Exp Med* **203**, 883-895, doi:10.1084/jem.20051776 (2006).
- 28 Okazaki, T. & Honjo, T. The PD-1-PD-L pathway in immunological tolerance. *Trends Immunol* **27**, 195-201, doi:10.1016/j.it.2006.02.001 (2006).
- 29 Brown, J. A. *et al.* Blockade of programmed death-1 ligands on dendritic cells enhances T cell activation and cytokine production. *J Immunol* **170**, 1257-1266 (2003).
- 30 Carreno, B. M. & Collins, M. The B7 family of ligands and its receptors: new pathways for costimulation and inhibition of immune responses. *Annu Rev Immunol* **20**, 29-53, doi:10.1146/annurev-immunol.20.091101.091806 (2002).
- 31 Dong, H. & Chen, L. B7-H1 pathway and its role in the evasion of tumor immunity. *J Mol Med (Berl)* **81**, 281-287, doi:10.1007/s00109-003-0430-2 (2003).
- 32 Day, C. L. *et al.* PD-1 expression on HIV-specific T cells is associated with T-cell exhaustion and disease progression. *Nature* **443**, 350-354, doi:10.1038/nature05115 (2006).
- 33 Huang, X. *et al.* PD-1 expression by macrophages plays a pathologic role in altering microbial clearance and the innate inflammatory response to sepsis. *Proc Natl Acad Sci U S A* **106**, 6303-6308, doi:10.1073/pnas.0809422106 (2009).
- 34 Horne-Debets, J. M. *et al.* PD-1 dependent exhaustion of CD8+ T cells drives chronic malaria. *Cell Rep* **5**, 1204-1213, doi:10.1016/j.celrep.2013.11.002 (2013).
- 35 Winkel, B. M. F. *et al.* Early Induction of Human Regulatory Dermal Antigen Presenting Cells by Skin-Penetrating Schistosoma Mansoni Cercariae. *Front Immunol* **9**, 2510, doi:10.3389/fimmu.2018.02510 (2018).
- 36 Xiao, J., Li, Y., Yolken, R. H. & Viscidi, R. P. PD-1 immune checkpoint blockade promotes brain leukocyte infiltration and diminishes cyst burden in a mouse model of Toxoplasma infection. *J Neuroimmunol* **319**, 55-62, doi:10.1016/j.jneuroim.2018.03.013 (2018).
- 37 Narasimhan, P. B. *et al.* Similarities and differences between helminth parasites and cancer cell lines in shaping human monocytes: Insights into parallel mechanisms of immune evasion. *PLoS Negl Trop Dis* **12**, e0006404, doi:10.1371/journal.pntd.0006404 (2018).
- 38 Ilingworth, J. *et al.* Chronic exposure to Plasmodium falciparum is associated with phenotypic evidence of B and T cell

- exhaustion. *J Immunol* **190**, 1038-1047, doi:10.4049/jimmunol.1202438 (2013).
- 39 Karunarathne, D. S. *et al.* Programmed Death-1 Ligand 2-Mediated Regulation of the PD-L1 to PD-1 Axis Is Essential for Establishing CD4(+) T Cell Immunity. *Immunity* **45**, 333-345, doi:10.1016/j.immuni.2016.07.017 (2016).
- 40 Treuting, P. M., Dintzis, S. M. & Montine, K. S. Comparative Anatomy and Histology: A Mouse and Human Atlas. *Academic Press, Elsevier Chapter 24*, 433-441 (2017).
- 41 Haniffa, M., Collin, M. & Ginhoux, F. Ontogeny and functional specialization of dendritic cells in human and mouse. *Adv Immunol* **120**, 1-49, doi:10.1016/B978-0-12-417028-5.00001-6 (2013).
- 42 Mestas, J. & Hughes, C. C. Of mice and not men: differences between mouse and human immunology. *J Immunol* **172**, 2731-2738 (2004).
- 43 Gueirard, P. *et al.* Development of the malaria parasite in the skin of the mammalian host. *Proc Natl Acad Sci U S A* **107**, 18640-18645, doi:10.1073/pnas.1009346107 (2010).
- 44 Prado, M. *et al.* Long-term live imaging reveals cytosolic immune responses of host hepatocytes against Plasmodium infection and parasite escape mechanisms. *Autophagy* **11**, 1561-1579, doi:10.1080/15548627.2015.1067361 (2015).
- 45 Kooij, T. W., Rauch, M. M. & Matuschewski, K. Expansion of experimental genetics approaches for Plasmodium berghei with versatile transfection vectors. *Mol Biochem Parasitol* **185**, 19-26, doi:10.1016/j.molbiopara.2012.06.001 (2012).
- 46 Sinden, R. E. Infection of mosquitoes with rodent malaria. *The Molecular Biology of Insect Disease Vectors: a Methods Manual* (ed. **J. M. Crampton, C. B. Beard and C. Louis**), pp. 67-91 (1997).
- 47 Ponnudurai, T., Leeuwenberg, A. D. & Meuwissen, J. H. Chloroquine sensitivity of isolates of Plasmodium falciparum adapted to in vitro culture. *Trop Geogr Med* **33**, 50-54 (1981).
- 48 Ponnudurai, T. *et al.* Infectivity of cultured Plasmodium falciparum gametocytes to mosquitoes. *Parasitology* **98 Pt 2**, 165-173 (1989).
- 49 Hussaarts, L. *et al.* Rapamycin and omega-1: mTOR-dependent and -independent Th2 skewing by human dendritic cells. *Immunol Cell Biol* **91**, 486-489, doi:10.1038/icb.2013.31 (2013).
- 50 Tarique, A. A. *et al.* Phenotypic, functional, and plasticity features of classical and alternatively activated human macrophages. *Am J Respir Cell Mol Biol* **53**, 676-688, doi:10.1165/rcmb.2015-0012OC (2015).
- 51 Cooper, J. A. Effects of cytochalasin and phalloidin on actin. *J Cell Biol* **105**, 1473-1478 (1987).
- 52 Bonelo, A. *et al.* Generation and characterization of malaria-specific human CD8(+) lymphocyte clones: effect of natural polymorphism on T cell recognition and endogenous cognate antigen presentation by liver cells. *Eur J Immunol* **30**, 3079-3088, doi:10.1002/1521-4141(200011)30:11<3079::AID-IMMU3079>3.0.CO;2-7 (2000).
- 53 Go, A., Ryu, Y. K., Lee, J. W. & Moon, E. Y. Cell motility is decreased in macrophages activated by cancer cell-conditioned medium. *Biomol Ther (Seoul)* **21**, 481-486, doi:10.4062/biomolther.2013.076 (2013).
- 54 Wynn, T. A. & Vannella, K. M. Macrophages in Tissue Repair, Regeneration, and Fibrosis. *Immunity* **44**, 450-462, doi:10.1016/j.immuni.2016.02.015 (2016).
- 55 Mosser, D. M. & Edwards, J. P. Exploring the full spectrum of macrophage activation. *Nat Rev Immunol* **8**, 958-969, doi:10.1038/nri2448 (2008).
- 56 Noy, R. & Pollard, J. W. Tumor-associated macrophages: from mechanisms to therapy. *Immunity* **41**, 49-61, doi:10.1016/j.immuni.2014.06.010 (2014).

- 57 Miles, S. A., Conrad, S. M., Alves, R. G., Jeronimo, S. M. & Mosser, D. M. A role for IgG immune complexes during infection with the intracellular pathogen *Leishmania*. *J Exp Med* **201**, 747-754, doi:10.1084/jem.20041470 (2005).
- 58 Baetselier, P. D. *et al.* Alternative versus classical macrophage activation during experimental African trypanosomiasis. *Int J Parasitol* **31**, 575-587 (2001).
- 59 Jenkins, S. J. & Allen, J. E. Similarity and diversity in macrophage activation by nematodes, trematodes, and cestodes. *J Biomed Biotechnol* **2010**, 262609, doi:10.1155/2010/262609 (2010).
- 60 Passos, L. S. *et al.* Regulatory monocytes in helminth infections: insights from the modulation during human hookworm infection. *BMC Infect Dis* **17**, 253, doi:10.1186/s12879-017-2366-0 (2017).
- 61 Wykes, M. N. & Lewin, S. R. Immune checkpoint blockade in infectious diseases. *Nat Rev Immunol* **18**, 91-104, doi:10.1038/nri.2017.112 (2018).
- 62 Cheong, C. *et al.* Microbial stimulation fully differentiates monocytes to DC-SIGN/CD209(+) dendritic cells for immune T cell areas. *Cell* **143**, 416-429, doi:10.1016/j.cell.2010.09.039 (2010).
- 63 Heide, J., Vaughan, K. C., Sette, A., Jacobs, T. & Schulze Zur Wiesch, J. Comprehensive Review of Human *Plasmodium falciparum*-Specific CD8+ T Cell Epitopes. *Front Immunol* **10**, 397, doi:10.3389/fimmu.2019.00397 (2019).
- 64 Crompton, P. D., Pierce, S. K. & Miller, L. H. Advances and challenges in malaria vaccine development. *J Clin Invest* **120**, 4168-4178, doi:10.1172/JCI44423 (2010).
- 65 Mogensen, T. H. Pathogen recognition and inflammatory signaling in innate immune defenses. *Clin Microbiol Rev* **22**, 240-273, Table of Contents, doi:10.1128/CMR.00046-08 (2009).
- 66 Gowda, D. C. TLR-mediated cell signaling by malaria GPIs. *Trends Parasitol* **23**, 596-604, doi:10.1016/j.pt.2007.09.003 (2007).
- 67 Mata, E., Salvador, A., Igartua, M., Hernandez, R. M. & Pedraz, J. L. Malaria vaccine adjuvants: latest update and challenges in preclinical and clinical research. *Biomed Res Int* **2013**, 282913, doi:10.1155/2013/282913 (2013).
- 68 Van Braeckel-Budimir, N. & Harty, J. T. CD8 T-cell-mediated protection against liver-stage malaria: lessons from a mouse model. *Front Microbiol* **5**, 272, doi:10.3389/fmicb.2014.00272 (2014).
- 69 Ewer, K. J. *et al.* Protective CD8+ T-cell immunity to human malaria induced by chimpanzee adenovirus-MVA immunisation. *Nat Commun* **4**, 2836, doi:10.1038/ncomms3836 (2013).
- 70 Bijker, E. M. *et al.* Cytotoxic markers associate with protection against malaria in human volunteers immunized with *Plasmodium falciparum* sporozoites. *J Infect Dis* **210**, 1605-1615, doi:10.1093/infdis/jiu293 (2014).
- 71 Chakravarty, S. *et al.* CD8+ T lymphocytes protective against malaria liver stages are primed in skin-draining lymph nodes. *Nat Med* **13**, 1035-1041, doi:10.1038/nm1628 (2007).
- 72 Obeid, M. *et al.* Skin-draining lymph node priming is sufficient to induce sterile immunity against pre-erythrocytic malaria. *EMBO Mol Med* **5**, 250-263, doi:10.1002/emmm.201201677 (2013).
- 73 Mazzini, E., Massimiliano, L., Penna, G. & Rescigno, M. Oral tolerance can be established via gap junction transfer of fed antigens from CX3CR1(+) macrophages to CD103(+) dendritic cells. *Immunity* **40**, 248-261, doi:10.1016/j.immuni.2013.12.012 (2014).
- 74 Radtke, A. J. *et al.* Lymph-node resident CD8alpha+ dendritic cells capture antigens from migratory malaria sporozoites and induce CD8+ T cell responses. *PLoS Pathog* **11**, e1004637, doi:10.1371/journal.ppat.1004637 (2015).

- 75 Klotz, C. & Frevert, U. *Plasmodium yoelii* sporozoites modulate cytokine profile and induce apoptosis in murine Kupffer cells. *Int J Parasitol* **38**, 1639-1650, doi:10.1016/j.ijpara.2008.05.018 (2008).
- 76 Stanisic, D. I., McCarthy, J. S. & Good, M. F. Controlled Human Malaria Infection: Applications, Advances, and Challenges. *Infect Immun* **86**, doi:10.1128/IAI.00479-17 (2018).
- 77 Roestenberg, M. *et al.* The frontline of controlled human malaria infections: A report from the controlled human infection models Workshop in Leiden University Medical Centre 5 May 2016. *Vaccine* **35**, 7065-7069, doi:10.1016/j.vaccine.2017.10.093 (2017).
- 78 Vogelpoel, L. T., Baeten, D. L., de Jong, E. C. & den Dunnen, J. Control of cytokine production by human fc gamma receptors: implications for pathogen defense and autoimmunity. *Front Immunol* **6**, 79, doi:10.3389/fimmu.2015.00079 (2015).
- 79 Vogelpoel, L. T. *et al.* Fc gamma receptor-TLR cross-talk elicits pro-inflammatory cytokine production by human M2 macrophages. *Nat Commun* **5**, 5444, doi:10.1038/ncomms6444 (2014).
- 80 Vanderberg, J. P. Studies on the motility of *Plasmodium sporozoites*. *J Protozool* **21**, 527-537 (1974).
- 81 Kurtovic, L. *et al.* Human antibodies activate complement against *Plasmodium falciparum* sporozoites, and are associated with protection against malaria in children. *BMC Med* **16**, 61, doi:10.1186/s12916-018-1054-2 (2018).
- 82 John, C. C. *et al.* Antibodies to pre-erythrocytic *Plasmodium falciparum* antigens and risk of clinical malaria in Kenyan children. *J Infect Dis* **197**, 519-526, doi:10.1086/526787 (2008).
- 83 White, M. T. *et al.* Immunogenicity of the RTS,S/AS01 malaria vaccine and implications for duration of vaccine efficacy: secondary analysis of data from a phase 3 randomised controlled trial. *Lancet Infect Dis* **15**, 1450-1458, doi:10.1016/S1473-3099(15)00239-X (2015).
- 84 Kester, K. E. *et al.* Randomized, double-blind, phase 2a trial of falciparum malaria vaccines RTS,S/AS01B and RTS,S/AS02A in malaria-naive adults: safety, efficacy, and immunologic associates of protection. *J Infect Dis* **200**, 337-346, doi:10.1086/600120 (2009)

SUPPLEMENTARY INFORMATION

Movie S1: MoMΦs phagocytize opsonized *Pf* SPZ in vitro

Movie S2: MoDCs do not interact with whole *Pf* SPZ in vitro

Movies available on: <https://doi.org/10.1371/journal.ppat.1008799>

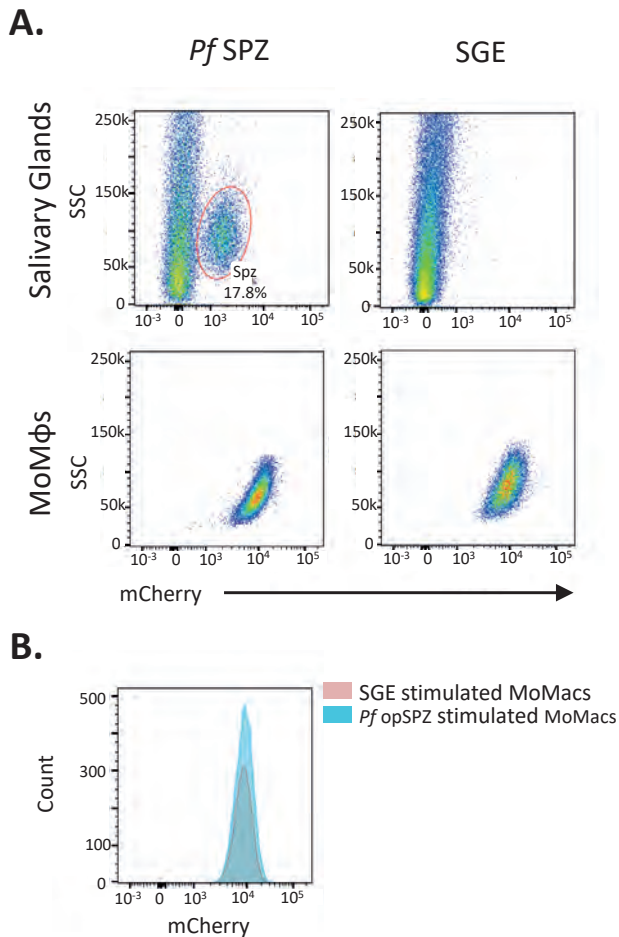
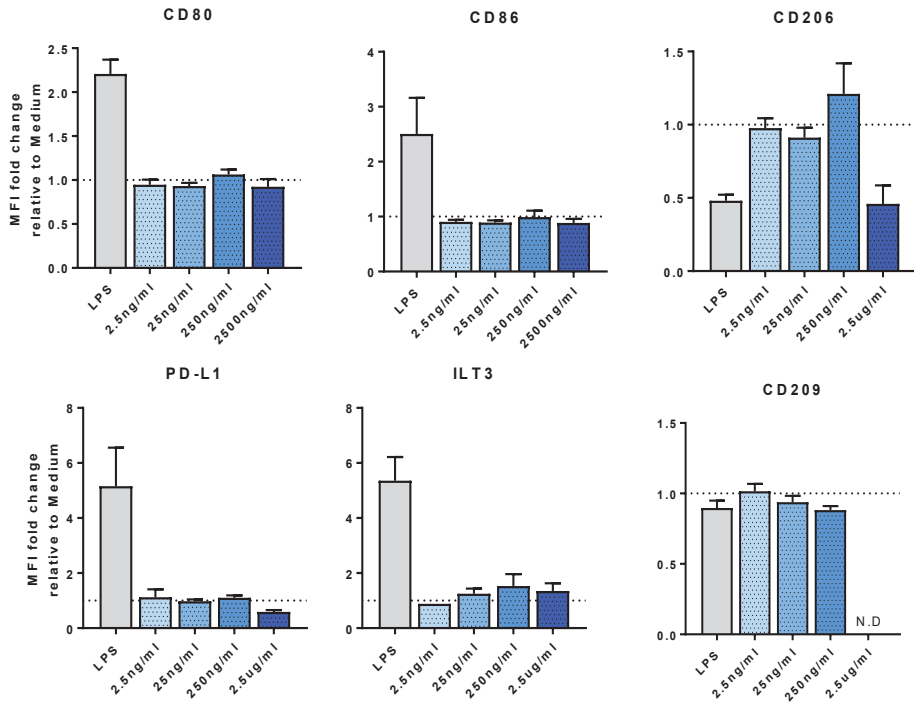


Figure S1. *Pf* SPZ uptake cannot be analyzed by flow cytometry due to high autofluorescence of (monocyte-derived) APCs. A. *Pf* SPZ mCherry fluorescence signal by flow cytometry of mosquito salivary glands alone (top panels, SPZ on the left, SGE control on the right) and after stimulation of MoMφs (bottom panels). Whereas SPZ mCherry signal can be easily distinguished when measuring SPZ in salivary gland samples, MoMφs show high autofluorescence in mCherry. **B.** Histogram of mCherry fluorescence in MoMφs stimulated with opsonized *Pf* SPZ (blue) or SGE control (red).

A.



B.

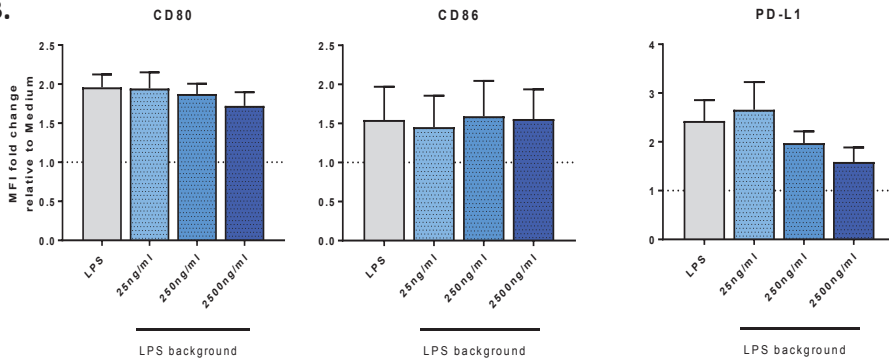


Figure S2. MoDC responses to recCSP. A. Surface marker responses to increasing doses of recCSP on immature MoDCs. **B.** Surface marker responses to increasing doses of recCSP on LPS matured MoDCs. Data shown as fold changes in Median Fluorescence Intensity (MFI) compared to medium stimulated controls (dotted line). N=8, at least 10 donors.

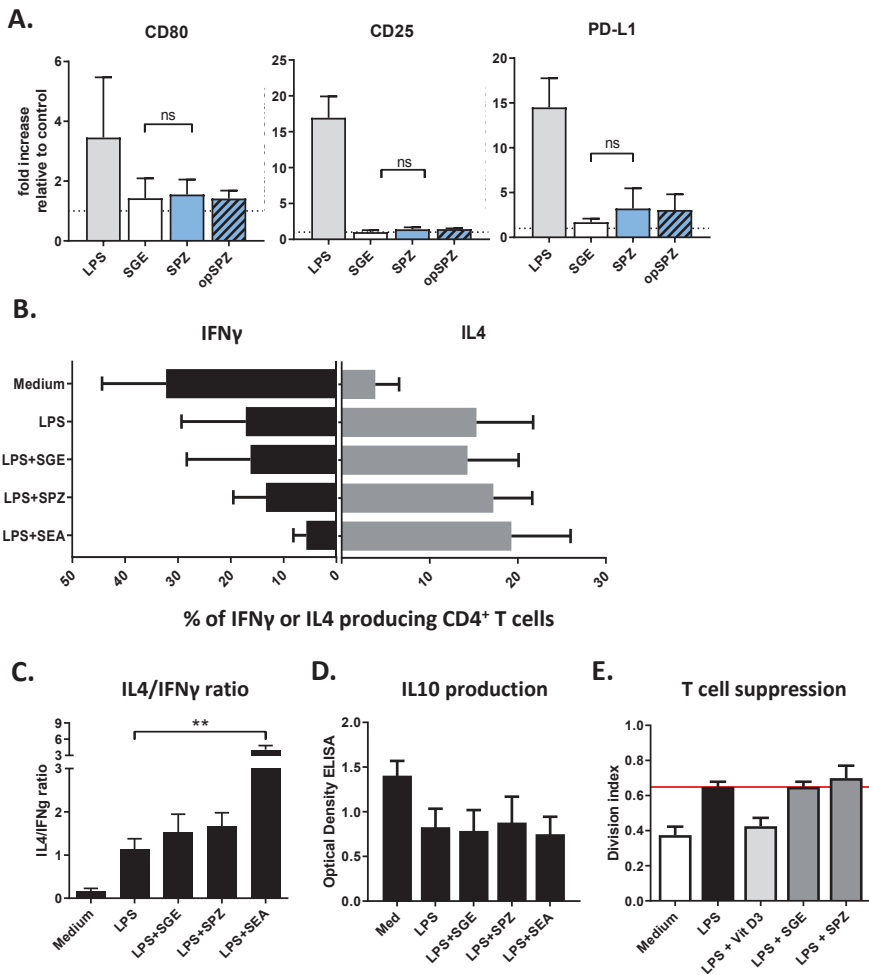


Figure S3. MoDC responses to *Pf* SPZ. A. MoDC surface marker expression after stimulation with SGE, *Pf* SPZ, opsonized *Pf* SPZ (opSPZ) or LPS control. Data shown in MFI (median fluorescence intensity) relative to unstimulated MoDC control. Data of 1 experiment, 3 donors. **B-C.** CD4⁺ T cell polarization after *Pf* SPZ stimulation. *Pf* SPZ stimulation of (LPS-matured) MoDCs does not polarize naïve T cells towards a Th1 (IFN γ) or Th2 response (IL-4; both measured by intracellular staining). (Data shown relative to LPS-matured MoDC control, N=3, 10 donors, soluble Schistosome Egg Antigen (SEA) used as a Th2 inducing control. **: P=<0.005.) **D.** CD4⁺ T cell regulatory response (IL-10; measured by ELISA after CD3/28 restimulation) after coculture with *Pf* SPZ stimulated (LPS matured) MoDCs. Data shown relative to LPS-matured MoDC control. N=3, 6 donors. **E.** MoDCs do not induce regulatory T cells in response to *Pf* SPZ. Data shown as the division index (average number of memory T cell divisions) of memory T cells after stimulation with LPS MoDCs in the presence of SPZ induced T cells, as calculated by FlowJo. Data from 1 experiment, 4 donors.

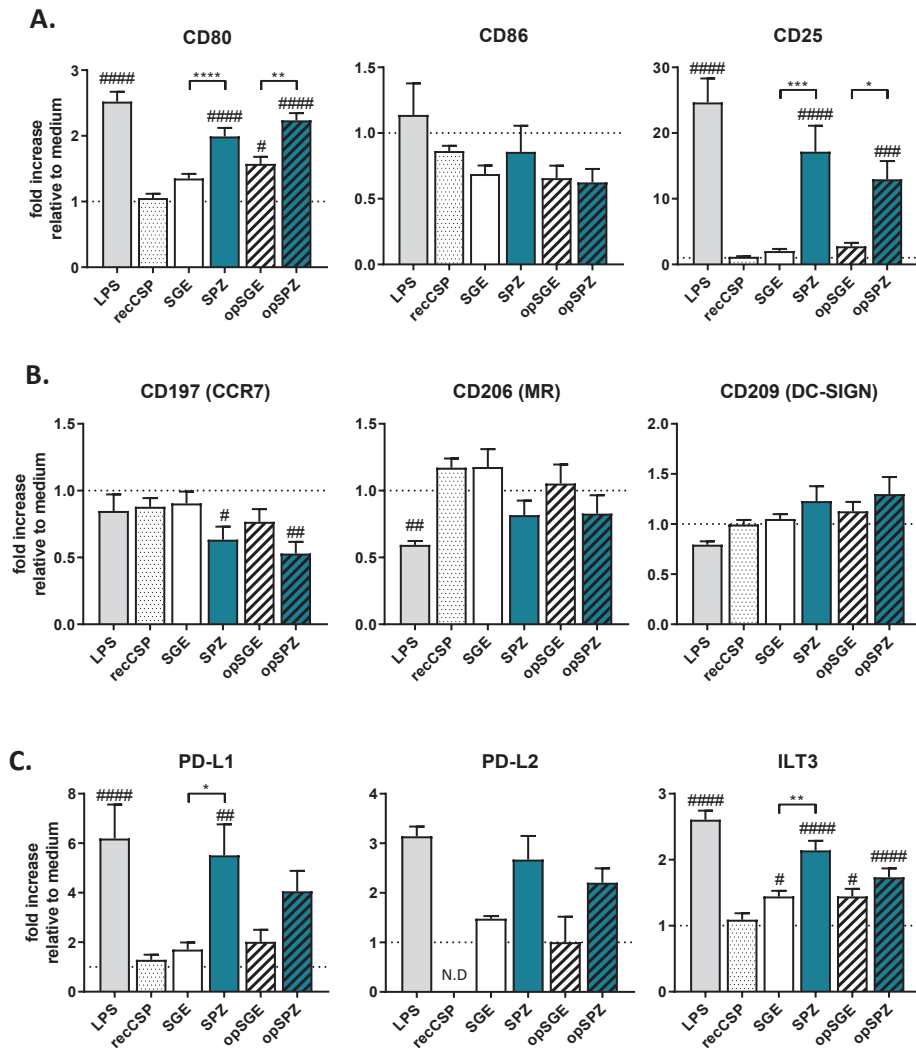


Figure S4. MoMΦ surface marker expression in response to recCSP or whole *Pf* SPZ. Surface marker expression of MoMΦs in response to stimulation with recCSP (250ng/ml), *Pf* SPZ and *Pf* opSPZ. **A.** SPZ stimulation induces increased activation marker expression (CD80, and CD25). No response to recCSP. **B.** SPZ stimulation reduces CD197 expression. No significant change in M2 markers CD206 and CD209. **C.** SPZ stimulation increases regulatory markers PD-L1, PD-L2 and ILT3. Data shown as fold changes in Median Fluorescence Intensity (MFI) compared to medium stimulated controls (dotted line). # indicates analysis compared to medium control. #: $P < 0.05$, ##: $P < 0.005$, ###: $P < 0.0005$ and ####: $P < 0.0001$, *: $P < 0.05$, **: $P < 0.001$, ***: $P < 0.005$, ****: $P < 0.0001$ using one way ANOVA. $N = 9$, at least 20 donors.

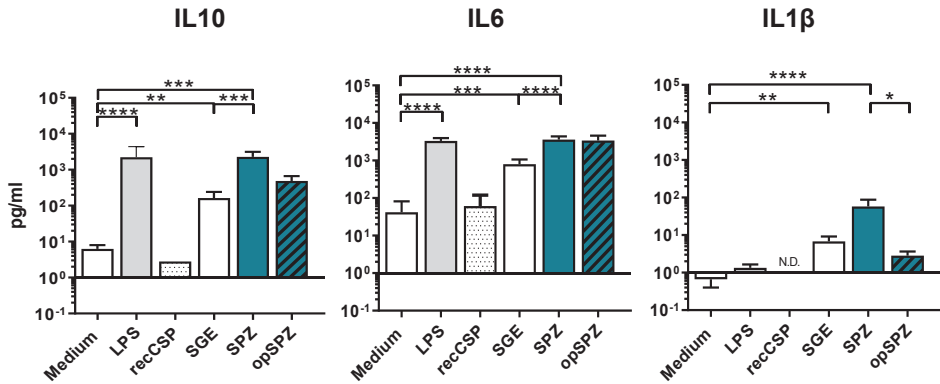


Figure S5. MoMΦ responses to recCSP and whole SPZ. Cytokine IL-10, IL-6 and IL1β responses to recCSP and *Pf* SPZ stimulation. Data shown in pg/ml; IL-10: N=8, 25 donors; IL-6: N=5, 17 donors; IL1β: N=3, 7 donors

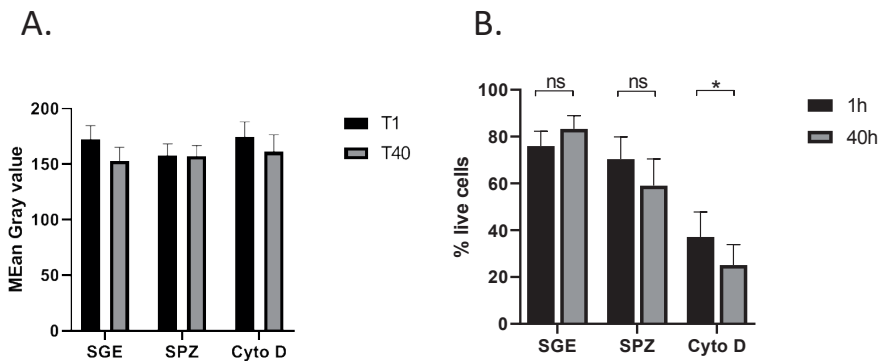


Figure S6. MoMΦ cell death *in vitro* over time. **A.** Mean gray value measured over the sides on both side of the scratch show no differences in cell density over time between or within groups, indicating the reduced gray value over the scratch is not due to overall cell loss. **B.** % of Live MoMΦs at 1 and 40h of stimulation with SGE, *Pf* SPZ and Cyto D, measured by Flow Cytometry. Statistical testing using two way ANOVA. *p<0.05. Although Cyto D reduces cell viability compared to SGE or *Pf* SPZ stimulation, we found no differences in cell viability of SGE and SPZ stimulated MoMΦs over time. N=2, 5 donors.

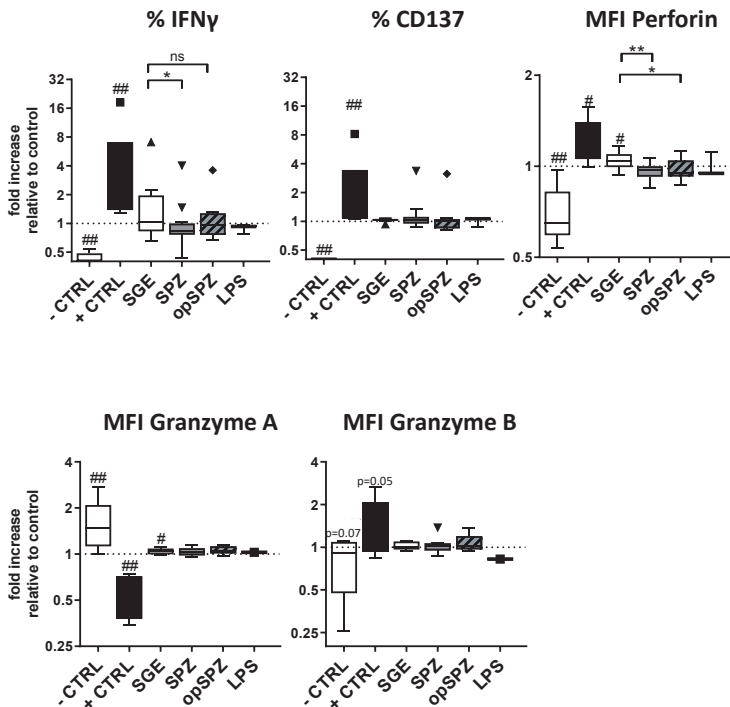


Figure S7. CD8 responses are altered by SPZ stimulated MoM ϕ . IFN γ , CD137 and perforin CD8⁺ T cell responses to control peptide stimulated MoDCs in the presence of SGE, *Pf* SPZ or *Pf* opSPZ stimulated MoM ϕ s. +CTRL represents response to peptide stimulated MoDCs in the presence of peptide stimulated MoM ϕ s. -CTRL represents baseline response to unstimulated MoDCs. Data shown as fold changes compared to peptide stimulated MoDCs only, in the absence of MoM ϕ . IFN γ and CD137 responses shown as a percentage of total CD8 T cells. Perforin and Granzyme responses shown as Median Fluorescence Intensity (MFI). # indicates analysis compared to medium control. #: P<0.05, ##: P<0.005, using Wilcoxon test. N=4, 8 donors

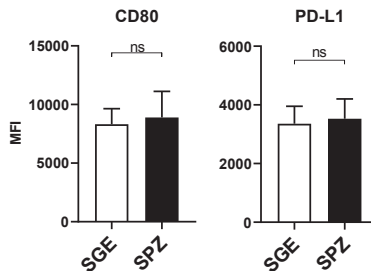
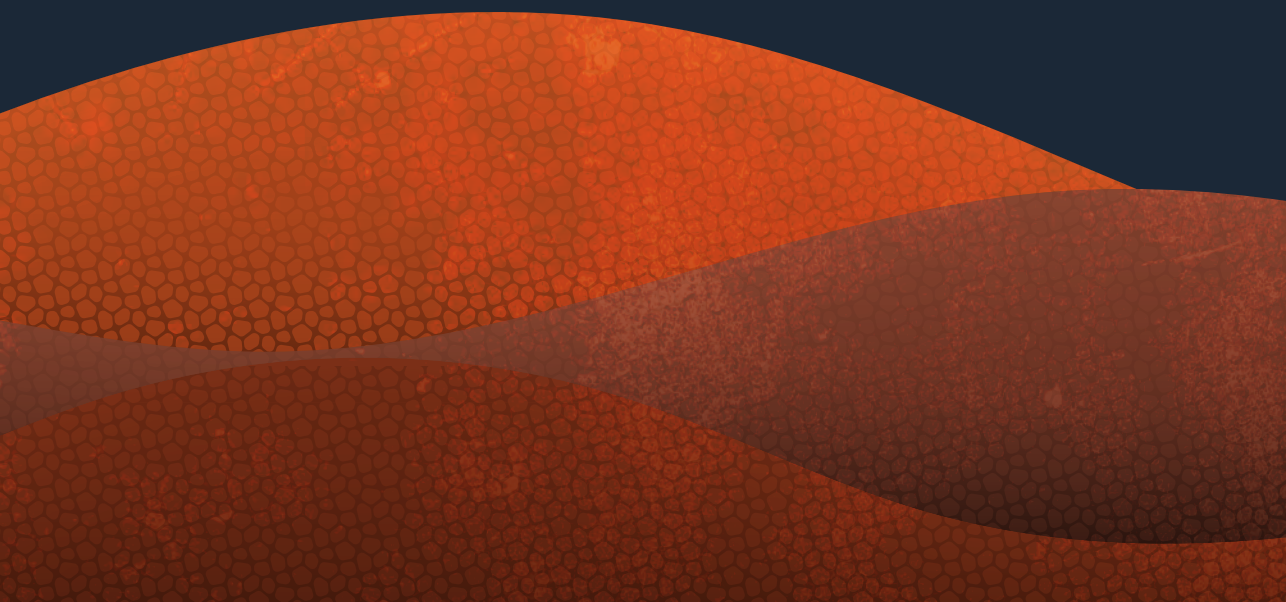


Figure S8. Surface CD80 and PD-L1 expression of dermal APCs from lysed human skin explants after stimulation with *Pf* SPZ or SGE control. Mean fluorescence intensity of CD80 and PD-L1 in dermal APCs from lysed human skin cells (HLA-DR⁺, CD11c⁺) stimulated with SGE or *Pf* SPZ. N=3, 4 donors.

3



Human dermal APC responses to needle- and mosquito bite-injected *Plasmodium falciparum* sporozoites

Béatrice M.F Winkel, Roos van Schuijlenburg, Els Baalbergen, Munisha S. Ganesh, Mirjam Daalenberg, Alwin van der Ham, Heleen Gerritsma, Geert-Jan van Gemert, Marijke C.C. Langenberg, Séverine C. Chevalley-Maurel, Maria Yazdanbakhsh, Toni van Capel, Esther C. de Jong, Bart Everts, Blandine Franke-Fayard, Meta Roestenberg

Manuscript in preparation



ABSTRACT

Whole sporozoite vaccines can yield sterile protection against malaria, however their efficacy critically depends on their route of administration. Early clinical trials demonstrated high levels of protection with mosquito bite administered parasites, whereas protection after needle injection was much reduced. Previously, we have shown that *Plasmodium* sporozoites induce a regulatory immune response in the dermis. To investigate whether differences in dermal immune regulation could underlie the differences in protection, we studied early dermal APC responses to mosquito bite and needle injected *Plasmodium falciparum* sporozoites directly in human skin explants. We analyzed subset distribution of the four main dermal APC subsets (CD14⁺, CD1a⁺, CD141⁺ dermal dendritic cells (DDCs) and Langerhans cells (LCs)), their surface expression of activation markers, their cytokine production and the subsequent effect on priming naïve CD4⁺ T cells. We found a small increase in the CD14⁺ DDC subset when sporozoites were administered by mosquito compared to needle. We did not detect changes in activation markers, cytokine production or polarization of naïve CD4⁺ T cells. In this study we take the first steps to elucidate the dermal immune responses during the uncharacterized human skin stage of malaria. Understanding the initial interaction of SPZ with the innate immune system and the subsequent effect on adaptive immunity may aid in the development of effective attenuated sporozoite malaria vaccines.

Keywords: *Plasmodium falciparum*, sporozoite, malaria, skin, innate immunity, dendritic cells

INTRODUCTION

Malaria infection starts with the bite of an infected *anopheles* mosquito injecting a motile form of the *Plasmodium* parasite, sporozoites (SPZ), into the dermis of the host. It is often thought that mosquitoes inoculate sporozoites directly into the blood stream. However, sporozoites are ejected when a probing mosquito salivates. Salivation stops when the mosquito has located a blood vessel^{1,2}. Interrupted feeding and bite site removal experiments², as well as video microscopic analysis³ have demonstrated a predominantly intradermal delivery of sporozoites by mosquito bite. These SPZ subsequently migrate through the dermal tissue and make their way into the vasculature with which they are transported to the liver, where they continue development in hepatocytes. Because the SPZ are still low in number and located extracellularly, where they are vulnerable to immune attack, SPZ antigens have been used as malaria vaccines.

The inoculation of live, radiation-attenuated malaria parasites is one of the most promising vaccine approaches. These vaccines are based on the whole sporozoite instead of its immunodominant antigen CSP, and are currently undergoing field efficacy trials. Remarkably, these parasites induce high levels of protection when administered by mosquito bite^{4,5}, but intradermal needle injection results in greatly reduced protective efficacy, both in clinical trials and in rodent models of malaria⁶⁻⁸. Given the inferiority of ID administration, we hypothesize that the interaction between SPZ and skin immune cells might downmodulate the ensuing immune responses.

Contrasting initial assumptions that the SPZ stay within the skin is only brief, experiments in both primates and rodents revealed that SPZ exit from the dermis can take up to many hours. Approximately half of injected sporozoites trickle out of the injection site over the course of several hours, the majority of these reaching the blood stream. A small portion ends up in lymphatic vessels where they are eliminated by immune cells in the skin draining lymph nodes. Surprisingly, a high amount of sporozoites remain inside the dermis, where they can be detected up to 7h after inoculation^{9,10}. During this dermal stage of the infection, malaria sporozoites are extracellularly located and secrete various proteins as they migrate¹¹. Combined, this results in significant antigen exposure at the skin site.

The skin is an important immunological organ containing different types of immune cells, including antigen-presenting cells (APCs) of the innate immune system such as dendritic cells (DCs) and macrophages (MΦ) that are capable of orchestrating subsequent innate immune responses. The dermal stage of disease is the first site of interaction of SPZ with the immune system. In the human skin, four APC subsets have

been identified based on their surface marker expression: CD14⁺, CD141⁺, and CD1a⁺ dermal dendritic cells (DDCs), and epidermal Langerhans cells (LCs). In general the different DDC subsets can be ascribed certain functionalities however, these depend on the type of antigen encountered. The functions of the various skin APC subsets in response to malaria sporozoites are currently unknown.

In order to understand why immune responses to malarial sporozoites are poor, it is essential to unravel the role of skin resident APCs in the activation or hindering of subsequent adaptive immune responses. To date research has focused solely on rodent models in order to elucidate the dermal stage. Indeed, in a murine model using *Plasmodium berghei* parasites, the lower levels of protection after ID vaccination were associated with an increase in lymphocytes producing IL-10 in the skin draining lymph node⁸. However, although murine models may provide valuable clues, using rodent skin poses obstacles for translation of the findings. Murine skin differs drastically from human skin both anatomically as well as immunologically¹²⁻¹⁵. Therefore, in order to address the immunological basis for the difference in protective efficacy between the two routes of administration we used human skin explants to study the phenotypic and functional effects of SPZ on human dermal APCs. It will be essential to increase our understanding of the skin immune response to sporozoites, in order to exploit the skin as an immunological priming site for the development and/or optimization of vaccines against malaria.

MATERIALS AND METHODS

Parasite materials

Sporozoites were obtained from the human parasite *Plasmodium falciparum* (Pf; NF5416, WT or GFP-luciferase expressing under the *pfCS* promotor) kindly provided by Radboudumc or TropiQ health sciences respectively, both Nijmegen, The Netherlands). Mosquitoes were infected by standard membrane feeding as previously described¹⁷. Salivary glands of infected and uninfected mosquitoes were manually dissected at day 14-21 post infection. Salivary glands were kept on ice until use within 1 hours. Immediately prior to their use, glands were homogenized to extract parasites. Parasites were counted using a Bürker chamber.

Animal use for this study was approved by the Animal Experiments Committee of the Leiden University Medical Center (DEC 14307). The Dutch Experiments on Animal

Act is established under European guidelines (EU directive no. 86/609/EEC regarding the Protection of Animals used for Experimental and Other Scientific Purposes). All experiments were performed in accordance with relevant guidelines and regulations.

Dermal APC emigration assay

Human skin explants were obtained from collaborating hospitals immediately after abdominal skin reduction surgery (IRB B18.009 see ethics statement) and kept at 4°C until use (within 6 hours). Subcutaneous fat was removed, and the epidermal side thoroughly cleaned with 70% ethanol. For injections, sporozoite solutions were diluted in RPMI (42401-042; Invitrogen, Carlsbad, CA, USA) to a concentration of 2×10^5 sporozoites/ml (104 sporozoites per 50 μ l injection). Additionally, uninfected salivary gland extract (SGE) was diluted to match salivary glands injected with the sporozoite solutions. 50 μ l solutions were injected intradermally using an insulin syringe (BD biosciences, Franklin lakes, NJ, USA). For mosquito bite conditions, skin pieces were wrapped around an electrically heated pad and placed upon mesh cages containing 100 infected *Anopheles* mosquitoes or uninfected control mosquitoes. Mosquitoes were allowed to probe the skin in an interrupted feeding schedule (2-5 min on, 30 seconds off for 15 total feeding minutes) in the dark, after which the sample was removed. The injection site or mosquito exposed area was cleaned and biopsied using 6mm punch biopsies (12-24 biopsies per condition). As controls, the injection site of 50 μ l intradermal injections of RMPI, lipopolysaccharide (LPS; 20 μ g/ml; Invivogen, San Diego, CA, USA) or 1,25-dihydroxyvitamin D3 (Vitamin D; 25 μ M; Invivogen) was biopsied. All controls were diluted in RMPI (42401-042; Invitrogen). Biopsies were rinsed in RPMI supplemented with 0.1% fetal calf serum (FCS, Bodinco, Alkmaar, The Netherlands) and transferred to a 48 wells plate containing 1ml RPMI 10% FCS per well supplemented with 500U/ml GM-CSF. Plates were incubated for 3 days at 37°C, 5% CO₂.

Biopsy supernatant was collected after 3 days. Supernatant was spun down to collect emigrated immune cells. And the supernatant was stored at -20 degrees for subsequent Luminex analysis. Emigrated cells were washed and stained for Flow Cytometric analysis or irradiated to a total dose of 3000 rad and brought into culture for co-culture assays.

Flow Cytometric analysis of emigrated cells

Cells were stained with 7AAD live/dead dye (Abcam, Cambridge, UK; uptake) or with Aqua fixable live/dead dye (Thermo Fischer Scientific, Waltham, MA, USA; phenotyping) antibodies against HLA-DR, CD11c, CD1a, CD14, CD141 and CD80 and analyzed by Flow

Cytometry using a BD FACSCanto II (BD Biosciences). Data was analyzed in FlowJo™ version 9.9.6 (FlowJo LLC, Ashlan, OR, USA). Gates were set using 'fluorescence minus one' (FMO) stained control samples.

Cytokine measurement

Biopsy supernatants were harvested 3 days after exposure to SPZ or controls. Supernatants were analyzed by commercially available custom Luminex kit including IFN γ , IL1 β , IL-10, IL-2, IL-23, IP10, MIP1 α , MIP1 β and TNF α (Affymetrix, Santa Clara, CA, USA).

Naïve CD4⁺ T cell co-culture

Naïve T cell co-culture analysis of T cell polarization was performed as described previously²⁴. In brief: 5x10³ emigrated APCs were irradiated (3000 rad) and co-cultured with 2x10⁴ allogeneic naïve CD4⁺ T cells isolated from buffy coat (Sanquin, Amsterdam, The Netherlands). Co-cultures were performed in the presence of staphylococcal enterotoxin B (10pg/ml). On days 6 and 8, recombinant human IL2 (10U/ml; R&D Systems) was added and the T cells were expanded until day 11. Intracellular cytokine production was analyzed after polyclonal restimulation with 100ng/ml phorbol myristate acetate (PMA) and 1 μ g/ml ionomycin (Sigma Aldrich) for 6 hours. Brefaldin A (10 μ g/ml; Sigma Aldrich) was added for the last 4 hours of restimulation. Cells were fixed in 3.7% paraformaldehyde (Sigma Aldrich), permeabilized with permeabilization buffer (Affymetrix, Santa Clara, CA, USA), stained with antibodies against IL-4 and IFN γ (BD bioscience) and analyzed with flow cytometry. In addition, 10⁵ expanded CD4 T cells were restimulated with antibodies against CD3 and CD28 for 24 hours in a 96-wells plate. Supernatants were harvested and analyzed for IL-10 secretion using standard ELISA (Sanquin, Amsterdam, The Netherlands).

Statistical analysis

Data was analyzed using GraphPad Prism (La Jolla, CA, USA) version 7. Comparisons between two or more independent data groups were made by student's T test or analysis of variance test (ANOVA; respectively). Luminex cytokine analysis was performed using the Kruskal-Wallis test for comparison of non-parametric data from multiple groups. P<0.05 was considered statistically significant.

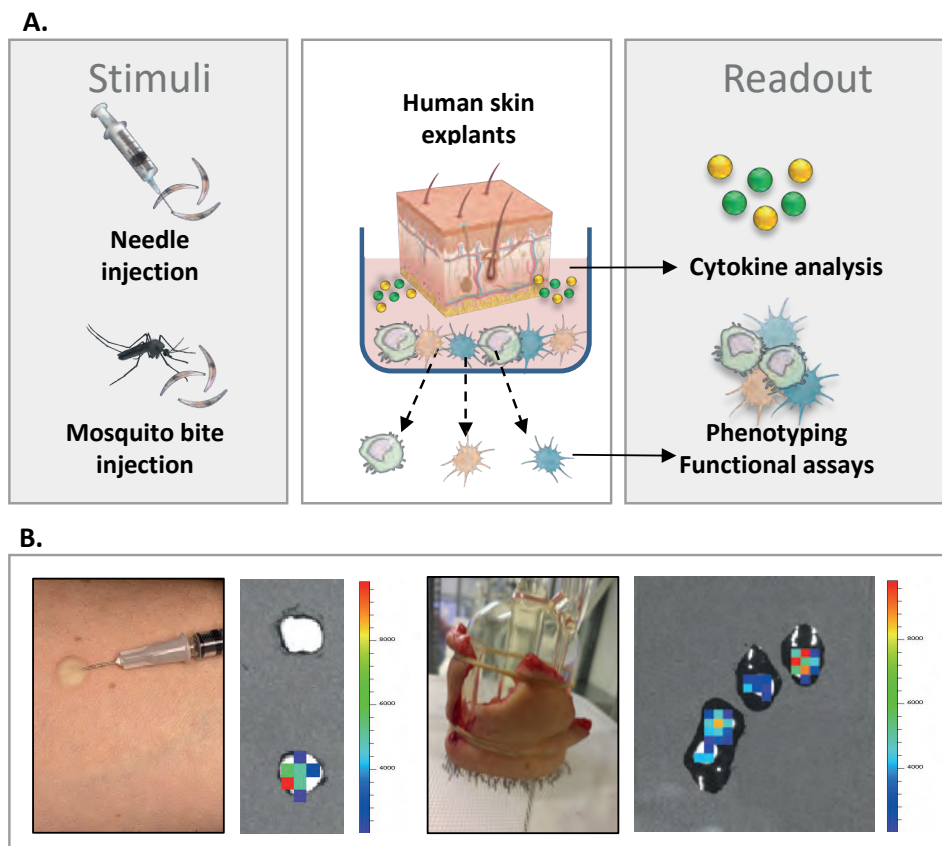


Figure 1. Experimental setup. **A.** Human skin explants were exposed to *Pf* infected mosquitoes or injected with *Pf* SPZ or controls (SGE, Medium, Vitamin D and LPS). The exposed or injected areas were then biopsied and cultured to allow emigration of migratory dermal APCs. We analysed the biopsy cytokine environment and the phenotype and function of emigrated APCs. **B.** Sporozoite luciferin signal seen after intradermal needle (left, bottom) or mosquito bite (right) injection of sporozoites confirms sporozoites are deposited in skin explants by mosquito bite. Uninjected biopsy as a control in top left.

RESULTS

In order to assess the responses of dermal immune cells to SPZ, we exposed full thickness human abdominal skin explants to SPZ injected by needle or by mosquito bite. We confirmed dermal location of 10 000 luciferase-expressing SPZ by IVIS (Figure 1B, left). Delivery of SPZ by the bites of 100 mosquitoes yielded lower signals, however still clearly detectable (right). As mosquitoes inject approximately 100 sporozoites per bite^{5,18}, we estimated approximately 85-fold fewer parasites in the mosquito bite delivered biopsies

(± 118 sporozoites per biopsy; $100 \text{ mosquitoes} * 100 \text{ sporozoites} = 10.000$ sporozoites in the total surface area of 23.8 cm^2 , compared to 10.000 injected sporozoites per single biopsy surface area of 0.28 cm^2).

Emigrating CD14⁺ DDCs are increased after mosquito bite administration of SPZ and decreased after needle injection.

We subsequently tested the phenotype and function of dermal APCs (Figure 1A). We measured approximately three to seven thousand emigrated HLA-DR⁺, CD11c⁺ dermal APCs per biopsy, and found a trend of decreased total APC emigration after exposure to SPZ both by mosquito bite and needle injection (Figure 2A). Examination of DDC subset distribution (CD14⁺, CD1a⁺, CD141⁺ DDCs and LCs), revealed only very small differences after exposure to salivary gland extract of uninfected (SGE) or Plasmodium infected mosquitoes (SPZ) with respect to the medium control (Figure 2B). These small differences were especially evident compared to the effects of LPS and Vitamin D controls (Supplementary Figure S1). We did find increased emigration of one subset of DDCs, the CD14⁺ subset, after SPZ exposure by infected mosquito bite, although this trend was not statistically significant ($P=0.09$). This effect was primarily due to an increase in the CD14⁺, Auto fluorescence⁺ population, which have previously been reported as “macrophage-like”²⁹ (Figure 2C). In contrast, emigration of the CD14⁺ subset was suppressed after needle injection of both SGE and SPZ (Figure 2B). We did not detect differences in the other DDC subsets. Additionally, analysis of surface expression of activation markers CD80, CD86 and HLA-DR showed that the changes in CD14⁺ DDCs were not accompanied by differences in activation marker expression with either administration method in either subset (Figure 3, Supplementary figure S2). We concluded that, although dermal APCs do not readily respond to intradermal SPZs administered either via mosquito bite or needle injection, emigration of total dermal APCs is reduced after SPZ exposure. In addition, the CD14⁺ DDC subset may be the subset of interest with regards to the route of administration of SPZ.

ID SPZ delivery does not result in changes in the dermal cytokine environment

Luminex analysis of 8 different cytokines and chemokines which can be produced by APCs in response to antigen encounter yielded no changes upon administration of SPZ. We tested proinflammatory cytokines IFN- γ , IL-1 β , TNF- α and IL-23, as well as proinflammatory chemokines MIP-1 α and MIP-1 β . In addition we measured regulatory cytokine IL-10 and chemokine IP-10. Although control injections using LPS showed clear increases in the production of both pro- and anti-inflammatory cytokines and chemokines (Supplementary figure S3), we did not detect any responses to mosquito

bite or needle injection of SPZ or SGE (Figure 4). Thus, we concluded that dermal APCs do not readily respond to intradermal SPZ or uninfected SGE by alteration of cytokine production.

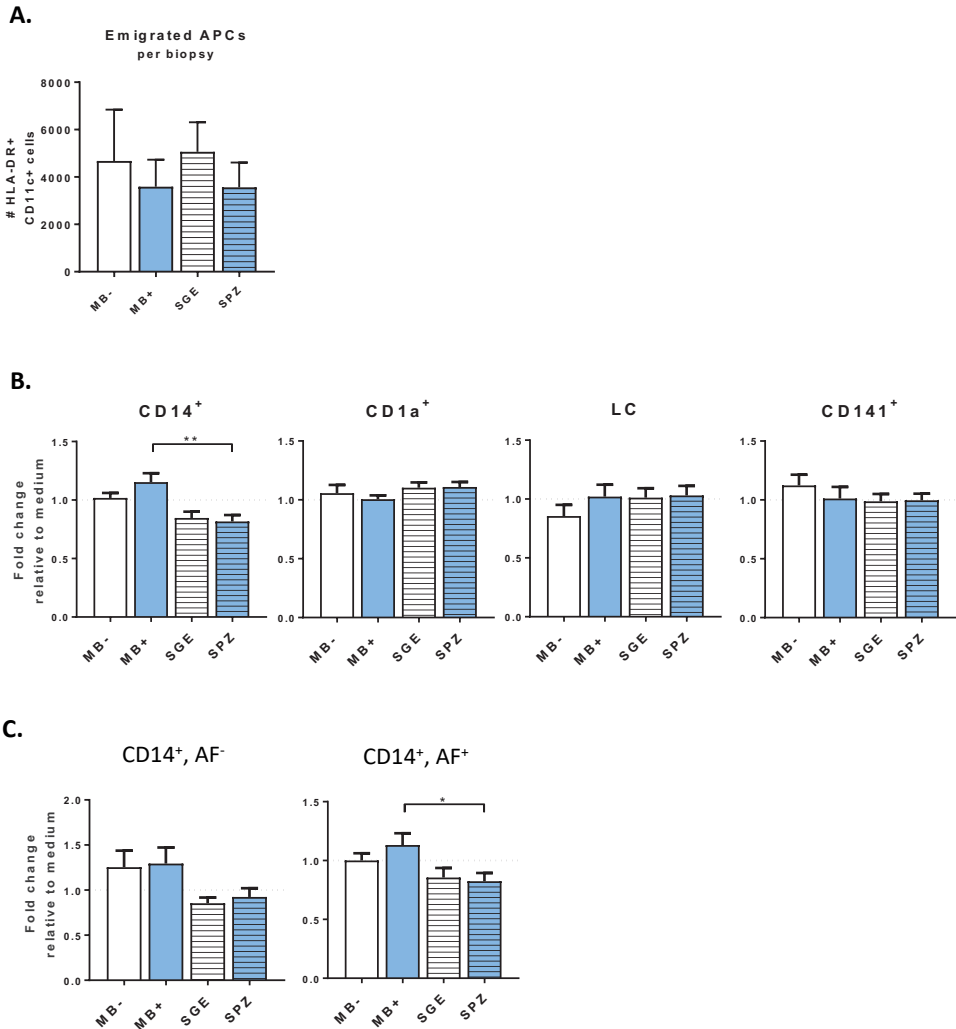


Figure 2. DDC subset distribution after ID SPZ inoculation via MB or needle. A. Total number of emigrated APCs per biopsy. Trend of a decrease in APC emigration upon exposure to SPZ, both with MB and needle injection. **B.** Subset distribution of emigrated DDCs. Statistical testing using paired student's T test. **C.** CD14⁺ subset consists of CD14⁺ DDCs (CD14+ Autofluorescence⁻) and Macrophage-like APCs (CD14⁺, Autofluorescence⁺).

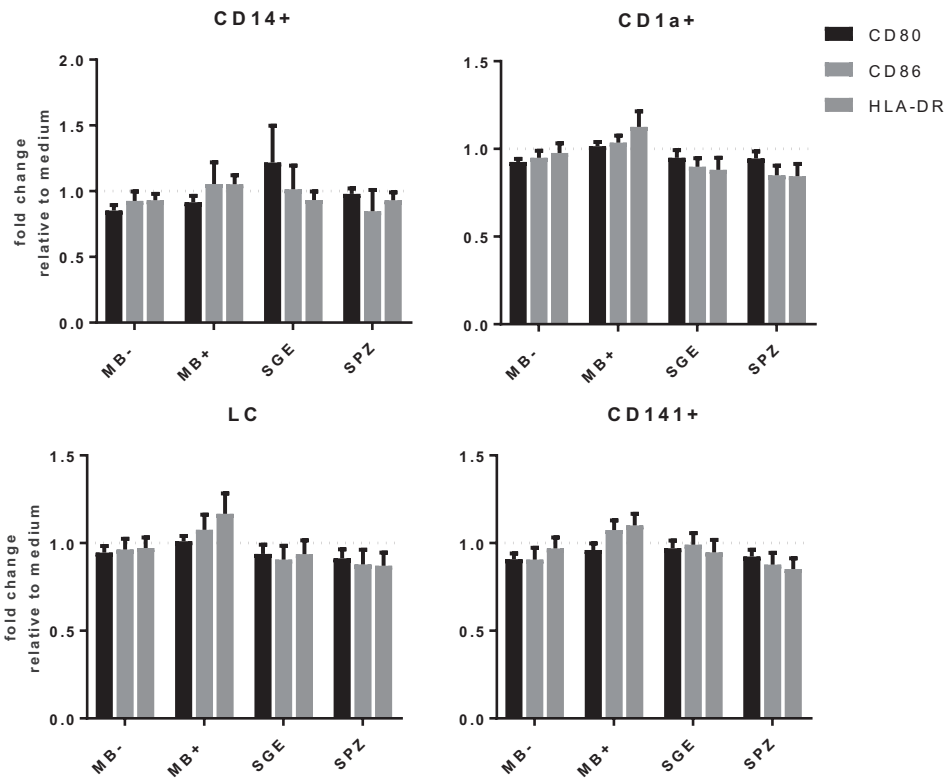


Figure 3. Activation status of emigrated DDCs. No changes in activation marker expression after exposure to SPZ either via mosquito bite (MB+) or needle (SPZ) or uninfected controls (MB- and SGE respectively). Data shown as CD80, CD86 and HLA-DR expression over the four main DDC subsets. Statistical testing using one way ANOVA.

No altered T cell polarization after dermal APC exposure to mosquito bite or needle injected SPZ

Next we investigated whether dermal APCs exposed to SPZ or SGE could affect naïve CD4⁺ T cell polarization. We co-cultured heterologous T cells from anonymous donors with emigrated DDCs from the previous setup, in the presence of staphylococcal enterotoxin B (SEB) to ligate the discordant MHC receptors and measured IFN- γ , IL-4 and IL-10 production by T cells. Using this method we did not detect altered CD4⁺ T cell polarization towards either Th1, Th2 or regulatory responses after DDC exposure to SPZ or SGE (Figure 5). In conclusion, dermal APC exposure to SPZ or uninfected SGE does not affect subsequent T cell polarization.

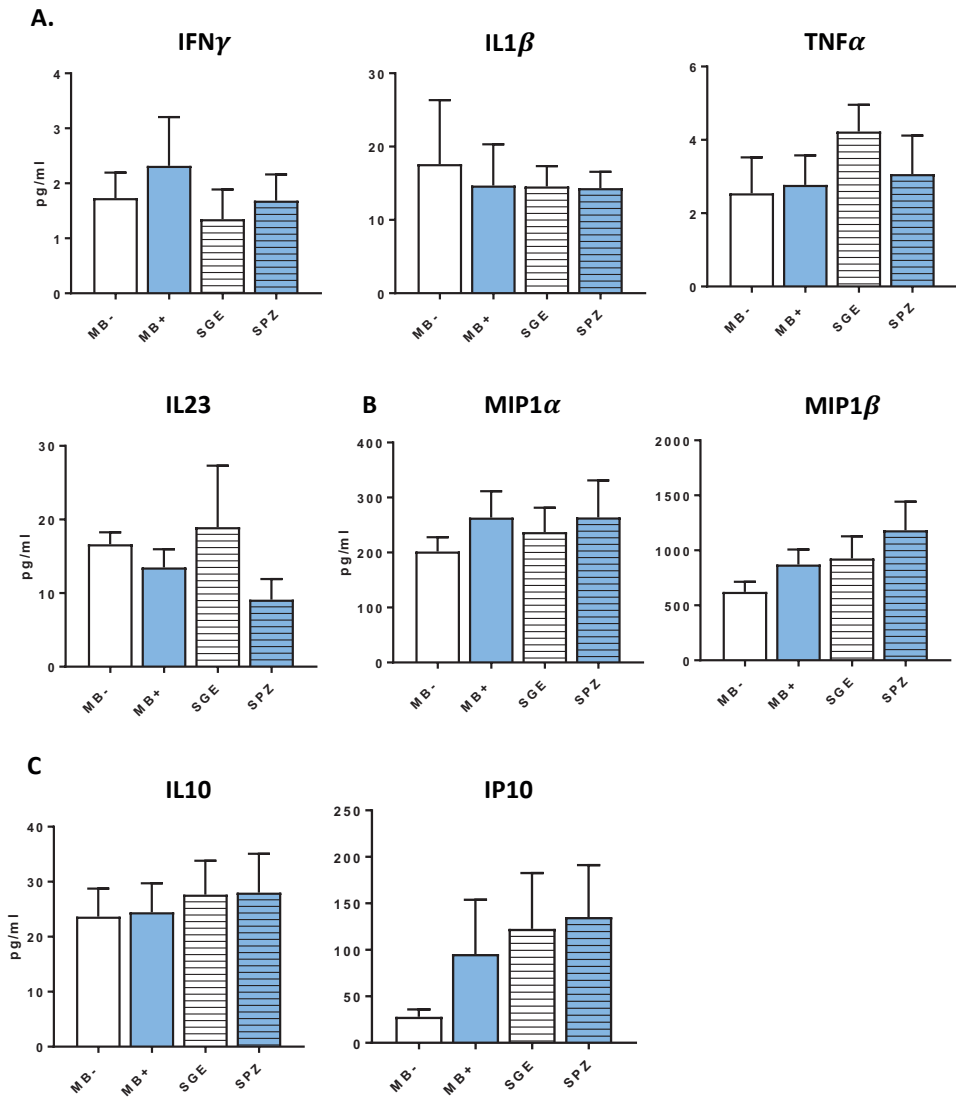


Figure 4. No changes in whole biopsy cytokine and chemokine environment after SPZ inoculation. A. Pro-inflammatory cytokines. **B.** Proinflammatory chemokines. **C.** Regular cytokine IL10 and chemokine IP10. Testing using Kruskal-Wallis test (unpaired one way ANOVA non-parametric)

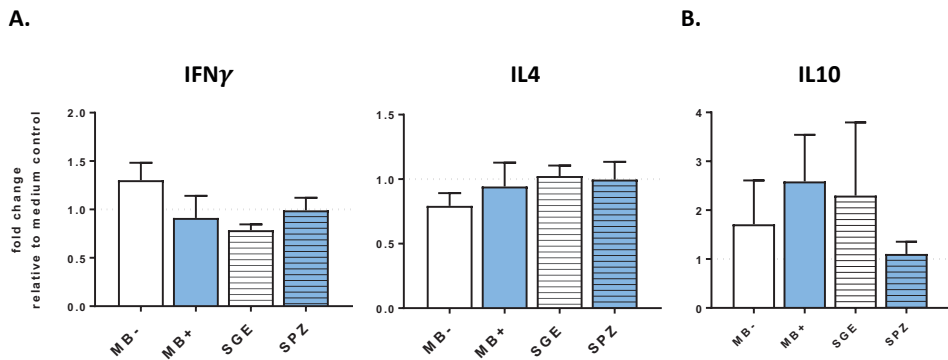


Figure 5. No skewing of naïve CD4⁺ T cells by stimulated DDCs. A. Naïve CD4 T cell polarization. IFN γ or IL-4 producing CD4⁺ T cells (Th1 and Th2 polarization respectively). **B.** IL-10 production by naïve CD4 T cells (after anti CD3/28 stimulation)

DISCUSSION

After sporozoite delivery, skin resident immune cells have been found capable of priming a protective immune response against infected hepatocytes. This response is initiated in the skin draining lymph node^{19,20}. However, we have recently shown that *Plasmodium falciparum* (*Pf*) SPZ are able to induce regulatory immune responses mediated through contact with APCs *in vitro* (Winkel 2020). These findings underline the importance of the skin stage in malaria, and could prove especially important in the field of vaccine development, where intradermal immunization has readily been shown to enhance vaccine potency for a great many diseases²¹⁻²³. In this study, we take the first steps to characterize human dermal immune responses after intradermal delivery of *Pf* SPZ. In order to address the immunological basis for the reduced protectivity of needle administered SPZ we compared needle injected and mosquito bite administered parasites. To the best of our knowledge this is the first study examining dermal immune responses to SPZ using human skin explants.

Overall, we see very few differences in the APC responses of our *ex vivo* skin explant model. A possible explanation could be that the explant emigration assay is not sensitive enough to pick up clear differences after three days of APC emigration. Another explanation is that the lack of vascularization in our setup excludes recruited blood-resident immune cells such as granulocytes and monocytes (including monocyte derived APCs). In spite of these limitations, a similar setup has been used to study APC responses to other pathogens such as *Schistosoma mansoni* cercariae and candida^{24,25}

as well as in vaccine delivery studies²⁶. Nevertheless, SPZ are single cell protozoa measuring 1x10 µm. Much smaller than the multicellular cercariae reaching 500 µm length or hyphae-forming candida. With a roughly similar number of parasites per biopsy (~118 for SPZ, ~140 for cercaria), the antigen load using cercariae is much higher than that of SPZ. This low SPZ antigen load however, is representative for both natural infection (mosquito bite) as well as attenuated SPZ vaccine trials (needle delivery). The discrepancy between responses to other pathogens and our findings with SPZ leads us to hypothesize the regulatory, suppressive propensity of *Pf*SPZ in the skin.

Previously, we demonstrated that SPZ are capable to induce regulatory macrophages *in vitro*, which can suppress subsequent antigen-specific CD8⁺ T cell responses (winkel 2020). These macrophages express high levels of activation marker CD80 as well as regulatory marker PD-L1. Additionally, they produce IL-10 and display reduced motility. These features align them with regulatory macrophages described in the context of tumor immunology^{27,28}. In our current study, we show decreased CD14⁺ APC emigration after needle injection of compounds. CD14⁺ APCs have been transcriptionally aligned to human monocytes and macrophages and have been postulated to be (related to) monocyte-derived macrophages²⁹⁻³¹. We therefore suggest that needle injection results in increased immunoregulation compared to mosquito bite. This effect is already seen in SGE delivery; however, it becomes more evident with SPZ inoculation.

We hypothesize that immune regulation starts at the earliest interaction of SPZ with the immune system of the host, where we propose a central role for regulatory macrophages. When SPZ are administered via needle injection, these regulatory macrophages are induced and remain inside the dermis due to their decreased motility. Here they can locally exert their immuno-suppressive effect, eventually resulting in the hindering of the adaptive immune response. We theorize that this regulation depends on the route of administration of SPZ due to a number of differences:

Firstly, the total SPZ load administered by needle injection greatly exceeds that of MB injection per biopsy. A higher SPZ load may proportionally result in increased immune-regulation within the skin. Especially the ratio between migrating (pro-inflammatory) and dermally-residing (regulatory) SPZ might be critical. Mosquito bite delivery deposits SPZ in close proximity to blood vessels as the mosquito probes, increasing their emigrating potential. In addition, it has been postulated that mosquito delivery of SPZ could select for the most mature and most motile SPZ to be injected. SPZ maturing inside the mosquito migrate to the salivary gland ducts and it is thought that the most mature SPZ are the first to be expelled in salivation³². In contrast, by extracting whole salivary glands from mosquitoes and injecting the homogenized product, this

selection is lost. Arguably, immature SPZ showing reduced migratory capacity are maintained within the skin longer and increase antigen exposure resulting in increased regulation. Secondly, there are large differences in the volumes used. Mosquitoes inject less than 1ul of saliva whereas standard intradermal injections used in vaccinations are 50µl³³. The larger volumes may result in flooding in the skin which hampers SPZ (and potentially also DDC) migration³⁴, resulting in increased antigen exposure at the inoculation site and decreased migration to either the skin draining lymph node or the liver. Corroborating this, 50µl needle injection of SGE also resulted in suppressed emigration of DDCs. Thirdly, the differences in depth of injection between mosquito bite and needle may bring SPZ in contact with different DDC subsets³⁰. As DDC subsets can respond differently to antigens, activation or bypassing of certain subsets may influence the final immunological outcome^{31,35-37}.

In summary, we took the first steps in characterizing human dermal immune responses after SPZ delivery directly in human skin explants. Although overall responses to SPZ were very limited, the decreased CD14⁺ emigration after needle injection of SPZ corresponds with our previous *in vitro* findings and could indicate a similarly regulatory effect within skin. Our study revealed differences in DDC migration after antigen delivery via two main routes of administration, with suppression most evident comparing needle to mosquito bite delivery of SPZ. More studies are needed to determine the nature and role of dermal macrophages in the route of administration of SPZ vaccines. Future studies will include biopsy lysis and analysis of cellular markers within the skin biopsy. Ideally, *in vivo* studies should be conducted to include vascularization and cellular influx. Alternatives for dermal immunity studies that can be translated to human infection could be the use of non-human primates^{38,39} or controlled human malaria infections⁴⁰. Using advanced imaging techniques on skin biopsies as well as flow cytometric or Cytof analysis, these models could elucidate the human skin stage of malaria in the *in vivo* setting.

SUPPLEMENTARY NOTES

Author contributions: The methodology was developed by BW, EJ and MR. Experiments were performed and interpreted by BW, LP, RS, EB, MG, HG, GG, RvS, ML, SC, BF and MR and supervised by MY, BE, BF and MR. BW and MR drafted the manuscript. All authors reviewed and contributed to finalizing the manuscript.

Acknowledgements: The research leading to these results has received funding from a ZONMW VENI grant (016.156.076) financed by the Netherlands Organization for Scientific Research (NWO) and a Gisela Thier fellowship of the LUMC.

Ethics statement: The use of human skin explants (obtained as waste material after abdominal reduction surgery) for this research was approved by the Commission Medical Ethics (CME) of the LUMC, Leiden. Approval number CME: B18-009.

Conflict of interest statement: The authors declare no conflict of interest.

REFERENCES

- 1 Matsuoka, H., Yoshida, S., Hirai, M. & Ishii, A. A rodent malaria, *Plasmodium berghei*, is experimentally transmitted to mice by merely probing of infective mosquito, *Anopheles stephensi*. *Parasitol Int* 51, 17-23, doi:10.1016/s1383-5769(01)00095-2 (2002).
- 2 Sidjanski, S. & Vanderberg, J. P. Delayed migration of *Plasmodium* sporozoites from the mosquito bite site to the blood. *Am J Trop Med Hyg* 57, 426-429, doi:10.4269/ajtmh.1997.57.426 (1997).
- 3 Choumet, V. et al. Visualizing non infectious and infectious *Anopheles gambiae* blood feedings in naive and saliva-immunized mice. *PLoS One* 7, e50464, doi:10.1371/journal.pone.0050464 (2012).
- 4 Roestenberg, M. et al. Protection against a malaria challenge by sporozoite inoculation. *N Engl J Med* 361, 468-477, doi:10.1056/NEJMoa0805832 (2009).
- 5 Medica, D. L. & Sinnis, P. Quantitative dynamics of *Plasmodium yoelii* sporozoite transmission by infected anopheline mosquitoes. *Infect Immun* 73, 4363-4369, doi:10.1128/IAI.73.7.4363-4369.2005 (2005).
- 6 Epstein, J. E. et al. Live attenuated malaria vaccine designed to protect through hepatic CD8(+) T cell immunity. *Science* 334, 475-480, doi:10.1126/science.1211548 (2011).
- 7 Seder, R. A. et al. Protection against malaria by intravenous immunization with a nonreplicating sporozoite vaccine. *Science* 341, 1359-1365, doi:10.1126/science.1241800 (2013).
- 8 Haeberlein, S. et al. Protective immunity differs between routes of administration of attenuated malaria parasites independent of parasite liver load. *Sci Rep* 7, 10372, doi:10.1038/s41598-017-10480-1 (2017).
- 9 Amino, R., Thiberge, S., Shorte, S., Frischknecht, F. & Menard, R. Quantitative imaging of *Plasmodium* sporozoites in the mammalian host. *C R Biol* 329, 858-862, doi:10.1016/j.crvi.2006.04.003 (2006).
- 10 Yamauchi, L. M., Coppi, A., Snounou, G. & Sinnis, P. *Plasmodium* sporozoites trickle out of the injection site. *Cell Microbiol* 9, 1215-1222, doi:10.1111/j.1462-5822.2006.00861.x (2007).
- 11 Garcia, J. E., Puentes, A. & Patarroyo, M. E. Developmental biology of sporozoite-host interactions in *Plasmodium falciparum* malaria: implications for vaccine design. *Clin Microbiol Rev* 19, 686-707, doi:10.1128/CMR.00063-05 (2006).
- 12 Pasparakis, M., Haase, I. & Nestle, F. O. Mechanisms regulating skin immunity and inflammation. *Nat Rev Immunol* 14, 289-301, doi:10.1038/nri3646 (2014).
- 13 Kashem, S. W., Haniffa, M. & Kaplan, D. H. Antigen-Presenting Cells in the Skin. *Annu Rev Immunol* 35, 469-499, doi:10.1146/annurev-immunol-051116-052215 (2017).
- 14 Mestas, J. & Hughes, C. C. Of mice and not men: differences between mouse and human immunology. *J Immunol* 172, 2731-2738 (2004).
- 15 Treuting, P. M., Dintzis, S. M. & Montine, K. S. *Comparative Anatomy and Histology: A Mouse and Human Atlas*. Academic Press, Elsevier Chapter 24, 433-441 (2017).
- 16 Ponnudurai, T., Leeuwenberg, A. D. & Meuwissen, J. H. Chloroquine sensitivity of isolates of *Plasmodium falciparum* adapted to in vitro culture. *Trop Geogr Med* 33, 50-54 (1981).
- 17 Ponnudurai, T. et al. Infectivity of cultured *Plasmodium falciparum* gametocytes to mosquitoes. *Parasitology* 98 Pt 2, 165-173 (1989).
- 18 Jin, Y., Kebaier, C. & Vanderberg, J. Direct microscopic quantification of dynamics of *Plasmodium berghei* sporozoite transmission from mosquitoes to mice. *Infect Immun* 75, 5532-5539, doi:10.1128/IAI.00600-07 (2007).

- 19 Chakravarty, S. et al. CD8+ T lymphocytes protective against malaria liver stages are primed in skin-draining lymph nodes. *Nat Med* 13, 1035-1041, doi:10.1038/nm1628 (2007).
- 20 Obeid, M. et al. Skin-draining lymph node priming is sufficient to induce sterile immunity against pre-erythrocytic malaria. *EMBO Mol Med* 5, 250-263, doi:10.1002/emmm.201201677 (2013).
- 21 Kenney, R. T., Frech, S. A., Muenz, L. R., Villar, C. P. & Glenn, G. M. Dose sparing with intradermal injection of influenza vaccine. *N Engl J Med* 351, 2295-2301, doi:10.1056/NEJMoa043540 (2004).
- 22 Okayasu, H. et al. Intradermal Administration of Fractional Doses of Inactivated Poliovirus Vaccine: A Dose-Sparing Option for Polio Immunization. *J Infect Dis* 216, S161-S167, doi:10.1093/infdis/jix038 (2017).
- 23 Denis, M. et al. An overview of the immunogenicity and effectiveness of current human rabies vaccines administered by intradermal route. *Vaccine* 37 Suppl 1, A99-A106, doi:10.1016/j.vaccine.2018.11.072 (2019).
- 24 Winkel, B. M. F. et al. Early Induction of Human Regulatory Dermal Antigen Presenting Cells by Skin-Penetrating *Schistosoma Mansoni* Cercariae. *Front Immunol* 9, 2510, doi:10.3389/fimmu.2018.02510 (2018).
- 25 Maboni, G. et al. A Novel 3D Skin Explant Model to Study Anaerobic Bacterial Infection. *Front Cell Infect Microbiol* 7, 404, doi:10.3389/fcimb.2017.00404 (2017).
- 26 Duinkerken, S. L., J; Stolk, D; Vree, J; Ambrosini, M; Kalay, H; van Kooyk, Y. Comparison of intradermal injection and epicutaneous laser microporation for antitumor vaccine delivery in a human skin explant model. *BioRxiv*, doi:https://doi.org/10.1101/861930 (2019).
- 27 Noy, R. & Pollard, J. W. Tumor-associated macrophages: from mechanisms to therapy. *Immunity* 41, 49-61, doi:10.1016/j.immuni.2014.06.010 (2014).
- 28 Wynn, T. A. & Vannella, K. M. Macrophages in Tissue Repair, Regeneration, and Fibrosis. *Immunity* 44, 450-462, doi:10.1016/j.immuni.2016.02.015 (2016).
- 29 McGovern, N. et al. Human dermal CD14(+) cells are a transient population of monocyte-derived macrophages. *Immunity* 41, 465-477, doi:10.1016/j.immuni.2014.08.006 (2014).
- 30 Wang, X. N. et al. A three-dimensional atlas of human dermal leukocytes, lymphatics, and blood vessels. *J Invest Dermatol* 134, 965-974, doi:10.1038/jid.2013.481 (2014).
- 31 Haniffa, M. et al. Differential rates of replacement of human dermal dendritic cells and macrophages during hematopoietic stem cell transplantation. *J Exp Med* 206, 371-385, doi:10.1084/jem.20081633 (2009).
- 32 Vanderberg, J. Development of infectivity by the *Plasmodium berghei* sporozoite. *J Parasitol* 61, 43-50 (1975).
- 33 Roestenberg, M. et al. Controlled human malaria infections by intradermal injection of cryopreserved *Plasmodium falciparum* sporozoites. *Am J Trop Med Hyg* 88, 5-13, doi:10.4269/ajtmh.2012.12-0613 (2013).
- 34 Vanderberg, J. P. Imaging mosquito transmission of *Plasmodium* sporozoites into the mammalian host: immunological implications. *Parasitol Int* 63, 150-164, doi:10.1016/j.parint.2013.09.010 (2014).
- 35 Klechevsky, E. et al. Functional specializations of human epidermal Langerhans cells and CD14+ dermal dendritic cells. *Immunity* 29, 497-510, doi:10.1016/j.immuni.2008.07.013 (2008).
- 36 de Jong, E. C., Smits, H. H. & Kapsenberg, M. L. Dendritic cell-mediated T cell polarization. *Springer Semin Immunopathol* 26, 289-307, doi:10.1007/s00281-004-0167-1 (2005).
- 37 Chu, C. C. et al. Resident CD141 (BDCA3)+ dendritic cells in human skin produce IL-10 and induce regulatory T cells that suppress skin inflammation. *J Exp Med* 209, 935-945, doi:10.1084/jem.20112583 (2012).

- 38 Martinelli, A. & Culleton, R. Non-human primate malaria parasites: out of the forest and into the laboratory. *Parasitology* 145, 41-54, doi:10.1017/S0031182016001335 (2018).
- 39 Avci, P. et al. Animal models of skin disease for drug discovery. *Expert Opin Drug Discov* 8, 331-355, doi:10.1517/17460441.2013.761202 (2013).
- 40 Roestenberg, M., Kamerling, I. M. C. & de Visser, S. J. Corrigendum: Controlled Human Infections As a Tool to Reduce Uncertainty in Clinical Vaccine Development. *Front Med (Lausanne)* 6, 23, doi:10.3389/fmed.2019.00023 (2019).

SUPPLEMENTARY INFORMATION

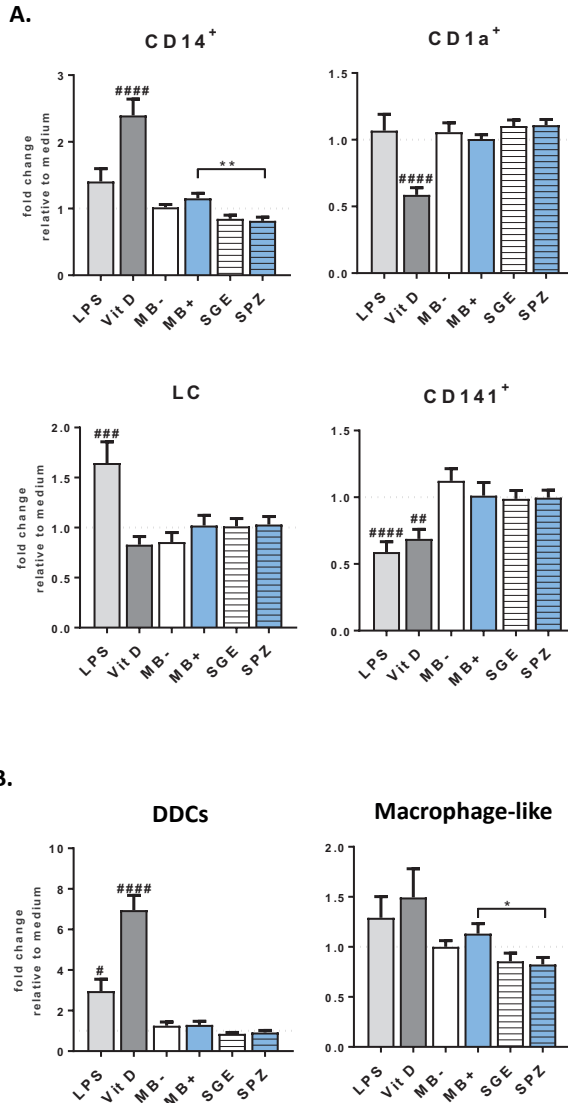


Figure S1. Small increase in macrophage like emigrated APCs after MB injection of SPZ compared needle injection. A. Subset distribution of emigrated DDCs. Statistical testing using one way ANOVA. **B.** CD14⁺ subset consists of CD14⁺ DDCs (CD14⁺ Autofluorescence) and Macrophage-like APCs (CD14⁺ Autofluorescence⁺).

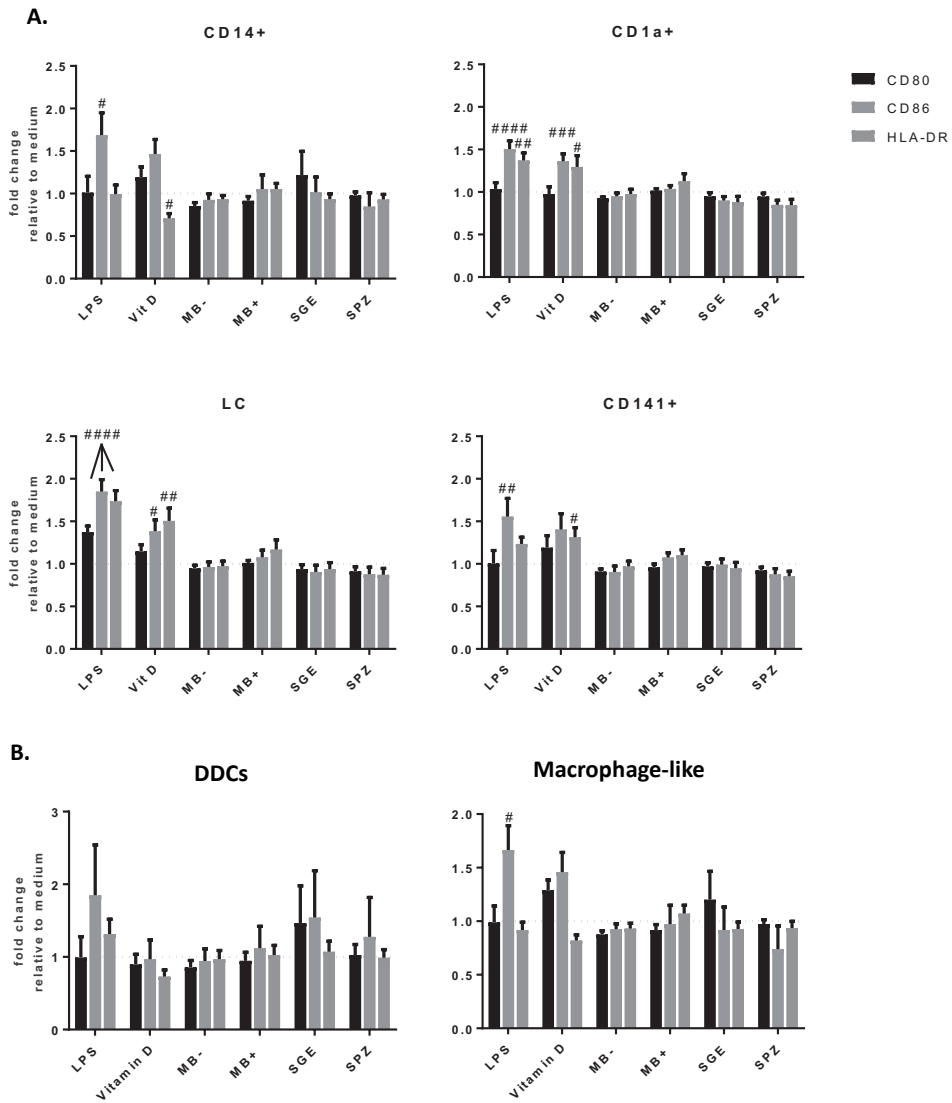


Figure S2. Activation status of emigrated DDCs. **A.** Changes in activation marker expression after exposure to SPZ delivered either via mosquito bite (MB+) or needle (SPZ), or controls (LPS, Vitamin D and uninfected controls (MB- and SGE respectively). Data shown as CD80, CD86 and HLA-DR expression over the four main DDC subsets. **B.** Activation markers of all DDC subsets combined (left) and on the macrophage-like, auto fluorescent CD14+ population alone (right). Statistical testing using one way ANOVA.

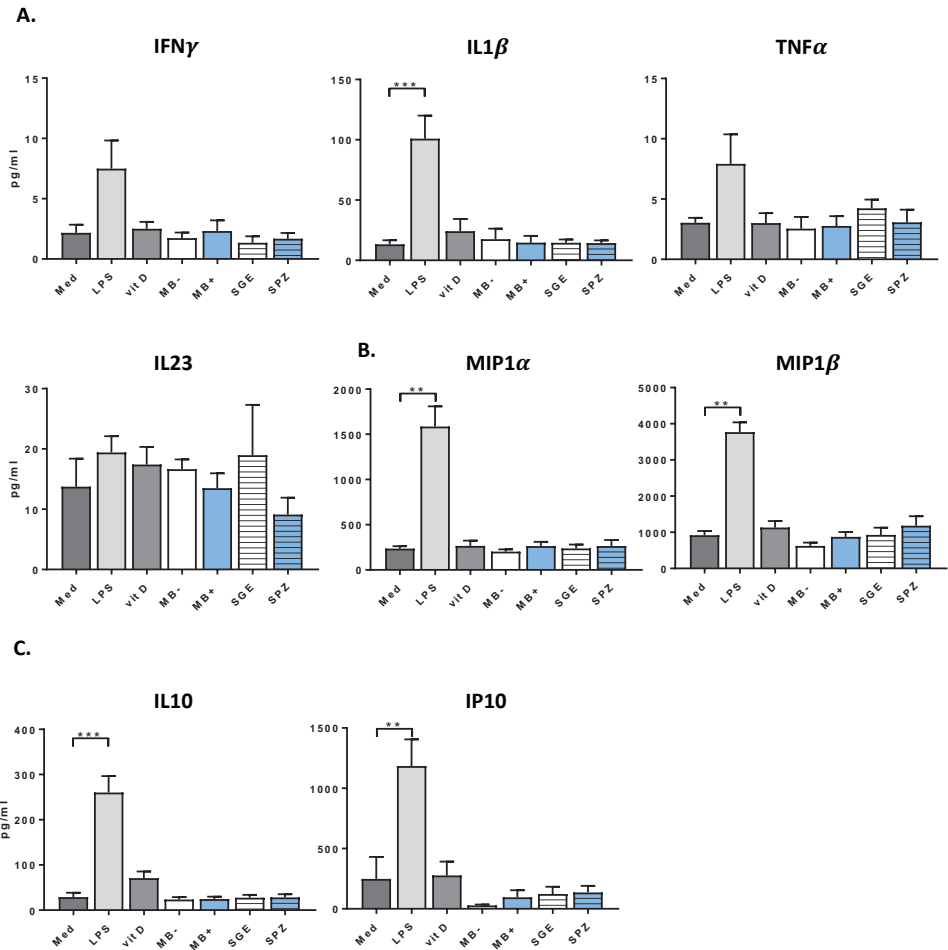


Figure S3. No changes in whole biopsy cytokine and chemokine environment after SPZ inoculation. A. Pro-inflammatory cytokines. **B.** Proinflammatory chemokines. **C.** Regular cytokine IL10 and chemokine IP10. Testing using Kruskal-Wallis test (unpaired one way ANOVA non-parametric).

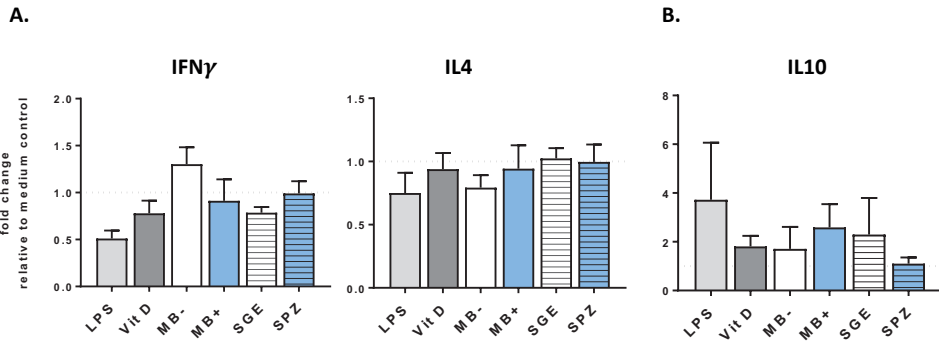
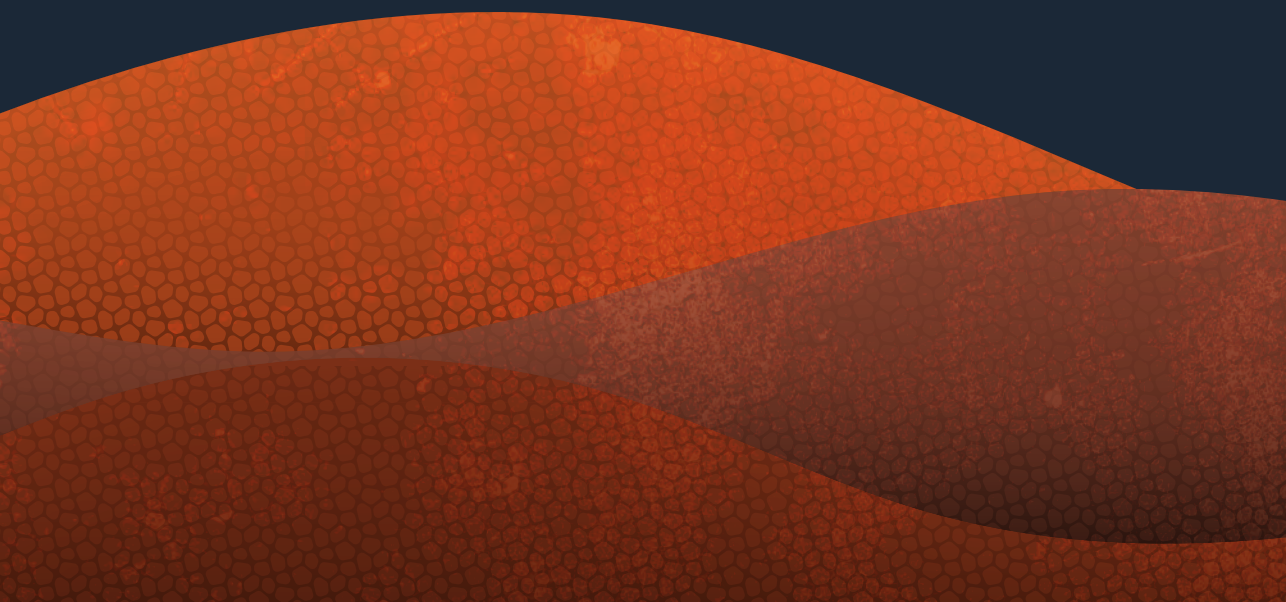


Figure S4. No skewing of naïve CD4⁺ T cells by stimulated DDCs. A. Naïve CD4 T cell polarization. **B.** IL-10 production by naïve CD4 T cells (aCD3/28 stimulation)

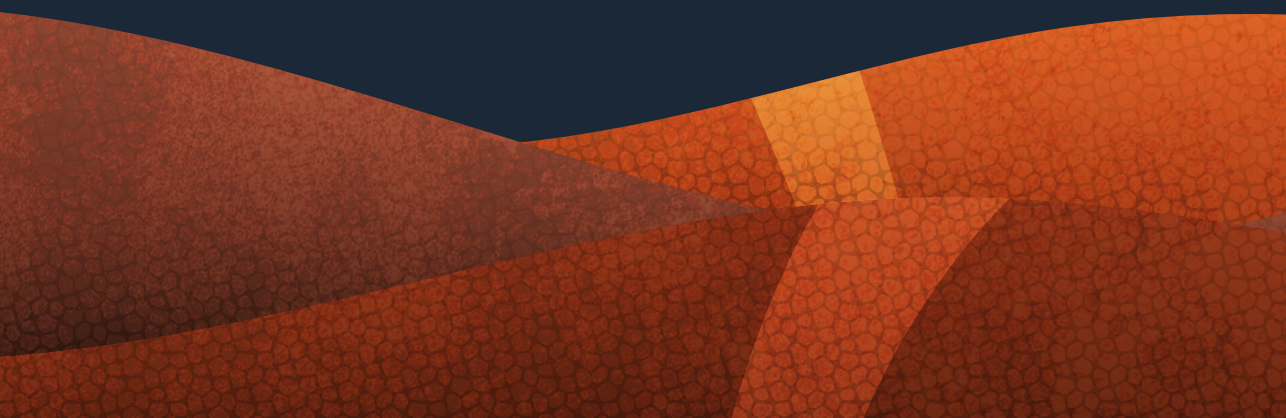
4



Early induction of human regulatory dermal antigen presenting cells by skin-penetrating *Schistosoma mansoni* cercariae

Béatrice M.F. Winkel, Mirjam R. Dalenberg, Clarize M. de Korne, Carola Feijt, Marijke C.C. Langenberg, Leonard Pelgrom, Munisha S. Ganesh, Maria Yazdanbakhsh, Hermelijn H. Smits, Esther C. de Jong, Bart Everts, Fijs W.B. van Leeuwen, Cornelis H. Hokke, Meta Roestenberg

Frontiers in Immunology 2018. Doi: [10.3389/fimmu.2018.02510](https://doi.org/10.3389/fimmu.2018.02510)



ABSTRACT

Following initial invasion of *Schistosoma mansoni* cercariae, schistosomula reside in the skin for several days during which they can interact with the dermal immune system. While murine experiments have indicated that exposure to radiation-attenuated (RA) cercariae can generate protective immunity which is initiated in the skin stage, contrasting non-attenuated cercariae, such data is missing for the human model. Since murine skin does not form a reliable marker for immune responses in human skin, we used human skin explants to study the interaction with non-attenuated and RA cercariae with dermal innate antigen presenting cells (APCs) and the subsequent immunological responses.

We exposed human skin explants to cercariae and visualized their invasion in real time (initial 30 min) using novel imaging technologies. Subsequently, we studied dermal immune responses and found an enhanced production of regulatory cytokine interleukin (IL)-10, pro-inflammatory cytokine IL-6 and macrophage inflammatory protein (MIP)-1 α within three days of exposure. Analysis of dermal dendritic cells (DDCs) for their phenotype revealed an increased expression of immune modulators programmed death ligand (PD-L) 1 and 2, and increased IL-10 production. *Ex vivo* primed DDCs suppress Th1 polarization of naïve T cells and increase T cell IL-10 production, indicating their regulatory potential. These immune responses were absent or decreased after exposure to RA parasites. Using transwells, we show that direct contact between APCs and cercariae is required to induce their regulatory phenotype.

To the best of our knowledge this is the first study that attempts to provide insight in the human dermal *S. mansoni* cercariae invasion and subsequent immune responses comparing non-attenuated with RA parasites. We reveal that cercariae induce a predominantly regulatory immune response whereas RA cercariae fail to achieve this. This initial understanding of the dermal immune suppressive capacity of *S. mansoni* cercariae in humans provides a first step towards the development of an effective schistosome vaccine.

Keywords: *Schistosoma mansoni*, human dermal immunity, immune regulation, fluorescence imaging

INTRODUCTION

After penetrating the skin, larvae of the *Schistosoma mansoni* (*S. mansoni*) parasite, termed cercariae, transform into schistosomula and reside locally for several days, during which they penetrate the epidermal-dermal junction and eventually continue onward migration¹⁻³. Until now, the dynamic aspects of this invasion into human skin remain largely unknown. As the skin is an immune-competent organ containing various immune cells⁴, it provides the first opportunity for host immune cells to recognize parasite antigens. This interaction could be important as it can drive an adaptive immune response against *S. mansoni*⁵. Although it is widely accepted that schistosomes are able to direct immune responses via egg-induced immune modulation at late stages of infection, the modulatory effects during the initial stages are less well defined.

Although human dermal immune responses to *S. mansoni* have not been studied to date, mouse models reveal a mixed immune response to cercariae. In mice, *S. mansoni* invasion induces inflammation, shown by a dermal infiltrate, which peaks by day 4 post infection^{6,7}. From the reports on acute schistosomiasis syndromes it is clear that there is considerable inter-individual variability in the human immune responses to schistosome infection, reflected by variation in cercarial dermatitis and onset of Katayama fever⁸⁻¹⁰. Analysis of murine dermal immune responses to *S. mansoni* larvae revealed an enhanced migration of innate antigen presenting cells (APCs) of such as macrophages (Mφ) and dendritic cells (DCs), to the skin draining lymph node as well as an increase in their activation markers, MCH class II and CD86^{5,7,11-13}. Nonetheless, exposure to cercariae does not readily induce protective immunity. This may be due to counteracting regulatory cytokine responses in the form of IL-10 and IL-1ra which are mounted in the dermis within 2 days post infection^{7,11,14}. Together these early innate responses in the dermis culminate in a short-lived mixed Th1/Th2 cytokine response in the skin draining lymph node which rapidly declines to baseline^{7,15} resulting in a failure to induce protective immunity against a subsequent infection. One possible way by which *S. mansoni* cercariae are suggested to achieve immune regulation is by the production of excretory/secretory (ES) products upon transformation into schistosomula, which can suppress (dermal) immune responses^{7,11,12,16-20}. Proteomic analysis of skin invasion identified a variety of secreted enzymes and factors that are able to degrade host immune defense molecules²⁰.

APCs orchestrate the adaptive immune response to antigens and one molecular mechanism by which APCs are able to inhibit an adaptive immune response is the PD-1/PD-L1 (Programmed Death-1/Programmed Death Ligand-1) interaction. PD-L1 has been described as a regulatory marker on APCs and is linked to the induction

of immunological tolerance²¹⁻²³. In tumor immunology, PD-L1 up regulation leads to immune-escape and T cell anergy upon ligation with PD-1²⁴⁻²⁶, and PD-L1 has been shown to play a pivotal role in the polarization of naïve CD4+ T cells to regulatory T cells (Tregs)²⁷. The role of PD-L2, the other known PD-1 ligand, is less clear. In addition to cancer cells, many pathogens have been shown to exploit the PD-1 pathway in order to escape the host's immune response^{26,28-31}. We aimed to determine whether this immune regulation pathway could potentially play a role in *S. mansoni* infection.

In contrast to non-attenuated cercariae, repeated exposure to radiation-attenuated (RA) cercariae induces protective immunity in animal models. RA cercariae yield a sustained IL12p40 mediated protective Th1 response, which has the capacity to kill migrating parasites in the host lungs^{7,32-37}. It has been reasoned that delayed dermal migration of RA cercariae, and thus prolonged antigen exposure, leads to an enhanced and sustained pro-inflammatory dermal cytokine response^{5,38}. Interestingly, in contrast to their non-attenuated counterparts, RA cercariae either induced delayed IL-10 responses⁷ or failed to induce IL-10 at all¹⁸. Corroborating this, IL-10 deficient mice mounted higher protective immunity after vaccination with RA cercariae³⁹. They also showed massive accumulation of inflammatory cells around invaded parasites, and a delay in schistosomula migration¹⁸. Taken together, these findings illustrate the importance of IL-10 in the down-regulation of the dermal immune response used by *S. mansoni* for the continuation of the parasite life cycle in mice.

Despite the numerous studies of the interaction between *S. mansoni* larvae and murine skin, human dermal APC responses in *ex vivo* skin have not been studied. There are, however, substantial differences between murine and human skin; human skin is anatomically (thickness, muscle layers, dermal papillae and hair follicle density^{40,41}), as well as immunologically distinct from murine skin and consequentially has different immune cell subsets⁴² and differential expression of receptors on dermal APCs⁴³. These features may limit the clinical relevance of findings in mice and demand a set-up that enables immune studies in human skin.

In this study we have used imaging technologies to monitor the human skin invasion of laboratory-reared *S. mansoni* (RA) cercariae *ex vivo*. We analyzed the ensuing human immune response characterizing the phenotype and PD-L1 expression on DDCs and their functional effects on CD4+ T cell polarization (Figure 1).

MATERIALS AND METHODS

Parasite materials

S. mansoni cercariae from the Puerto Rican-strain were shed from *Biomphalaria glabrata* watersnails for 2.5h at 30°C in water. Radiation attenuation was performed by irradiating cercariae at room temperature to a total dose of 20krad using a Cesium radiation source.

For the production of cercarial excretory/secretory products (ES), (RA) cercariae were transformed into schistosomula *in vitro* by centrifugation of 100,000-300,000 cercariae at 1600 rpm for 5 min, after which supernatant was removed and replaced by 12.5 mL of pre-warmed (37°C) RPMI (Invitrogen, Carlsbad, CA, USA) supplemented with Penicillin, Streptomycin, 20 µM pyruvate and 20 µM L-glutamine (Sigma-Aldrich, Zwijndrecht, The Netherlands). Cercariae were incubated at 37°C and 5% CO₂ for 20 min to induce transformation. Tails were separated from schistosomula bodies using an orbital shaker and schistosomula were collected and cultured for 3h at 37°C and 5% CO₂ in a 96-wells plate (4000 schistosomula/mL at 100ul per well). After the culture period, supernatant containing cercarial ES was collected and pooled.

Skin explants

Human skin explants were obtained from collaborating hospitals immediately after abdominal skin reduction surgery (ERB number B18.009, see ethics statement) and kept at 4°C until use (within 6 hours). Subcutaneous fat was removed and the epidermal side thoroughly cleaned with 70% ethanol. Skin pieces were wrapped around an electrically heated pad and placed upon petri dishes filled with either 15ml water or 15 ml water containing (RA) cercariae. Twelve thousand (RA) cercariae were allowed to penetrate a circular skin piece with a diameter of 5cm (surface area 19.6cm²) for 30 minutes, after which the sample was removed, cleaned and biopsied using 6mm punch biopsies. Biopsies were rinsed in RPMI supplemented with 0.1% fetal calf serum (FCS, Bodinco, Alkmaar, The Netherlands) and transferred to a 48 wells plate containing 1ml RPMI 10% FCS per well supplemented with 500U/ml GM-CSF. Emigrated immune cells were collected from the supernatant after 3 days, washed, filtered and stained for Flow Cytometric analysis or irradiated to a total dose of 3000 rad and brought into culture for co-culture assays.

Visualization of cercarial invasion of human skin explants

Small skin explant pieces (4x8 mm) were placed into a confocal dish (ø35mm; MatTek Corporation). To enable imaging, the cercariae were labelled with the fluorescent cyanine dye Cy5-methyl-methyl (500 nM; Interventional molecular imaging group

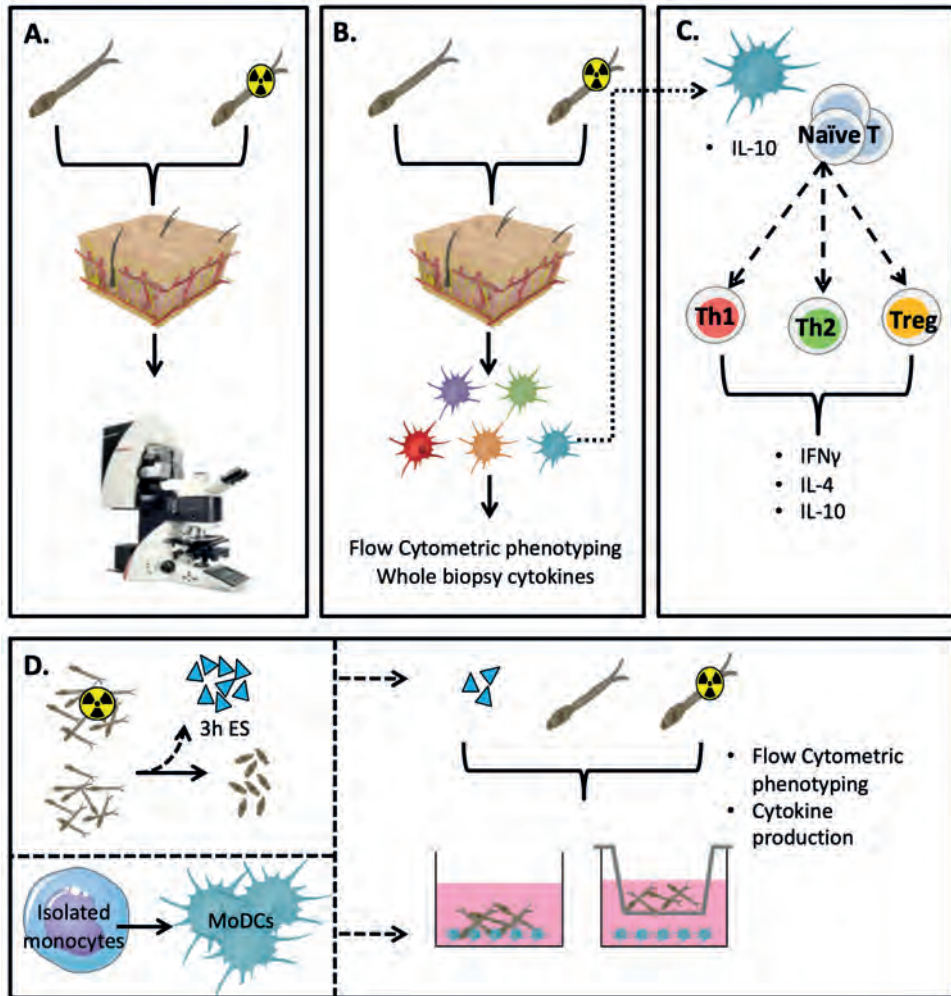


Figure 1. General presentation of the skin invasion set up and immunological markers studied. Skin invasion imaging setup: *S. mansoni* (RA) cercariae are irradiated or kept at RT. Human skin explant pieces are mounted on confocal microscopy dishes and cercariae are added to the epidermal side. Explants are imaged with a confocal microscope. **(A)** Skin explants are exposed to (RA) cercariae in water and cultured to harvest emigrating DDCs **(B)**. DDCs are co-cultured with naive T cells to assess functional effects **(C)**. Monocyte derived dendritic cells (MoDCs) are differentiated from human monocytes. 3h ES products are generated from (RA) schistosomula. Stimulation of MoDCs with (RA) cercariae or their ES products in presence or absence of a transwell.

LUMC, Leiden, The Netherlands⁴⁴). The labelled cercariae were added to the epidermal side of the skin piece and invasion was imaged using the time-lapse function of the Leica TCS (true confocal scanning) SP8X WLL (white light laser) microscope (Leica Microsystems, Wetzlar, Germany; 10x objective). Cy5-methyl-methyl was excited at 633 nm and emission was collected between 650-700 nm. The UV-laser (excitation: 405 nm, emission: 420-470 nm) was used to visualize skin structures (epidermis, epidermal-dermal junction, dermis) based on its auto fluorescence. The cercariae invasion was analyzed using the Leica Application Suite X software (Leica Microsystems, Wetzlar, Germany).

Flow Cytometric analysis

Emigrated dermal dendritic cells were distinguished from other immune cells by their forward and side scatter properties, in addition to high expression of CD11c and HLA-DR. The different DDC subsets were determined using the expression of CD1a, CD14 and CD141: CD141⁺CD14⁻ (referred to as CD141⁺ DDCs), CD1a^{high}CD14⁻ (referred to as LCs), CD1a^{int}CD14⁻ (referred to as CD1a⁺ DDCs) and CD1a⁻CD14⁺ (referred to as CD14⁺ DDCs). Antibodies used were HLA-DR-PerCP-ef710 (L243, eBioscience), CD11c-PE-Cy7 (B-Ly6, BD Pharmingen), CD80-BV650 (L307.4, BD Biosciences), CD1a-AF700 (HI149), CD141-BV421 (M80), lineage cocktail-APC (CD3/19/20/56; Biolegend), CD14-PE-Texas Red (Tuk4, Life Technologies), PDL1-APC (MIH1) and PDL2-PE or PECy7 (MIH18; eBioscience). All conditions were incubated with CD16/32 Fc receptor inhibitor (eBioscience) and Aqua live/dead staining (Invitrogen). Samples were measured using a FACS canto-II (BD Bioscience Franklin Lakes, NJ, USA) and analyzed in FlowJo™ (FlowJo LLC, Ashland, OR, USA).

Naïve CD4⁺ T cell co-culture

For analysis of T cell polarization, 5x10³ emigrated DDCs were irradiated (3000 rad) and co-cultured with 2x10⁴ allogeneic naïve CD4⁺ T cells isolated from buffy coat (Sanquin, Amsterdam, The Netherlands). Co-cultures were performed in the presence of staphylococcal enterotoxin B (10pg/ml). On days 6 and 8, recombinant human IL2 (10U/ml; R&D Systems) was added and the T cells were expanded until day 11. Intracellular cytokine production was analyzed after polyclonal restimulation with 100ng/ml phorbol myristate acetate (PMA) and 1ug/ml ionomycin (Sigma Aldrich) for 6 hours. Brefaldin A (10ug/ml; Sigma Aldrich) was added for the last 4 hours of restimulation. Cells were fixed in 3.7% paraformaldehyde (Sigma Aldrich), permeabilized with permeabilization buffer (eBioscience), stained with antibodies against IL-4 and IFN γ (BD bioscience) and analyzed with flow cytometry. In addition, 10⁵ expanded CD4⁺T cells were restimulated

with antibodies against CD3 and CD28 for 24 hours in a 96-wells plate. Supernatants were harvested and analyzed for IL-10 secretion using standard ELISA (Sanquin, Amsterdam, The Netherlands).

Table 1: Skin invasion by cercariae

| | Cercariae | RA Cercariae |
|------------------------|------------------|---------------------|
| No of imaged cercariae | 45 | 35 |
| Invaded | 23 (51%) | 15 (51%) |
| Lodged in epidermis | 4 | 5 |
| Intact penetration | 14 | 4 |
| Tail shedding | 5 | 9 |

J558-CD40L co-culture

DDCs were co-cultured with a CD40L expressing J558 myeloma line at a 1:1 ratio in a round bottom 96-wells plate. After 24 hours supernatants were harvested and kept at -20 until analyzed for cytokine production by standard ELISA.

Monocyte derived dendritic cells (MoDCs)

Monocytes were isolated from venous whole blood from healthy volunteers and differentiated as described previously⁴⁵. On Day 5, MoDCs were harvested, counted and re-cultured at 35×10^4 cells/well in a 24 wells plate and rested for 24 hours. On day 6 the immature MoDCs were stimulated with *S. mansoni* cercariae or RA cercariae or their ES products (in water, 100 cercariae/well), water control (equivalent volume to cercarial stimulation), LPS (100ng/ml) or medium. For transwell experiments, transwell inserts with 8µm pore size were used (Costar, Corning NY, USA).

RESULTS

Invasion of cercariae into human skin explants

Using our fluorescence-based *S. mansoni* cercariae imaging technique, we were able to monitor the invasion in human skin in real-time (Figure 2; supplementary video 1 and 2). The infectious potential of non-attenuated as well as RA cercariae was confirmed by microscopically imaging the skin interaction. Larvae were seen to attach to the epidermal surface with their tails thrashing, after which they invaded deeper into the epidermis with gliding motion. 23 of the 45 non-attenuated and 18 of the 35 RA

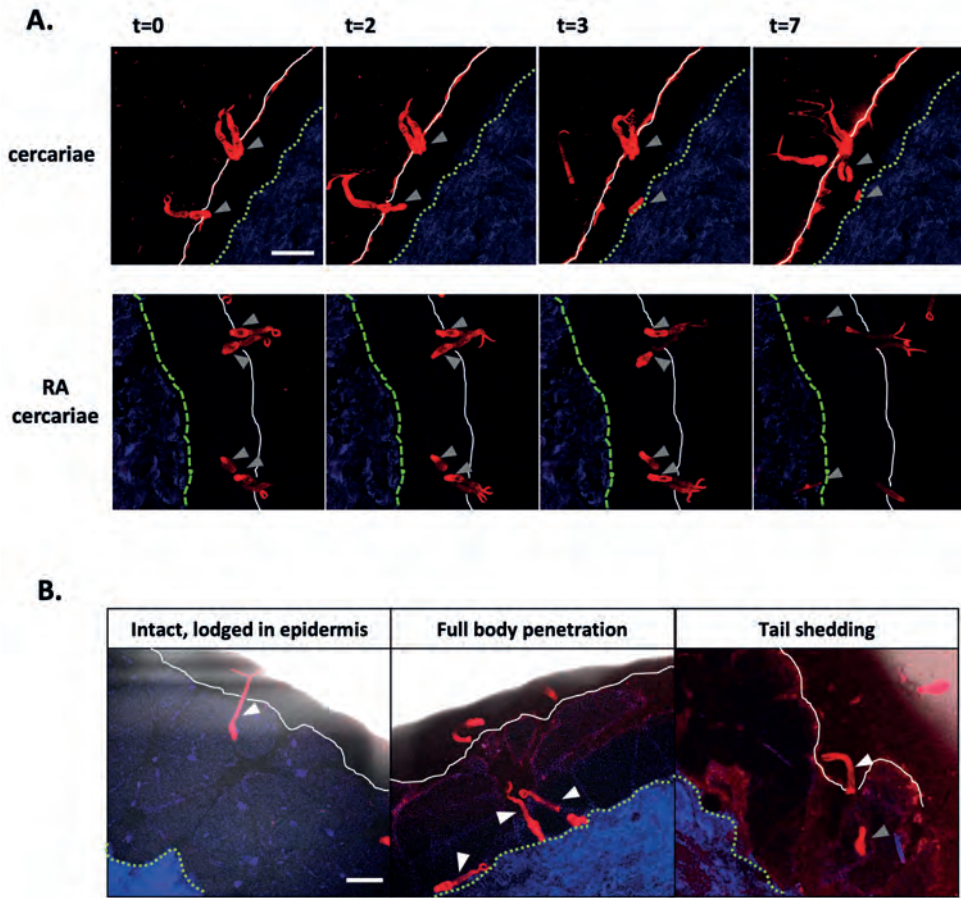


Figure 2. Visualization of cercarial invasion into a human skin explant. Cercariae attach and penetrate the epidermis of the human skin explant. Cercariae depicted in red, the dermis in blue, the epidermal surface as a white solid line and the basal membrane as a green dashed line T=0 to 7 minutes. Gray arrowheads: cercarial heads/schistosomula. Top panels: non-attenuated cercariae, lower panels: RA cercariae (A). Cercariae penetrate the skin in different ways. White arrowheads: cercariae/tails (B). Scale bar: 200 μ m.

cercariae studied (51%) entered the human skin within 30 minutes (non-attenuated cercariae median: 8.5 min, range: 5-10 min Inter Quartile Range (IQR) 2.13 min; RA cercariae median 7.5 min, range 6.5-30 min, IQR 1.5 min) (Figure 2A; Table 1). This invasion time roughly corresponds with previous data in which the authors self-infected with RA cercariae (mean penetration time 6.58 min, 1.57-13.13 min⁴⁶). In general we recorded three different ways of invasion; 1) cercariae penetrated with their heads, remain intact and stay lodged in the epidermis, 2) intact cercariae penetrated the full

thickness of the epidermis, and 3) cercariae penetrated with their heads, shedding their tail on the surface, continuing on as schistosomula (Figure 2B; Table 1). These different ways of invasion were seen for both non-attenuated as well as RA cercariae, although RA cercaria seemed to shed their tail more readily. It is interesting to note that all cercariae which penetrated the epidermis halted migration at the epidermal-dermal junction (time frame 30 min).

Non-attenuated cercariae induce regulatory dermal immune responses

To start addressing the innate immunological responses to cercarial exposure in *ex vivo* exposed human skin biopsies, we determined the subset distribution of the various crawl-out DC populations. Neither exposure of human skin to *S. mansoni* non-attenuated or RA cercariae induced migration of skin APCs or altered their subset distribution (Figure 3; Supplementary Figure S1). However, analysis of the whole biopsy cytokine environment exposed to non-attenuated cercariae revealed an average 2.7 fold increase in the regulatory cytokine IL-10, a 1.4 fold increase in the pro-inflammatory cytokine IL6 and a 3.7-fold increase in inflammatory chemokine of the innate immune response, macrophage inflammatory protein (MIP)1 α (Figure 4A) compared to water exposed controls. These cytokine responses were less pronounced (1.7-fold for IL-10 and 1.6-fold for MIP1 α) or absent (IL-6) in tissue exposed to RA cercariae (Figure 4A). Additionally, we measured chemokines and cytokines previously reported in murine dermal *S. mansoni* models (MIP-1 β , IL-4, IL-12p40, IL-18, IL-23 and IFN γ ^{7,11,12,47}). However, IL-4, IL-12p40, IL-18, IL-23 and IFN γ were not detectable in our model. A trend similar to MIP-1 α was seen for MIP-1 β (data not shown). Next we studied whether skin APCs could be the source of IL-10 by co-culturing crawl-out DDCs with a CD40L-expressing B cell myeloma line, mimicking T cell interaction. We found that DDCs increased their IL-10 production upon exposure to non-attenuated cercariae, which was not seen in DDCs exposed to RA cercariae (Figure 4B). We continued to investigate the phenotype of the exposed crawl-out DDCs in more detail and found an increased expression of immunomodulatory molecules programmed death ligand (PD-L) 1 and 2.

(1.9-fold and 2-fold respectively; Figure 5A) after exposure to non-attenuated cercariae. PD-L1 was primarily upregulated in the CD1a+ DDC population, whereas PD-L2 was overall more prominent in the CD14+ subset and in Langerhans cells (LCs; Figure 5B). For RA cercariae, this upregulation was less pronounced (1.3-fold increase for PD-L1) or absent (PD-L2; Figure 5A). Crawl-out DDCs did not up regulate activation markers CD80 and HLA-DR after (RA) cercariae exposure (Figure 5C).

To assess the ensuing T cell responses, we performed a co-culture assay of allogeneic naïve CD4⁺ T cells with (RA) cercariae exposed crawl-out DDCs. After co-culture with

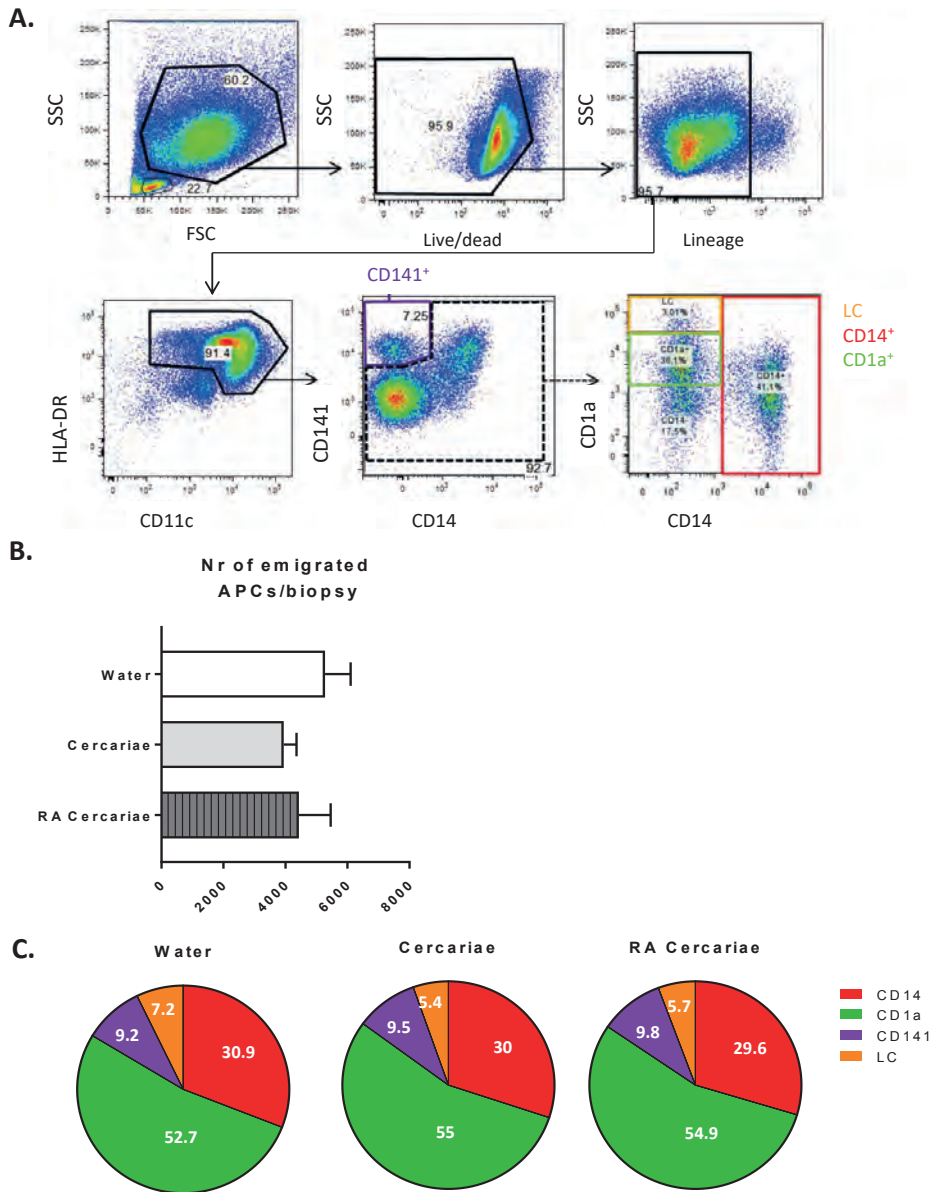


Figure 3. *S. mansoni* cercariae do not induce DDC emigration from the skin. DDC gating strategy. Antigen presenting cells are selected by forward scatter (FSC) and side scatter (SSC) characteristics. Doublets are excluded (not shown). Live cells are gated and selected for the lack of lineage markers (CD56, CD3, CD19, CD20). APCs are selected on the expression of HLA-DR as well as intermediate to high levels of CD11c. HLA-DR⁺, CD11c⁺ cells can be divided into the different DDC populations: CD141⁺, LC, CD1a⁺ and CD14⁺ (A). Subset distribution of emigrated cells (B). Total emigrated HLA-DR⁺, CD11c⁺ antigen presenting cells from dermal biopsies at 3 days post exposure to *S. mansoni* cercariae or water control. Mean ± SEM, n=7 (C).

DDCs exposed to non-attenuated cercariae, CD4⁺T cells produced less IFN γ and showed a trend of increased IL-10 production (Figure 6), suggesting regulatory potential of these DDCs. In line with our phenotypic analysis, this functional regulatory potential was not seen for RA cercariae exposed DDCs (Figure 6). A summary of the detected dermal immune responses can be found in Table 2.

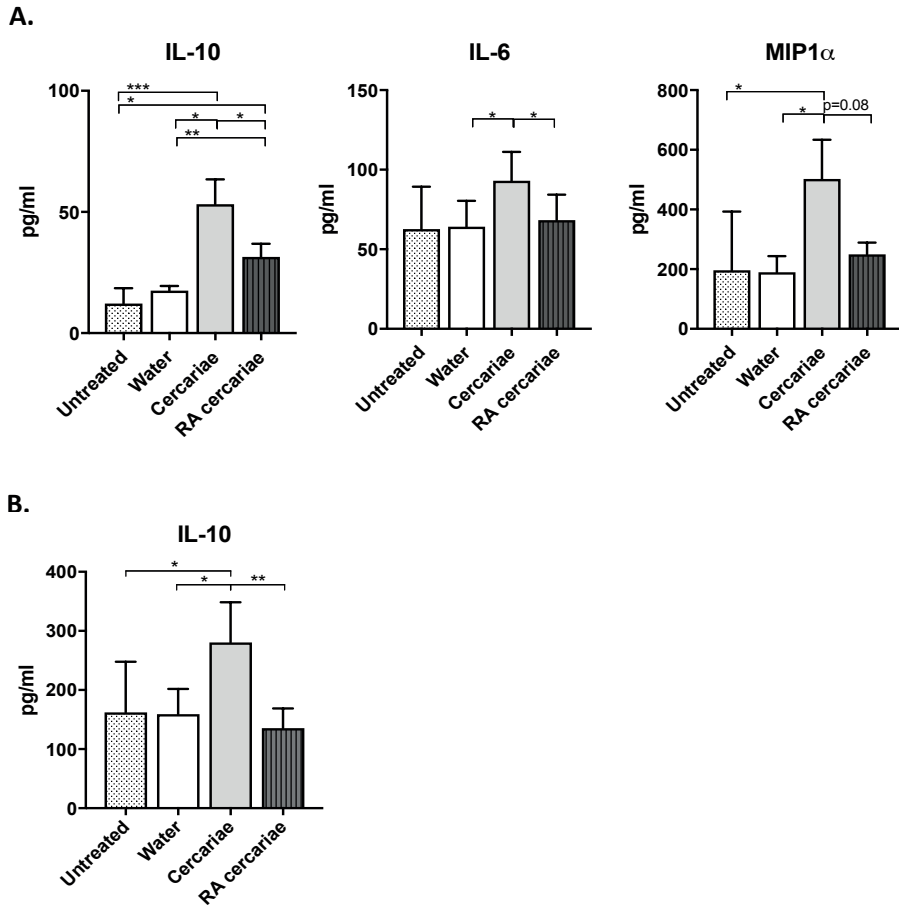


Figure 4. Increased production of IL-6 and IL-10 and MIP1 α in skin exposed to cercariae. Whole biopsy cytokine analysis at 3 days post exposure to non-attenuated *Sm* cercariae show an increase in IL-6, IL-10 and MIP1 α . The effect is less pronounced in radiation attenuated cercariae. (A). IL-10 production by DDCs after co-culture of emigrated DDCs with CD40L expressing cell line, 7 donors. (B). Data shown in pg/ml, mean \pm SEM. * = $p < 0.05$, ** = $p < 0.01$, *** = $p < 0.001$ using paired Student's T test on log transformed data.

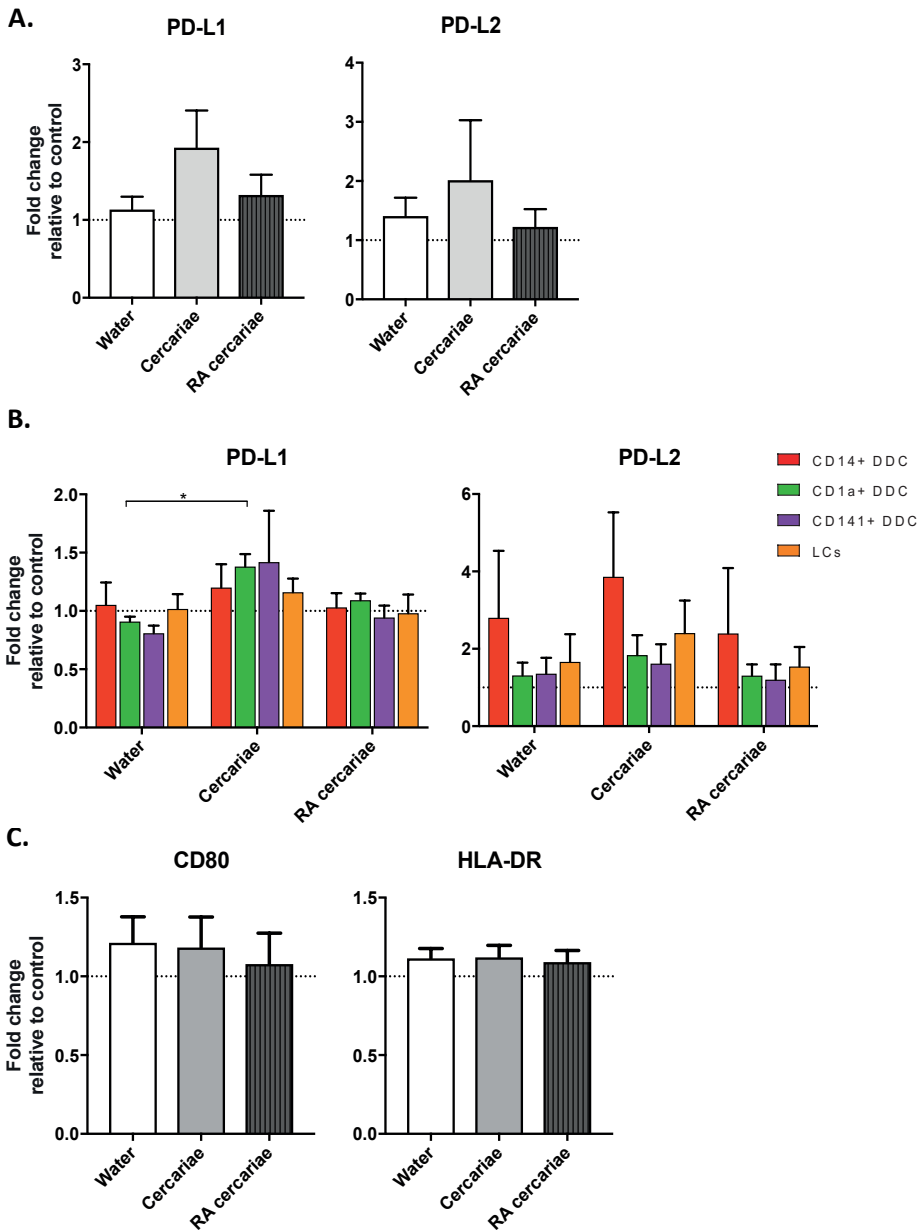


Figure 5. DDCs do not increase activation markers upon cercaria exposure but do show a trend of increased levels of immunoregulatory markers PD-L1 and PD-L2. Immunoregulatory markers PD-L1 and 2 are up regulated in DDCs when exposed to Cercariae but not RA Cercariae (n=3) (A). PD-L1 expression primarily occurs in CD1a⁺ DDCs. (n=3) (B). CD80 and HLA-DR expression in total emigrated HLA-DR⁺, CD11c⁺ antigen presenting cells from dermal biopsy at 84 hours post exposure to *S. mansoni* cercariae or water control (n=7) (C). Mean ± SEM.

Direct contact with (RA) cercariae is necessary to induce a regulatory phenotype in monocyte-derived dendritic cells

To further investigate APC phenotype in response to *S. mansoni* antigens, we generated monocyte-derived dendritic cells (moDCs) isolated from healthy volunteers and incubated these cells with (RA) cercariae. We found increased expression of activation markers CD80, CD86 and CD40, but not HLA-DR, (Figure 7A) in stimulated MoDCs. However, similar to their DDC counterparts, MoDCs strongly up regulated expression of immune regulatory molecules PD-L1 and PD-L2 (Figure 7B). Complementing these findings, MoDCs give an increased production of IL-10 upon stimulation with (RA) cercariae (Figure 7C). In contrast to exposure in skin, there was no significant difference between non-attenuated and RA cercariae in this *in vitro* setup. Table 3 summarizes the MoDC phenotype findings.

In order to dissect whether the immunosuppressive phenotype of DCs was induced by direct interaction of the APC with *S. mansoni* or a response to their ES products, we performed a transwell assay which physically separates the MoDCs from the (RA) cercariae. Interestingly, PD-L1 and PD-L2 upregulation was partly dependent on the direct contact of cells with (RA) cercariae (Figure 8A). And indeed, incubation of MoDCs with ES products of transformed (RA) cercariae alone did not induce PD-L1 and PD-L2 expression (Figure 8B). In addition to PD-L1 and PD-L2 up regulation, MoDCs increased their production of IL-10 only when allowed direct contact with (RA) cercariae, whereas transwell stimulation or ES stimulation did not induce IL-10 production (Figure 8C).

DISCUSSION

For the first time we visualized human skin invasion by *S. mansoni* cercariae and show that these larvae subsequently drive expression of PD-L1 and 2 and IL-10 by human DDCs, indicative of a regulatory phenotype. In line with their regulatory phenotype, these DDCs suppress Th1 priming, and favor the induction of regulatory cytokine IL-10 by T cells. RA cercariae were less capable of inducing skin immune suppression. These findings may help to explain why, in contrast to RA cercariae, exposure to non-attenuated cercariae fails to initiate a protective immune response. The early differences in the immune responses to non-attenuated and RA cercariae imply that priming of the protective immune response against RA *S. mansoni*, is initiated immediately after invasion, by APCs of the dermis. Whether immune priming in the skin draining lymph node alone is sufficient to establish protective immunity remains a long-standing matter of debate⁴⁸⁻⁵⁰. Previously published epidemiological data revealed that individuals infected with parasitic worms (helminths) such as *S. mansoni* show elevated

serum levels of IL-10⁵¹⁻⁵⁴. Taken together, our results support the hypothesis that active suppression of immune responses is initiated immediately after infection, at the dermal stages of *S. mansoni* infection. This propensity of *S. mansoni* larvae to promote T cell hyporesponsiveness may, in part, explain why cercarial dermatitis is a subtle clinical phenomenon^{10,18}.

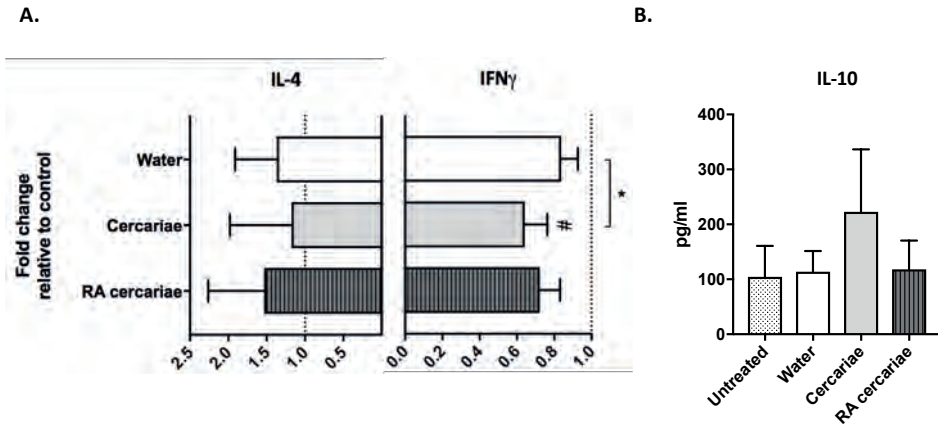


Figure 6. Stimulation with cercariae reduces pro-inflammatory potential of DDCs. Emigrated DDCs were co-cultured with CD4⁺ T cells to assess immunomodulatory potential. Data shown as percentages IFN γ or IL4 producing CD4⁺ T cells cultured with *ex vivo* stimulated DDCs relative to CD4⁺ T cells cultured with DDCs from untreated skin after PMA/ionomycin stimulation. Mean \pm SEM. * = $p < 0.05$, using paired Student's T test (A). IL-10 production by CD4⁺ T cells after co-culture with DDCs. ELISA on culture supernatants after 24h stimulation with anti CD3/28 (B). Data shown in pg/ml. Mean \pm SEM.

The human skin cytokine responses to *S. mansoni* correspond with data in murine models, which also show a dermal invasion site rich in IL-10 and a less pronounced increase in pro-inflammatory cytokines IL6 and MIP- α and β ^{7,11,12,47}. The source of IL-10 in the skin is still unclear. Several dermal cell-types, such as lymphocytes and keratinocytes have been shown to produce IL-10 in response to *S. mansoni* larvae^{18,55}. Additionally, dermal mast cells are a known source of IL-10 in a variety of skin diseases⁵⁵ and cercarial ES products have been shown to affect these cells by triggering their degranulation. Our data, however, suggests that dermal APCs are an important source of dermal IL-10 enrichment in response to cercariae. In addition, we observed a small increase in the levels of pro-inflammatory cytokine IL-6 and innate inflammatory chemokine MIP-1 α . These results are in line with previous reports using murine dermal *S. mansoni* models⁷ and highlight that the cumulative dermal immune response to *S. mansoni* is

a delicate balance between innate pro-inflammatory signals and a modulatory IL-10 response. In RA cercariae, this immune suppression is less pronounced, corroborating murine skin data⁷. Also in line with murine data⁴⁷, our research shows increased IL-10 production by naïve CD4+ T cells after co-culture with cercariae-exposed DDCs. However, contrary to what has previously been found in the murine skin draining lymph node⁵⁶ we detected a significant reduction in Th1 priming of CD4+ T cells in response to non-attenuated cercariae, highlighting differences between human and mouse skin responses in *S. mansoni* infection. Despite the fact that the *ex vivo* human skin explant model lacks blood flow, excellent viability of dermal cells in cultured skin biopsies is maintained for a long period of time^{57,58}, making this model a valuable method which can aid in understanding human immune responses during natural infections in a three dimensional organization.

Table 2. Immune phenotype of (RA) cercariae stimulated DDCs.

| | Cercariae | RA Cercariae |
|---------------------------------------|-----------|--------------|
| DDC Phenotype | | |
| CD80 | = | = |
| HLA-DR | = | = |
| PD-L1 | ↑ | = |
| PD-L2 | ↑ | = |
| IL-10 production | ↑↑ | = |
| Dermal Cytokines | | |
| IL-10 | ↑↑ | ↑ |
| IL-6 | ↑ | = |
| MIP-1 | ↑↑ | ↑ |
| Naïve T-cell Responses to DDCs | | |
| IFNg | ↓ | = |
| IL-4 | = | = |
| IL-10 | ↑ | = |

The symbols =, ↓ and ↑ signify similar levels, a decrease or an increase respectively, compared to water exposed control

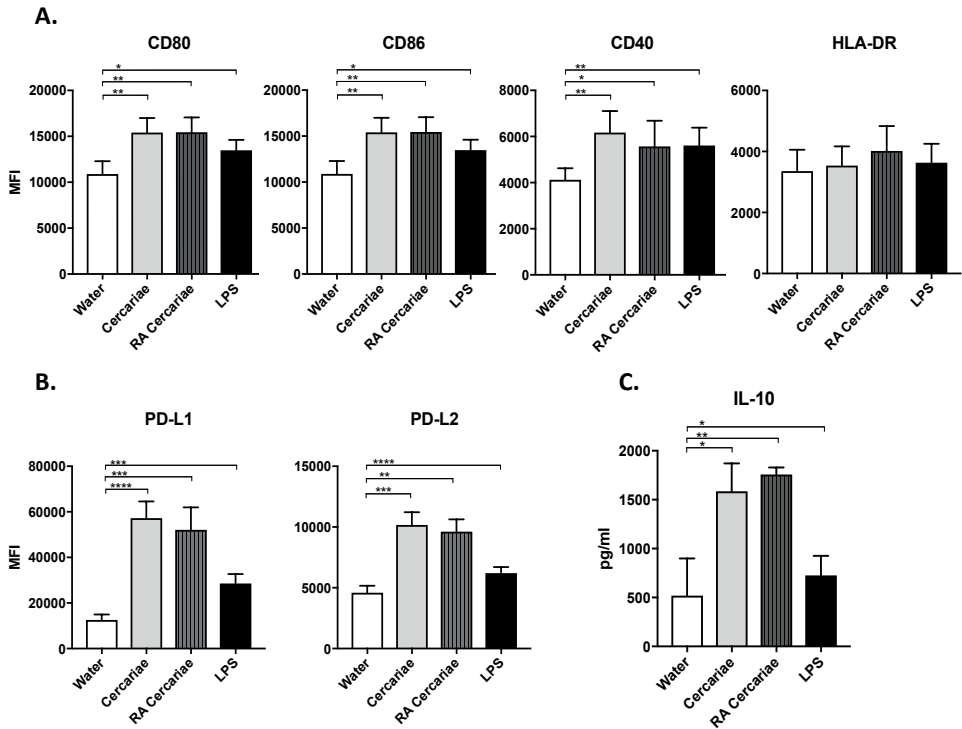


Figure 7. Cercaria stimulation activates MoDCs but also induces up regulation of immunoregulatory markers PD-L1 and 2 and regulatory cytokine IL-10 production. Stimulation of MoDCs with (RA) cercariae up regulates activation markers CD80, CD86 and CD40. **(A)** PD-L1 and PD-L2 up regulation after cercaria stimulation. **(B)** IL-10 production by MoDCs after 48h stimulation, data shown as pg/ml **(C)** Mean \pm SEM. * $p < 0.05$, ** $p < 0.005$, *** $p < 0.0005$, **** $p < 0.0001$ using paired student's T test (on log transformed data for IL-10).

A potential mechanism by which *S. mansoni* is able to regulate immune activation is the excretion of ES products, which have been described to exhibit regulatory potential^{119,59-61}. However, we find that direct contact of the parasite with immune cells is needed to induce the immunosuppressive effects on human MoDCs. Interestingly, immunomodulatory markers PD-L1 and 2 were primarily induced by non-attenuated cercariae in the skin explant model, while *in vitro* MoDCs up regulated these markers in response to direct contact with both non-attenuated as well as RA cercariae. This may indicate that dermal migratory behavior of (RA) cercariae may influence DDC-cercarial contact and thus alter the ensuing immune responses as has been previously suggested^{5,38}. Because migration does not affect the cellular contacts in the *in vitro* assay, this effect may be lost *in vitro*. Using a cell-labelling dye we visualized *S. mansoni* cercarial penetration in

human skin and confirmed cercarial penetration. Using this technique, we could clearly visualize the fate of the tail in the skin. A previous study applying confocal imaging to investigate cercarial invasion into mouse ear pinnae showed comparable invasion behavior, although all cercariae imaged in this study displayed tail loss upon entry⁶². Tail loss at the moment of skin entry has been assumed previously, but contradicted by some authors^{46,63,64}. It has been suggested that delayed tail loss might be a mechanism by which the host immune response is diverged away from targeting adult worms⁶³. RA cercaria seem to be less capable of doing so. Potentially, differences in the timing of tail shedding between non-attenuated and RA cercariae may be responsible for the differential immunological effect in skin. After penetration, *S. mansoni* cercariae shed their surrounding glycocalyx, which protects them during the aquatic stage of the life cycle. This shedding exposes the cercarial membrane and its molecules and therefore timing may be critical to the ensuing immune response. Although phagocytosis of cercarial ES products by APCs in the dermis results in their activation and the production of pro-inflammatory cytokines⁶², surprisingly little is known about membrane-bound molecules on cercariae and/or schistosomula and the DDC receptors that recognize them during direct contact. Further research is needed to fully understand the molecular basis through which *S. mansoni* modifies APC function at this stage of the life cycle.

Table 3. Immune phenotype of (RA) cercariae stimulated Monocyte derived DCs.

| | Cercariae | RA Cercariae |
|-----------------------|-----------|--------------|
| MoDC Phenotype | | |
| CD80 | ↑ | ↑ |
| CD86 | ↑ | ↑ |
| CD40 | ↑ | ↑ |
| HLA-DR | = | = |
| PD-L1 | ↑↑ | ↑↑ |
| PD-L2 | ↑↑ | ↑↑ |
| IL-10 production | ↑↑ | ↑↑ |

The symbols =, ↓ and ↑ signify similar levels, a decrease or an increase respectively, compared to water exposed control.

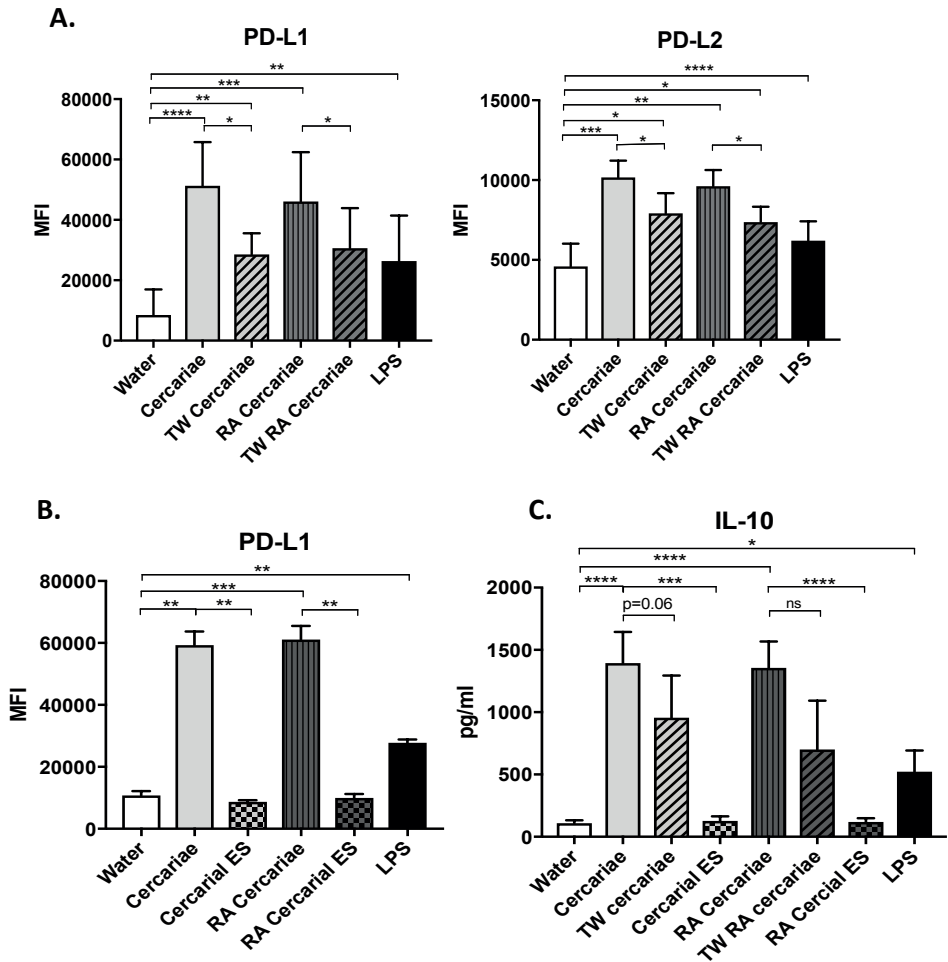


Figure 8. Direct contact with cercariae but not cercarial ES products increases immunoregulatory markers PD-L1 and 2 and IL-10 secretion. PD-L1 and PD-L2 up regulation after cercaria stimulation in presence or absence of direct contact (TW=transwell) (A). PD-L1 expression after stimulation with cercariae or cercarial ES alone. The ES dose was matched to the number of cercariae used for stimulation (B). IL-10 production of MoDCs after stimulation with cercariae or their products (C). Mean \pm SEM. * $p < 0.05$, ** $p < 0.005$, *** $p < 0.0005$ using paired student's T test (on log transformed data for IL-10).

Our finding that *S. mansoni* cercariae induce upregulation of PD-L1/2 in both DDCs as well as MoDCs suggests that, similar to cancer cells, *S. mansoni* may exploit the PD-1 pathway to inhibit the adaptive immune response starting in the human dermis. Recently, PD-L1 and PD-L2 upregulation has been demonstrated in monocytes exposed to *Brugia malayi*, the causative parasitic agent for filariasis⁶⁵, indicating that the effect on PD-L1/2 in phagocytic APCs may be part of an immune-regulatory pathway employed by different parasites. This suggests PD-1 or PD-L1/2 targets could potentially be used in the development of vaccines against parasitic diseases.

In conclusion, we visualized cercarial invasion into human skin and demonstrate that, similarly to rodent models, *S. mansoni* cercariae are able to induce a regulatory dermal immune response. In our human model, this response is characterized by expression of PD-L1/2, excretion of IL-10 and the suppression of IFN γ producing CD4+ T cells. This process is less well mastered by RA cercariae, which may explain, in part, why they are superior immunogens. An understanding of the immune suppressive capacity of *S. mansoni* in human skin may give clues towards the development of novel therapies, or directly impact the development of an effective schistosome vaccine.

SUPPLEMENTARY NOTES

Author Contributions Statement: The methodology was developed by BW, CK, FL, BE, LP, MY, EJ and MR. Experiments were performed and interpreted by BW, MD, CF, ML, CK, MG and LP and supervised by HS, RH, BE and MR. BW and MR drafted the manuscript. All authors reviewed and contributed to finalizing the manuscript.

Acknowledgments: The authors would like to thank Janneke Kos-van Oosterhoud and Arifa Ozir-Fazalalikhani for their efforts on maintaining the parasite life cycle and Toni van Capel for her help in establishing the skin explant protocol. MR was supported by a VENI grant from ZONMW and a Gisela Thier fellowship from the LUMC.

Ethics statement: The use of human skin explants (obtained as waste material after abdominal reduction surgery) for this research was approved by the Commission Medical Ethics (CME) of the LUMC, Leiden. Approval number CME: B18-009.

Conflict of Interest Statement: The authors declare no conflict of interest.

REFERENCES

1. Wheeler P. R., Wilson R. A. *Schistosoma mansoni*: a histological study of migration in the laboratory mouse. *Parasitology*. 1979;79(1):49-62.
2. Mangold B. L., Dean D. A. Autoradiographic analysis of *Schistosoma mansoni* migration from skin to lungs in naive mice. Evidence that most attrition occurs after the skin phase. *Am J Trop Med Hyg*. 1983;32(4):785-9.
3. Wilson R. A., Coulson P. S., Sturrock R. F., Reid G. D. Schistosome migration in primates: a study in the olive baboon (*Papio anubis*). *Trans R Soc Trop Med Hyg*. 1990;84(1):80-3.
4. Di Meglio P., Perera G. K., Nestle F. O. The multitasking organ: recent insights into skin immune function. *Immunity*. 2011;35(6):857-69.
5. Mountford A. P., Trottein F. Schistosomes in the skin: a balance between immune priming and regulation. *Trends Parasitol*. 2004;20(5):221-6.
6. Incani R. N., McLaren D. J. Histopathological and ultrastructural studies of cutaneous reactions elicited in naive and chronically infected mice by invading schistosomes of *Schistosoma mansoni*. *Int J Parasitol*. 1984;14(3):259-76.
7. Hogg K. G., Kumkate S., Anderson S., Mountford A. P. Interleukin-12 p40 secretion by cutaneous CD11c+ and F4/80+ cells is a major feature of the innate immune response in mice that develop Th1-mediated protective immunity to *Schistosoma mansoni*. *Infect Immun*. 2003;71(6):3563-71.
8. Bottieau E., Clerinx J., de Vega M. R., Van den Enden E., Colebunders R., Van Esbroeck M., et al. Imported Katayama fever: clinical and biological features at presentation and during treatment. *J Infect*. 2006;52(5):339-45.
9. Ross A. G., Vickers D., Olds G. R., Shah S. M., McManus D. P. Katayama syndrome. *Lancet Infect Dis*. 2007;7(3):218-24.
10. Langenberg M. C. C., Hoogerwerf M., Janse J. J., van Lieshout L., van Dam G. J., Roestenberg M. Katayama fever in an experimental *Schistosoma mansoni* infection without eggs (Manuscript submitted 2018).
11. Hogg K. G., Kumkate S., Mountford A. P. IL-10 regulates early IL-12-mediated immune responses induced by the radiation-attenuated schistosome vaccine. *Int Immunol*. 2003;15(12):1451-9.
12. Angeli V., Faveeuw C., Roye O., Fontaine J., Teissier E., Capron A., et al. Role of the parasite-derived prostaglandin D2 in the inhibition of epidermal Langerhans cell migration during schistosomiasis infection. *J Exp Med*. 2001;193(10):1135-47.
13. Kumkate S., Jenkins G. R., Paveley R.A., Hogg K.G., Mountford A.P. CD207+ Langerhans cells constitute a minor population of skin-derived antigen-presenting cells in the draining lymph node following exposure to *Schistosoma mansoni*. *Int J Parasitol*. 2007;37(2):209-20.
14. He Y. X., Chen L., Ramaswamy K. *Schistosoma mansoni*, *S. haematobium*, and *S. japonicum*: early events associated with penetration and migration of schistosomes through human skin. *Exp Parasitol*. 2002;102(2):99-108.
15. Kourilova P., Hogg K. G., Kolarova L., Mountford A. P. Cercarial dermatitis caused by bird schistosomes comprises both immediate and late phase cutaneous hypersensitivity reactions. *J Immunol*. 2004;172(6):3766-74.
16. Salafsky B., Fusco A. C. *Schistosoma mansoni*: a comparison of secreted vs nonsecreted eicosanoids in developing schistosomulae and adults. *Exp Parasitol*. 1987;64(3):361-7.
17. Ramaswamy K., Salafsky B., Potluri S., He Y. X., Li J. W., Shibuya T. Secretion of an anti-inflammatory, immunomodulatory factor by Schistosomulae of *Schistosoma mansoni*. *J Inflamm*. 1995;46(1):13-22.
18. Ramaswamy K., Kumar P., He Y. X. A role for parasite-induced PGE2 in IL-10-mediated host immunoregulation by skin stage

- schistosomula of *Schistosoma mansoni*. *J Immunol.* 2000;165(8):4567-74.
19. Sanin D. E., Mountford A. P. Sm16, a major component of *Schistosoma mansoni* cercarial excretory/secretory products, prevents macrophage classical activation and delays antigen processing. *Parasit Vectors.* 2015;8:1.
 20. Hansell E., Braschi S., Medzihradsky K. F., Sajid M., Debnath M., Ingram J., et al. Proteomic analysis of skin invasion by blood fluke larvae. *PLoS Negl Trop Dis.* 2008;2(7):e262.
 21. Keir M. E., Liang S. C., Guleria I., Latchman Y.E., Qipo A., Albacker L. A., et al. Tissue expression of PD-L1 mediates peripheral T cell tolerance. *J Exp Med.* 2006;203(4):883-95.
 22. Okazaki T., Honjo T. The PD-1-PD-L pathway in immunological tolerance. *Trends Immunol.* 2006;27(4):195-201.
 23. Brown J. A., Dorfman D. M., Ma F. R., Sullivan E. L., Munoz O., Wood C. R., et al. Blockade of programmed death-1 ligands on dendritic cells enhances T cell activation and cytokine production. *J Immunol.* 2003;170(3):1257-66.
 24. Carreno B. M., Collins M. The B7 family of ligands and its receptors: new pathways for costimulation and inhibition of immune responses. *Annu Rev Immunol.* 2002;20:29-53.
 25. Dong H., Chen L. B7-H1 pathway and its role in the evasion of tumor immunity. *J Mol Med (Berl).* 2003;81(5):281-7.
 26. Keir M. E., Butte M. J., Freeman G. J., Sharpe A. H. PD-1 and its ligands in tolerance and immunity. *Annu Rev Immunol.* 2008;26:677-704.
 27. Francisco L. M., Salinas V. H., Brown K. E., Vanguri V. K., Freeman G. J., Kuchroo V. K., et al. PD-L1 regulates the development, maintenance, and function of induced regulatory T cells. *J Exp Med.* 2009;206(13):3015-29.
 28. Day C. L., Kaufmann D. E., Kiepiela P., Brown J. A., Moodley E. S., Reddy S., et al. PD-1 expression on HIV-specific T cells is associated with T-cell exhaustion and disease progression. *Nature.* 2006;443(7109):350-4.
 29. Horne-Debets J. M., Faleiro R., Karunarathne D. S., Liu X. Q., Lineburg K. E., Poh C. M., et al. PD-1 dependent exhaustion of CD8+ T cells drives chronic malaria. *Cell Rep.* 2013;5(5):1204-13.
 30. Huang X., Venet F., Wang Y. L., Lepape A., Yuan Z., Chen Y., et al. PD-1 expression by macrophages plays a pathologic role in altering microbial clearance and the innate inflammatory response to sepsis. *Proc Natl Acad Sci U S A.* 2009;106(15):6303-8.
 31. Xiao J., Li Y., Yolken R. H., Viscidi R. P. PD-1 immune checkpoint blockade promotes brain leukocyte infiltration and diminishes cyst burden in a mouse model of *Toxoplasma* infection. *J Neuroimmunol.* 2018;319:55-62.
 32. Smythies L. E., Pemberton R. M., Coulson P. S., Mountford A. P., Wilson R. A. T cell-derived cytokines associated with pulmonary immune mechanisms in mice vaccinated with irradiated cercariae of *Schistosoma mansoni*. *J Immunol.* 1992;148(5):1512-8.
 33. Bickle Q., Bain J., McGregor A., Doenhoff M. Factors affecting the acquisition of resistance against *Schistosoma mansoni* in the mouse: III. The failure of primary infections with cercariae of one sex to induce resistance to reinfection. *Trans R Soc Trop Med Hyg.* 1979;73(1):37-41.
 34. Wilson R. A. Leaky livers, portal shunting and immunity to schistosomes. *Parasitol Today.* 1990;6(11):354-8.
 35. de Jesus A. R., Araujo I., Bacellar O., Magalhaes A., Pearce E., Harn D., et al. Human immune responses to *Schistosoma mansoni* vaccine candidate antigens. *Infection and Immunity.* 2000;68(5):2797-803.
 36. Wynn T. A., Reynolds A, James S., Cheever A. W., Caspar P., Hieny S., et al. IL-12 enhances vaccine-induced immunity to schistosomes by augmenting both humoral and cell-mediated immune responses against the parasite. *J Immunol.* 1996;157(9):4068-78.
 37. Anderson S., Shires V. L., Wilson R. A., Mountford A. P. In the absence of IL-12, the induction of Th1-mediated protective

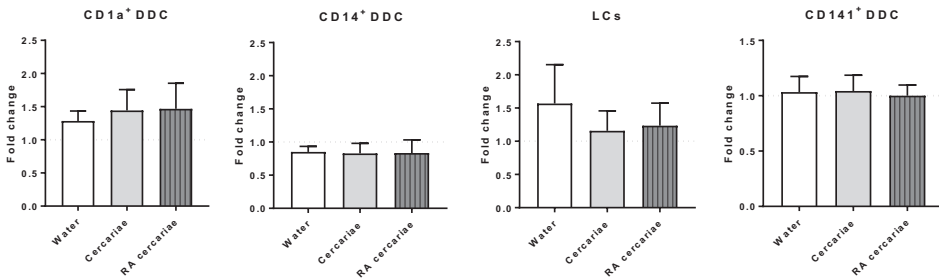
- immunity by the attenuated schistosome vaccine is impaired, revealing an alternative pathway with Th2-type characteristics. *Eur J Immunol.* 1998;28(9):2827-38.
38. Mountford A. P., Coulson P. S., Wilson R. A. Antigen localization and the induction of resistance in mice vaccinated with irradiated cercariae of *Schistosoma mansoni*. *Parasitology.* 1988;97 (Pt 1):11-25.
 39. Hoffmann K. F., James S. L., Cheever A. W., Wynn T. A. Studies with double cytokine-deficient mice reveal that highly polarized Th1- and Th2-type cytokine and antibody responses contribute equally to vaccine-induced immunity to *Schistosoma mansoni*. *J Immunol.* 1999;163(2):927-38.
 40. Pasparakis M., Haase I., Nestle F. O. Mechanisms regulating skin immunity and inflammation. *Nat Rev Immunol.* 2014;14(5):289-301.
 41. Treuting P. M., Dintzis S. M., Liggitt D., Frevert C. W. *Comparative Anatomy and Histology: A Mouse and Human Atlas.* Academic Press, Elsevier. 2012;Chapter 23:433-41.
 42. Mestas J., Hughes C. C. Of mice and not men: differences between mouse and human immunology. *J Immunol.* 2004;172(5):2731-8.
 43. Kashem S. W., Haniiffa M., Kaplan D. H. Antigen-Presenting Cells in the Skin. *Annu Rev Immunol.* 2017;35:469-99.
 44. Winkel B. M. F., van Oosterom M. N., de Korne C. M., Staphorst D., Bunschoten A., Langenberg M. C. C., et al. A tracer-based method enables tracking of *Plasmodium falciparum* malaria parasites during human skin infection. *Theranostics* 2019 13;9(10):2768-2778.
 45. Hussaarts L., Smits H. H., Schramm G., van der Ham A. J., van der Zon G. C., Haas H., et al. Rapamycin and omega-1: mTOR-dependent and -independent Th2 skewing by human dendritic cells. *Immunol Cell Biol.* 2013;91(7):486-9.
 46. Haas W., Haeberlein S. Penetration of cercariae into the living human skin: *Schistosoma mansoni* vs. *Trichobilharzia szidati*. *Parasitol Res.* 2009;105(4):1061-6.
 47. Sanin D. E., Prendergast C. T., Bourke C. D., Mountford A. P. Helminth Infection and Commensal Microbiota Drive Early IL-10 Production in the Skin by CD4+ T Cells That Are Functionally Suppressive. *PLoS Pathog.* 2015;11(5):e1004841.
 48. Mountford A. P., Coulson P. S., Pemberton R. M., Smythies L. E., Wilson R. A. The generation of interferon-gamma-producing T lymphocytes in skin-draining lymph nodes, and their recruitment to the lungs, is associated with protective immunity to *Schistosoma mansoni*. *Immunology.* 1992;75(2):250-6.
 49. Coulson P. S., Wilson R. A. Recruitment of lymphocytes to the lung through vaccination enhances the immunity of mice exposed to irradiated schistosomes. *Infect Immun.* 1997;65(1):42-8.
 50. Mountford A. P., Wilson R. A. *Schistosoma mansoni*: the effect of regional lymphadenectomy on the level of protection induced in mice by radiation-attenuated cercariae. *Exp Parasitol.* 1990;71(4):463-9.
 51. Anthony R. M., Rutitzky L. I., Urban J. F., Stadecker M. J., Gause W. C. Protective immune mechanisms in helminth infection. *Nat Rev Immunol.* 2007;7(12):975-87.
 52. Araujo M. I., Lopes A. A., Medeiros M., Cruz A. A., Sousa-Atta L., Sole D., et al. Inverse association between skin response to aeroallergens and *Schistosoma mansoni* infection. *Int Arch Allergy Immunol.* 2000;123(2):145-8.
 53. van den Biggelaar A. H., van Ree R., Rodrigues L. C., Lell B., Deelder A. M., Kremsner P. G., et al. Decreased atopy in children infected with *Schistosoma haematobium*: a role for parasite-induced interleukin-10. *Lancet.* 2000;356(9243):1723-7.
 54. Yazdanbakhsh M., Kremsner P. G., van Ree R. Allergy, parasites, and the hygiene hypothesis. *Science.* 2002;296(5567):490-4.

55. Galli S. J., Grimaldeston M., Tsai M. Immunomodulatory mast cells: negative, as well as positive, regulators of immunity. *Nat Rev Immunol.* 2008;8(6):478-86.
56. Kumar P, Ramaswamy K. Vaccination with irradiated cercariae of *Schistosoma mansoni* preferentially induced the accumulation of interferon-gamma producing T cells in the skin and skin draining lymph nodes of mice. *Parasitol Int.* 1999;48(2):109-19.
57. Frade M. A., Andrade T. A., Aguiar A. F., Guedes F. A., Leite M. N., Passos W. R., et al. Prolonged viability of human organotypic skin explant in culture method (hOSEC). *An Bras Dermatol.* 2015;90(3):347-50.
58. Gunawan M., Jardine L., Haniffa M. Isolation of Human Skin Dendritic Cell Subsets. *Methods Mol Biol.* 2016;1423:119-28.
59. Harn D. A., Cianci C. M., Caulfield J. P. *Schistosoma mansoni*: immunization with cercarial glycocalyx preparation increases the adult worm burden. *Exp Parasitol.* 1989;68(1):108-10.
60. Fallon P. G., Teixeira M. M., Neice C. M., Williams T. J., Hellewell P. G., Doenhoff M. J. Enhancement of *Schistosoma mansoni* infectivity by intradermal injections of larval extracts: a putative role for larval proteases. *J Infect Dis.* 1996;173(6):1460-6.
61. Paveley R. A., Aynsley S. A., Turner J. D., Bourke C. D., Jenkins S. J., Cook P. C., et al. The Mannose Receptor (CD206) is an important pattern recognition receptor (PRR) in the detection of the infective stage of the helminth *Schistosoma mansoni* and modulates IFN γ production. *Int J Parasitol.* 2011;41(13-14):1335-45.
62. Paveley R. A., Aynsley S. A., Cook P. C., Turner J. D., Mountford A.P. Fluorescent imaging of antigen released by a skin-invading helminth reveals differential uptake and activation profiles by antigen presenting cells. *PLoS Negl Trop Dis.* 2009;3(10):e528.
63. Whitfield P. J., Bartlett A., Khammo N., Brain A. P., Brown M. B., Marriott C., et al. Delayed tail loss during the invasion of human skin by schistosome cercariae. *Parasitology.* 2003;126(Pt 2):135-40.
64. Wang T, Fang Z. M., Lei J. H., Guan F., Liu W. Q., Bartlett A., et al. Delayed tail loss during the invasion of mouse skin by cercariae of *Schistosoma japonicum*. *Parasitology.* 2012;139(2):244-7.
65. Narasimhan P. B., Akabas L., Tariq S., Huda N., Bennuru S., Sabzevari H., et al. Similarities and differences between helminth parasites and cancer cell lines in shaping human monocytes: Insights into parallel mechanisms of immune evasion. *PLoS Negl Trop Dis.* 2018;12(4):e0006404

SUPPLEMENTARY INFORMATION

Supplementary information, including video material, is available at *frontiers in Immunology* online: <https://www.frontiersin.org/articles/10.3389/fimmu.2018.02510/full#supplementary-material>

A.



B.

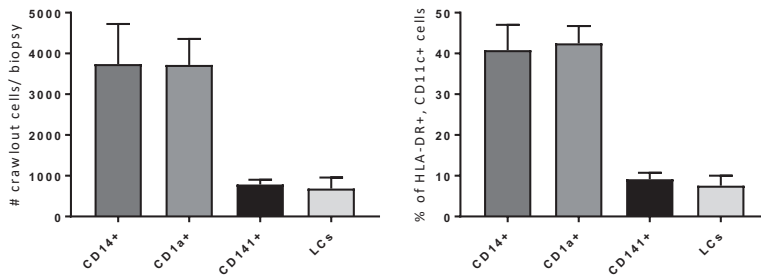


Figure S1. Subset distribution of DDCs in skin. A. DDC subset changes upon exposure to Water, Cercariae or RA cercariae as compared to uninjected skin. **B.** Baseline DDC subset distribution in un-injected control skin.

Part 2

Wanderings *noun*

◀ /'wɒndərɪŋz

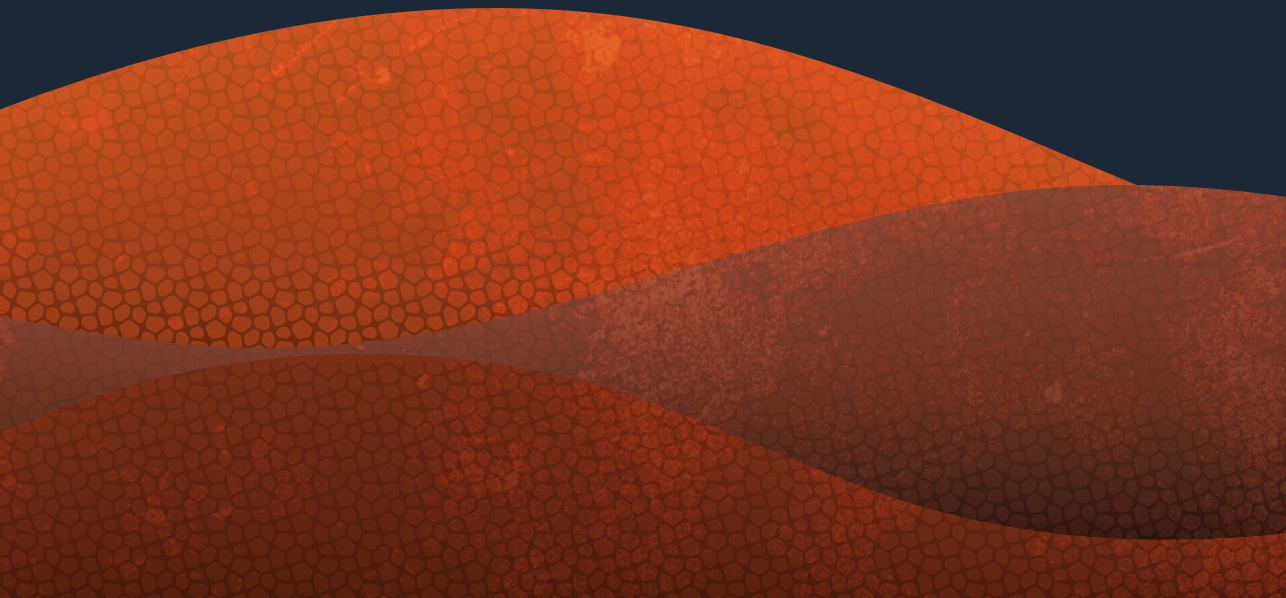
Leisurely or aimless travels; journeys
from place to place

— Oxford Dictionary

“

When sporozoite wanderings through human skin tissue are characterized and quantified, it appears these parasites are not so aimless after all

5

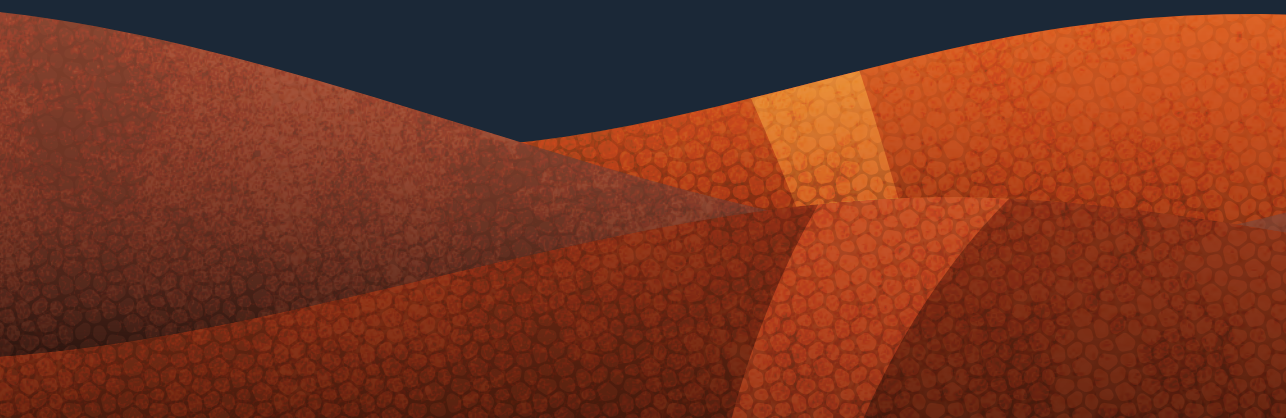


Quantification of wild-type and radiation attenuated *Plasmodium falciparum* sporozoite motility in human skin

Béatrice M.F. Winkel*, Clarize M. de Korne*, Matthias N. van Oosterom, Diego Staphorst, Mark Meijhuis, Els Baalbergen, Munisha S. Ganesh, Koen J. Dechering, Martijn W. Vos, Séverine C. Chevalley-Maurel, Blandine Franke-Fayard, Fijs W.B. van Leeuwen, Meta Roestenberg

*These authors contributed equally to this work

Scientific Reports 2019. Doi: [10.1038/s41598-019-49895-3](https://doi.org/10.1038/s41598-019-49895-3)



ABSTRACT

Given the number of global malaria cases and deaths, the need for a vaccine against *Plasmodium falciparum* (*Pf*) remains pressing. Administration of live, radiation-attenuated *Pf* sporozoites can fully protect malaria-naïve individuals. Despite the fact that motility of these attenuated parasites is key to their infectivity and ultimately protective efficacy, sporozoite motility in human tissue (e.g. skin) remains wholly uncharacterized to date. We show that the ability to quantitatively address the complexity of sporozoite motility in human tissue provides an additional tool in the development of attenuated sporozoite vaccines. We imaged *Pf* movement in the skin of its natural host and compared wild-type and radiation-attenuated GFP-expressing *Pf* sporozoites. Using custom image analysis software and human skin explants we were able to quantitatively study their key motility features. This head-to-head comparison revealed that radiation attenuation impaired the capacity of sporozoites to vary their movement angle, velocity and direction, promoting less refined movement patterns. Understanding and overcoming these changes in motility will contribute to the development of an efficacious attenuated parasite malaria vaccine.

Keywords: *Plasmodium falciparum*, Sporozoite, Motility, Malaria, skin, imaging, Radiation attenuation, vaccine

INTRODUCTION

Nearly half the human population lives in areas with an increased risk of malaria transmission, resulting in more than 200 million cases each year¹, illustrating the urgent need for a highly effective malaria vaccine. Vaccines based on live attenuated *Plasmodium falciparum* (*Pf*) parasites obtained from the mosquito salivary gland, so-called sporozoites, are currently most promising. Clinical trials that used mosquitoes to transmit the *Pf* parasites into the human subjects yielded 100% protection in non-endemic settings²⁻⁴. When translating the seminal mosquito-bite studies into a needle-based cryopreserved vaccine formulation³, intradermal (ID) injection of isolated live attenuated sporozoites, were found to induce inferior protective immunity in humans⁵. Further research showed that an impractical intravenous (IV) route of attenuated parasite injection was more effective, because IV administration promotes transportation of parasites to the liver^{3,4,6}, which is key to the induction of protection^{7,8}. To date, the factors which affect motility of *Pf* from human skin to liver have not been studied.

Imaging studies using genetically modified fluorescent *Plasmodium berghei* (*Pb*) or *yoelii* (*Py*) sporozoites in mouse skin yielded insight into the migration patterns of sporozoites, with contrasting differences between *in vitro* and *in vivo* motility or the site of injection (tail or ear)⁹⁻¹⁴. Because the anatomical structure of murine skin differs from human skin, with respect to thickness, muscle layers, dermal papillae and hair follicle density^{15,16}, a human skin model would provide a valuable contribution. Despite differences such as the lack of blood flow, *ex vivo* skin explant models have shown excellent viability of dermal cells over long periods of time^{17,18}. Analysis of *Pf* migration in human tissue is an important first step to understanding *Pf* transmission and attenuated parasite vaccine delivery. In addition, a human skin model could also allow for future evaluation of subunit vaccines¹⁴.

Attenuated sporozoite vaccines have been produced using radiation attenuation (RA), gene modification or concomitant drug administration¹⁹. RA is the most commonly used method, whereby RA sporozoite vaccines are currently entering phase 3 clinical trials^{20,21}. RA introduces double strand breaks in DNA²² and has been shown to impact the sporozoites gene expression and ultrastructure²³⁻²⁵. In both ways, sporozoite motility might be influenced. At present, preservation of motility following RA can only be validated using an *in vitro* gliding assay²⁶, where the sporozoite is allowed to glide on a glass surface. However, this assay does not mimic the complexity of environmental interactions that are observed in tissue (e.g. physical confinement)^{10,27}. Therefore, *ex vivo* imaging technologies that make use of human tissue are required.

The pioneering literature that presents image analysis of rodent sporozoite (*Pb*) movement in murine tissue, has focused on an often used measure of random diffusion of particles, the mean squared displacement (MSD)^{9,10,28}. This measurement separates anomalous diffusion (with a non-linear relation to time), from the classic linear diffusion process. This has supported quantitative investigations towards motility changes over time and in relation to dermal structures^{9,10}. As sporozoite movement through tissue suits a specific purpose, it makes sense for motility analyses to include quantitative parameters for directionality rather than limit the analysis to parameters that present random diffusion. Analysis of directional movement, referred to as tortuosity, is a common approach to study e.g. animal migration through the desert²⁹ and analysis of disease severity in cognitively impaired patients³⁰, but has also been applied during cell tracking studies³¹. The tortuosity of movement indicates whether it is directional or random. We reasoned that the concept of directional movement could complement the diffusion-based in skin sporozoite analysis and could provide a more detailed insight in sporozoite motility in complex environments such as human skin tissue.

The aim of this study was to image and quantitatively assess motility of wild-type, GFP-expressing *Pf* sporozoites (Pf^{WT}) in human skin (Figure. 1). For image analysis we developed a software tool for in skin analysis called SMOOTHhuman skin (Sporozoite Motility Orienting and Organizing Tool) that can output tortuosity and velocity related motility parameters of individual *Pf* sporozoites. In order to assess the effect of RA on sporozoite migration, we subsequently compared the motility of Pf^{WT} and RA sporozoite (Pf^{RA}) populations in human skin explants (tail or ear).

MATERIALS AND METHODS

Study Design

In order to explore movement characteristics of *Pf* sporozoites in human skin explants, we performed a controlled laboratory experiment, in which we compared motility parameters (outputted by our custom software SMOOTHhuman skin, see below) of unattenuated *Pf* parasites Pf^{WT} : 352 sporozoites (14 movie sections of 400 frames/11 min) with those of radiation attenuated *Pf* parasites Pf^{RA} : 350 sporozoites (18 movie sections 400 frames/11 min). The movies were made of sporozoites injected in skin explants of two donors (in two independent experiments), comparing Pf^{WT} with Pf^{RA} in both donors at two different locations in the skin ending up with four unique locations for both Pf^{WT} and Pf^{RA} . The experiments were evaluated individually (Supplementary figure

S1), thereafter the data was pooled (Supplementary figure S2) and the final analysis of the motility of Pf^{ANT} vs Pf^{RA} was performed on the pooled dataset. The study was not randomized and not blinded.

Parasites

Anopheles stephensi mosquitoes infected with a transgenic *Pf* line that constitutively expresses fluorescent reporter protein GFP under the pfCS promotor (M.W. Vos et al, manuscript in preparation), were killed using ethanol spray and rinsed in RPMI 1640 (Invitrogen, Carlsbad, CA, USA). Salivary glands were dissected manually at day 14-21 post infection, incubated in RPMI 1640 and kept on ice. Radiation attenuation of sporozoites was performed by irradiating intact salivary glands to a total dose of 20krad using a Cesium radiation source (total of 28 minutes) on ice. During this time control sporozoites were also kept on ice. Within one-hour, glands were homogenized to release *Pf* sporozoites. Sporozoites were then counted using a Burkler chamber, brought to a concentration of 20×10^6 /ml in RPMI 1640 containing 10% Fetal Calf Serum (FCS; Bodinco, Alkmaar, The Netherlands) and used for imaging experiments immediately.

Skin explants

We obtained human skin explants from collaborating hospitals immediately after abdominal skin reduction surgery (CME B18.009) and kept skin explants at 4°C for 3 hours until use. Subcutaneous fat was removed, and the epidermal side was cleaned with 70% ethanol. One million sporozoites were injected intradermally in a 50µl injection using a 0.3ml insulin syringe (30G; BD, Franklin Lakes, NJ, USA). In order to facilitate quick localization of the injection site by confocal microscopy the injection formulation contained Yellow-Green fluorescent 500nm Latex nanoparticles (Sigma Aldrich). Immediately after injection, the injection site was biopsied using a 6mm biopsy punch, sliced longitudinally through the center and mounted on a microscopy slide with a 1 mm depression in RPMI 10% FCS. Slides were imaged within 30 minutes post injection.

Confocal video-microscopy

Skin biopsy slides were imaged using the time-lapse function of the Leica TSC SP8 Confocal microscope (Leica, Wetzlar, Germany) at a temperature of 37 degrees Celsius, 5% CO₂. 2D images (no z-stacks) were obtained using an exposure time of 1.7 seconds per frame and a 40x objective (400 frames per movie, 11 minutes). Microscopy videos were rendered using accompanying Leica LASX software and were analyzed using custom software SMOOTHhuman skin.

SMOOTHuman skin

MATLAB (The MathWorks Inc. Natick, MA, USA) software was created for in skin sporozoite analysis, which we called Sporozoite Motility Orienting and Organizing Tool (SMOOT_{human skin}). This tool is an extended version compared to the SMOOT_{human skin} tool previously used to determine the velocity and movement pattern distribution of Cy5M₂ labeled Pf sporozoites⁵⁴. Similar to our recently published *in vitro* tool SMOOT_{In vitro}⁴¹, the upgraded SMOOT_{human skin} software now also includes turn angle and displacement. In addition, SMOOT_{human skin} takes into account the directionality by computing: angular dispersion, straightness index and the direction of sporozoite tracks. Firstly, sporozoite tracks were characterized as motile or stationary based on their displacement. Subsequently, motile tracks were subdivided into movement patterns: sharp turn, slight turn and linear.

To investigate the influence of RA on sporozoite motility, we compared SMOOT_{human skin} parameter outcomes of 14 *Pf*^{MT} motility movie files (11 minutes/movie, 154 minutes total, 352 sporozoite tracks consisting of 511 segments and 26932 frames; Sup. Movie S1) with 18 *Pf*^{RA} motility files (11 minutes/ movie, 198 minutes total, 350 sporozoite tracks consisting of 563 segments and 25804 frames; Sup. Movie S2). Software output was manually validated.

Velocity was determined by measuring the displacement between frames. We defined step number in the track *i* to measure velocity *v* using formula (1), with *x* as the median pixel location of the segmented structure and *t* as the time passed in seconds.

$$v(i) = \frac{x_i - x_{i-1}}{t_i - t_{i-1}} = \frac{dx}{dt} \quad (1)$$

The mean squared displacement (MSD) is a common measure to distinguish random versus non-random motion for moving particles and was previously used to analyze sporozoite motility^{5,6}. The squared displacement (SD) is a measure of the displacement per time point of an individual track, which can be calculated with formula (2):

$$SD(i) = (x_n(i) - x_n(0))^2 \quad (2)$$

The MSD was derived from the SD of all linear tracks using formula (3):

$$MSD(i) = \langle (x(i) - x_0)^2 \rangle = \frac{1}{N} \sum_{n=1}^N (x_n(i) - x_n(0))^2 \quad (3)$$

The turn angle (θ) of the sporozoite was defined by the angle difference between path directions in consecutive frames. If we start calculating the turn angle from location x_0 then the sporozoite reaches x_i after i steps. The angle of x_i is the angle δ_i between point x_i and the horizontal. The turn angle was then defined as described in formula (4).

$$\theta_i = \delta_i - \delta_{i-1} \quad (4)$$

The straightness index (SI) is the most basic approach to quantify tortuosity and is defined as the ratio of distance between track end points (C) and track length (L), as calculated using formula (5). This parameter quantifies deviation from a straight line, e.g. SI = 1 in a perfect linear path, SI = 0 in circular motion.

$$St = \frac{C_{track}}{L_{track}} = \frac{x(i) - x(0)}{\sum_{k=1}^i (x(k) - x(k-1))} \quad (5)$$

Angular dispersion (AD) quantifies the number of turning angles diverging from the main angle of movement. It describes tortuosity by quantifying changes in direction. It is calculated using the turn angles (formula (4)) according to the following formula:

$$AD = \frac{1}{I} \sqrt{C^2 + S^2} \quad (6)$$

Where I is the last step of the track and C and S are defined as:

$$C = \sum_{i=1}^I \cos \theta_i \quad S = \sum_{i=1}^I \sin \theta_i$$

Statistics

Data extracted from $SMOOT_{\text{human skin}}$ was analyzed in IBM (Armonk, NY, USA) SPSS version 23 or GraphPad Prism (La Jolla, CA, USA) version 7. Comparisons between two or more independent categorical data groups were made by Chi-squared test, continuous nonparametric parameters were compared by Mann-Whitney U test. $P < 0.05$ was considered statistically significant. Bonferroni correction was applied for post hoc analysis after Chi-squared testing.

RESULTS

Generation of a semi-automated sporozoite migration analysis tool

Firstly, we generated confocal microscopy movies of Pf^{WT} and Pf^{RA} migrating through human skin explants by a trans sectional skin setup (fourteen 11 min movie sections of Pf^{WT} and eighteen 11 min movie sections of Pf^{RA} , yielding a total of 352 and 350 analyzed sporozoites, respectively). Experiments were performed in two independent donor samples and while splitting the batch of sporozoites in a Pf^{WT} and Pf^{RA} group. Using our semi-automated software tool $SMOOT_{\text{human skin}}$, we were able to track sporozoite movement (Figure 1) by identifying sporozoites based on their shape and fluorescence intensity (Figure 1B) and connecting their location over time (see Supplementary figure S1 for an overview of the data per individual location and supplementary movie S1 and S2 for examples). Sporozoite locations per frame were stitched together in order to generate track segments, where multiple segments in the same 2D plane build up a full track (Figure 1B-C). Depending on the straightness index (SI) of the individual segments, their movement patterns (sharp turn, slight turn and linear) were determined and color coded (Figure 1C). Slight turns were defined as the turns which resulted from the natural curvature of the sporozoites ($0,21-0,23$ ($1/\mu\text{m}$)³².

Sharper turns, requiring extra bending of the sporozoite, were defined as sharp turns³². Furthermore, the following movement parameters were calculated at track level: SI and angular dispersion (AD), at segment level: turn direction (clockwise or counterclockwise) and at frame level: MSD and velocity. Using the unique ID allocated to each individual sporozoite track, all computed parameters were extracted for the individual sporozoites and, where relevant, analyzed over time. In the experiments 81% of the sporozoites were characterized as motile, which surpasses the 66% reported earlier for *Pb* sporozoites in murine skin⁹.

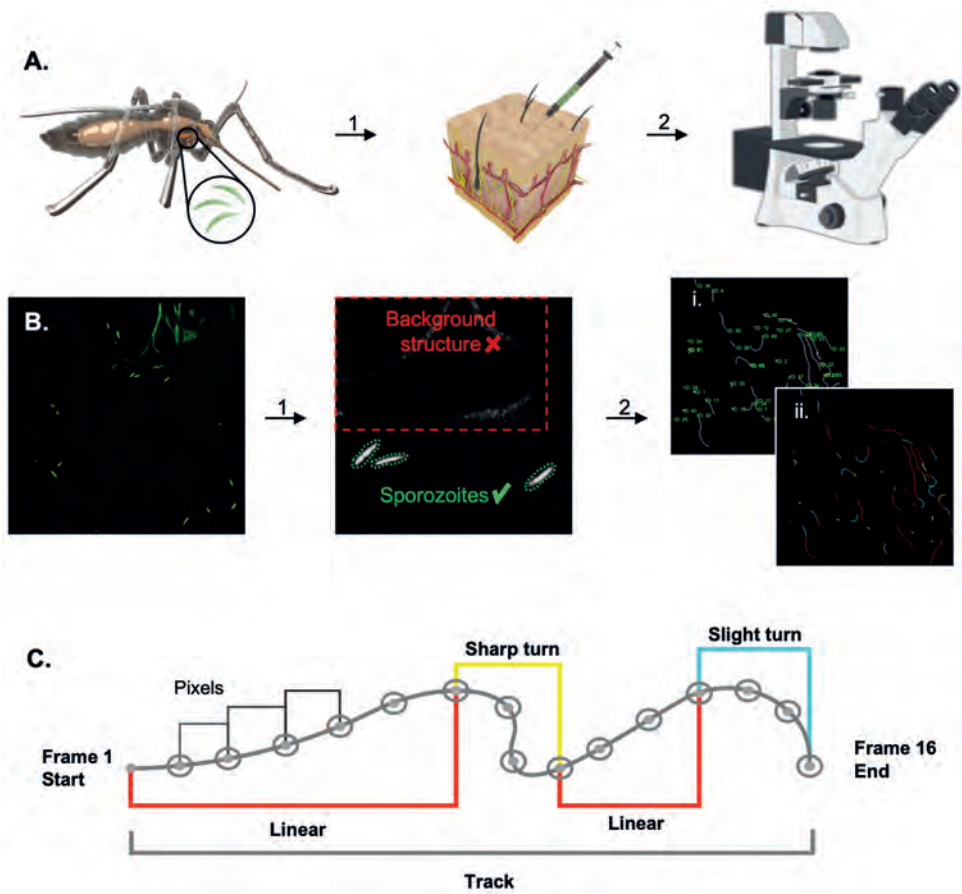


Figure 1. Schematic of experimental setup and SMOOT_{human skin} analysis. **A.** Schematic of an *Anopheles* mosquito as the host of *Plasmodium* sporozoites within its salivary glands. Isolated sporozoites, Pf^{WT} or Pf^{RA} , were injected into human skin (1). The skin samples containing sporozoites were filmed using a confocal microscope (2) (Images of needle and microscope were adapted from image copyright <https://smart.servier.com>, Creative Commons Attribution 3.0 Unported License, <https://creativecommons.org/licenses/by/3.0/>). **B.** Raw confocal video images were uploaded into SMOOT_{human skin}. Per video frame individual sporozoites were semi-automatically segmented (1). Segmented sporozoites in consecutive frames were stitched to generate tracks. Generated tracks have a unique sporozoite ID (i) in order to extract measured parameters (for example movement pattern (ii)) per sporozoite over time (2). **C.** Sporozoite tracks are divided into segments based on the underlying movement pattern.

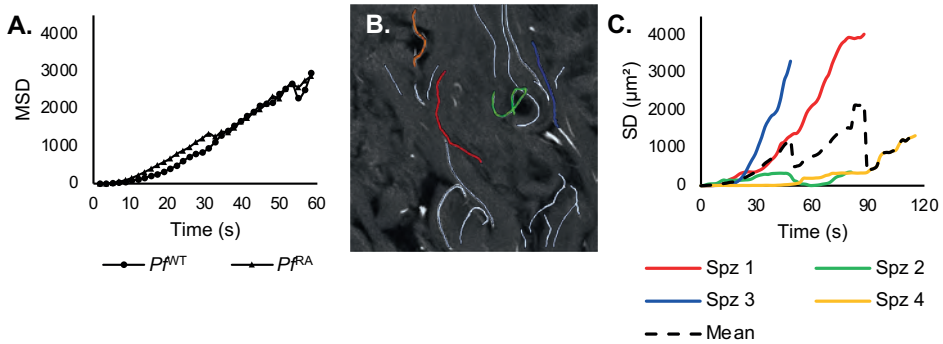


Figure 2. Mean squared displacement of sporozoites. **A.** Mean squared displacement (MSD in μm^2) of the sporozoites plotted against time, only linear tracks are taken into account. **B.** Examples of individual sporozoite tracks in a single movie file. **C.** The four differently colored individual tracks from B. are presented as squared displacement (SD in μm^2) over time and presented relative to the dotted line, which presents the MSD of all four lines.

Mean Squared Displacement (MSD) data alone does not reflect individual sporozoite movement heterogeneity

In analogy to previous protocols for *Pb* sporozoites¹⁰, we evaluated the MSD of linear Pf^{WT} tracks (37% of tracks). Comparing the MSD of Pf^{WT} with the Pf^{RA} population (containing 18.5% total linear tracks) yielded no significant difference (Figure 2A). This analysis, however, excluded a large fraction of sporozoites that exhibited non-linear movement (slight and sharp turn; 81.5% for Pf^{RA} and 63% for Pf^{WT}). We thus concluded that this analysis methodology was not suitable to fully grasp the complexity of *Pf* motility in human skin. In addition, we found that squared displacement plots of sporozoites revealed a high level of heterogeneity. A typical example of this heterogeneity is shown in figure 2B-C, where we plotted the squared displacement (SD; where displacement is the difference in sporozoite position between begin and endpoint of a track) of 4 very different individual sporozoite tracks from the same movie file. In order to do justice to the sample heterogeneity, we aimed to include other parameters of movement, such as the tortuosity, in the motility analysis.

Tortuosity analysis reveals differences in sporozoite motility after RA

Using tortuosity-based analysis we quantified pattern characteristics of sporozoite tracks. First, the individual experiments were evaluated (Supplementary figure S1), thereafter the data of all Pf^{RA} and Pf^{WT} was pooled (Supplementary figure S2) and further analyzed. Automated pattern classification of sporozoite tracks showed that 37% of Pf^{WT} sporozoite tracks were linear, 42% classified as sharp turn and 21% as slight turn (Figure

3A). Pf^{WT} sporozoite tracks displayed a median SI of 0.86, indicating relatively straight tracks (i.e. indices close to 1; Figure 3B) and a balanced AD of 0.45 indicating random meandering of sporozoites (AD close to 1 indicates a consistent track, AD close to 0 indicate random direction changes; Figure 3C).

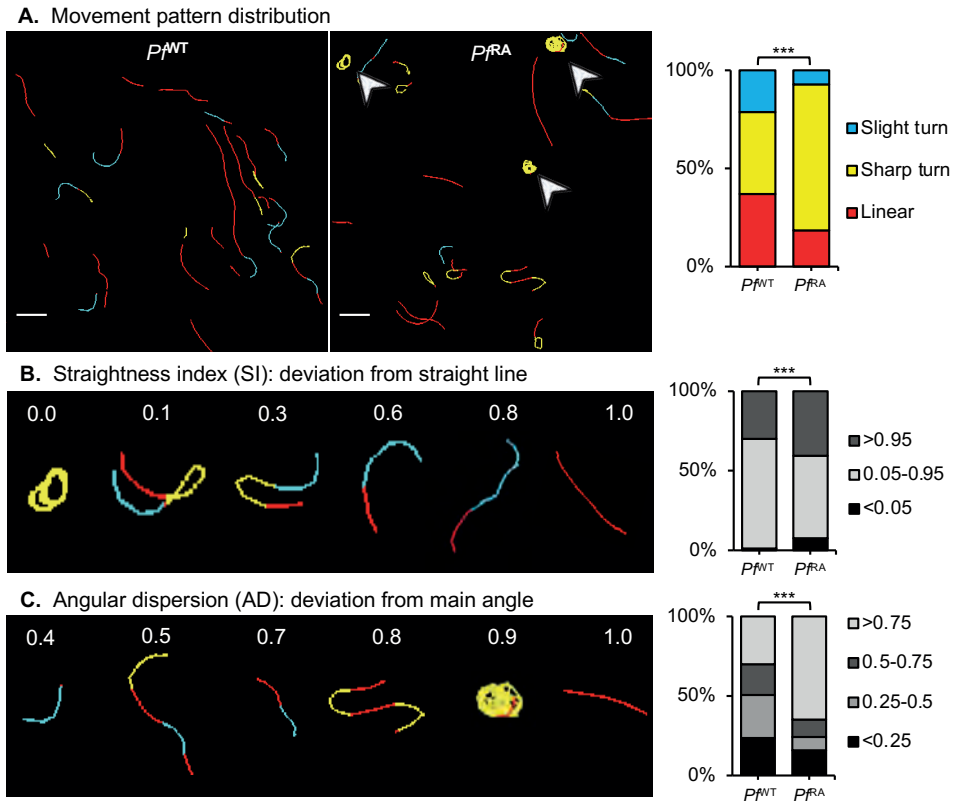


Figure 3. Tortuosity of sporozoite tracks. **A.** Two examples of movement pattern maps of tracked sporozoites; Pf^{WT} in skin (left) and Pf^{RA} in skin (middle). Linear segments are depicted in red, slight turns in blue and sharp turns in yellow. Arrowheads indicate circular sporozoite tracks comparable to *in vitro* movement. The movement pattern distribution of the Pf^{WT} and Pf^{RA} is quantified for all sporozoite tracks based on frames (right). Scale bar: 20 μ m. **B.** To illustrate the concept of straightness index (SI) in relation to sporozoite tracks, 6 tracks are displayed out of the movement pattern maps shown in A. The SI distribution is quantified based on the SI values of total tracks (Pf^{WT} median: 0.89, IQR: 0.66-0.96; Pf^{RA} median: 0.90, IQR: 0.46-0.98). **C.** To illustrate the concept of angular dispersion (AD) in relation to sporozoite tracks, 6 tracks are displayed out of the movement pattern maps shown in A. The AD distribution is quantified based on the AD values of total tracks (Pf^{WT} median: 0.47, IQR: 0.26-0.80; Pf^{RA} median: 0.93, IQR: 0.51-0.99). ***= $p < 0.0001$ using Chi squared test.

In contrast, the Pf^{RA} population displayed significantly more slight and sharp turn segments (7.2% blue and 74.3% yellow color coding respectively), and a decrease in linear patterns (18.5%, red) as compared to the Pf^{WT} (Figure 3A). This difference was caused by continuous circular turning behavior of sporozoites (arrowheads Figure 3A), as well as a back and forth motion (180° turn; hereafter termed "reversal"). Although *in vitro* on circular movement of *Pf* is reported on coated surfaces, under the conditions studied *Pf* did not show such movement (see Sup. Movie S4). This was confirmed by an increase in SI values close to 0, representing these turning tracks (Figure 3B; post hoc Chi squared test $p=0.008$ and $p<0.0001$ respectively).

In addition, Pf^{RA} sporozoites showed significantly more persistent straight tracks compared to Pf^{WT} i.e. increased indices close to 1 (Overall Chi squared test $p<0.0001$; median SI 0.89). Similarly, Pf^{RA} showed more consistent tracks with fewer deviations from the mean angle of movement patterns compared to Pf^{WT} (Figure 3C; angular dispersion median 0.92; overall Chi squared test $p<0.001$ post hoc Chi squared test $AD >0.75$ $p<0.0001$). Taken together, the pattern analysis and tortuosity parameters indicate that Pf^{RA} exhibit reduced motility variation compared to Pf^{WT} and preferentially display continuous circling patterns.

RA causes sporozoites to circle consistently in a clockwise direction

Possibly due to the tilted arrangement of the sporozoite polar-ring³³, circularly moving sporozoites display a preferred clockwise (CW) turn direction *in vitro*³⁴. In the three-dimensional (3D) skin environment this preference was lost; SMOOT_{human skin} analysis demonstrated Pf^{WT} sporozoites turned equally CW and counterclockwise (CCW; Figure 4A). Surprisingly, analysis of turn direction in the Pf^{RA} population yielded a preference for CW directionality (Figure 4A; 65.2% CW; $p=0.013$). Analysis of the duration of the turns (number of frames) revealed that Pf^{RA} sporozoites continued turning in circles when this pattern was initiated.

Per frame analysis of velocity reveals decreased velocity alterations after RA

In line with previous findings^{9,10,35}, we recorded an average sporozoite velocity per track of 1.1 $\mu\text{m/s}$ (time did not seem to have an effect on the average velocity (Supplementary figure S3)). SMOOT_{human skin} also allowed analysis of the velocity per captured frame within a track (Figure 5), revealing marked variations over time. Examples illustrated in figure 5A show a single sporozoite can display non-parametric velocity changes between 0 and 3.5 $\mu\text{m/s}$ over the course of one track (Figure 5A upper panel; Spz 3, red). While the velocity changes occurred within all movement patterns, the median velocity

was highest in linear segments followed by slight turns and in sharp turns (Figure 5B). Pf^{RA} consistently showed higher velocity in all movement patterns (median 1.1 $\mu\text{m/s}$ vs 0.85 $\mu\text{m/s}$ for linear tracks, 0.6 $\mu\text{m/s}$ vs 0.48 for slight turns and 0.34 $\mu\text{m/s}$ vs 0.24 for sharp turns in Pf^{RA} vs Pf^{WT} respectively, $p < 0.0001$). Despite the fact that Pf^{RA} displayed more "slow" sharp turns, in a per frame analysis its overall median velocity at 0.37 $\mu\text{m/s}$ was higher than the median velocity of Pf^{WT} (0.35 $\mu\text{m/s}$; $p < 0.0001$). This difference was caused by a reduction in stop-and-go action (frames with velocity $< 0.5 \mu\text{m/s}$ were 56.8 % for Pf^{RA} and 59.6 % for Pf^{WT} , $p = 0.037$). Furthermore, velocity variability was smaller in Pf^{RA} (Figure 5A, range 0-4.1 $\mu\text{m/s}$) compared to Pf^{WT} (0-4.8 $\mu\text{m/s}$). Corroborating this finding, Pf^{RA} velocities of linear tracks were normally distributed compared to a nonparametric velocity distribution for Pf^{WT} (Figure 5B, $p < 0.0001$), whereas velocities in other movement patterns were nonparametrically distributed for both Pf^{RA} and Pf^{WT} . Taken together, Pf^{RA} less readily alternated their velocity.

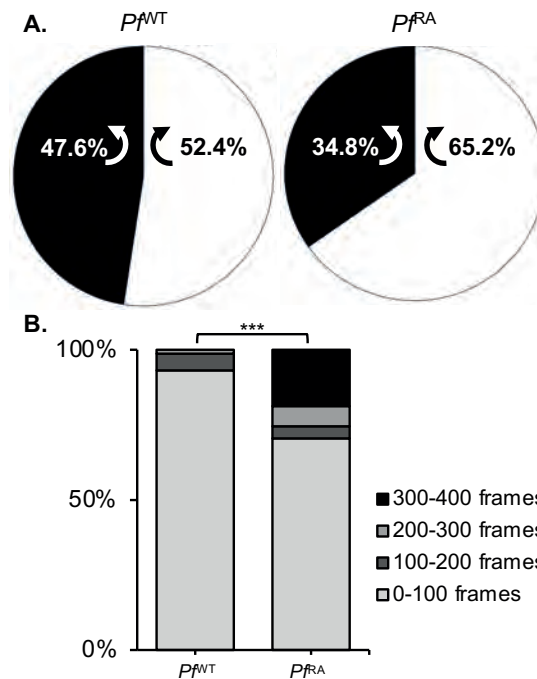


Figure 4. Direction of turning sporozoites. **A.** Turn direction of Pf^{WT} and Pf^{RA} in skin. Pf^{RA} turn significantly more CW than Pf^{WT} , $p = 0.013$ using Chi-Squared test. **B.** The sharp turns of Pf^{RA} contain significantly more frames than the turns of Pf^{WT} (Pf^{WT} median: 32, IQR: 22-55; Pf^{RA} median: 33, IQR: 14-218; $p > 0.000$ using Chi-Squared test). Indicating persistent circular motion.

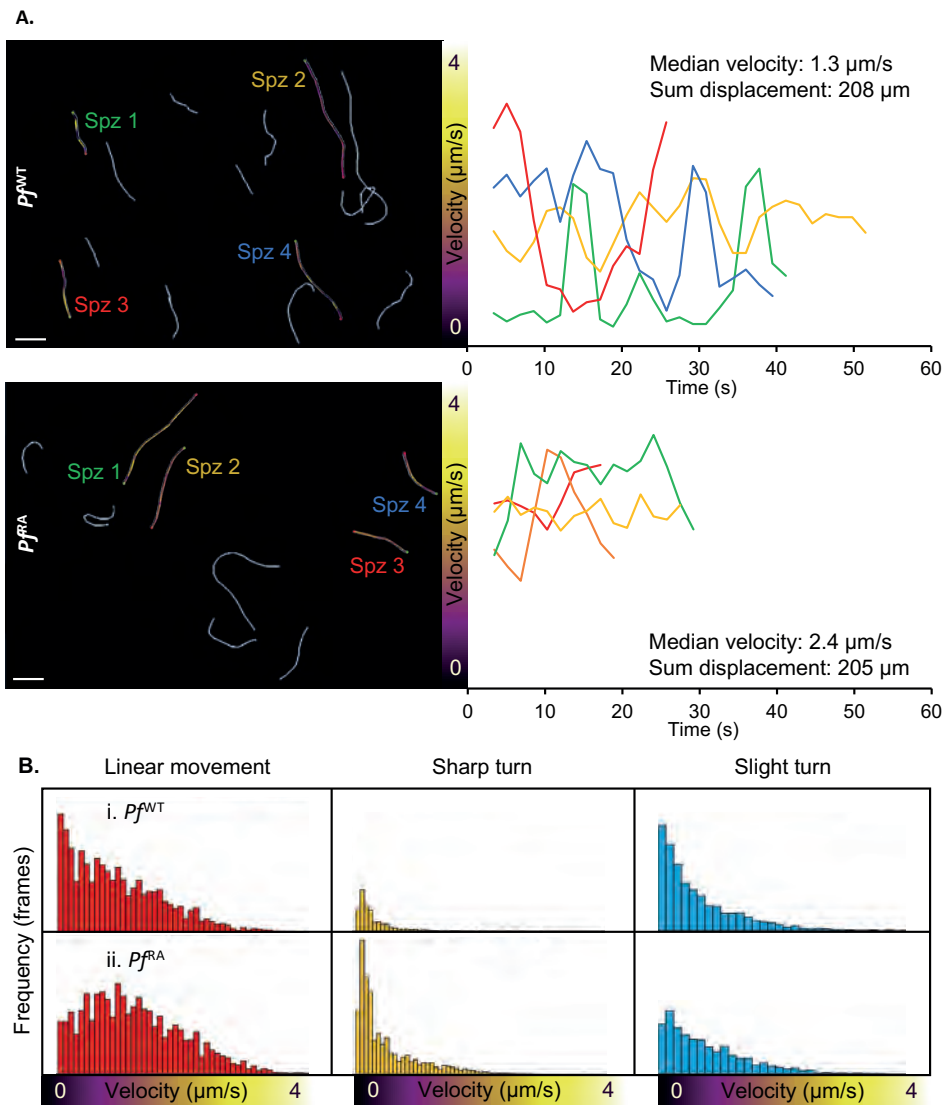


Figure 5. Velocity of sporozoites. **A.** Four Pf^{WT} (above) and 4 Pf^{RA} (below) tracks are color-coded based on velocity. Scalebar: 20 μm . Their individual velocity is plotted over time (right). **B.** Velocity distribution of Pf^{WT} and Pf^{RA} per movement pattern.

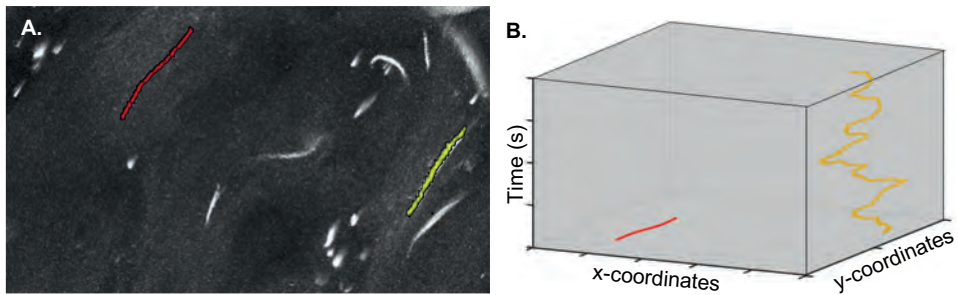


Figure 6. Reverse movement. **A.** In this example, one sporozoite was moving in a linear direction and one sporozoite was moving back and forth. The linear track is depicted in red, the reverse movement is classified as a sharp turn, thereby depicted in yellow. **B.** The coordinates of the linear and the reversal track are plotted in a xyt coordinate axis system.

***Pf^{RA}* display a default motility pattern: reversal**

Interestingly, some sporozoites in the *Pf^{RA}* group (9% of motile *Pf^{RA}* tracks) revealed pendulum movement, whereby they reverse direction repeatedly moving up and down a short path (Figure 6; Sup. Movie S3). This is in line with earlier findings where sporozoites moved in this particular fashion while residing in the mosquito³⁶⁻³⁸. Plotting this movement (over x and y axis) over time yielded a sinuous track (yellow) that is clearly distinct from the short linear track (red) observed in the same movie segment. Strikingly, this movement pattern was not observed in *Pf^{WT}*.

DISCUSSION

In this study we compared movement of wild-type with irradiated *Pf* malaria sporozoites in a human skin explant using our semi-automated custom analysis tool for sporozoite tracking. We found that *Pf^{RA}* display increased circular motility patterns, more extreme SI values and higher AD compared to *Pf^{WT}*. In addition, *Pf^{RA}* exhibit less variability in velocity over the course of their track and “reversal” patterns were unique to this group. Combined, the data indicates that attenuation via radiation alters sporozoite motility.

In vitro, sporozoites display very elementary circular movement with little variation in velocity, angle or direction^{34,39,40}. Recently, we reported that for *Pb* sporozoites a complex interplay of various nutrients including albumin, glucose and certain amino acids and vitamins regulates parasite motility *in vitro*⁴¹. Under the conditions used to study the movement in human skin explants (uncoated glass; RPMI 160 + 10% FCS) *Pf* sporozoites did not display this movement pattern *in vitro* (Sup. Movie S4). In skin, however, sharp

turns (combination of circular and reversal movement) were observed in addition to linear and slight turn movement patterns. This indicates that the environment influences the *Pf* sporozoite movement and in particular its directionality. It was previously shown for *Pb* sporozoites that an environment with artificial physical constraints in the form of pillars increases the movement directionality as function of interstitial space²⁷. This trend is in line with the reported increase of tortuosity in porous materials that occurs when reducing the interstitial space⁴². An influence of tissue structure on directionality of *Pb* sporozoites can also be extrapolated from the different motility patterns in the skin of mouse ears as compared to the skin of a mouse tail¹⁰. Our findings suggest that the highly complex heterogeneity of human skin composition, in combination with the mixed nutrient availability, may similarly impact individual sporozoites.

Although *Pf* sporozoites display average track velocities in line with previous reports (average 1.1µm/s as compared to previous studies reporting averages of 0.9-1.5µm/s in mouse skin^{9,10,35}), a per frame velocity analysis revealed ongoing stop-and-go actions (see Figure 5). These heterogeneous patterns in combination with the high level of path tortuosity suggests that environmental cues and cellular interactions such as traversal⁴³ impact heterogeneity of direction and speed of the sporozoites. Indeed, the sporozoite surface displays many proteins such as CSP, SPECT1 and CelTOS which facilitate interaction with targets like heparan sulphate and αvβ3 integrin which are available in the human skin^{11,44,45}. Because these alterations in velocity result in a nonparametric velocity distribution which is different for sporozoites taking sharp or slight turns or moving straight, we reason that average velocity alone is insufficient to unravel complex migratory behavior.

Our findings suggest that radiation not only effectively attenuates *Pf* sporozoites at the liver stage, which has been described before⁸, but could also influence their motility at the skin stage. Similar to what has been described before with respect to the effect of cryopreservation on *Pb* sporozoite motility⁴⁶, RA also seems to induce small alterations in motility. The differences in motility between *Pf*^{WT} and *Pf*^{RA} (observed in both donors), although minor, are indicative of a reduced complexity of the *Pf*^{RA} interaction with the tissue environment. Moreover, the increased AD of *Pf*^{RA}, and the increased duration of their turns seems to suggest that once a “default” movement pattern has been initiated, the movement pattern persists. As circling and reversal patterns mean the *Pf* sporozoites stay in a single location, one could argue this movement pattern would render parasites at risk for elimination by phagocytic dermal immune cells, which could impact antigen presentation and vaccine efficacy.

Understanding how radiation attenuation interferes with these pathogen-host interactions could be important to identify novel vaccine targets or improve the efficacy of existing radiation attenuated sporozoite vaccines. Here it should be noted that for our studies we solely used 20Krad attenuation dose as described previously in murine studies^{47,48}, meaning we cannot state if a similar difference would be observed at lower radiation doses. However, increased radiation dosages result in reduced infectivity of *Plasmodium* species and reduced effectivity of attenuated parasite immunization^{8,49}. The altered motility induced by radiation may contribute to this reduced infectivity. Whether similar effects also occur when using genetically modified sporozoites vaccines⁵⁰⁻⁵², remains to be investigated.

Use of viable human skin explants allowed us to analyze *Pf* sporozoite movement in their natural skin environment thereby enhancing the possibilities to gain insight in their behavior. Obviously, also this model system has limitations. Although not per se relevant for the field of live attenuated *Pf* vaccines, intradermal syringe-based injections may not accurately represent the mosquito based transmission of the disease⁵³. The lack of blood and lymphatic circulation limited prevents *Pf* to migrate out of the skin, which means the motility of the total population of administered *Pf* is analyzed. Due to the light attenuation of tissue the analysis of sporozoite movement was restricted to 2D, which shortened the length of the more linear tracks and thus biased circular and reversal movement patterns occurring in plane. Finally, the location in the dermis that was imaged seemed to effect the sporozoite movement patterns (Supplementary figure S1) even when the same batch of *Pf* was used. Nevertheless, we feel confident that the analysis performed in *ex vivo* human skin helps building a bridge between *in vitro* assays and *in vivo* assays of *Pb* sporozoites in mouse skin^{9,10} and controlled human infection studies^{21,50}.

In conclusion, we imaged *Pf* sporozoite migration in the dermis of its natural host and performed an in-depth analysis of the motility of WT and RA *Pf* sporozoites. We demonstrate loss of movement variability after radiation attenuation which might reflect reduced viability and ultimately decreased infectivity. Because of the ability of SMOOT_{human skin} to analyze complex migration, it may contribute to the refinement of live sporozoite vaccine formulations.

SUPPLEMENTARY NOTES

Data availability: The data can be made available upon request

Ethics statement: The use of human skin explants (obtained as waste material after abdominal reduction surgery) for this research was approved by the Commission Medical Ethics (CME) of the LUMC, Leiden. Approval number CME: B18-009. The methods were carried out in accordance with the relevant guidelines and regulations. Informed consent was obtained from all participants.

Acknowledgements: The authors would like to thank Sven van Leeuwen for his contribution to the images in this article. The research leading to these results has received funding from a ZONMW VENI grant (016.156.076) financed by the Netherlands Organization for Scientific Research (NWO) and a Gisela Thier fellowship of the LUMC.

Author contributions: The methodology was developed by BW, CK, KD, MV, FL and MR. Experiments were performed and interpreted by BW, CK, DS, MvO, MM, MG, EB, SC, BF, FL and MR and supervised by FL and MR. BW, CK, FL and MR drafted the manuscript. All authors reviewed and contributed to finalizing the manuscript.

Competing interests: The authors declare no competing interest.

REFERENCES

- 1 [Internet] WHO: Geneva Switzerland. 19 November 2018, World Malaria report 2018. <https://www.who.int/malaria/media/world-malaria-report-2018/en/>.
- 2 Roestenberg, M. et al. Protection against a malaria challenge by sporozoite inoculation. *N Engl J Med* 361, 468-477, doi:10.1056/NEJMoa0805832 (2009).
- 3 Seder, R. A. et al. Protection against malaria by intravenous immunization with a nonreplicating sporozoite vaccine. *Science* 341, 1359-1365, doi:10.1126/science.1241800 (2013).
- 4 Ishizuka, A. S. et al. Protection against malaria at 1 year and immune correlates following PfSPZ vaccination. *Nat Med* 22, 614-623, doi:10.1038/nm.4110 (2016).
- 5 Epstein, J. E. et al. Live attenuated malaria vaccine designed to protect through hepatic CD8(+) T cell immunity. *Science* 334, 475-480, doi:10.1126/science.1211548 (2011).
- 6 Mordmuller, B. et al. Sterile protection against human malaria by chemoattenuated PfSPZ vaccine. *Nature* 542, 445-449, doi:10.1038/nature21060 (2017).
- 7 Cochrane, A. H., Nussenzweig, R. S. & Nardin, E. H. Immunization against sporozoites. *Malaria in Man and Experimental Animals*, Academic Press, New York, Editor: Kreier, J.P. Pages 163-202 (1980).
- 8 Silvie, O. et al. Effects of irradiation on *Plasmodium falciparum* sporozoite hepatic development: implications for the design of pre-erythrocytic malaria vaccines. *Parasite Immunol* 24, 221-223 (2002).
- 9 Hopp, C. S. et al. Longitudinal analysis of *Plasmodium* sporozoite motility in the dermis reveals component of blood vessel recognition. *Elife* 4, doi:10.7554/eLife.07789 (2015).
- 10 Hellmann, J. K. et al. Environmental constraints guide migration of malaria parasites during transmission. *PLoS Pathog* 7, e1002080, doi:10.1371/journal.ppat.1002080 (2011).
- 11 Amino, R. et al. Quantitative imaging of *Plasmodium* transmission from mosquito to mammal. *Nat Med* 12, 220-224, doi:10.1038/nm1350 (2006).
- 12 Vanderberg, J. P. & Frevert, U. Intravital microscopy demonstrating antibody-mediated immobilisation of *Plasmodium berghei* sporozoites injected into skin by mosquitoes. *Int J Parasitol* 34, 991-996, doi:10.1016/j.ijpara.2004.05.005 (2004).
- 13 Douglas, R. G., Reinig, M., Neale, M. & Frischknecht, F. Screening for potential prophylactics targeting sporozoite motility through the skin. *Malar J* 17, 319, doi:10.1186/s12936-018-2469-0 (2018).
- 14 Aliprandini, E. et al. Cytotoxic anti-circumsporozoite antibodies target malaria sporozoites in the host skin. *Nat Microbiol* 3, 1224-1233, doi:10.1038/s41564-018-0254-z (2018).
- 15 Pasparakis, M., Haase, I. & Nestle, F. O. Mechanisms regulating skin immunity and inflammation. *Nat Rev Immunol* 14, 289-301, doi:10.1038/nri3646 (2014).
- 16 Treuting, P. M., Dintzis, S. M. & Montine, K. S. *Comparative Anatomy and Histology: A Mouse and Human Atlas*. Academic Press, Elsevier Chapter 24, 433-441 (2017).
- 17 Frade, M. A. et al. Prolonged viability of human organotypic skin explant in culture method (hOSEC). *An Bras Dermatol* 90, 347-350, doi:10.1590/abd1806-4841.20153645 (2015).
- 18 Gunawan, M., Jardine, L. & Haniffa, M. Isolation of Human Skin Dendritic Cell Subsets. *Methods Mol Biol* 1423, 119-128, doi:10.1007/978-1-4939-3606-9_8 (2016).
- 19 Menard, R. et al. Looking under the skin: the first steps in malarial infection and immunity. *Nat Rev Microbiol* 11, 701-712, doi:10.1038/nrmicro3111 (2013).

- 20 Richie, T. L. et al. Progress with Plasmodium falciparum sporozoite (PfSPZ)-based malaria vaccines. *Vaccine* 33, 7452-7461, doi:10.1016/j.vaccine.2015.09.096 (2015).
- 21 Hoffman, S. L. et al. Protection of humans against malaria by immunization with radiation-attenuated Plasmodium falciparum sporozoites. *J Infect Dis* 185, 1155-1164, doi:10.1086/339409 (2002).
- 22 Jeggo, P. A. & Lobrich, M. DNA double-strand breaks: their cellular and clinical impact? *Oncogene* 26, 7717-7719, doi:10.1038/sj.onc.1210868 (2007).
- 23 Oakley, M. S. et al. Molecular Markers of Radiation Induced Attenuation in Intrahepatic Plasmodium falciparum Parasites. *PLoS One* 11, e0166814, doi:10.1371/journal.pone.0166814 (2016).
- 24 Hoffman, B. U. & Chattopadhyay, R. Plasmodium falciparum: effect of radiation on levels of gene transcripts in sporozoites. *Exp Parasitol* 118, 247-252, doi:10.1016/j.exppara.2007.08.014 (2008).
- 25 Singer, M. et al. Zinc finger nuclease-based double-strand breaks attenuate malaria parasites and reveal rare microhomology-mediated end joining. *Genome Biol* 16, 249, doi:10.1186/s13059-015-0811-1 (2015).
- 26 Prinz, H. L., Sattler, J. M. & Frischknecht, F. Plasmodium Sporozoite Motility on Flat Substrates. *Bio-protocol* 7, e2395, doi:10.21769/BioProtoc.2395. (2017).
- 27 Battista, A., Frischknecht, F. & Schwarz, U. S. Geometrical model for malaria parasite migration in structured environments. *Phys Rev E Stat Nonlin Soft Matter Phys* 90, 042720, doi:10.1103/PhysRevE.90.042720 (2014).
- 28 Beltman, J. B., Maree, A. F. & de Boer, R. J. Analysing immune cell migration. *Nat Rev Immunol* 9, 789-798, doi:10.1038/nri2638 (2009).
- 29 Miller, C., Christman, M. C. & Estevez, I. Movement in a confined space: Estimating path tortuosity. *Applied Animal Behaviour Science*, 13-23 (2011).
- 30 Kearns, W. D., Fozard, J. L. & Nams, V. O. Movement Path Tortuosity in Free Ambulation: Relationships to Age and Brain Disease. *IEEE J Biomed Health Inform* 21, 539-548, doi:10.1109/JBHI.2016.2517332 (2017).
- 31 Loosley, A. J., O'Brien, X. M., Reichner, J. S. & Tang, J. X. Describing directional cell migration with a characteristic directionality time. *PLoS One* 10, e0127425, doi:10.1371/journal.pone.0127425 (2015).
- 32 Muthinja, M. J. et al. Microstructured Blood Vessel Surrogates Reveal Structural Tropism of Motile Malaria Parasites. *Adv Healthc Mater* 6, doi:10.1002/adhm.201601178 (2017).
- 33 Kudryashev, M. et al. Structural basis for chirality and directional motility of Plasmodium sporozoites. *Cell Microbiol* 14, 1757-1768, doi:10.1111/j.1462-5822.2012.01836.x (2012).
- 34 Vanderberg, J. P. Studies on the motility of Plasmodium sporozoites. *J Protozool* 21, 527-537 (1974).
- 35 Amino, R. et al. Imaging malaria sporozoites in the dermis of the mammalian host. *Nat Protoc* 2, 1705-1712, doi:10.1038/nprot.2007.120 (2007).
- 36 Quadt, K. A., Streichfuss, M., Moreau, C. A., Spatz, J. P. & Frischknecht, F. Coupling of Retrograde Flow to Force Production During Malaria Parasite Migration. *ACS Nano* 10, 2091-2102, doi:10.1021/acsnano.5b06417 (2016).
- 37 Frischknecht, F. et al. Imaging movement of malaria parasites during transmission by Anopheles mosquitoes. *Cell Microbiol* 6, 687-694, doi:10.1111/j.1462-5822.2004.00395.x (2004).
- 38 Munter, S. et al. Plasmodium sporozoite motility is modulated by the turnover of discrete adhesion sites. *Cell Host Microbe* 6, 551-562, doi:10.1016/j.chom.2009.11.007 (2009).
- 39 Yoeli, M. Movement of the Sporozoites of Plasmodium Berghei (Vincke Et Lips, 1948). *Nature* 201, 1344-1345 (1964).

- 40 Stewart, M. J. & Vanderberg, J. P. Malaria sporozoites leave behind trails of circumsporozoite protein during gliding motility. *J Protozool* 35, 389-393 (1988).
- 41 de Korne, C. M. et al. Regulation of Plasmodium sporozoite motility by formulation components. *Malar J* 18, 155, doi:10.1186/s12936-019-2794-y (2019).
- 42 Pisani, L. Simple Expression for the Tortuosity of Porous Media. *Transp Porous Med*, 193-203, doi:10.1007/s11242-011-9734-9 (2011).
- 43 Amino, R. et al. Host cell traversal is important for progression of the malaria parasite through the dermis to the liver. *Cell Host Microbe* 3, 88-96, doi:10.1016/j.chom.2007.12.007 (2008).
- 44 Coppi, A. et al. The malaria circumsporozoite protein has two functional domains, each with distinct roles as sporozoites journey from mosquito to mammalian host. *J Exp Med* 208, 341-356, doi:10.1084/jem.20101488 (2011).
- 45 Dundas, K. et al. Alpha-v-containing integrins are host receptors for the Plasmodium falciparum sporozoite surface protein, TRAP. *Proc Natl Acad Sci U S A* 115, 4477-4482, doi:10.1073/pnas.1719660115 (2018).
- 46 Prinz, H. et al. Immunization efficacy of cryopreserved genetically attenuated Plasmodium berghei sporozoites. *Parasitology Research* 117, 2487-2497, doi:10.1007/s00436-018-5937-0 (2018).
- 47 Hafalla, J. C., Sano, G., Carvalho, L. H., Morrot, A. & Zavala, F. Short-term antigen presentation and single clonal burst limit the magnitude of the CD8(+) T cell responses to malaria liver stages. *Proc Natl Acad Sci U S A* 99, 11819-11824, doi:10.1073/pnas.182189999 (2002).
- 48 Ocana-Morgner, C., Mota, M. M. & Rodriguez, A. Malaria blood stage suppression of liver stage immunity by dendritic cells. *J Exp Med* 197, 143-151 (2003).
- 49 Mellouk, S., Lunel, F., Sedegah, M., Beaudoin, R. L. & Druilhe, P. Protection against malaria induced by irradiated sporozoites. *Lancet* 335, 721, doi:10.1016/0140-6736(90)90832-p (1990).
- 50 Roestenberg, M. et al. Controlled human malaria infections by intradermal injection of cryopreserved Plasmodium falciparum sporozoites. *Am J Trop Med Hyg* 88, 5-13, doi:10.4269/ajtmh.2012.12-0613 (2013).
- 51 Belhoue, E. et al. Protective T cell immunity against malaria liver stage after vaccination with live sporozoites under chloroquine treatment. *J Immunol* 172, 2487-2495 (2004).
- 52 Mueller, A. K., Labaied, M., Kappe, S. H. & Matuschewski, K. Genetically modified Plasmodium parasites as a protective experimental malaria vaccine. *Nature* 433, 164-167, doi:10.1038/nature03188 (2005).
- 53 Haeberlein, S. et al. Protective immunity differs between routes of administration of attenuated malaria parasites independent of parasite liver load. *Sci Rep* 7, 10372, doi:10.1038/s41598-017-10480-1 (2017).

SUPPLEMENTARY INFORMATION

Movie S1. Example of a confocal microscopy movie showing Pf^{WT} sporozoites migrating through human skin explant tissue.

Movie S2. Example of a confocal microscopy movie showing Pf^{RA} sporozoites migrating through human skin explant tissue.

Movie S3. Example of reversal movement exhibited by Pf^{RA} sporozoites.

Movie S4. Example of Pf^{WT} sporozoite motility on uncoated glass surfaces.

Movies available on: <https://www.nature.com/articles/s41598-019-49895-3#Sec18>

Evaluation and pooling of individual experiments

Two independent experiments were performed to investigate the effect of radiation attenuation on sporozoite motility. During each experiment sporozoites were obtained by dissection and half of them were radiated to obtain a Pf^{WT} and Pf^{RA} sample. One million Pf^{WT} and Pf^{RA} were injected intradermally in a skin explant from the same donor and imaged by confocal microscopy, both samples at two different locations. The movies made at the 4 different locations per donor were divided in sections of 400 frames, because the length of the movies varied from 800-2000 frames and SMOOT_{human skin} is optimized to process movies of 400 frames.

The color-coded track overviews of the movies made at the eight different locations are shown in Supplementary figure S1. Linear segments are depicted in red, slight turns in blue and sharp turns in yellow. The latter consisted of both sporozoites moving forward while turning sharply and sporozoites moving back and forth making a 180° turn, called reversal movement. In both donors more sharp turns were found in the Pf^{RA} sample. In donor 1 Pf^{WT} did make some sharp turns and one sporozoite started circling, while Pf^{RA} made more sharp turns in the form of reversal movement (Supplementary S1a-d). In donor 2 the Pf^{RA} exhibited the circling movement, which is observed *in vitro* (Supplementary figure S1g-h). The difference in movement pattern distribution seen for the Pf^{RA} in donor 2 (Supplementary figure S1g-h) revealed the effect of location on movement pattern and underlined that the location needs to be standardized as much as possible by using the same part of the skin and imaging at the same depth.

The data from the eight different locations was pooled before the detailed motility analysis was performed which is reported in the main manuscript. Supplementary figure S2 shows the effect of pooling per donor and the effect of pooling the data from both donors. The same trend is visible when comparing the movement pattern distribution of Pf^{WT} and Pf^{RA} per donor or after pooling the data from both donors.

Pooling of individual experiments

The data from the eight different locations was pooled before the detailed motility analysis was performed which is reported in the main manuscript. Supplementary figure S2 shows the effect of pooling per donor and the effect of pooling the data from both donors. The same trend is visible when comparing the movement pattern distribution of Pf^{WT} and Pf^{RA} per donor or after pooling the data from both donors.

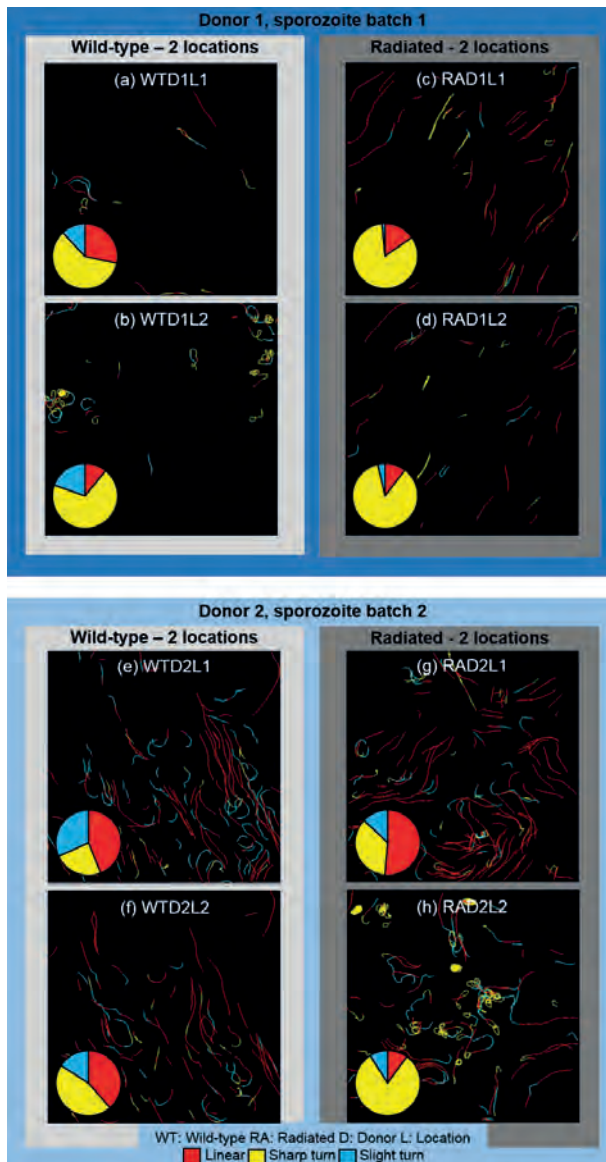


Figure S1. Overview sporozoite tracks for individual locations. (a-b) Track overview and movement pattern distribution for wild-type sporozoites injected into the skin explant from donor 1 and imaged at two different location. (c-d) Track overview and movement pattern distribution for radiation attenuated sporozoites injected into the skin explant from donor 1 and imaged at two different location. (e-f) Track overview and movement pattern distribution for wild-type sporozoites injected into the skin explant from donor 2 and imaged at two different location. (g-h) Track overview and movement pattern distribution for radiation attenuated sporozoites injected into the skin explant from donor 2 and imaged at two different location. The field of view was 290x290 μm for all movies.

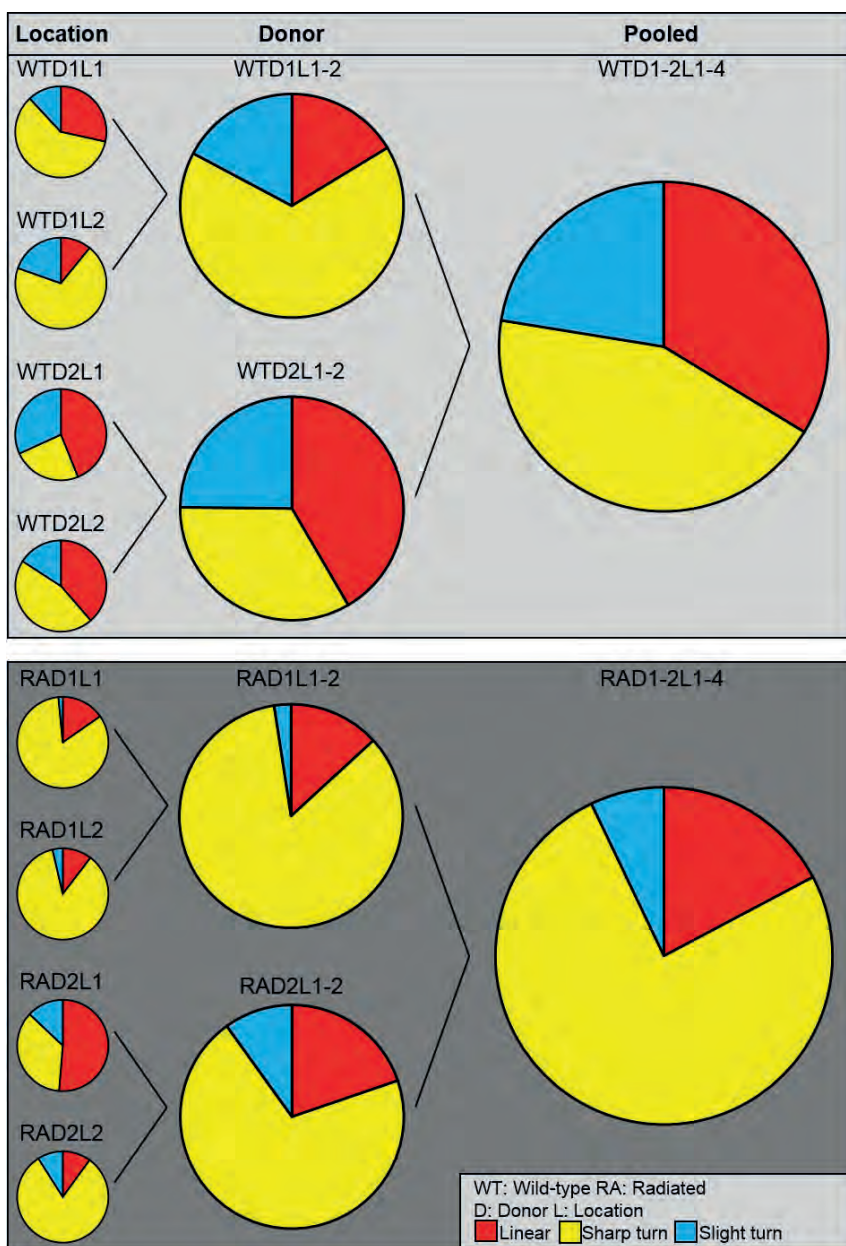


Figure S2. Pooling process of sporozoite motility data. The movement pattern distribution is shown for wild-type (WT) and radiation attenuated (RA) sporozoites per individual location (L), per donor (D) and after pooling. The movement pattern distribution of radiation attenuated sporozoites was significantly different from the movement pattern distribution of wild-type sporozoites, both per donor and after pooling ($p < 0.0001$; Chi-Squared test).

In vitro assay with *Plasmodium falciparum*

For the in vitro assay, the sporozoites were obtained in the same way as for the experiments in human skin explants. For imaging of the sporozoites, 10 μl of the spz solution was pipetted on the cover slip of a confocal dish without any precoating ($\varnothing 14\text{mm}$; MatTek Corporation), covered with another cover slip ($\varnothing 12\text{mm}$; VWR Avantor) and imaged within half an hour (Sup. Movie 4).

Sporozoite velocity and movement pattern distribution over time

To assess the influence of the time on sporozoite velocity we longitudinally sampled 1 movie file over a 2h time period, see Supplementary figure S3. This data suggested that in the current setting time had little influence on the velocity of *Plasmodium falciparum* (trendline slope: decrease of $0.0023 \mu\text{m}/\text{sec}$ per minute; R^2 : 0.3). In the same movie we assessed the influence of time on the turning behavior of sporozoites and again, there seem to be little to no influence (trendline slope: decrease of 0.09 percent per min; R^2 : 0.4).

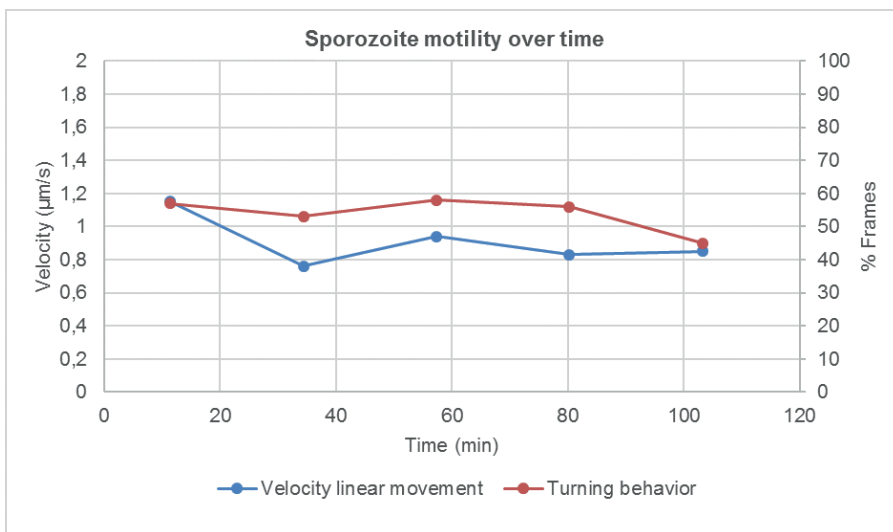
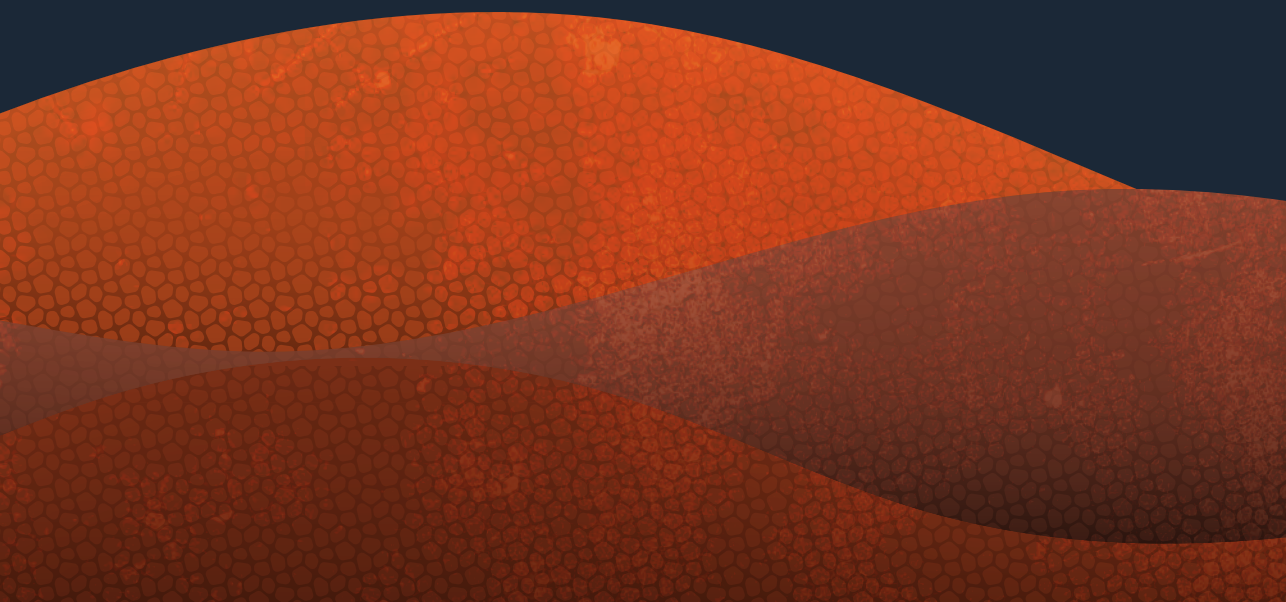


Figure S3. Sporozoite motility over time. A 4000 frames movie file was longitudinally sampled in 5 sections of 800 frames (23 min). The velocity of the sporozoites during linear movement is depicted in blue and the percentage of turns (calculated at frame level) is depicted in red.

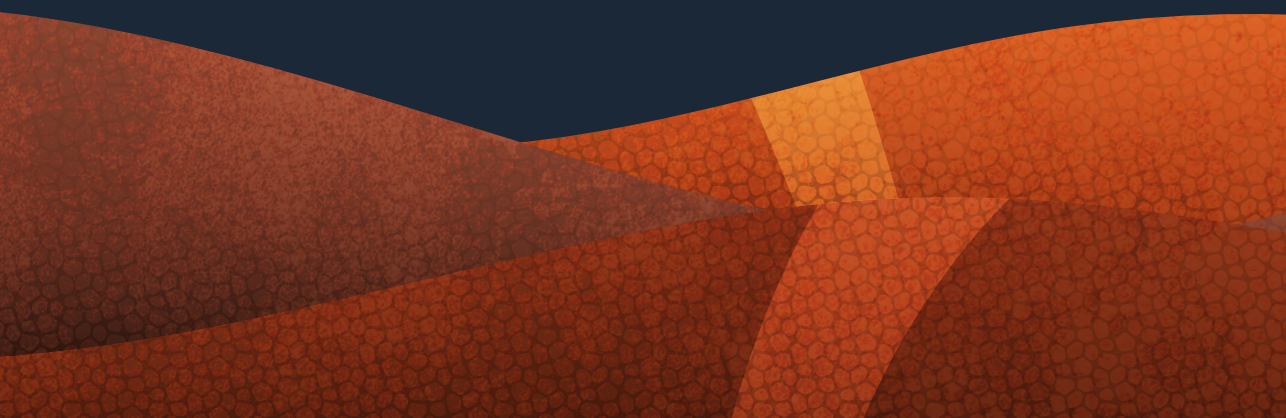
6



A tracer-based method enables tracking of *Plasmodium falciparum* malaria parasites during human skin infection

Béatrice M.F. Winkel, Clarize M. de Korne, Matthias N. van Oosterom, Diego Staphorst, Anton Bunschoten, Marijke C.C. Langenberg, Séverine C. Chevalley-Maurel, Chris J. Janse, Blandine Franke-Fayard, Fijs W.B. van Leeuwen, Meta Roestenberg

Theranostics 2018. Doi: [10.7150/thno.33467](https://doi.org/10.7150/thno.33467)



ABSTRACT

Introduction: The skin stage of malaria is a vital and vulnerable migratory life stage of the parasite. It has been characterized in rodent models, but remains wholly uninvestigated for human malaria parasites. To enable in depth analysis of not genetically modified (non-GMO) *Plasmodium falciparum* (Pf) sporozoite behavior in human skin, we devised a labelling technology (Cy5M₂, targeting the sporozoite mitochondrion) that supports tracking of individual non-GMO sporozoites in human skin.

Methods: Sporozoite labelling with Cy5M₂ was performed *in vitro* as well as via the feed of infected Anopheles mosquitos. Labelling was validated using confocal microscopy and flow cytometry and the fitness of labelled sporozoites was determined by analysis of infectivity to human hepatocytes *in vitro*, and *in vivo* in a rodent infection model. Using confocal video microscopy and custom software, single-sporozoite tracking studies in human skin-explants were performed.

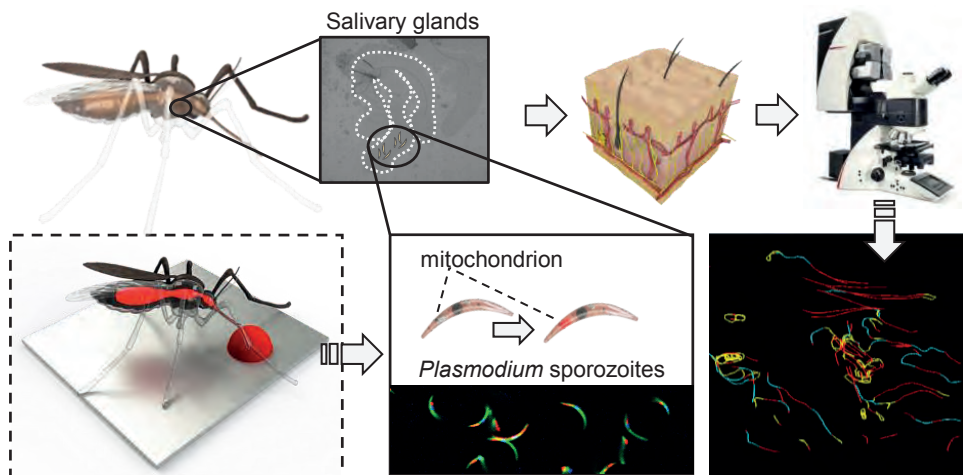
Results: Both *in vitro* and in mosquito labelling strategies yielded brightly fluorescent sporozoites of three different *Plasmodium* species. Cy5M₂ uptake colocalized with MitoTracker® green and could be blocked using the known Translocator protein (TSPO)-inhibitor PK11195. This method supported the visualization and subsequent quantitative analysis of the migration patterns of individual non-GMO Pf sporozoites in human skin and did not affect the fitness of sporozoites.

Conclusions: The ability to label and image non-GMO *Plasmodium* sporozoites provides the basis for detailed studies on the human skin stage of malaria with potential for *in vivo* translation. As such, it is an important tool for development of vaccines based on attenuated sporozoites and their route of administration.

Keywords: malaria, sporozoites, skin, molecular Imaging, cell tracking.

Graphical Abstract

Mitochondria of malaria sporozoites can be labelled *in vitro* or within mosquito glands using Cy5M₂. Using custom software, labelled non-GMO *Pf* sporozoites are tracked and their migration is studied in human skin.



INTRODUCTION

Despite global control efforts, malaria remains the most deadly parasitic disease worldwide accounting for 435,000 deaths in 2017 alone¹, particularly among children below 5 years of age in Sub-Saharan Africa. Decades of research into malaria vaccine development has led to a focus on immune recognition of the clinically silent pre-erythrocytic stage of *Plasmodium* parasites, i.e. sporozoites injected by an infected mosquito that infect liver cells. At this stage, the number of parasites is still low (~100 sporozoites are injected per mosquito bite²) and during their migration from the skin inoculation site to the liver the extracellular sporozoites are vulnerable to attack by immunoglobulins^{3,4}. Ultimately, only around a quarter of injected sporozoites will make their way from the injection site to the liver, leaving the majority behind in the skin⁵.

Pre-erythrocytic immunity to malaria can be induced by repeated exposure to attenuated *Plasmodium falciparum* (*Pf*) sporozoites that arrest development in the liver⁶. Remarkably, these sporozoites induce a strong protective immune response when delivered by the bite of *Pf* infected mosquitoes^{2,6} or following intravenous (IV)

administration of purified attenuated *Pf* parasites^{7,8}, but intradermal (ID) syringe injection of the latter yields inferior protective immunity both in human and in rodent models of malaria^{7,9,10}. However, the use of live mosquitoes or IV administration for large scale vaccination in sub-Saharan countries is not practical.

To rationally design a highly potent malaria vaccine that helps trigger immunity at the pre-erythrocytic stage, more insight into the skin-liver migration mechanisms and immune priming by sporozoites is urgently needed. In rodents, genetically engineered murine *Plasmodium* parasites expressing reporter proteins such as green fluorescent protein (GFP) or luciferase provided unprecedented insight into host-to-host parasite transmission and subsequent migratory behavior of sporozoites from skin to liver. With the use of such tools, sporozoite motility in the skin was visualized¹¹⁻¹³ and the initial dermal immunological responses to injected parasites could be characterized^{14,15}. The clinical translation of these rodent malaria characteristics poses some challenges: 1) the difference between rodent and human skin in anatomy and the population of skin-resident immune cells makes it difficult to translate rodent data to humans, and 2) application of transgenic reporter parasites in humans is undesirable. As a consequence, there is demand for imaging technologies that support tracking of single not genetically modified (non-GMO) *Pf* sporozoites in human skin.

Molecular imaging provides a means to monitor the location of pathology *in vivo*¹⁶. While this technology is most advanced in oncological settings, it also proved to be of value for the detection of infectious diseases, particularly in bacterial infections¹⁷. Uniquely, many imaging modalities and targets in biomedical imaging are universal. Exogenous fluorescent tracers are not only standard tools in biomedical *in vitro* assays, but are also increasingly clinically employed to provide high resolution real-time guidance during interventions e.g. for skin cancers¹⁸. Based on these utilities, we reasoned fluorescent tracers could also be used to track non-GMO sporozoites in human skin.

We investigated the receptor specific uptake of the mitochondrial Cy5-methyl-methyl (Cy5M₂) tracer. Based on the chemical properties of Cy5M₂: lipophilicity and charge, as well as structure, we hypothesized that translocator proteins (TSPO), formally known as the peripheral-type benzodiazepine receptor (PBR), at the outer mitochondrial membrane^{19,20} could be a potential target of this tracer. We demonstrate Cy5M₂mitochondrial labelling capacity of sporozoites which can be blocked by the known TSPO inhibitor PK1119521. Cy5M₂enables labelling of multiple *Plasmodium* species, both *in vitro* and in the mosquito host. Additionally, we studied the cell-tracking

utility of Cy5M₂-labelled *Pf* sporozoites in a human skin explant model. As a proof of concept for their future use, the fitness of Cy5M₂-labelled sporozoites was studied in an *in vitro* human hepatocyte infection assay as well as *in vivo* in a rodent infection model.

MATERIALS AND METHODS

Parasites and animals

Sporozoites were obtained from two rodent malaria species *Plasmodium berghei* (*Pb*) and *Plasmodium yoelli* (*Py*). We used the following wild type and transgenic lines that express fluorescent and/or luminescent reporter proteins: Wild type *Pb* ANKA (cl15cy122); *Pb* line 1868cl1 expressing mCherry and luciferase under the constitutive HSP70 and eef1a promoters respectively²³ (RMgm-1320, www.pberghei.eu) *Pb* line Bergreen²⁴, Wild type *Py* 17XNL (RMgm-688, www.pberghei.eu22); *Py* line 1971cl125 expressing green fluorescent protein (GFP) and luciferase under the constitutive eef1a promoter (RMgm-689, www.pberghei.eu). Mosquitoes were infected by feeding on infected mice as described previously²⁶. For all experiments we used female Swiss mice (6-7 weeks old; Charles River, Leiden, The Netherlands). In addition, sporozoites were obtained from the human parasite *Pf* (NF5427, kindly provided by Radboudumc, Nijmegen, The Netherlands). Mosquitoes were infected by standard membrane feeding as previously described²⁸.

All animal experiments of this study were approved by the Animal Experiments Committee of the Leiden University Medical Center (DEC 14307). The Dutch Experiments on Animal Act is established under European guidelines (EU directive no. 86/609/EEC regarding the Protection of Animals used for Experimental and Other Scientific Purposes). All experiments were performed in accordance with relevant guidelines and regulations.

In vitro Cy5M2 labelling of sporozoites

Salivary glands from infected mosquitoes were dissected manually at day 14-21 (*Py* and *Pf*) or day 21-28 post infection (*Pb*). Glands were incubated in RPMI 1640 (Invitrogen, Carlsbad, CA, USA) supplemented with 10% heat inactivated Fetal Calf Serum (FCS; Bodinco, Alkmaar, The Netherlands) containing 2,6µM Cy5-methyl-methyl (Cy5M2; 1ug/ml; for compound details see supporting information; Figure S1) or, 100nM MitoTracker® Green for 30 minutes at 28°C or mock stained using RPMI 10% FCS only. TSPO blocking experiments were performed by incubating sporozoites with the known TSPO inhibitor PK11195 21 (50 µM; 40 minutes at 37°C; see supporting information) before the incubation with Cy5M2. Subsequently, salivary glands were washed twice in RPMI

10% FCS and either imaged directly, or homogenized and filtered over a 40µm filter (Falcon, Corning, Amsterdam, The Netherlands). The whole salivary gland, or solution containing sporozoites was pipetted onto a microscopy slide for live imaging using either a confocal (Leica TCS SP8, Wetzlar, Germany, 40x objective) or a conventional fluorescence microscope (Leica AF6000LX, Wetzlar, Germany, 40x objective). Nuclei were counterstained with Hoechst 33342 10 minutes before imaging.

In vivo Cy5M₂ labelling of sporozoites

Mosquitoes were infected either with wild type (WT) or transgenic *Pb* or *Py*. In addition, mosquitoes were infected with WT *Pf* as previously described²⁸. Infected mosquitoes were fed on fresh whole blood or 5% glucose in water containing 26µM Cy5M₂ (10µg/ml) at day 21-28 (*Pb*) or day 14-21 post infection (*Py* and *Pf*). Feeding was performed using water-heated, glass mosquito feeders at 39°C as previously described²⁸, in an interrupted feeding schedule of five times two minutes. To maximize feeding behavior, we withheld glucose 24 hours prior to feeding. Immediately after feeding, salivary glands of fed mosquitoes were dissected and placed on a microscopy slide for imaging. Nuclei were counterstained *in vitro* using Hoechst 33342. Slides were imaged using a Leica TCS SP8 confocal microscope with a 40x objective.

Flow Cytometry

Salivary glands containing GFP expressing *Pb* (Bergreen) sporozoites were labelled with Cy5M₂ using either the *in vitro* or the *in vivo* labelling technique (see above) or mock stained *in vitro*. Glands were homogenized, stained with Hoechst 33342 *in vitro*, and resuspended in FACS (Flow Cytometric Cell Sorting) buffer (Phosphate-buffered saline (PBS; Braun, Melsungen, Germany) containing 2mM Ultra-pure EDTA (Invitrogen, Carlsbad CA, USA) and 0.5% Bovine serum albumin; BSA (Roche, Basel, Switzerland)). Samples were measured by LSR FortessaTM (BD Bioscience, Franklin Lakes, NJ, USA) and analyzed in FlowJoTM version 9.9.5 (FlowJo LLC, Ashland, OR, USA). Sporozoites were selected by gating on GFP-positive events and Cy5M₂ fluorescence signal was quantified in Median Fluorescent Intensity (MFI). Events were normalized to FlowJo algorithms (% of max) to account for the differences in numbers of sporozoites measured per sample.

In vitro sporozoite fitness assay

Sporozoite fitness after labelling was established by measuring *in vitro* infection of hepatocytes and development within hepatocytes as described previously²⁹. In brief, 5x10⁴ *Pb* sporozoites of line 1868cl1 expressing mCherry were stained *in vitro* with Cy5M₂ or mock stained as described above. Sporozoites were incubated with cells of a HUH7 human hepatoma cell line in a 1:1 ratio in RPMI 10% FCS at 37 degrees for 44

hours. Hepatoma nuclei were stained using Hoechst 33342. Live imaging of liver stage parasite development (presence of liver schizonts) was performed using a conventional fluorescent microscope (Leica AF6000LX). In addition, infectivity was quantified by real-time PCR. DNA was isolated from infected cells 4 hours post infection using a QIAamp DNA Mini Kit (Qiagen, Hilden, Germany) and a real-time PCR was performed as previously described using a cross-species 18S gene based cross species *Plasmodium* probe³⁰.

In vivo sporozoite fitness assay

Sporozoite fitness after labelling was established by measuring parasite liver loads *in vivo* after infection of mice with labelled parasites. Whole salivary glands of mosquitoes infected with *Pb* line 1868cl1 were collected in RPMI medium and stained with Cy5M₂ *in vitro* or mock stained in medium as described above. Sporozoites were isolated as described above (section *In vitro* Cy5M₂ labelling of sporozoites). The free sporozoites were counted in a Bürker counting chamber using phase-contrast microscopy. A total number of 5x10⁴ sporozoites was administered to mice by ID injection of 10 µl at both upper thighs using a 30G x 8 mm needle (BD Micro-Fine, BD Biosciences, Breda, The Netherlands). Prior to administration of sporozoites, mice were anesthetized using the isoflurane-anesthesia system (XGI-8, Caliper Life Sciences, Waltham, MA, USA) and shaved in order to optimize the precision of administration.

Parasite liver loads were determined in live mice at 44 hours post infection by real time *in vivo* imaging of luciferase-expressing liver stages as previously described³¹. Liver stages were visualized by measuring luciferase activity of parasites in whole bodies of anesthetized mice using the IVIS Lumina II Imaging System (Perkin Elmer Life Sciences, Waltham, MA, USA). D-luciferin was dissolved in PBS (100 mg/kg; Caliper Life Sciences) and injected subcutaneously in the neck. Animals were kept anesthetized during the measurements, which were performed within 8 minutes after the injection of D-luciferin. Quantitative analysis of bioluminescence of whole bodies was performed by measuring the luminescence signal intensity using the ROI (region of interest) settings of the Living Image® 4.4 software (Perkin Elmer Life Sciences). Presence of blood parasitemia and prepatent period was determined by Giemsa-stained blood smear at day 4 to 10 post sporozoite infection. The prepatent period (measured in days post sporozoite infection; prepatency) ends at the day that blood stage infection with 0.5-2% parasitemia is observed.

Imaging of *Pf* sporozoites in human skin explants

Human skin explants were obtained from patients undergoing abdominal reduction surgery (CME approval number: B18-009). Immediately after surgery, skin explants

were injected intradermally with 106 *in vitro* Cy5M₂-labelled *Pf* sporozoites. Sporozoites were mixed with Yellow-Green fluorescent 500nm Latex nanoparticles (Sigma Aldrich) in order to locate the injection site microscopically. A 6mm punch biopsy was taken at the injection site. Biopsies were sliced longitudinally through the injection site and mounted on a microscopy slide with a 1 mm depression in RPMI 10% FCS. Slides were imaged for 30-60 consecutive minutes using a Leica TSC SP8 Confocal microscope with accompanying Leica LASX software, using an exposure time of approximately 1.7 seconds per frame and a 40x objective. Recorded microscopy movies were analyzed for sporozoite motility, using a custom MATLAB software (The MathWorks Inc. Natick, MA, USA) termed SMOOT_{human skin}. In this application tailored software package, sporozoite locations were segmented per movie frame, based on both fluorescence intensity and shape. To reconstruct sporozoite movement over time, median pixel locations per segmented sporozoite shape were connected in time, based on both pixel and frame locations. Based on the dynamic behavior of the sporozoites it was possible to i.a. isolate the following features: migration pattern, speed and parameters of track tortuosity (see supporting information for more detail). SMOOT_{human skin} software can be made available upon request.

RESULTS

In vitro labelling of sporozoites with Cy5M₂

Salivary glands of mosquitoes containing GFP-expressing *Plasmodium berghei* (*Pb*) sporozoites were incubated with Cy5M₂ to achieve labelling of sporozoite mitochondria *in vitro*. Confocal microscopy of salivary sporozoites revealed a single fluorescent spot adjacent to the nucleus, in agreement with the presence of single parasite mitochondrion (Figure 1A)^{32,33}. The universal applicability of this *in vitro* labelling technique for sporozoites of different *Plasmodium* species was demonstrated by labelling murine *Plasmodium yoelii* (*Py*) and *Pb* and human *Pf* sporozoites (Supporting information; Supplementary figure S2). Cy5M₂ uptake by sporozoites was quantified by flow cytometry, which showed a 430-fold increase in median fluorescence intensity (MFI) of Cy5M₂ labelled parasites (Cy5M₂ MFI of 7493) compared to unlabeled controls (Cy5M₂ MFI of 17.5; Figure 1B). All sporozoites exposed to Cy5M₂ showed tracer uptake, however, a small proportion of sporozoites (8.47%) take up Cy5M₂ less readily, as reflected by their lower mean fluorescent intensity (Figure 1B).

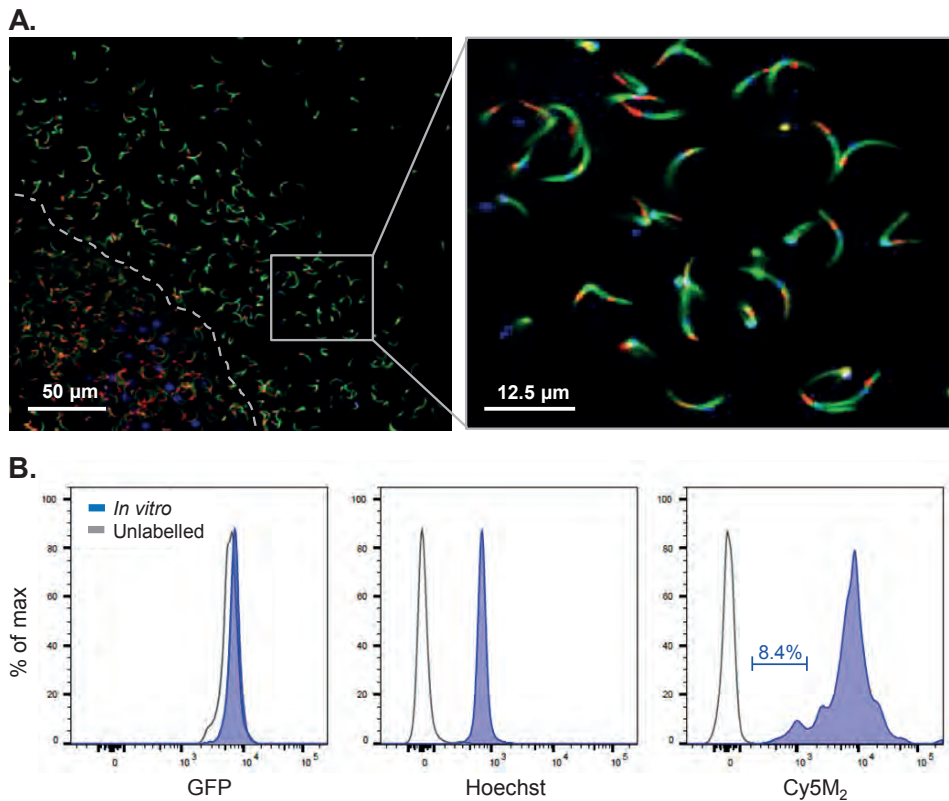


Figure 1. Cy5M labels sporozoites *in vitro*. (A) Fluorescence-microscopy analysis of *In vitro* labelled *Pb* sporozoites (Berg2green) expressing GFP (green; cytoplasmic) and a single spot Cy5M (red). Parasite nuclei are stained with Hoechst (blue). Dotted line demarcates the salivary gland edge, separating expelled sporozoites from gland sporozoites. (B) Quantification of fluorescence by Flow Cytometry. Gray lines represent background signal in unlabelled sporozoites. Blue lines show signal after labelling with Hoechst and Cy5M₂. All sporozoites are GFP⁺. Fluorescence intensity on x-axis, Events normalized using FlowJo algorithms in order to account for the differences in numbers of sporozoites measured per sample (% of max; y-axis).

Co-staining with MitoTracker® green confirmed Cy5M₂ labelling was restricted to the mitochondrion (Figure 2A; Supporting information Supplementary figure S3). In line with our assumptions that mitochondrial TSPO could be a potential target of Cy5M₂, competition with the known TSPO inhibitor PK11195 reduced the mitochondrial uptake in a breast cancer cell line (X4-cells), schwannoma cell line (RT4-D6P2T; Supplementary figure S4) as well as directly in *Pb* sporozoites (Figure 2B).

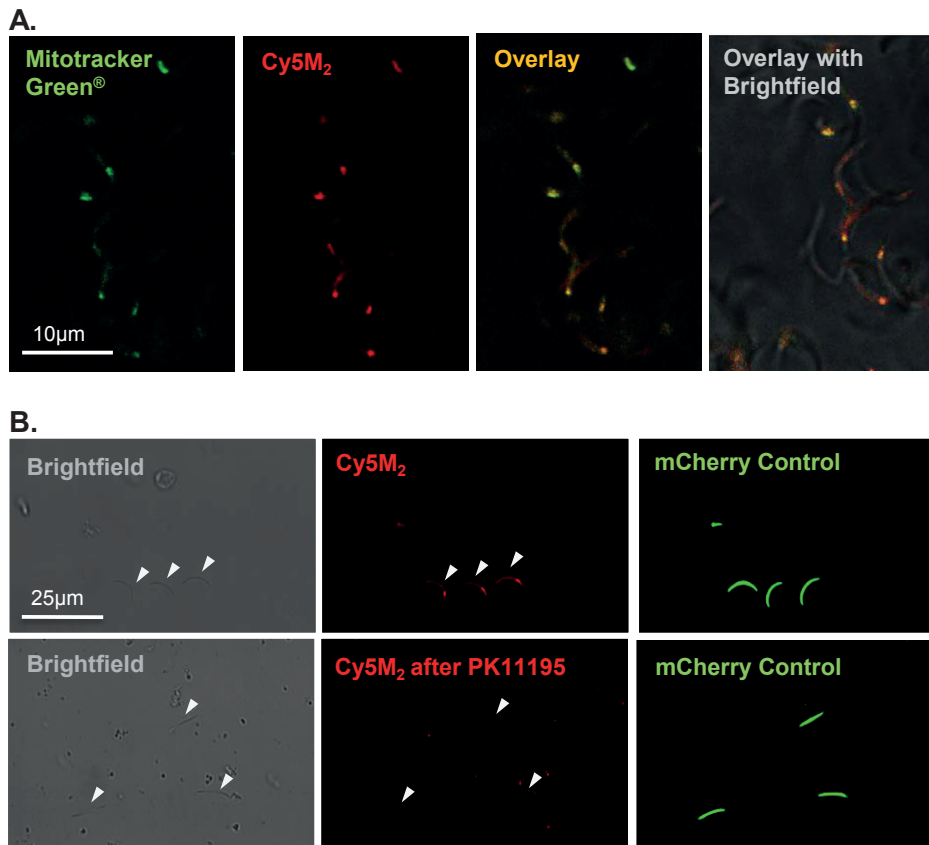
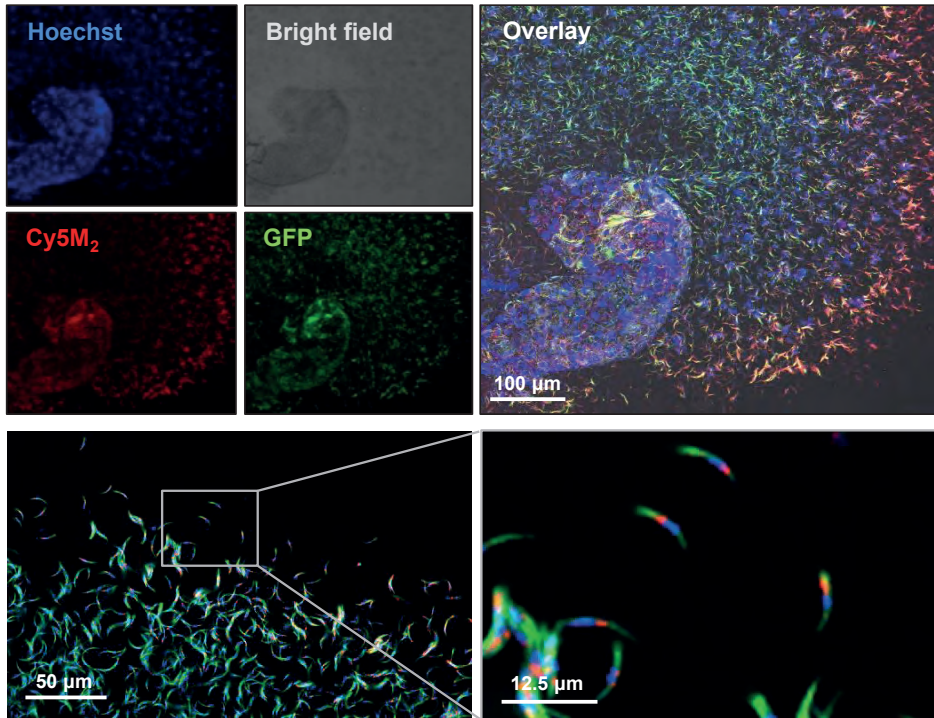


Figure 2. Cy5M₂ labels sporozoite mitochondria and can be blocked by TSPO inhibitor PK11195. (A) Double staining of Cy5M₂ (red) with Mitotracker green (green) shows mitochondrial staining in labelled *Pb* sporozoites. (B) Cy5M₂ (red) labelling in mCherry expressing (green) sporozoites can be blocked by addition of the known TSPO inhibitor PK11195.

Labeling of sporozoites with Cy5M₂ in mosquitoes

Infected mosquitoes containing salivary gland sporozoites were exposed to Cy5M₂ by membrane feeding. As a result of the tracer's molecular size (383,25 Mw) it rapidly diffused through the mosquito to label sporozoites within salivary glands (Figure 3). In order to study the tracer distribution throughout highly auto fluorescent mosquitoes, we collected midguts and salivary glands of Cy5M₂ fed mosquitoes and imaged those organs separately. This indicated universal staining of mosquito organs, including the salivary glands and gland residing sporozoites (Figure 3, Supplementary figure S5). Quantification of the *in vivo* tracer uptake in sporozoites by flow cytometry revealed

A.



B.

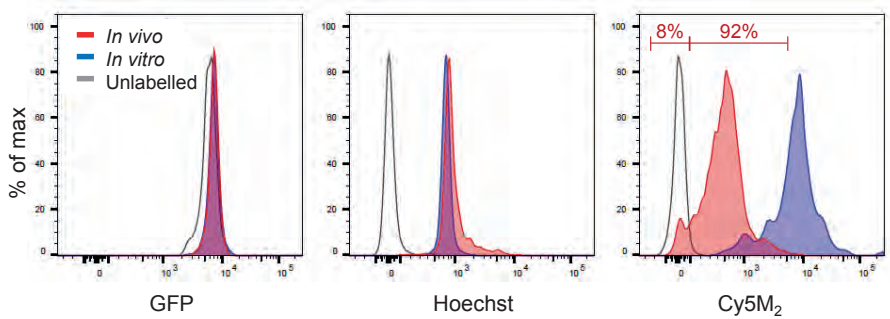


Figure 3. Feeding infected mosquitoes on blood containing Cy5M labels sporozoites. (A) Fluorescence-microscopy analysis showing a whole salivary gland with a cloud of expelled, *in vivo* Cy5M (red) labelled, GFP expressing (green) *Pb* sporozoites. Nuclei are stained with Hoechst (blue). Scale bar 100 µm. Below: magnification shows mitochondrial staining. (B) Flow Cytometric quantification shows a 30 fold increase in fluorescence in 92% of mosquito-fed sporozoites (*in vivo*, red) compared to unlabelled controls (grey line). Highest uptake was seen with *in vitro* labelled parasites (blue). Fluorescence intensity on x-axis. Events are normalized using FlowJo algorithms in order to account for the differences in numbers of sporozoites measured per sample (% of max; y-axis).

clear fluorescence uptake by 92% of sporozoites and a 30-fold increase of Cy5M₂ MFI compared to unlabeled control sporozoites (Figure 3B; Cy5M₂ MFI of labelled sporozoites was 515 compared to 17.5 of unlabeled controls).

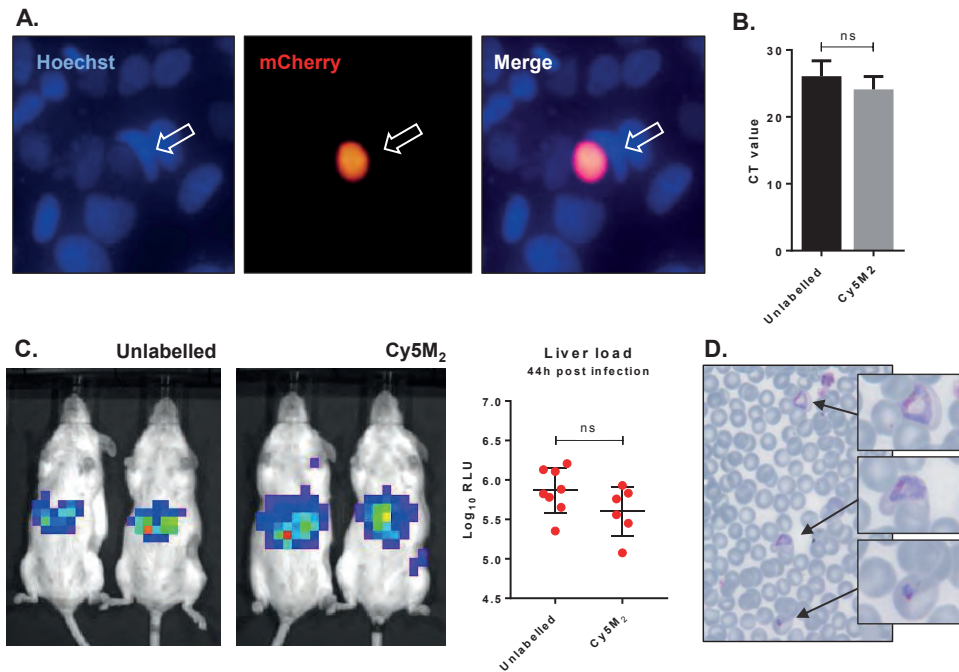


Figure 4. Labeled sporozoites retain their infectivity *in vitro* and *in vivo*. (A) Human hepatoma (HUH7) cell line infection with *in vitro* Cy5M₂ labelled, mCherry expressing *Pb* sporozoites shows liver schizont (arrow) formation at 44h post infection. (B) PCR data showing similar levels of HUH7 cell infection with Cy5M₂ labelled sporozoites compared to unlabeled controls. ($p=0.52$) (C) Representative IVIS Lumina image of Swiss mice injected with luciferase expressing sporozoites. Mice injected with *in vitro* Cy5M₂ labelled *Pb* (right panel) show similar liver load 44h post injection compared to mice injected with mock labelled controls (left panel). Quantification of liver loads in relative light units (RLU), pooled data of two experiments. Eight mice per group. $p=0.18$ (D) Representative blood smear at day 7 post infection with Cy5M₂ labelled *Pb* shows blood stage malaria.

Fitness of Cy5M₂ labelled sporozoites.

The fitness of Cy5M₂ labelled sporozoites was first analyzed by determination of *in vitro* infectivity of mCherry-expressing *Pb* sporozoites to human Huh7 hepatoma cells. As Cy5M₂ is lost during liver stage development of parasites, we detected fully mature liver stages using mCherry expression at 44 hours after infection. Figure 4A shows a

liver schizont, demonstrating that labelled sporozoites are able to infect hepatocytes and develop into mature forms. Quantification of *Pb* DNA within Huh7 monolayers by reverse transcriptase-polymerase chain reaction (RT-PCR) showed comparable levels of invasion of hepatocytes and development into liver-schizonts in cells infected with labelled versus unlabeled sporozoites ($p=0.52$); Figure 4B).

Next we analyzed sporozoite fitness *in vivo* by determination of parasite liver loads in mice infected with labelled *Pb* sporozoites. Parasite liver loads were determined by real-time imaging of luciferase expressing parasites in livers of live mice 44 hours after ID sporozoite injection. We did not observe a difference in parasite liver load between mice infected with Cy5M₂-labeled sporozoites and mice infected with mock stained controls (5.6 ± 0.31 versus 5.7 ± 0.25 mean Log₁₀ relative light units (RLU) respectively, $p=0.18$; Figure 4C). We tested Cy5M₂ concentrations of 50nM to 2.6 μ M, which did not affect sporozoite infectivity in HUH7 cells nor in mice (Figure 4A, Supplementary figure S6). The ability of Cy5M₂-labeled sporozoites to develop into blood stage malaria was demonstrated by positive blood smears at day seven post injection (Figure 4D) The prepatency of mice infected with Cy5M₂ labelled sporozoites was comparable to that of mice infected with unlabeled parasites, both at 6-7 days post infection.

Imaging of migration of Cy5M₂ labelled sporozoites in a human skin explant model

Since the aim of the development of a tracer labelling technique was to realize tracking of individual non-GMO sporozoites in human skin, we studied the migratory behavior of *in vitro* Cy5M₂-labelled non-GMO *Pf* sporozoites in human skin by confocal microscopy. (Figure 5A; movie S1). Using our custom analysis tool SMOOTHhuman skin (Sporozoite Motility Orienting and Organizing Tool) it was possible to isolate individual *Pf* sporozoites based on their Cy5M₂ fluorescent signature, and to record their migration over time. We generated 10 movies during which we were able to visualize 310 individual Cy5M₂ labelled non-GMO sporozoite tracks. 265 of imaged sporozoites were motile (85.5%) and allowed for segmentation of distinct movement patterns: sharp turns (39%), slight turns (13%) and linear movement (48%) (Figure 5B and C). Additionally, we were able to analyze the velocity of individual sporozoites over the full duration of their tracks (Figure 5D) or within individual movement pattern (Figure 5E). The latter revealed that linear segments displayed the highest velocity (median 0.86 μ m/s) and velocity decreases with increased turning behavior (median 0.43 μ m/s for slight turn and 0.29 μ m/s for sharp turn, $p<0.0001$; Figure 5E). Next to these motility characteristics, SMOOTHhuman skin extracts parameters of track tortuosity e.g. straightness index and angular dispersion (Supplementary figure S7). Taken together, these data demonstrate the potential of our custom tracer in imaging and analyzing non-GMO sporozoites in human skin.

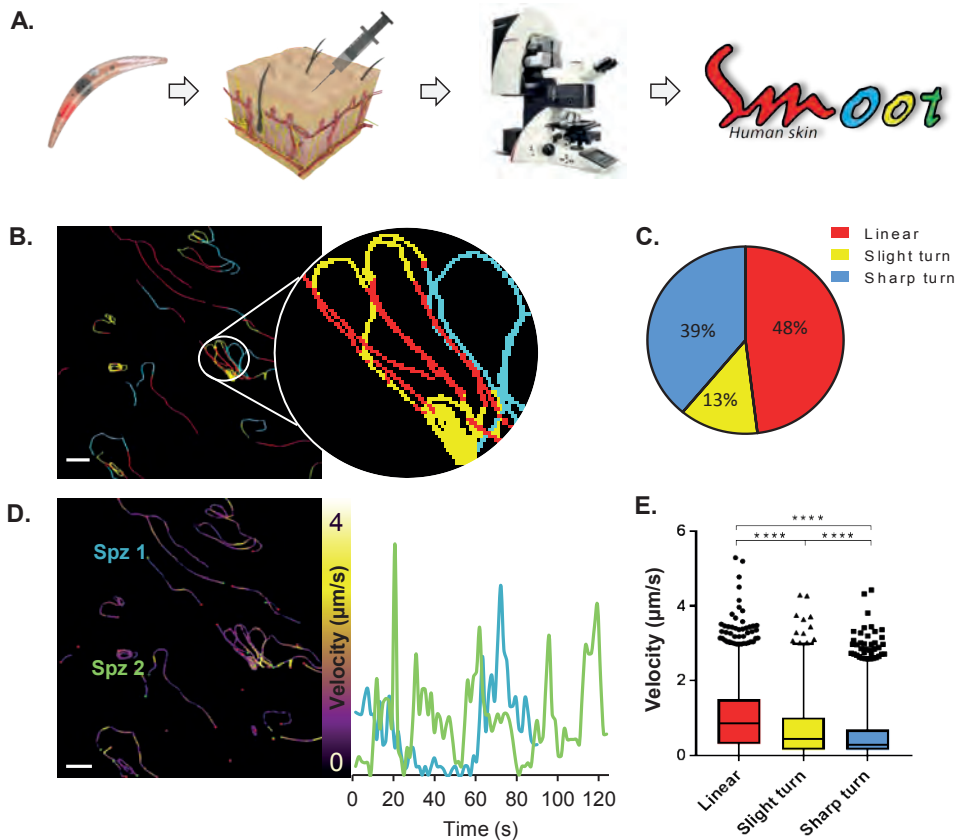


Figure 5. Labelled sporozoites can be tracked in a human skin explant model. (A) Non-GMO *Pf* sporozoites, *in vitro* labelled with Cy5M are injected into human skin explants. Sliced punch biopsies are imaged using confocal microscopy. 2D² video microscopy images are analyzed using SMOOT^{human skin}. (B) Individual sporozoites tracks visualized by migration pattern (linear in red, sharp turn in yellow slight turn in blue) and quantification of patterns (C). Velocity is tracked (D) and quantified (E) over the full duration of the track. ****: $p < 0.0001$ using one way analysis of variance (ANOVA) test.

DISCUSSION

Here we present a novel method to label live sporozoites using a mitochondrion-targeting labelling technique. This method allowed us to perform molecular imaging of non-GMO *Pf* in human skin and quantitatively analyze their motility. Uniquely, the Cy5M2 tracer could be universally applied to the *Plasmodium* species *Pb*, *Py* and *Pf*, and could be utilized to efficiently label sporozoites *in vitro* or to directly label sporozoites within the salivary glands of live mosquitoes. Subsequently, the labelling approach

allowed for cell-tracking of sporozoites. With that, a valuable step has been made towards the realization of *Pf* sporozoite imaging in human skin. We are convinced the application of the Cy5M₂ as a tool for imaging malaria sporozoites is of importance to the development of vaccines consisting of live-attenuated sporozoites.

There is a desperate need for tools that help unravel the mechanism of immune protection induced by malaria vaccine candidates. Antibody binding of sporozoites is likely to be an important effector mechanism after immunization with attenuated sporozoites^{8,34,35} and results in altered motility of sporozoites under antibody attack^{36,37}. Additionally, the recently EMA-approved malaria vaccine Mosquirix™ targets the highly abundant circumsporozoite protein (CSP) on the outer membrane of sporozoites and is associated with elevated anti-CSP antibody titres^{34,38,39}. Despite this, the role of anti-CSP antibodies in the overall immune response against malaria remains controversial. For example, it is unknown what the relative contribution of these antibodies is in either blocking sporozoite migration from the skin to the blood or in blocking invasion of hepatocytes^{35,37}. By allowing molecular-imaging based cell-tracking, the sporozoite-tracking technology presented in this study opens up novel possibilities on functional assays that study the effect that anti CSP antibodies (or antibodies against other sporozoite proteins) exert on sporozoite migration in human skin. Such studies may reveal pathways that support the development of new strategies that prevent infection.

To utilize molecular imaging to investigate the skin migratory behavior of *Plasmodium* sporozoites in humans, a highly expressed biomarker is required that can be targeted with a clinically acceptable tracer design. One of the prominent biomarkers in viable cells is mitochondrial metabolism. Therefore, we explored the use of the single mitochondrion in sporozoites as molecular target for *Plasmodium* sporozoite labelling. This targeting was verified through co-localization with MitoTracker® green. A competition assay with the known TSPO inhibitor PK11195 indicated that our mitochondrial dye Cy5M₂ targets a *Plasmodium* ortholog of TSPO. Uniquely, the presence of TSPO has not been previously been annotated in the *Plasmodium* genome. That said, the presence of TSPO analogues is considered universal in eukaryotic as well as prokaryotic cells⁴⁰⁻⁴². It thus seems likely that *Plasmodium* mitochondria are equipped with a structure resembling mammalian TSPO, or at least a structure that binds similar ligands. This assumption is in line with reports that indicate TSPO inhibition affects blood stages of *Plasmodium* species *in vitro*^{43,44}. A wide range of cell permeable small molecule benzodiazepine-, isoquinoline-, and pyrimidine-analogues have been reported to bind to TSPO19 and because TSPO is widespread in many cell types across species, some of these compounds have already been successfully translated to molecular imaging applications⁴⁵. The same may become true for Cy5M₂, which may also be used to e.g. track different cell types.

The Cy5M₂ labelling technology enabled us to target more than 90% of all sporozoites within the mosquito and *in vitro* whereby 100% of all sporozoites were efficiently labelled. *In vitro* labelling was approximately 15 times more efficient compared to labelling within the mosquito. Flow cytometric analysis of *in vitro* labelled sporozoites identified only a small percentage (8.47%) of sporozoites exhibiting decreased staining efficiency. Whether the differences in Cy5M₂ staining within sporozoites reflect functional differences for example in infectivity or migrating potential, will be the subject of further studies. Interestingly, the decreased staining efficiency might be the result of different factors, such as the presence of transporters⁴⁶⁻⁴⁹.

Our fitness assays did not reveal any evidence for toxicity of Cy5M₂ to sporozoites at the dose used. When extrapolating the current data for future use of Cy5M₂-labelled sporozoites in humans, we expect Cy5M₂ toxicity to the human host to be negligible. Reasoning that even if all Cy5M₂ is taken up during *in vitro* labelling of 10⁶ *Pf* sporozoites (2.6 μM in 1 ml), this would result in a total maximum dose of 1 μg Cy5M₂ or (1 pg per sporozoite). At this dose, toxicity assessments of this compound would fall within the tracer dose regime, a property that supports the translational nature of the presented labelling technology^{50,51}. Obviously, when increased understanding of the in human behavior of *Pf* sporozoites allows for the doses of attenuated sporozoites to be lowered, overall toxicity risk decreases even further.

Our quantitative assessment of migrating *Pf* sporozoites in human skin underlines the potential of this new cell-tracking technology for imaging of non-GMO *Pf* sporozoites in the human skin to study factors and mechanisms influencing host-to-host transmission. Using our custom SMOOT_{human skin} software we were able to extract dermal migration behavior data from individual non-GMO *Pf* sporozoites both in detail and over time. Our data show highly directional movement patterns of migrating sporozoites, as well as high velocity variability within sporozoite tracks. Velocity correlated with movement pattern, with parasites slowing down as their tortuosity increased. Variations in velocity and/or movement pattern may correspond with sporozoite interactions with the tissue environment and may therefore indicate sites of particular interest^{5,52}.

With the presented technology we have been able to study sporozoite behavior skin deep. To extend the use of this technology for imaging beyond the skin stage, a matching nuclear medicine-based imaging approach, or preferably a hybrid imaging approach will have to be developed⁵³. Increased signal intensity per sporozoite through potentiated mitochondrial targeting, may be realized with the use of recent chemical developments in the area of nanotechnology⁵⁴. Such developments will facilitate

further use in malaria research, where imaging of small numbers of parasites will help to elucidate the mystery of non-hepatic development of sporozoites and lymph node trafficking, analogous to experiments with *Pb* in rodents¹³.

Conclusion

We have implemented a fluorescence-based molecular imaging approach based on an exogenous fluorescent tracer that allows direct imaging of *Plasmodium* sporozoites in human tissue. Uniquely, the Cy5M₂ labelling approach is a universally applicable technology which even permits labelling of *Plasmodium* sporozoites while still residing in the live mosquito host. This initial study demonstrated that this technology has the potential to help unravel the fundamental features of skin migration of malaria parasites in humans. Molecular imaging of sporozoite migration in humans allows investigation of factors and mechanisms influencing host-to-host transmission, knowledge that is essential for further development of highly effective vaccines targeting the sporozoite stage.

SUPPLEMENTARY NOTES

Author contribution statement: BW, MO,DS, AB, ML, BF, SC and CK performed the experiments. BW, MO, CK, CJ, FvL and MR interpreted the data. BW, FvL and MR drafted the manuscript. All authors reviewed and contributed to finalizing the manuscript.

Acknowledgements: The research leading to these results has received funding from the European Research Council under the European Union's Seventh Framework Programme (FP7/2007-2013) (2012-306890), a ZONMW VENI grant (016.156.076) financed by the Netherlands Organization for Scientific Research (NWO) and a Gisela Thier fellowship of the LUMC. We thank Geert-Jan van Gemert and Prof. dr. Robert Sauerwein for providing NF54 *Plasmodium falciparum* infected mosquitoes.

Ethics statement: The use of human skin explants (obtained as waste material after abdominal reduction surgery) for this research was approved by the Commission Medical Ethics (CME) of the LUMC, Leiden. Approval number CME: B18-009.

Competing interests: The authors declare no competing financial interests.

REFERENCES

- 1 [Internet] WHO: Geneva Switzerland. 19 November 2018, World Malaria report 2018. <https://www.who.int/malaria/media/world-malaria-report-2018/en/>.
- 2 Medica, D. L. & Sinnis, P. Quantitative dynamics of *Plasmodium yoelii* sporozoite transmission by infected anopheline mosquitoes. *Infect Immun* 73, 4363-4369, doi:10.1128/IAI.73.7.4363-4369.2005 (2005).
- 3 Sack, B. K. et al. Model for in vivo assessment of humoral protection against malaria sporozoite challenge by passive transfer of monoclonal antibodies and immune serum. *Infect Immun* 82, 808-817, doi:10.1128/IAI.01249-13 (2014).
- 4 Vanderberg, J. P. & Frevert, U. Intravital microscopy demonstrating antibody-mediated immobilisation of *Plasmodium berghei* sporozoites injected into skin by mosquitoes. *Int J Parasitol* 34, 991-996, doi:10.1016/j.ijpara.2004.05.005 (2004).
- 5 Amino, R. et al. Quantitative imaging of *Plasmodium* transmission from mosquito to mammal. *Nat Med* 12, 220-224, doi:10.1038/nm1350 (2006).
- 6 Roestenberg, M. et al. Protection against a malaria challenge by sporozoite inoculation. *N Engl J Med* 361, 468-477, doi:10.1056/NEJMoa0805832 (2009).
- 7 Epstein, J. E. et al. Live attenuated malaria vaccine designed to protect through hepatic CD8(+) T cell immunity. *Science* 334, 475-480, doi:10.1126/science.1211548 (2011).
- 8 Bastiaens, G. J. et al. Safety, Immunogenicity, and Protective Efficacy of Intradermal Immunization with Aseptic, Purified, Cryopreserved *Plasmodium falciparum* Sporozoites in Volunteers Under Chloroquine Prophylaxis: A Randomized Controlled Trial. *Am J Trop Med Hyg* 94, 663-673, doi:10.4269/ajtmh.15-0621 (2016).
- 9 Haeberlein, S. et al. Protective immunity differs between routes of administration of attenuated malaria parasites independent of parasite liver load. *Sci Rep* 7, 10372, doi:10.1038/s41598-017-10480-1 (2017).
- 10 Seder, R. A. et al. Protection against malaria by intravenous immunization with a nonreplicating sporozoite vaccine. *Science* 341, 1359-1365, doi:10.1126/science.1241800 (2013).
- 11 Hopp, C. S. et al. Longitudinal analysis of *Plasmodium* sporozoite motility in the dermis reveals component of blood vessel recognition. *Elife* 4, doi:10.7554/eLife.07789 (2015).
- 12 Yamauchi, L. M., Coppi, A., Snounou, G. & Sinnis, P. *Plasmodium* sporozoites trickle out of the injection site. *Cell Microbiol* 9, 1215-1222, doi:10.1111/j.1462-5822.2006.00861.x (2007).
- 13 Gueirard, P. et al. Development of the malaria parasite in the skin of the mammalian host. *Proc Natl Acad Sci U S A* 107, 18640-18645, doi:10.1073/pnas.1009346107 (2010).
- 14 da Silva, H. B. et al. Early skin immunological disturbance after *Plasmodium*-infected mosquito bites. *Cell Immunol* 277, 22-32, doi:10.1016/j.cellimm.2012.06.003 (2012).
- 15 Mac-Daniel, L. et al. Local immune response to injection of *Plasmodium* sporozoites into the skin. *J Immunol* 193, 1246-1257, doi:10.4049/jimmunol.1302669 (2014).
- 16 Massoud, T. F. & Gambhir, S. S. Molecular imaging in living subjects: seeing fundamental biological processes in a new light. *Genes Dev* 17, 545-580, doi:10.1101/gad.1047403 (2003).
- 17 Bunschoten, A., Welling, M. M., Termaat, M. F., Sathekge, M. & van Leeuwen, F. W. Development and prospects of dedicated tracers for the molecular imaging of bacterial infections. *Bioconjug Chem* 24, 1971-1989, doi:10.1021/bc4003037 (2013).
- 18 van den Berg, N. S. et al. Multimodal Surgical Guidance during Sentinel Node Biopsy for

- Melanoma: Combined Gamma Tracing and Fluorescence Imaging of the Sentinel Node through Use of the Hybrid Tracer Indocyanine Green-(99m)Tc-Nanocolloid. *Radiology* 275, 521-529, doi:10.1148/radiol.14140322 (2015).
- 19 Rupprecht, R. et al. Translocator protein (18 kDa) (TSPO) as a therapeutic target for neurological and psychiatric disorders. *Nat Rev Drug Discov* 9, 971-988, doi:10.1038/nrd3295 (2010).
 - 20 Li, F. et al. Translocator Protein 18 kDa (TSPO): An Old Protein with New Functions? *Biochemistry* 55, 2821-2831, doi:10.1021/acs.biochem.6b00142 (2016).
 - 21 Hatty, C. R. & Banati, R. B. Protein-ligand and membrane-ligand interactions in pharmacology: the case of the translocator protein (TSPO). *Pharmacol Res* 100, 58-63, doi:10.1016/j.phrs.2015.07.029 (2015).
 - 22 Otto, T. D. et al. A comprehensive evaluation of rodent malaria parasite genomes and gene expression. *BMC Biol* 12, 86, doi:10.1186/s12915-014-0086-0 (2014).
 - 23 Prado, M. et al. Long-term live imaging reveals cytosolic immune responses of host hepatocytes against *Plasmodium* infection and parasite escape mechanisms. *Autophagy* 11, 1561-1579, doi:10.1080/15548627.2015.1067361 (2015).
 - 24 Kooij, T. W., Rauch, M. M. & Matuschewski, K. Expansion of experimental genetics approaches for *Plasmodium berghei* with versatile transfection vectors. *Mol Biochem Parasitol* 185, 19-26, doi:10.1016/j.molbiopara.2012.06.001 (2012).
 - 25 Lin, J. W. et al. A novel 'gene insertion/marker out' (GIMO) method for transgene expression and gene complementation in rodent malaria parasites. *PLoS One* 6, e29289, doi:10.1371/journal.pone.0029289 (2011).
 - 26 Sinden, R. E. Infection of mosquitoes with rodent malaria. *The Molecular Biology of Insect Disease Vectors: a Methods Manual* (ed. J. M. Crampton, C. B. Beard and C. Louis), pp. 67-91 (1997).
 - 27 Ponnudurai, T., Leeuwenberg, A. D. & Meuwissen, J. H. Chloroquine sensitivity of isolates of *Plasmodium falciparum* adapted to in vitro culture. *Trop Geogr Med* 33, 50-54 (1981).
 - 28 Ponnudurai, T. et al. Infectivity of cultured *Plasmodium falciparum* gametocytes to mosquitoes. *Parasitology* 98 Pt 2, 165-173 (1989).
 - 29 Fougere, A. et al. Variant Exported Blood-Stage Proteins Encoded by *Plasmodium* Multigene Families Are Expressed in Liver Stages Where They Are Exported into the Parasitophorous Vacuole. *PLoS Pathog* 12, e1005917, doi:10.1371/journal.ppat.1005917 (2016).
 - 30 Rougemont, M. et al. Detection of four *Plasmodium* species in blood from humans by 18S rRNA gene subunit-based and species-specific real-time PCR assays. *J Clin Microbiol* 42, 5636-5643, doi:10.1128/JCM.42.12.5636-5643.2004 (2004).
 - 31 van der Velden, M. et al. Protective Efficacy Induced by Genetically Attenuated Mid-to-Late Liver-Stage Arresting *Plasmodium berghei* Deltamrp2 Parasites. *Am J Trop Med Hyg* 95, 378-382, doi:10.4269/ajtmh.16-0226 (2016).
 - 32 De Niz, M. et al. Progress in imaging methods: insights gained into *Plasmodium* biology. *Nat Rev Microbiol* 15, 37-54, doi:10.1038/nrmicro.2016.158 (2017).
 - 33 Sturm, A., Mollard, V., Cozijnsen, A., Goodman, C. D. & McFadden, G. I. Mitochondrial ATP synthase is dispensable in blood-stage *Plasmodium berghei* rodent malaria but essential in the mosquito phase. *Proc Natl Acad Sci U S A* 112, 10216-10223, doi:10.1073/pnas.1423959112 (2015).
 - 34 Ishizuka, A. S. et al. Protection against malaria at 1 year and immune correlates following PfSPZ vaccination. *Nat Med* 22, 614-623, doi:10.1038/nm.4110 (2016).
 - 35 Flores-Garcia, Y. et al. Antibody-Mediated Protection against *Plasmodium* Sporozoites

- Begins at the Dermal Inoculation Site. *MBio* 9, doi:10.1128/mBio.02194-18 (2018).
- 36 Stewart, M. J., Nawrot, R. J., Schulman, S. & Vanderberg, J. P. Plasmodium berghei sporozoite invasion is blocked in vitro by sporozoite-immobilizing antibodies. *Infect Immun* 51, 859-864 (1986).
- 37 Aliprandini, E. et al. Cytotoxic anti-circumsporozoite antibodies target malaria sporozoites in the host skin. *Nat Microbiol* 3, 1224-1233, doi:10.1038/s41564-018-0254-z (2018).
- 38 Casares, S., Brumeanu, T. D. & Richie, T. L. The RTS,S malaria vaccine. *Vaccine* 28, 4880-4894, doi:10.1016/j.vaccine.2010.05.033 (2010).
- 39 Cohen, J., Nussenzweig, V., Nussenzweig, R., Vekemans, J. & Leach, A. From the circumsporozoite protein to the RTS,S/AS candidate vaccine. *Hum Vaccin* 6, 90-96 (2010).
- 40 Yeliseev, A. A. & Kaplan, S. A sensory transducer homologous to the mammalian peripheral-type benzodiazepine receptor regulates photosynthetic membrane complex formation in *Rhodobacter sphaeroides* 2.4.1. *J Biol Chem* 270, 21167-21175 (1995).
- 41 Chapalain, A. et al. Bacterial ortholog of mammalian translocator protein (TSPO) with virulence regulating activity. *PLoS One* 4, e6096, doi:10.1371/journal.pone.0006096 (2009).
- 42 Papadopoulos, V. et al. Translocator protein (18kDa): new nomenclature for the peripheral-type benzodiazepine receptor based on its structure and molecular function. *Trends Pharmacol Sci* 27, 402-409, doi:10.1016/j.tips.2006.06.005 (2006).
- 43 Marginedas-Freixa, I. et al. TSPO ligands stimulate ZnPPiX transport and ROS accumulation leading to the inhibition of *P. falciparum* growth in human blood. *Sci Rep* 6, 33516, doi:10.1038/srep33516 (2016).
- 44 Dzierszinski, F. et al. Ligands of the peripheral benzodiazepine receptor are potent inhibitors of *Plasmodium falciparum* and *Toxoplasma gondii* in vitro. *Antimicrob Agents Chemother* 46, 3197-3207 (2002).
- 45 Vivash, L. & O'Brien, T. J. Imaging Microglial Activation with TSPO PET: Lighting Up Neurologic Diseases? *J Nucl Med* 57, 165-168, doi:10.2967/jnumed.114.141713 (2016).
- 46 Koenderink, J. B., Kavishe, R. A., Rijpma, S. R. & Russel, F. G. The ABCs of multidrug resistance in malaria. *Trends Parasitol* 26, 440-446, doi:10.1016/j.pt.2010.05.002 (2010).
- 47 Wongsrichanalai, C., Pickard, A. L., Wernsdorfer, W. H. & Meshnick, S. R. Epidemiology of drug-resistant malaria. *Lancet Infect Dis* 2, 209-218 (2002).
- 48 Rijpma, S. R. et al. Multidrug ATP-binding cassette transporters are essential for hepatic development of *Plasmodium* sporozoites. *Cell Microbiol* 18, 369-383, doi:10.1111/cmi.12517 (2016).
- 49 Mu, J. et al. Multiple transporters associated with malaria parasite responses to chloroquine and quinine. *Mol Microbiol* 49, 977-989 (2003).
- 50 KleinJan, G. H. et al. Fluorescence guided surgery and tracer-dose, fact or fiction? *Eur J Nucl Med Mol Imaging* 43, 1857-1867, doi:10.1007/s00259-016-3372-y (2016).
- 51 [internet] European Medicines Agency EMA. 2018, <http://www.ema.europa.eu/ema>.
- 52 Battista, A., Frischknecht, F. & Schwarz, U. S. Geometrical model for malaria parasite migration in structured environments. *Phys Rev E Stat Nonlin Soft Matter Phys* 90, 042720, doi:10.1103/PhysRevE.90.042720 (2014).
- 53 KleinJan, G. H. et al. Multimodal imaging in radioguided surgery. *Clin Transl Imaging* 1, 433-444 (2013).
- 54 Lynn E. Samuelson, B. M. A., Mingfeng Bai, Madeline J Dukes,, Colette R. Hunt, J. D. C., Zeqiu Han, Vassilios Papadopoulosc & Bornhop, a. D. J. A self-internalizing mitochondrial TSPO targeting imaging probe for fluorescence, MRI and EM. *RSC Adv.* 4, 9003 (2014).

SUPPLEMENTARY INFORMATION

Methods

Synthesis of Cy5-methyl-methyl (Cy5M₂)

Indol-Methyl

In brief, 2,3,3-trimethylindolenine (25 mmol) and methyl iodide (30 mmol) were stirred in toluene (40 ml) for 16h at 40 °C. The formed suspension was filtered, and the precipitate was dried in vacuo yielding pink crystals (4 g) and used without further purification.

Cy5-Methyl-Methyl

Indol-Methyl (13.28 mmol), 3-anilinoacraldehyde (6.64 mmol) and sodium acetate (15.49 mmol) were stirred in ethanol absolute (150 ml) and refluxed for 8h under nitrogen atmosphere followed by stirring at room temperature for 6h. The mixture was concentrated and purified by silica gel chromatography using acetonitrile:methanol 3:1, followed by methanol, followed by methanol + 0.25%AcOH. After lyophilization a dark powder (148 mg) was obtained.

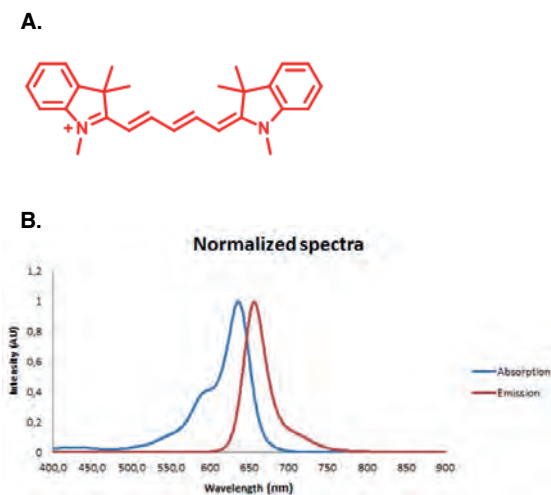


Figure S1. Properties of Cy5M₂. Molecular structure (A) and normalized absorption (blue) and emission spectra (red) of Cy5M₂ (B).

Cy5M₂ binding specificity for TSPO

Confocal microscopy

The binding specificity of Cy5M₂ was initially evaluated *in vitro* using two mammalian cell lines that have a higher mitochondrial density and thus TSPO expression levels than sporozoites: Human breast cancer cell line MDAMB213 X4 cells (X4-cells), kindly provided by Dr. G. Luker (University of Michigan, Ann Arbor, USA), wherein CXCR4 expression was acquired after transfection with a GFP-tagged version of the human CXCR4-gene¹ and RT4-D6P2T rat Schwannoma cell line (RT4-cells), obtained from ATCC (American Type Culture Collection, Manassas, VA, USA). Both cell lines were maintained in Dulbecco's modified Eagle medium (DMEM) enriched with 10% fetal bovine serum and 1% penicillin/streptomycin (all Life Technologies Inc. Carlsbad, CA, USA). Cells were kept under standard culture conditions. The cultured cells were trypsinized and seeded onto coverslips (ø35mm; MatTek Corporation) and incubated overnight in medium.

To validate the mitochondrial localization, Cy5M₂ was applied together with Mitotracker[®] green (Thermo Fisher Scientific, Waltham, MA, USA). RT-4 cells were incubated with 1 µM Mitotracker green[®] (for 1 hour at 37°C) before the incubation with Cy5M₂ (5 min at RT with 3nM). To confirm TSPO binding specificity of Cy5M₂, blocking experiments were performed with the known TSPO inhibitor PK11195² (Sigma Aldrich). Both RT4-cells and X4-cells were incubated with 50 µM PK11195 (40 minutes at 37°C), before the incubation with Cy5M₂ (5 min at room temperature (RT); 3nM). All samples were washed with PBS prior to confocal microscopy analysis (Leica TCS SP8X WLL microscope (Leica Microsystems, Wetzlar, Germany)). Cy5 was excited at 633 nm and the emission was collected between 650-700 nm, the laser power was kept constant during the comparative experiments.

SMOOT_{human skin}

MATLAB (The MathWorks Inc. Natick, MA, USA) software was created for in skin sporozoite analysis. Using this software, we were able to extract the following features per sporozoite over time: movement pattern, angular dispersion, straightness index and velocity. Sporozoite tracks were characterized as motile or stationary based on their displacement. Subsequently, the movement patterns: *sharp turn*, *slight turn* and *linear* were segmented from motile tracks.

Straightness index (SI)

The SI is a measurement for the deviation of a track from a straight line and is used to quantify track tortuosity. It is defined as the ratio of distance between track end point (C) and track length (L), as calculated using formula (1). e.g. SI = 1 in a perfect linear path, SI = 0 when the path describes a circle.

$$SI = \frac{C_{track}}{L_{track}} = \frac{x(i) - x(0)}{\sum_{k=1}^i (x(k) - x(k-1))} \quad (1)$$

Angular dispersion (AD)

The AD describes tortuosity by quantifying changes in direction by measuring deviation from the mean angle of movement. It is calculated according to the following formula:

$$AD = \frac{1}{I} \sqrt{C^2 + S^2} \quad (2)$$

Where I is the last step of the track and C and S are defined as:

$$C = \sum_{i=1}^I \cos \theta_i \quad S = \sum_{i=1}^I \sin \theta_i$$

Where θ is the turn angle of the sporozoite track, defined by the angle difference between path directions in consecutive frames.

$$\theta_i = \delta_i - \delta_{i-1}$$

e.g. AD = 1 indicates a consistent angle (either a straight line or a perfect circle) and smaller AD values represent the presence of random turns over the track course.

Velocity

Sporozoite velocity was measured using the displacement between frames. We defined step number in the track i to measure velocity v using formula (3), with x as the median pixel location of the sporozoite and t as the time duration in seconds.

$$v(i) = \frac{x_i - x_{i-1}}{t_i - t_{i-1}} = \frac{dx}{dt} \quad (3)$$

Supplementary video 1 available on:

<https://www.thno.org/v09/p2768/thnov09p2768s2.mp4>

Results

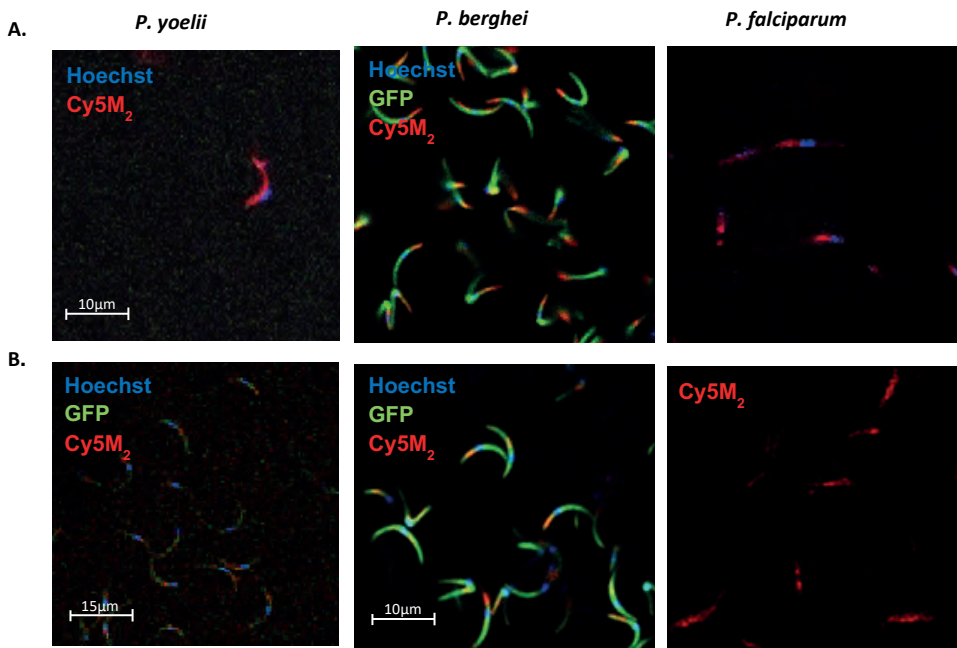


Figure S2. Cy5M₂ labels rodent and human malaria sporozoites. Labelling of different *Plasmodium* species with Cy5M₂, both *in vitro* (A, upper panels) as well as *in vivo* (B, lower panels) within the mosquito host. Overlay images of indicated colours. Brightfield in grey, Hoechst in blue, GFP in green and Cy5M₂ in red. Scale bar 10 μM

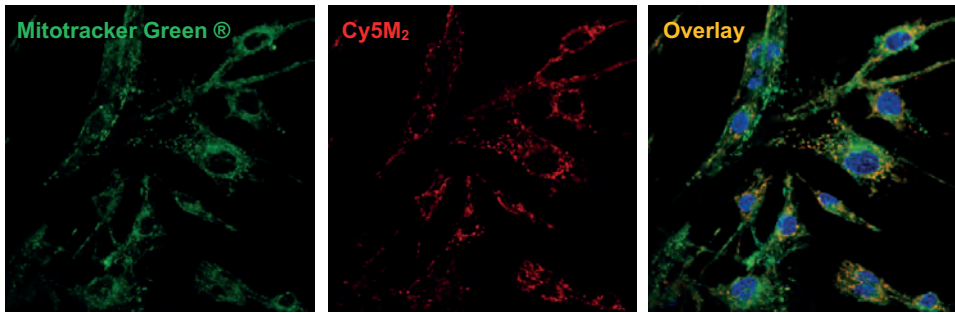


Figure S3. Co-localization of mitochondrial Cy5M₂ and MitoTracker® Green. RT4-cells were stained with MitoTracker® green (green) and Cy5M₂ (red). Nuclei are stained with Hoechst (blue). Scale bar 50µM.

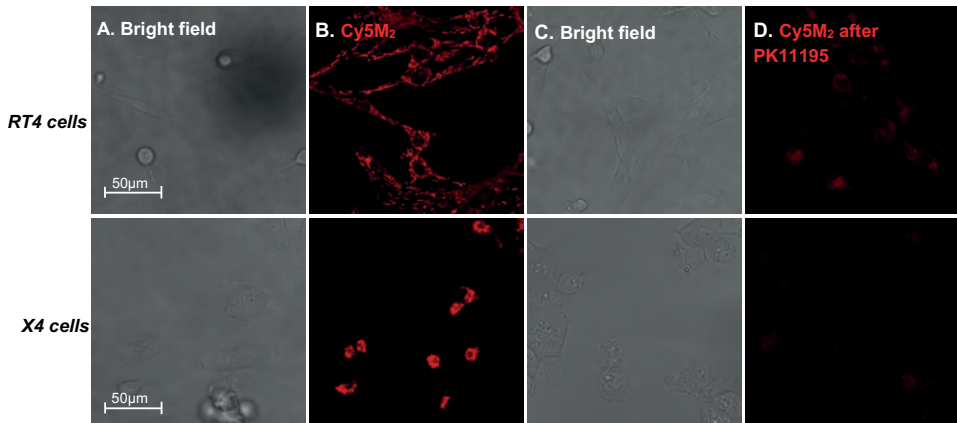


Figure S4. Competitive binding assay of Cy5M₂ with PK11195 in cell lines. A,B. RT4-cells (top panels) and X4-cells (bottom panels) are stained with Cy5M₂ (red). C,D. Cy5M₂ binding is blocked with PK11195.

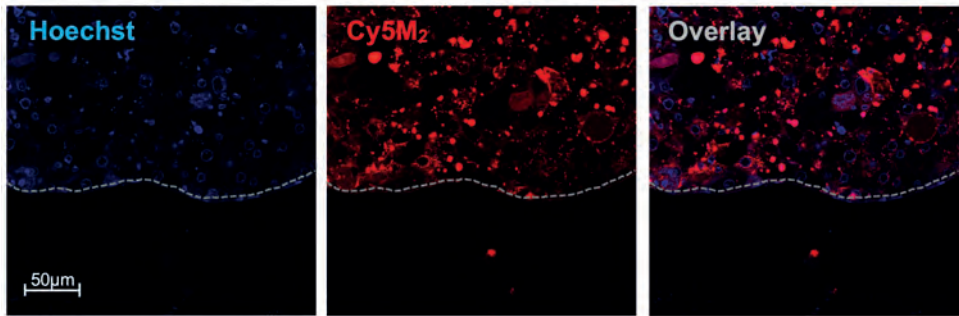


Figure S5. Cy5M₂ staining of the mosquito midgut. Midguts of *Pb* infected *Anopheles* mosquitoes fed on Cy5M₂. Mosquitoes were dissected 15 minutes after feeding. Midgut cells stained with Cy5M₂ (red), nuclei are stained with Hoechst (blue). Scale bar 50µM

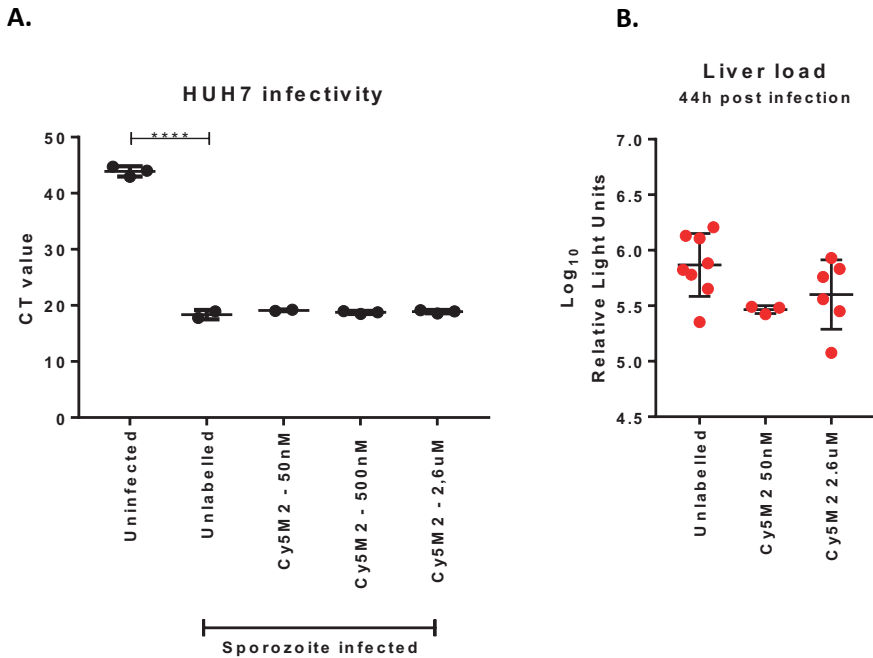


Figure S6. Sporozoite infectivity after Cy5M₂ labelling. Sporozoite infectivity in HUH7 hepatoma cells (A) or in mice (B) was not affected by increased dosages of Cy5M₂. **A.** PCR data showing similar levels of HUH7 cell infection with all dosages of Cy5M₂ labelled sporozoites compared to unlabelled controls. **B.** Quantification of liver load measured by IVIS 44h post infection. Cumulative results from 2 separate experiments (n=8 unlabelled; n=3 TCy5M₂ 50µM and n=8 Cy5M₂ 2,6µM). Statistical analysis: Student's T test. ****= p<0,0001

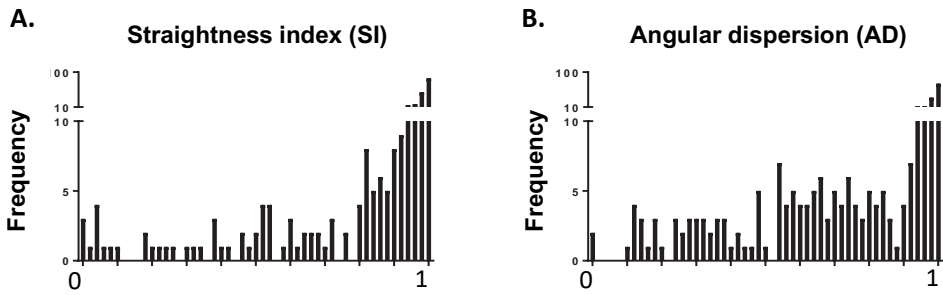
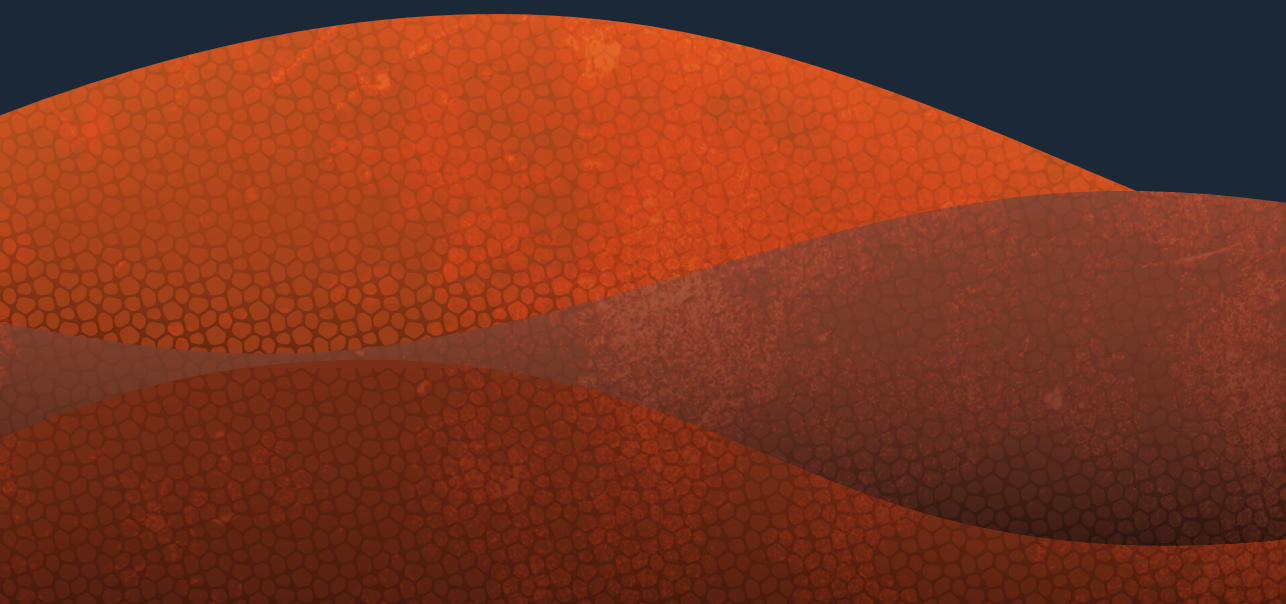


Figure S7. Tortuosity *Pf* tracks in human skin. The tortuosity of sporozoite tracks is quantified using the Straightness index (SI; **A**) and Angular dispersion (AD; **B**). The SI was non-parametrically distributed with the majority of tracks displaying high values (relatively straight tracks; median SI 0.97). Track AD values showed three peaks, indicating three subgroups of tracks. The majority of tracks had a high AD, indicating consistent directions of movement, as opposed to random variations.

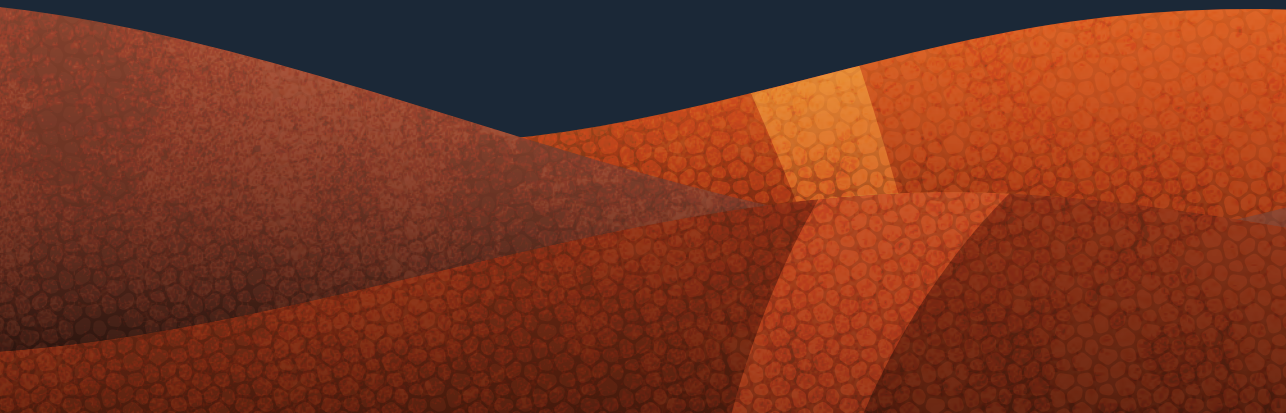
REFERENCES

- 1 Luker, K. E., Gupta, M., & Luker, G. D. Bioluminescent CXCL12 fusion protein for cellular studies of CXCR4 and CXCR7. *BioTechniques*. 2009; 47: 625-632
- 2 Hatty, C. R., & Banati, R. B. Protein-ligand and membrane-ligand interactions in pharmacology: the case of the translocator protein (TSPO). *Pharmacological Research*. 2015; 100, 58-63.

7



Summarizing discussion



With this thesis we attempted to shed light on the thus far uncharacterized human skin stage of skin-penetrating parasites. We present three novel key concepts to the field.

1. By analyzing immune responses to both malaria and schistosomiasis in the skin of their natural host, we have demonstrated that parasite exposure initiates immune regulation at the dermal site, by exploiting host immune-regulatory mechanisms. A characteristic relating them to tumor cells, which have been described to recruit immune cells to their aid in a similar fashion (**Chapter 2 and 4**).
2. We applied imaging techniques which allowed us to quantitatively image parasite movement within skin tissue. Our efforts yielded the first video-microscopic images of *Plasmodium falciparum* migrating through human skin, as well as of invading *Schistosoma mansoni* cercariae and allowed us to quantitatively compare the *in-skin* motility of radiation-attenuated and non-attenuated parasites. We describe how sporozoite migration is altered after radiation-attenuation (**Chapter 5 and 6**).
3. Importantly, our studies are performed directly in human skin, using either *Schistosoma mansoni* or the deadliest *Plasmodium* species to man; *Plasmodium falciparum*. Thus far, investigation into the skin-stage of both schistosomiasis and malaria was performed solely on rodents and non-human primates. Using human skin explants allows for a more direct translation of our findings to the *in vivo* setting in the human host (**all chapters**).

In this final chapter our findings will be discussed in the context of the known pathophysiology of disease and with regards to future prospects in parasite vaccine development. Additionally, we will draw parallels between the two very different skin-penetrating parasites investigated in this thesis.

Dermal immune responses to malaria and schistosomiasis; of mice and men

The discovery that the majority of *Plasmodium* sporozoites remain in the skin and that a large quantity of injected parasites drains to the skin draining lymph node (sdLN)^{1,2}, combined with the fact that protective immune responses can be primed in the sdLN^{3,4}, has sparked new interest in the skin-stage of malaria. In mice, intradermal delivery of sporozoites results in a local inflammatory response consisting of sustained neutrophil and monocyte recruitment as well as mast cell activation⁵⁻⁷. 2-4 hours after injection, neutrophil and monocyte recruitment can also be seen into the sdLN. Additionally, both in the skin as well as in the sdLN, sporozoites were seen to co-localize with CD11b⁺ myeloid cells^{2,5}. Within the sdLN, both a Th1 response as well as an immune regulatory response,

indicated by an increase in IFN γ producing T cells and IL10 producing, CTLA-4 expressing T cells respectively, has been shown previously^{3,5,8}. Although research has focused solely on murine dermal responses, the importance of dermal mechanisms in the human host is demonstrated by the crucial role of the route of administration of whole-sporozoite vaccines to their protective effect. Both in controlled mouse and human models of malaria infection, intradermal vaccine delivery greatly reduces their efficacy compared to both mosquito bite delivery as well as intravenous injection^{8,9}. We aimed to elucidate the immunological mechanisms underlying these differences by examining the effects of sporozoites on APCs, and their subsequent effect on T cell responses (**Chapter 2**) as well as comparing the dermal immune responses after needle or mosquito bite delivery of parasites (**Chapter 3**). Our findings show that immune regulation by parasites is not limited to the blood stage of infection but initiates at the first site of interaction with the host immune system, the skin site. We show clear upregulation of immunoregulatory mechanisms on monocyte-derived macrophages with a concomitant similar response by primary dermal APCs after sporozoite stimulation *in vitro*. However, despite our *ex vivo* method indicating a role for the CD14⁺ APC subset (proposed to be macrophages; **Chapter 3**), it did not shed light on whether specific DDC subsets are involved. Whether skin-resident DCs have no place in the response to skin-stage malaria, or it reflects the limitations of the *ex vivo* protocol (described in **chapter 3**) remains to be determined.

Skin-penetration by *Schistosoma* cercariae results in dermal inflammation maximal at day 4 post invasion in mice^{10,11}. Dermal APCs show increased activation and increase their migration to the skin draining lymph node. However, already at day 2 post invasion a regulatory response mounts in the skin characterized by IL-10 and IL-1ra production eventually resulting in a quick abrogation of the inflammatory responses and failure to induce a protection against reinfection¹¹. In humans, cercarial dermatitis has been described after exposure showing that at least some form of immune activation exists¹²⁻¹⁴, however the human skin-stage of schistosomiasis remained uncharacterized to date. We show that the initiation of the regulatory response in humans occurs in the skin by IL-10 producing DDCs and that attenuated cercariae are less capable of inducing this response. These findings corroborate with murine skin responses¹⁵.

For both parasite species lasting sterile natural and vaccine-induced immunity fails to develop, although vaccination efforts using live attenuated parasites show promising results¹⁵⁻¹⁸. However, parasites do not go entirely undetected by the host immune system, as residents in endemic areas do show increased levels of circulating antibodies and altered cytokine responses¹⁹. So why does it seem impossible to initiate a lasting sterile immune response? We hypothesized that either, 1) parasites divert immune responses by inactivation of host immune cells through their (secreted) products or

direct interactions with host immune cells, or 2) the response mounted by the host is abrogated by activation of host regulatory mechanisms. In **chapter 2** we tested whether the regulatory propensity of sporozoites was the result of responses to the immunodominant circumsporozoite protein (CSP), secreted by sporozoites upon migration. We did not find any effect of CSP on both dendritic cells and macrophages, indicating CSP plays no role in immune-modulation through APCs. CSP has been proposed to be a 'decoy' protein. A protein shed in large quantities in order to generate 'smokescreen' for antibody development, leading away from the migrating sporozoite²⁰. In vaccination studies using RTS,S, antibodies against CSP do correlate with protection²¹. However, recently it was found that RTS,S also increases vaccine-unrelated antibody responses against *Plasmodium*²². In the case of *Schistosoma*, although early studies have demonstrated a role for schistosome excretory/secretory (ES) products in the suppression of (dermal) immune responses by cercariae, our results in chapter 4 did not show cercarial ES products to have an effect on immune responses *in vitro*. We show that direct contact of cercariae is necessary for modulation of the response. However, as our results suggest that the *in vitro* setting (used to determine the effect of ES products) is not affected by changes in migration or motility, an effect of ES on the motility of APCs, and thereby altering their function cannot be ruled out. Whether other (secreted) proteins or compounds such as parasite exosomes²³ play a role in the activation of immune regulation on APCs remains to be determined.

Surviving in a hostile host: where tumor cells and parasites intersect.

For microbes residing in an immune competent host, exploitation of immune regulatory pathways is a powerful tool to steer clear of elimination. The same can be said for tumor cells. Tumor cells use a variety of mechanisms in order to escape the immune system, including the expansion of regulatory T cells (Tregs), increased production of regulatory cytokines such as IL-10 and TGF β ²⁴ as well as affecting the phenotype and function of APCs leading to decreased T cell activation. These mechanisms are also utilized by some parasites^{25,26}.

Our findings implicate a central role for the regulatory macrophage (Mreg) in malaria dermal immunology (**Chapter 2**). Macrophages are terminally differentiated skin resident cells that have antigen presenting abilities and display high levels of plasticity. Historically, macrophages were subdivided into categories based on their response to either TLR ligands or Th2 cytokines: (classically activated) M1 macrophages secreting high levels of pro-inflammatory Th1 cytokines and (alternatively activated) M2 macrophages involved in tissue repair respectively. Further investigation led to a subdivision of M2 macrophages in Mregs and tissue repair macrophages based on

their cytokine production and role in wound healing. It is currently thought that the classification of macrophages in M1, M2 and Mreg might be an over-simplification of a continuous spectrum of macrophage phenotypes^{27,28}. Primarily described in the context of tumor immunology, the regulatory macrophage is characterized as a macrophage producing large quantities of IL-10 and expressing PD-L1 on its surface despite its retained ability to produce proinflammatory cytokines and express activation markers such as CD80^{27,29}. They are described to have a local effect on the tumor environment by production of cytokines and chemokines as well as on the recruitment of circulating immune cells homing to the tumor and induction of T cell anergy³⁰. This is distinct from parasite infection, where parasites actively migrate away from the site of injection and do not wait for immune cells to arrive. However, as the majority of parasites remain in the skin, and a large proportion is found in the skin draining lymph node where immune responses to malaria can be primed, this local effect may still have widespread consequences to the overall induction of immunity. In addition, antigen uptake by macrophages does not only influence them directly, but also shapes their behavior and responses to subsequent antigen-sensing, therefore containing an integrated adaptive component³¹. This indicates that the first exposure to (malaria) parasites in the right context may be crucial in order to launch a protective response. Therefore, it could have implications for the translation of vaccine studies on malaria-naïve individuals to the endemic field.

We established a role for DDCs in the immune-regulation by *Schistosoma* parasites. However, we did not examine dermal macrophages in our skin explant setup due to difficulties in the distinction between DDCs and skin-residing macrophages in human tissues lacking clear macrophage markers such as F4/80 in mice. Interestingly, alternatively activated macrophages have been implicated to prevent helminth and protozoan killing in mice³². In addition, PD-L1/2 expression on macrophages has been demonstrated in splenic macrophages of mice infected with *S. mansoni* and was found to induce T cell anergy³³. These findings could indicate that macrophages might also be involved in dermal immune regulation by *S. mansoni* and should be the topic of future investigation.

Although PD-L1 is generally described as a regulatory marker, its upregulation does not inherently mean a cell has immunosuppressive capabilities. We see PD-L1 also upregulated after exposure to LPS, a finding previously described as a negative feedback loop preventing excessive inflammation in the context of endotoxin tolerance. We use salivary gland extract of similarly handled uninfected mosquitoes as a control in all our experiments, ruling out that the effect on phenotype and function is due to endotoxin contamination of the sporozoites. However, although the macrophages with regulatory

phenotype investigated in this thesis did result in a suppression of T cell responses, where LPS stimulated macrophages were not, the induction of this phenotype as a feedback response cannot be completely ruled out. Indeed, blocking of the PD-1/PD-L1 pathway in bystander macrophages did not influence CD8⁺ T cell responses to DCs, however, blocking of the IL-10 pathway partially restored CD8⁺ T cell IFN γ production, indicating that IL-10 production by these macrophages may be critical to their suppressive effect.

The proposed model of immune-modulation

We propose a model where regulatory macrophages impair immune priming against parasite antigens from skin-penetrating parasites, starting in the dermis (Figure 1). In the case of *Plasmodium* sporozoites, the majority of injected parasites are sacrificed for the greater cause and are phagocytosed by macrophages, be it directly at the injection site or after passive transfer to the skin draining lymph node. These macrophages decrease their migration (**Chapter 2 and 3**) in order to remain at the hot spot of parasite entry and gain a regulatory phenotype which hinders the activation of CD8⁺ T cells by dendritic cells (**Chapter 2**). The site of this interaction might well be extended to the sdLN³⁸. CD8⁺ T cells that DDCs did manage to activate and prime enter the skin and find themselves in a regulatory environment containing high concentrations of IL-10 which may directly impair their function³⁴ (Figure 1a).

Schistosoma mansoni cercariae utilize similar mechanisms in order to suppress dermal immune responses. Direct interaction with this parasite pushes dermal dendritic cells towards a regulatory phenotype and results in a decreased Th1 response by CD4⁺ T cells. A role for dermal macrophages is possible but has not been studied to date (**Chapter 4**). Additionally, a role for liver-resident macrophages, Kupffer cells, in the modulation of immune responses is possible, and should be studied in the future. (Figure 1c). Sporozoites have been shown to primarily utilize Kupffer cells in order to enter the liver. Contact with sporozoites could result in a similar response of these cells thereby initiating an equally regulatory environment at the site of hepatocyte infection³⁵⁻³⁷.

Establishing immunity to malaria and schistosomiasis is a complex and multi parasite-stage endeavor that is not limited to the importance of one cell type during one parasite-stage, but most likely hinges on the combined efforts of both innate and adaptive immune cells during all stages of infection. Although the exact molecular mechanisms and cellular interactions underlying the regulatory responses shown still remain unclear, our findings are a first step in the characterization of the human skin-stage of skin-penetrating parasites and may help to explain the inferiority of the intradermal route of vaccination, why natural immunity fails to develop in endemic areas and why no effective vaccine to either disease exists to date.

Common ground for all skin-penetrating parasites? The ‘fallen heroes’ hypothesis.

Whether exploitation of the IL-10 and/or the PD-1 pathway is conserved across different parasites remains an interesting question. In **chapter 3 and 4** we show upregulation of PD-L1 in *Plasmodium* sporozoite as well as *S. mansoni* cercariae stimulation. In addition, a role for PD-1 has recently been demonstrated for yet another skin-penetrating parasite species, *Brugia malayi*, one of the causative agents of lymphatic filariasis^{38,39}. If immune suppression via conserved pathways is characteristic for skin-penetrating parasite species, this pathway would be a promising target for vaccine development, potentially in the form of adjuvants or adaptations to existing parasite proteins. Evolutionarily, initiation of immune regulation as early as possible has advantages for the parasite life cycle. As for all skin-penetrating parasites described, only a minority of invading parasites will make it to adult-hood. Regulation at early stages in this ‘funnel-effect’ is primarily important for parasites such as *S. mansoni*, which do not replicate inside the human host. We propose that parasites stranding in the skin and/or skin draining lymph node, initiating a regulatory response, is an important mechanism to overall parasite survival. We named this the ‘fallen heroes’ hypothesis. For malaria, where the sporozoite stage is relatively short-lived, and where after the initial pre-erythrocytic stage the subsequent expansion leads to high levels of parasite antigen during blood stage, this is potentially less crucial. Having immune regulatory mechanisms in play during the blood stage of malaria might aid parasite invasion during subsequent infection⁴⁰.

Future skin focus

Although the use of *ex vivo* skin circumvents the pitfalls regarding the use of murine models for human dermal immunology questions (**Chapter 2-5**), the limitations of explant models (described in **chapter 3 and 4**) highlight the additional need for alternatives. Given the advances in the field of controlled human infections⁴¹⁻⁴⁴, future research should focus on *in vivo* application of both immunological assays as well imaging. Controlled human infections have the capacity to elucidate these mechanisms directly within the host, without facing the challenges of either *ex vivo* or murine models of disease. Taking dermal biopsies from volunteers would allow for cytological, histological as well as functional read-outs directly *in vivo*. However, murine models should be used additionally, in order to systematically examine possible mechanisms for dermal immune regulation. Furthermore, mouse models and non-human primate models are not limited to skin and blood samples but allow for determination of responses in both the sdLN as well as the liver. Non-human primate skin has the advantage of being more comparable to human skin, and although more costly, should be considered as a valuable alternative. Knockout models can be used to investigate the role of dermal

dendritic cells and macrophages. The effect of neutralizing the PD-1 pathway or other checkpoint molecules is worth investigating using neutralizing antibodies, siRNA or specific genetic knockouts. In addition, targeting dermal dendritic cells and/or macrophages specifically by administration of liposomes containing parasite proteins, or coupling of antigens and adjuvants to dendritic cell-specific antibodies should be studied in order to gain insight in the regulatory mechanisms in play⁴⁵⁻⁴⁷.

Implications of dermal immune regulation to vaccine refinement

In order to generate an effective live attenuated parasite vaccine, parasites should initiate sustained adaptive immune responses without the interference of modulatory mechanisms. One obvious possibility to circumvent dermal immune regulation is to bypass the skin altogether. Intravenous injection of cryopreserved sporozoites can indeed induce sterile protection in volunteers^{16,48,49}. However, also after IV vaccine injection protection wanes over time¹⁷, indicating an additional role for regulatory mechanisms outside of the skin such as in the liver. Furthermore, intravenous injection of attenuated parasite vaccines is currently possible for malaria sporozoites, but not for the multicellular, and much larger, *Schistosoma* parasites.

In order to skew immunity to pro-inflammatory responses, adjuvants are often used. RTS,S for example is delivered in a hepatitis B envelope and is co-administered with adjuvant AS01B to increase antibody responses⁵⁰. Adjuvants used for dermal applications such as imiquimod (a TLR7 agonist) and resiquimod (a TLR 7 and 8 agonist) can be tested in order to stimulate dermal macrophages and DDCs and to increase the pro-inflammatory response to intradermal delivered vaccines⁵¹⁻⁵³. In addition, if the molecular pathways underlying immune regulation are elucidated, parasites could hypothetically be genetically modified to circumvent these pathways.

Lastly, our findings on dermal immunity could potentially have great implications for the immunization protocols used in vaccine efficacy studies. In **chapter 2**, we show that antibody opsonization of sporozoites greatly increases their uptake by macrophages, without affecting the subsequent regulatory response. This could imply that a prime-boost protocol using high numbers of cryopreserved sporozoites may not be optimal for vaccination. Firstly, increased phagocytosis results in fewer parasites able to initiate a protective response in the skin draining lymph node or after reaching the liver. In addition, the increased numbers of phagocytosed parasites result in larger numbers of immune-suppressive macrophages further tempering immune responses with each boost. It can be argued that a selection of only the most potent and viable sporozoites should be used as a vaccine in order to decrease the amount of skin-residing (and

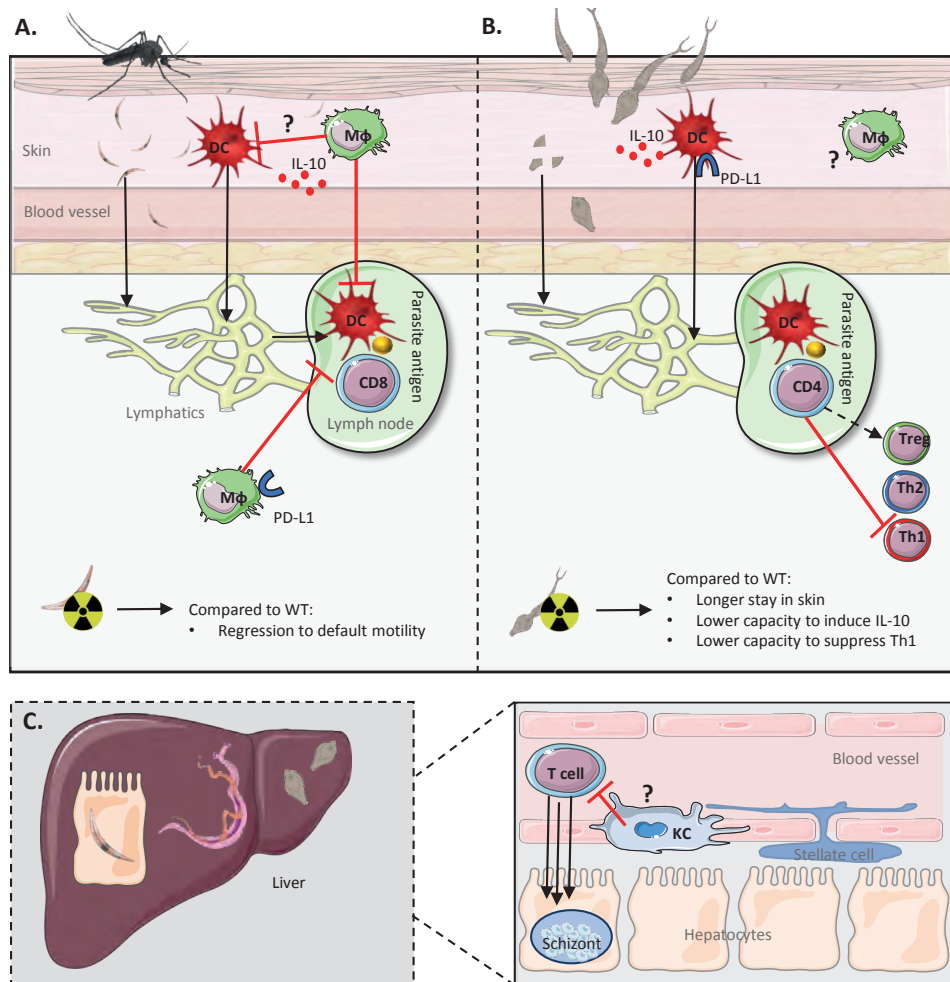


Figure 1. Proposed model of immune regulation by sporozoites. A. An infected anopheles mosquito injects SPZ into the dermis of the host. SPZ migrate through the dermis to reach a blood or lymphatic vessel. The majority stay within the skin. Skin resident macrophages (MΦ, green) phagocytose SPZ and gain a regulatory phenotype and are able to modulate CD8 responses to antigen loaded dendritic cells (DCs, red). Additionally (sdLN resident?) macrophages can interfere with CD8 T cell priming directly through cell-cell interactions. **B.** *S. mansoni* cercariae bore their way into the skin, shed their tails and migrate as schistosomula to the vasculature. Direct contact with skin resident dendritic cells (DC, red) leads to upregulation of PD-L1 and the production of IL-10. This eventually results in a decrease in Th1 skewing of naive T cells. The role for skin resident macrophages remains to be determined. Irradiated cercariae are not as efficient as wild-type cercariae to induce this phenotype. **C.** Whether Liver resident macrophages, Kupffer cells (KC), play a similar role in immune regulation remains to be determined.

thereby immunoregulatory) parasites. The same can be argued for vaccine application in the endemic setting, where residents already have circulating anti-CSP antibodies ready to immobilize parasites upon entry.

Overall, our findings may have widespread implications in the field of live-attenuated parasite vaccine development. In order to refine current vaccine formulations, these important questions should be addressed before costly, grand-scale clinical trials take place in the field.

The effect of radiation attenuation on live parasite vaccines

We characterized the effect of radiation-attenuation of parasites on both their immune-suppressive function (*Schistosoma*, **Chapter 4**) as well as their motility (malaria, **Chapter 5**). Although radiation-attenuation is a powerful method to inhibit parasite maturation, our findings indicate that its effect is much more extensive and has previously uncharacterized repercussions.

Using *S. mansoni* parasites, we demonstrated decreased immune regulatory propensity after radiation attenuation. Irradiation of cercariae has been demonstrated to reduce migration through the skin^{11,54} and it was proposed that prolonged antigen exposure underlies the improved immunogenicity of radiation-attenuated cercariae. We show that direct interaction of radiation-attenuated cercariae leads to decreased PD-L1 expression on and decreased IL-10 production by DDCs, and their increased ability to skew towards Th1 responses (Figure 1b). Whether radiation-attenuation alters cercarial surface antigens or whether molecular mechanisms used to inactivate host immune responses are hampered by radiation is not yet clear.

In line with motility alteration previously described after radiation-attenuation of cercariae, *Plasmodium falciparum* sporozoites were shown to display impaired motility after irradiation (**Chapter 5**, Figure 1a). Potentially RAS will remain longer in the skin than their non-attenuated counterparts, as movement was shown to revert to default patterns including circulatory and reversal patterns. Whether these patterns also increase their chances of passive transfer to skin draining lymph nodes has not been investigated due to the limitations of the explant model.

In addition, whether radiation attenuation has a similar effect on the sporozoites ability to modulate APC responses is the subject of further research. Both radiation effects have the potential to work in synergy: the slower migration indeed does prolong

antigen exposure at the immunocompetent skin site, and priming is now potentially able to occur since the immune-regulatory propensity of parasites is diminished upon attenuation.

A role for (molecular) imaging in vaccine advancement

Molecular imaging is a powerful tool to directly analyze the behavior of (live-attenuated) parasites. In **chapter 5 and 6** we used novel imaging strategies in order to visualize and characterize dermal migration of malaria sporozoites. Motility and migration are important features of parasite infection especially during the skin stage where their most important objective is to exit the skin and enter the vasculature. Indeed, genetically modified parasites deficient of proteins crucial for migration fail to establish an infection and, in attenuated form, fail to confer protection⁵⁵⁻⁵⁸. Therefore, a detailed understanding of this movement may be crucial to design and optimize attenuated-parasite vaccines.

Next to mapping of parasite motility alone, (molecular) imaging has the potential to go deeper into dermal immune interactions. In example, it can be used to answer the question whether irradiation of sporozoites results in prolonged exposure to dermal regulatory cells. Optimization of our protocols can potentially chart cellular interactions of sporozoites with immune cells. The altered movement patterns within our dataset could signify these interactions, however, the complexity of the interactions warrant visualization to a level of detail not yet feasible in our current setup. Immunofluorescent staining of cell types by camelid single-domain antibodies could overcome the limitations faced in *ex vivo* staining of dermal structures^{59,60}. Additionally, the use of spinning-disk confocal systems or the optimization of tracer penetration by emission in the far-red spectrum could potentially increase the depth of analysis.

Not only would molecular imaging advance our understanding of dermal immune interactions, it could facilitate testing of novel anti-sporozoite antibodies as well as the characterization, optimization and comparison of different parasite-attenuation techniques. Antibody binding of attenuated sporozoites likely contributes to protective immunity by altering sporozoite motility⁶¹⁻⁶³. Yet the role of these antibodies in the overall immune response against malaria remains controversial, despite anti-CSP antibody titers correlating with protection. To date, the relative contribution of anti-CSP antibodies in sporozoite migration or invasion blocking remains uninvestigated. Molecular-imaging based techniques that allow for sporozoite tracking can be used as a novel tool to study the effect of antibodies on dermal sporozoite migration.

Additionally, molecular imaging could be extended to imaging beyond the skin stage with a nuclear medicine-based approach. Hybrid (both fluorescent and nuclear) tracer development would facilitate its use in controlled human infections where it could help to elucidate the role of lymph node trafficking and extra-hepatic parasite development in parasite immunity⁶⁴. Lastly, dermal imaging of pathogens is not limited to host-parasite interactions but could be used in the visualization and movement quantification of all manner of pathogens.

Concluding remarks

By studying the combined immune response to parasites as well as parasite motility, this thesis offers a new scope to enhance our understanding of parasite skin stages. Although the molecular mechanisms and cellular interactions that play a role in the dermal immune-regulatory propensity of parasites require further investigation, this thesis highlights the importance of the skin stage of different skin-penetrating parasites and offers novel (imaging) strategies in order to further characterize and subsequently optimize attenuated-parasite vaccine design. These insights are a pivotal first step in broadening our understanding of pre-erythrocytic natural immunity and the pitfalls of intradermal vaccination-induced immunity.

Outstanding questions

- Where does immune modulation take place? Solely in the dermis, or in addition in the sdLN and/or liver?
- What is the role of liver-resident macrophages (Kupffer cells) in pre-erythrocytic immune modulation?
- Do macrophages themselves also present sporozoite antigen to T cells or are their effects modulated via dermal- or lymph node-resident dendritic cells?
- Does the PD-1/PD-L1 pathway indeed play a role *in vivo*?
- Is there a role for neutrophils and/or monocyte-derived macrophages in dermal immune modulation?
- How do sporozoites exert their effects on macrophages? Which molecular pathways are involved in the upregulation of PD-L1 and IL-10?
- Can we use adjuvants, delivered directly to dermal macrophages in order to circumvent the modulatory response?
- What is the duration of the APC mediated immune-suppressive effect? Does this impact prime-boost vaccination strategies?
- Does radiation attenuation alter sporozoite-dermal APC interaction?
- What is the role of sporozoite motility on their interaction with dermal immune cells?

REFERENCES

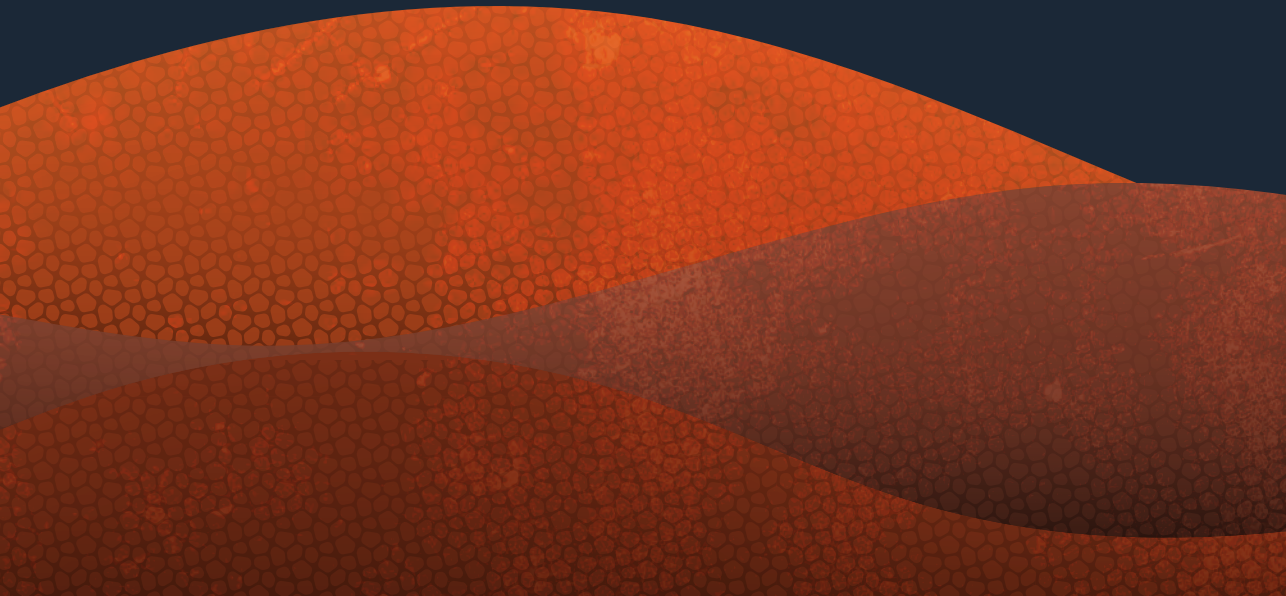
- 1 Amino, R., Thiberge, S., Shorte, S., Frischknecht, F. & Menard, R. Quantitative imaging of *Plasmodium* sporozoites in the mammalian host. *C R Biol* 329, 858-862, doi:10.1016/j.crvi.2006.04.003 (2006).
- 2 Amino, R. et al. Quantitative imaging of *Plasmodium* transmission from mosquito to mammal. *Nat Med* 12, 220-224, doi:10.1038/nm1350 (2006).
- 3 Chakravarty, S. et al. CD8+ T lymphocytes protective against malaria liver stages are primed in skin-draining lymph nodes. *Nat Med* 13, 1035-1041, doi:10.1038/nm1628 (2007).
- 4 Obeid, M. et al. Skin-draining lymph node priming is sufficient to induce sterile immunity against pre-erythrocytic malaria. *EMBO Mol Med* 5, 250-263, doi:10.1002/emmm.201201677 (2013).
- 5 Mac-Daniel, L. et al. Local immune response to injection of *Plasmodium* sporozoites into the skin. *J Immunol* 193, 1246-1257, doi:10.4049/jimmunol.1302669 (2014).
- 6 Wilainam, P., Nintasen, R. & Viriyavejakul, P. Mast cell activation in the skin of *Plasmodium falciparum* malaria patients. *Malar J* 14, 67, doi:10.1186/s12936-015-0568-8 (2015).
- 7 Huang, B. et al. Activation of Mast Cells Promote *Plasmodium berghei* ANKA Infection in Murine Model. *Front Cell Infect Microbiol* 9, 322, doi:10.3389/fcimb.2019.00322 (2019).
- 8 Haeberlein, S. et al. Protective immunity differs between routes of administration of attenuated malaria parasites independent of parasite liver load. *Sci Rep* 7, 10372, doi:10.1038/s41598-017-10480-1 (2017).
- 9 Epstein, J. E. et al. Live attenuated malaria vaccine designed to protect through hepatic CD8(+) T cell immunity. *Science* 334, 475-480, doi:10.1126/science.1211548 (2011).
- 10 Incani, R. N. & McLaren, D. J. Histopathological and ultrastructural studies of cutaneous reactions elicited in naive and chronically infected mice by invading schistosomula of *Schistosoma mansoni*. *Int J Parasitol* 14, 259-276 (1984).
- 11 Mountford, A. P. & Trottein, F. Schistosomes in the skin: a balance between immune priming and regulation. *Trends Parasitol* 20, 221-226, doi:10.1016/j.pt.2004.03.003 (2004).
- 12 Kourilova, P., Hogg, K. G., Kolarova, L. & Mountford, A. P. Cercarial dermatitis caused by bird schistosomes comprises both immediate and late phase cutaneous hypersensitivity reactions. *J Immunol* 172, 3766-3774 (2004).
- 13 Bottieau, E. et al. Imported Katayama fever: clinical and biological features at presentation and during treatment. *J Infect* 52, 339-345, doi:10.1016/j.jinf.2005.07.022 (2006).
- 14 Ross, A. G., Vickers, D., Olds, G. R., Shah, S. M. & McManus, D. P. Katayama syndrome. *Lancet Infect Dis* 7, 218-224, doi:10.1016/S1473-3099(07)70053-1 (2007).
- 15 Hogg, K. G., Kumkate, S., Anderson, S. & Mountford, A. P. Interleukin-12 p40 secretion by cutaneous CD11c+ and F4/80+ cells is a major feature of the innate immune response in mice that develop Th1-mediated protective immunity to *Schistosoma mansoni*. *Infect Immun* 71, 3563-3571 (2003).
- 16 Seder, R. A. et al. Protection against malaria by intravenous immunization with a nonreplicating sporozoite vaccine. *Science* 341, 1359-1365, doi:10.1126/science.1241800 (2013).
- 17 Ishizuka, A. S. et al. Protection against malaria at 1 year and immune correlates following PfSPZ vaccination. *Nat Med* 22, 614-623, doi:10.1038/nm.4110 (2016).
- 18 Hewitson, J. P., Hamblin, P. A. & Mountford, A. P. Immunity induced by the radiation-attenuated schistosome vaccine. *Parasite Immunol* 27, 271-280, doi:10.1111/j.1365-3024.2005.00764.x (2005).
- 19 Idris, Z. M. et al. Naturally acquired antibody response to *Plasmodium falciparum* describes

- heterogeneity in transmission on islands in Lake Victoria. *Sci Rep* 7, 9123, doi:10.1038/s41598-017-09585-4 (2017).
- 20 Schofield, L. The circumsporozoite protein of *Plasmodium*: a mechanism of immune evasion by the malaria parasite? *Bull World Health Organ* 68 Suppl, 66-73 (1990).
- 21 White, M. T. et al. Immunogenicity of the RTS,S/AS01 malaria vaccine and implications for duration of vaccine efficacy: secondary analysis of data from a phase 3 randomised controlled trial. *Lancet Infect Dis* 15, 1450-1458, doi:10.1016/S1473-3099(15)00239-X (2015).
- 22 Dobano, C. et al. RTS,S/AS01E immunization increases antibody responses to vaccine-unrelated *Plasmodium falciparum* antigens associated with protection against clinical malaria in African children: a case-control study. *BMC Med* 17, 157, doi:10.1186/s12916-019-1378-6 (2019).
- 23 Wu, Z. et al. Extracellular Vesicle-Mediated Communication Within Host-Parasite Interactions. *Front Immunol* 9, 3066, doi:10.3389/fimmu.2018.03066 (2018).
- 24 Dranoff, G. Cytokines in cancer pathogenesis and cancer therapy. *Nat Rev Cancer* 4, 11-22, doi:10.1038/nrc1252 (2004).
- 25 McSorley, H. J. & Maizels, R. M. Helminth infections and host immune regulation. *Clin Microbiol Rev* 25, 585-608, doi:10.1128/CMR.05040-11 (2012).
- 26 Horne-Debets, J. M. et al. PD-1 dependent exhaustion of CD8+ T cells drives chronic malaria. *Cell Rep* 5, 1204-1213, doi:10.1016/j.celrep.2013.11.002 (2013).
- 27 Mosser, D. M. & Edwards, J. P. Exploring the full spectrum of macrophage activation. *Nat Rev Immunol* 8, 958-969, doi:10.1038/nri2448 (2008).
- 28 Biswas, S. K. & Mantovani, A. Macrophage plasticity and interaction with lymphocyte subsets: cancer as a paradigm. *Nat Immunol* 11, 889-896, doi:10.1038/ni.1937 (2010).
- 29 Wynn, T. A. & Vannella, K. M. Macrophages in Tissue Repair, Regeneration, and Fibrosis. *Immunity* 44, 450-462, doi:10.1016/j.immuni.2016.02.015 (2016).
- 30 Chanmee, T., Ontong, P., Konno, K. & Itano, N. Tumor-associated macrophages as major players in the tumor microenvironment. *Cancers (Basel)* 6, 1670-1690, doi:10.3390/cancers6031670 (2014).
- 31 Bowdish, D. M., Loffredo, M. S., Mukhopadhyay, S., Mantovani, A. & Gordon, S. Macrophage receptors implicated in the "adaptive" form of innate immunity. *Microbes Infect* 9, 1680-1687, doi:10.1016/j.micinf.2007.09.002 (2007).
- 32 Jang, J. C. & Nair, M. G. Alternatively Activated Macrophages Revisited: New Insights into the Regulation of Immunity, Inflammation and Metabolic Function following Parasite Infection. *Curr Immunol Rev* 9, 147-156, doi:10.2174/1573395509666131210232548 (2013).
- 33 Smith, P. et al. *Schistosoma mansoni* worms induce anergy of T cells via selective up-regulation of programmed death ligand 1 on macrophages. *J Immunol* 173, 1240-1248, doi:10.4049/jimmunol.173.2.1240 (2004).
- 34 Smith, L. K. et al. Interleukin-10 Directly Inhibits CD8(+) T Cell Function by Enhancing N-Glycan Branching to Decrease Antigen Sensitivity. *Immunity* 48, 299-312 e295, doi:10.1016/j.immuni.2018.01.006 (2018).
- 35 Klotz, C. & Frevort, U. *Plasmodium yoelii* sporozoites modulate cytokine profile and induce apoptosis in murine Kupffer cells. *Int J Parasitol* 38, 1639-1650, doi:10.1016/j.ijpara.2008.05.018 (2008).
- 36 Steers, N. et al. The immune status of Kupffer cells profoundly influences their responses to infectious *Plasmodium berghei* sporozoites. *Eur J Immunol* 35, 2335-2346, doi:10.1002/eji.200425680 (2005).
- 37 Usynin, I., Klotz, C. & Frevort, U. Malaria circumsporozoite protein inhibits the respiratory burst in Kupffer cells. *Cell*

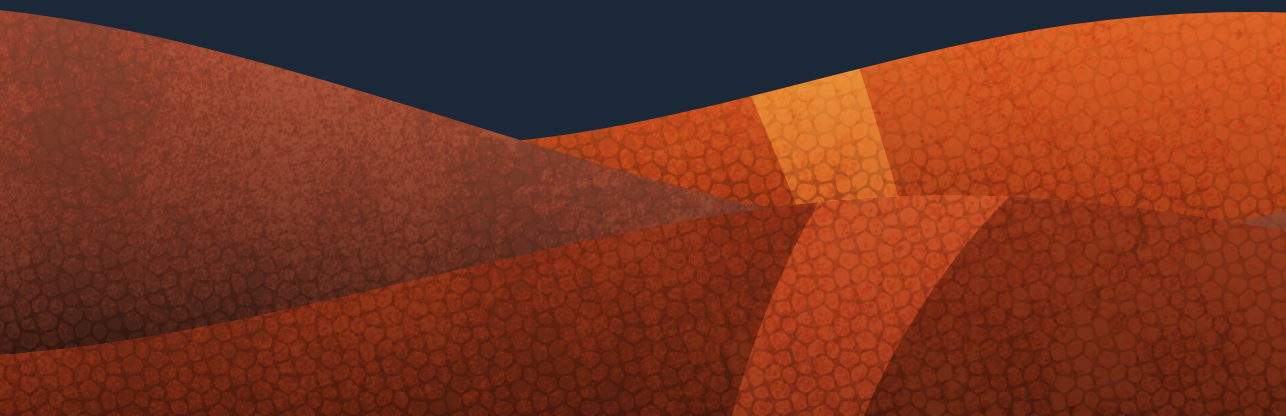
- Microbiol 9, 2610-2628, doi:10.1111/j.1462-5822.2007.00982.x (2007).
- 38 Loke, P., MacDonald, A. S., Robb, A., Maizels, R. M. & Allen, J. E. Alternatively activated macrophages induced by nematode infection inhibit proliferation via cell-to-cell contact. *Eur J Immunol* 30, 2669-2678, doi:10.1002/1521-4141(200009)30:9<2669::AID-IMMU2669>3.0.CO;2-1 (2000).
- 39 Narasimhan, P. B. et al. Similarities and differences between helminth parasites and cancer cell lines in shaping human monocytes: Insights into parallel mechanisms of immune evasion. *PLoS Negl Trop Dis* 12, e0006404, doi:10.1371/journal.pntd.0006404 (2018).
- 40 Ocana-Morgner, C., Mota, M. M. & Rodriguez, A. Malaria blood stage suppression of liver stage immunity by dendritic cells. *J Exp Med* 197, 143-151, doi:10.1084/jem.20021072 (2003).
- 41 de, M. C. C. L. M. H. J. R. K. J. J. J. K.-v. O. C. F. S. P. J. C. J. A controlled human *Schistosoma mansoni* infection model to advance novel drugs, vaccines and diagnostics. *Nature Medicine* (2020).
- 42 Stanicic, D. I., McCarthy, J. S. & Good, M. F. Controlled Human Malaria Infection: Applications, Advances, and Challenges. *Infect Immun* 86, doi:10.1128/IAI.00479-17 (2018).
- 43 Roestenberg, M. et al. The frontline of controlled human malaria infections: A report from the controlled human infection models Workshop in Leiden University Medical Centre 5 May 2016. *Vaccine* 35, 7065-7069, doi:10.1016/j.vaccine.2017.10.093 (2017).
- 44 Roestenberg, M., Hoogerwerf, M. A., Ferreira, D. M., Mordmuller, B. & Yazdanbakhsh, M. Experimental infection of human volunteers. *Lancet Infect Dis* 18, e312-e322, doi:10.1016/S1473-3099(18)30177-4 (2018).
- 45 Boks, M. A. et al. In situ Delivery of Tumor Antigen- and Adjuvant-Loaded Liposomes Boosts Antigen-Specific T-Cell Responses by Human Dermal Dendritic Cells. *J Invest Dermatol* 135, 2697-2704, doi:10.1038/jid.2015.226 (2015).
- 46 Unger, W. W. & van Kooyk, Y. 'Dressed for success' C-type lectin receptors for the delivery of glyco-vaccines to dendritic cells. *Curr Opin Immunol* 23, 131-137, doi:10.1016/j.coi.2010.11.011 (2011).
- 47 Romani, N. et al. Targeting skin dendritic cells to improve intradermal vaccination. *Curr Top Microbiol Immunol* 351, 113-138, doi:10.1007/82_2010_118 (2012).
- 48 Mordmuller, B. et al. Sterile protection against human malaria by chemoattenuated PfSPZ vaccine. *Nature* 542, 445-449, doi:10.1038/nature21060 (2017).
- 49 Roestenberg, M. et al. Protection against a malaria challenge by sporozoite inoculation. *N Engl J Med* 361, 468-477, doi:10.1056/NEJMoa0805832 (2009).
- 50 Regules, J. A., Cummings, J. F. & Ockenhouse, C. F. The RTS,S vaccine candidate for malaria. *Expert Rev Vaccines* 10, 589-599, doi:10.1586/erv.11.57 (2011).
- 51 Zhang, W. W. & Matlashewski, G. Immunization with a Toll-like receptor 7 and/or 8 agonist vaccine adjuvant increases protective immunity against *Leishmania major* in BALB/c mice. *Infect Immun* 76, 3777-3783, doi:10.1128/IAI.01527-07 (2008).
- 52 Igartua, M. & Pedraz, J. L. Topical resiquimod: a promising adjuvant for vaccine development? *Expert Rev Vaccines* 9, 23-27, doi:10.1586/erv.09.135 (2010).
- 53 Cheng, W. K., Wee, K., Kollmann, T. R. & Dutz, J. P. Topical CpG adjuvantation of a protein-based vaccine induces protective immunity to *Listeria monocytogenes*. *Clin Vaccine Immunol* 21, 329-339, doi:10.1128/CVI.00734-13 (2014).
- 54 Mountford, A. P., Coulson, P. S. & Wilson, R. A. Antigen localization and the induction of resistance in mice vaccinated with irradiated cercariae of *Schistosoma mansoni*. *Parasitology* 97 (Pt 1), 11-25 (1988).

- 55 Sultan, A. A. et al. TRAP is necessary for gliding motility and infectivity of plasmodium sporozoites. *Cell* 90, 511-522, doi:10.1016/s0092-8674(00)80511-5 (1997).
- 56 Barry, A. et al. Functional antibodies against *Plasmodium falciparum* sporozoites are associated with a longer time to qPCR-detected infection among schoolchildren in Burkina Faso. *Wellcome Open Res* 3, 159, doi:10.12688/wellcomeopenres.14932.2 (2018).
- 57 Ejigiri, I. et al. Shedding of TRAP by a rhomboid protease from the malaria sporozoite surface is essential for gliding motility and sporozoite infectivity. *PLoS Pathog* 8, e1002725, doi:10.1371/journal.ppat.1002725 (2012).
- 58 Coppi, A. et al. The malaria circumsporozoite protein has two functional domains, each with distinct roles as sporozoites journey from mosquito to mammalian host. *J Exp Med* 208, 341-356, doi:10.1084/jem.20101488 (2011).
- 59 Fernandes, C. F. C. et al. Camelid Single-Domain Antibodies As an Alternative to Overcome Challenges Related to the Prevention, Detection, and Control of Neglected Tropical Diseases. *Front Immunol* 8, 653, doi:10.3389/fimmu.2017.00653 (2017).
- 60 Muyldermans, S. Nanobodies: natural single-domain antibodies. *Annu Rev Biochem* 82, 775-797, doi:10.1146/annurev-biochem-063011-092449 (2013).
- 61 Flores-Garcia, Y. et al. Antibody-Mediated Protection against *Plasmodium* Sporozoites Begins at the Dermal Inoculation Site. *mBio* 9, doi:10.1128/mBio.02194-18 (2018).
- 62 Vanderberg, J. P. & Frevert, U. Intravital microscopy demonstrating antibody-mediated immobilisation of *Plasmodium berghei* sporozoites injected into skin by mosquitoes. *Int J Parasitol* 34, 991-996, doi:10.1016/j.ijpara.2004.05.005 (2004).
- 63 Stewart, M. J., Nawrot, R. J., Schulman, S. & Vanderberg, J. P. *Plasmodium berghei* sporozoite invasion is blocked in vitro by sporozoite-immobilizing antibodies. *Infect Immun* 51, 859-864 (1986).
- 64 KleinJan, G. H. et al. Multimodal imaging in radioguided surgery. *Clin Transl Imaging* 1, 433-444 (2013).

A



Appendix



ENGLISH SUMMARY

Skin-penetrating parasites have something in common; they all need to evade the initial immune response in the skin in order to avoid being evicted by their hostile host and establish an infection. To do so, they are equipped with the necessary cunning stratagems. For example, they can act directly on immune cells to alter their function and they can optimize their migration patterns to their hostile environment. This thesis is aimed at unravelling those mechanisms.

Malaria and Schistosomiasis are two deadly and debilitating parasitic diseases. With over 200 million (malaria) and over 240 million (schistosomiasis) cases annually, the global disease burden remains very high and the need for potent vaccines is evident. Whole weakened parasites can be used to vaccinate individuals against parasitic diseases like malaria. However, delivery of these parasites in the skin, as is commonly done in vaccinations, reduces their protectivity. We hypothesize that this reduction is caused by parasite-mediated immune-regulatory mechanisms that are initiated upon their first encounter with immune cells in the skin.

The skin is an important and active immune organ. Its main function is to maintain the immunological balance between swift and powerful elimination of disease-inducing microbes called pathogens and gentle tolerance towards commensals, the “good microbes” living on our body. In order to do its job properly, the human skin contains a wide variety of immune cells. Among these cells are antigen presenting cells (APCs). They have the ability to take up foreign particles (antigens), process them into small fragments, and present these fragments to T cells. T cells can then launch an immune attack when they recognize these fragments as pathogenic. The type of T cell response, either inflammation (an active immune attack) or tolerance, depends on APC signaling during presentation. Certain molecules on the APC’s surface can signal T cells to induce a tolerizing immune response. These molecules, termed immune checkpoint-molecules, like PD-L1, can deactivate T cells. We investigated whether skin penetrating parasites exploit these existing mechanisms in human skin in order to enhance their survival.

In the first part of this thesis, *wiles*, we demonstrate that *Plasmodium falciparum* and *Schistosoma mansoni*, the causative agents of Malaria and Schistosomiasis or Bilharzia respectively, exploit existing APC mechanisms in the skin to induce T cell tolerance. We show that both *Plasmodium* sporozoites and *Schistosoma* larvae increase PD-L1 on the surface of skin APCs and the production of regulatory cytokines by these cells. In addition, we confirm the immune regulatory propensity of these parasite stimulated APCs by looking at their effect on T cell activation (**chapter 2** and **4**). **Chapter 3**

investigates whether the method of intradermal delivery of parasites into the skin affects APC responses by investigating cellular responses to mosquito bite or needle injected parasites in human skin explants. In **chapter 4** we show that the attenuation (weakening) of *Schistosoma* parasites decreases their regulatory effect in the skin. This may help to explain why attenuated parasites are capable of initiating protection, where repeated natural infection is not.

In the second part of this thesis, *wanderings*, we employed imaging techniques to investigate the motility of malaria parasites in human skin. In **chapter 5** we presented a semi-automatic software program that detects and tracks *plasmodium* sporozoites in microscopy videos of sporozoites moving through human tissue. This method allowed us to comprehensibly quantify movement patterns and compare radiation attenuated with non-attenuated genetically-modified fluorescent parasites, ultimately showing that irradiated sporozoites revert to less variable, “default” movement patterns. In **chapter 6** we showed a novel molecular imaging method in order to label wild type *plasmodium* parasites using a mitochondrial dye, enabling us to visualize wild type parasite movement in human skin.

Lastly, in **chapter 7** our findings are discussed in the broader context of our current understanding of parasite immunity as well as the implications for live-attenuated parasite vaccine development.

NEDERLANDSE SAMENVATTING

Parasieten die de huid penetreren hebben iets gemeen: stuk voor stuk moeten ze, voordat zij een infectie kunnen initiëren, het immuunsysteem in de huid van de gastheer omzeilen en daarmee voorkomen dat zij door dit immuunsysteem worden opgeruimd. Om dit te bewerkstelligen beschikken zij over de nodige slimme listen. Zo kunnen zij direct actie uitoefenen op afweercellen of hun migratiegedrag aanpassen aan de leefomstandigheden waarin zij zich bevinden. Dit proefschrift is erop gericht om de mechanismen van deze tactieken op te helderen.

Malaria en schistosomiasis (ook wel bilharzia genoemd) zijn twee dodelijke en belastende ziekten. Met respectievelijk meer dan 200 en 240 miljoen jaarlijkse infecties blijft de wereldwijde ziektelast zeer hoog en is de noodzaak voor een goedwerkend vaccin reeds lange tijd duidelijk. Levende, verzwakte parasieten kunnen worden gebruikt om mensen te vaccineren tegen parasitaire ziekten zoals bovenstaande. Echter, wanneer deze parasieten via de gebruikelijke route voor vaccintoediening worden toegediend (namelijk via de huid), resulteert dat in een verminderde werking van het vaccin. Wij stellen als hypothese dat deze verminderde werking wordt veroorzaakt door parasiet-gemedieerde immuun-regulatorische mechanismen en dat dit reeds bij de eerste interactie met het immuunsysteem in de huid gebeurt.

De huid is een belangrijk en actief orgaan in de menselijke afweer. Naast zijn barrièrefunctie is zijn belangrijkste taak om de immunologische balans te waarborgen tussen snelle en efficiënte eliminatie van ziekmakende microben (pathogenen) en tolerantie voor de goedaardige commensalen, de "goede" microben die op de huid wonen. Om deze functie goed uit te kunnen oefenen beschikt de huid over een grote variëteit in afweercellen. Enkele van deze cellen zijn antigeen-presenterende cellen (APCs). Deze cellen hebben de functie om lichaamsvreemde deeltjes (antigenen) op te nemen, te verwerken tot kleine fragmenten en te presenteren aan T cellen. T cellen kunnen hierop een afweer-aanval lanceren wanneer zij deze fragmenten als pathogeen herkennen. Het type T-celreactie, ofwel inflammatie (een actieve afweer-aanval) ofwel tolerantie, hangt mede af van signalen die APCs afgeven tijdens de presentatie van de antigeenfragmenten. Bepaalde moleculen op het oppervlak van de APCs kunnen een signaal afgeven aan de T cellen om tolerantie te induceren. Deze moleculen, genaamd "checkpoint moleculen" zoals PD-L1, kunnen T cellen deactiveren. Wij onderzochten of parasieten die de huid penetreren deze mechanismen in de humane huid exploiteren om zelf te kunnen overleven in de gastheer.

In het eerste gedeelte van dit proefschrift, "wiles" oftewel listen, demonstreren wij dat *Plasmodium falciparum* en *Schistosoma mansoni*, respectievelijk de veroorzakers van malaria en schistosomiasis, inderdaad bestaande APC-mechanismen in de huid exploiteren om T-celtolerantie te induceren. In **hoofdstuk 2 en 4** laten wij zien dat zowel *Plasmodium*-sporozoïten als *Schistosoma*-larven zorgen voor toename van PD-L1-expressie op het oppervlak van dermale APCs en deze cellen aanzetten tot het produceren van regulatoire signaalstoffen (cytokinen). Daarnaast bevestigen wij de regulatoire werking van deze cellen door het effect op T-celactivatie te bestuderen. In **hoofdstuk 3** onderzoeken wij of de methode van intradermale toediening van parasieten de APC-reactie beïnvloedt: in dit hoofdstuk vergelijken wij het effect van parasiettoediening via muggenbeten met dat van injectie-naaldtoediening in humane huidexplantaten. In **hoofdstuk 4** laten we zien dat het verzwakken van *Schistosoma*-larven het regulatoire effect in de huid vermindert. Dit kan helpen verklaren waarom blootstelling aan verzwakte parasieten mensen kan beschermen, maar (herhaaldelijke) natuurlijke infectie niet.

In het tweede gedeelte van dit proefschrift, "wanderings" oftewel omzwervingen, gebruiken wij beeldvormende technieken om de motiliteit van malariaparasieten in de huid te karakteriseren. In **hoofdstuk 5** presenteren wij een semi-automatisch softwareprogramma dat *Plasmodium*-sporozoïten kan herkennen en deze kan volgen in microscopievideo's van parasieten in de humane huid. Deze methode leidde ertoe dat wij bewegingspatronen konden classificeren en kwantificeren en daarmee verzwakte parasieten met niet-verzwakte parasieten konden vergelijken. Onze resultaten laten zien dat verzwakking van sporozoïten door middel van bestraling (de meest gebruikte vorm van parasietverzwakking voor vaccinatie) tot veranderingen in bewegingspatronen leidt. Bestraalde parasieten toonden "default" bewegingspatronen, waarbij zij de variabiliteit in hun beweging en snelheid verloren. In **hoofdstuk 6** presenteren wij een nieuwe moleculaire beeldvormingstechniek die gebruikt kan worden om wild-type (niet genetisch gemanipuleerde) *Plasmodium*-parasieten aan te kleuren middels een kleurstof die de mitochondriën kleurt. Deze methode maakte het voor ons mogelijk om de motiliteit van wild-type parasieten in menselijke huid te onderzoeken.

Als laatste bediscussiëren wij in **hoofdstuk 7** onze bevindingen in de bredere context van de huidige inzichten in de afweer tegen parasieten. Hierbij worden tevens de implicaties van ons onderzoek voor de ontwikkeling van levende, verzwakte parasietvaccinaties besproken.

RESÚMEN NA PAPIAMENTU

Parásitonan ku ta penetrá den kueru tin un karakteristiká komun: promé ku nan por kousa un infekshon, nan mester evitá e sistema inmunológiko di kueru di e anfitrión i asina prevení ku e sistema inmunológiko ta eliminá nan. Pa logra esei, parásitonan ta disponé di trikinan sofistiká. Por ehèmpel, nan por ehersé akshon direkto riba sélulanan di defenza òf nan por adaptá nan komportashon migratorio na e ambiente ku nan ta aden. E tésis akí tin komo meta aklará e mekanismonan di e táktikanan en kuestion.

Malaria i schistosomiasis (konosí tambe komo bilharzia) ta dos enfermedat mortal, ku ta pone un peso enorme riba pashènt i sosiedat. Ku respektivamente mas di 200 i 240 mion kaso di infekshon kada aña, e peso mundial di e dos enfermedatnan akí ta ketu bai mashá haltu. P'esei hopi tempu kaba ta eksistí e nesiesidat di un bakuna efektivu. Por hasi uso di parásitonan bibu debilitá pa bakuná hende kuné kontra enfermedatnan parasitario manera e dosnan ya mensioná. Sin embargo, ora bakuná ku e parásitonan akí mediante inyekshon den kueru (un sistema usual di bakunashon) esei ta redusí efekto di e bakuna. Nos ta presentá komo hipótesis ku ta e parásitonan ku ta influensia nos mekanismonan immunoregulatorio, kousando redukshon di efekto di e bakuna, i ku esei ta sosodé for di e promé interakshon ku e sistema inmunológiko den nos kueru.

Kueru humano ta un órganu importante i aktivo di defenza. Aparte di su funshon di barera, su prinsipal tarea ta garantisá e ekilibrio inmunológiko entre, di un banda, eliminashon rápido i efikas di mikrobionan ku ta kousa enfermedat (mikrobionan patógeno) i, di otro banda, toleransia pa e huéspednan benigno, e "bon" mikrobionan ku ta biba riba nos kueru. Pa e por ehersé su funshon debidamente, kueru ta disponé di gran variedat di sélula di defenza. Algun di e sélulanan akí ta sélula ku ta presentá antígenonan ('APC'-nan). E funshon di e sélulanan akí ta pa apsorbé antígenonan, ku ta partikulan foráneo, antó konvertí nan den fragmento chikitu i presentá nan na sélulanan T. E sélulanan T por lansa un atake di defenza na momento ku nan rekonosé e fragmentonan komo patógeno. E reakshon di sélulanan T ta sea inflamashon (un atake aktivo di defenza), sea toleransia, loke ta dependé tambe di e señalnan ku e APC-nan ta manda, ora nan ta presentá fragmentonan antígeno. Sierto molékulonan na superfisie di e APC-nan por manda un señal pa e sélulanan T pa esakinan komportá tolerante. E molékulonan akí, ku na ingles yama "checkpoint molecules", manera PD-L1, por desaktivá sélulanan T. Nos a investigá si parásitonan ku penetrá den kueru humano ta probechá di e mekanismonan akí den kueru humano, pa nan mes por sobreviví den e anfitrión.

Den promé parti di e tésis akí, "wiles" (trikinan), nos ta demostrá ku efektivamente *Plasmodium falciparum* i *Schistosoma mansoni* — e kousantenan di, respektivamente, malaria i schistosomiasis — ta probechá di e mekanismonan APC eksistente den kueru humano pa sélulanan T komportá tolerante. Na **kapítulo 2 i 4** nos ta mustra ku tantu sporozoites di *Plasmodium* komo larva di *Schistosoma* ta kousa oumento di ekspreshon di PD-L1 riba superfisie di APC-nan di kueru humano, i ta aktivá e sélulanan akí pa nan produsí molékulonan di señal regulatorio (citokina). Ademas, nos ta konfirmá e efekto imunoregulatorio di e sélulanan akí, mirando nan efekto riba aktivashon di sélulanan T. Na **kapítulo 3** nos ta investigá si e método di inyekta parásito den kueru ta afektá e reakshon di APC: nos ta kompará e efekto en kaso di piká di sangura ku e efekto en kaso di inyekshon mediante angua, den eksplante di kueru humano. Na **kapítulo 4** nos ta demostrá ku debilitashon di larva di *Schistosoma* ta redusí e efekto regulatorio den kueru. Esaki por yuda splika di kon eksposishon na parásitonan debilitá por protehé hende, kontrali na ora ta trata di infekshon natural (ripití).

Den di dos parti di e tésis akí, "wanderings" (odisea), nos ta hasi uso di téknikanan di representashon gráfiko pa karakterisá e motilidat di parásito di malaria den kueru. Na **kapítulo 5** nos ta presentá un programa di software semi-automátiko ku por rekonosé i sigui sporozoites di *Plasmodium* riba vídeo di mikroskop di parásitonan den kueru humano. Danki na e método akí nos por a klasifiká i kuantifiká e patronchinan di moveshon pa asina nos por a kompará parásitonan debilitá ku parásitonan no-debilitá. Nos resultatonan ta demostrá ku debilitashon di sporozoites pa medio di radiashon (*bestraling*, e sistema mas usual pa debilitashon di parásito pa apliká den bakuna) ta kondusí na kambio den e patronchinan di moveshon. Parásitonan ku a trata ku radiashon tabata manifestá patronchinan di moveshon "default", perdiendo nan variabilidat di moveshon i velosidat. Na **kapítulo 6** nos ta presentá un téknika nobo di representashon molekular gráfiko, ku por usa pa marka parásitonan di *Plasmodium* den nan forma natural (esta, no genétikamente manipulá) pa medio di un kolorante ku ta duna e mitokondrianan un koló. E método akí ta brinda nos e posibilidat pa investigá e motilidat di parásitonan den nan forma natural den kueru humano.

Finalmente, nos ta diskutí na **kapítulo 7** e resultatonan di nos investigashon den e konteksto mas general di konosementu aktual riba tereno di defensa kontra parásitonan. I nos ta trata a la bes tambe e implikashonnan di nos investigashon pa desaroyo di bakuna di parásitonan bibu debilitá.

CURRICULUM VITAE

Béatrice Marguélite Françoise Winkel was born on Curaçao on August 28th 1985. She moved to the Netherlands in 1996, where she graduated high school (Dalton Vatel Gymnasium, Voorburg, the Netherlands) in 2002. After a period of travelling she started medical school at the Leiden University in 2004 and obtained both her medical degree and master diploma in Biomedical Sciences in 2014. During her master she employed imaging techniques to map the spatial distribution of hematopoietic stem cells in the bone marrow microenvironment at the laboratory of Prof. Silberstein (Children's Hospital, Harvard university, Boston, USA), and at the Interventional Molecular Imaging group of Dr. van Leeuwen (Leiden University medical Center (LUMC), the Netherlands) she studied novel nuclear navigation technologies in the context of sentinel node surgery. A longstanding interest in tropical infectious diseases led her to continue with a PhD in the field of immuno-parasitology at the Parasitology department of the LUMC, where the work in this thesis was conducted. After a residency period at the internal medicine department of the HMC in The Hague, Béatrice started formal training in clinical microbiology at the UMC Utrecht in 2020. She plans to pursue a career in infectious diseases as a medical specialist and hopes to continue to do research in the field of parasitology.

LIST OF ABBREVIATIONS

| | |
|-------------------|-----------------------------------|
| ANOVA | Analysis of variance |
| APC | Antigen presenting cell |
| aSPZ | attenuated sporozoites |
| Cy5M ₂ | Cy5-Methyl-Methyl |
| DC | Dendritic cell |
| ELISA | Enzyme-linked immunosorbent assay |
| FACS | Flow cytometric cell sorting |
| GFP | Green Fluorescent Protein |
| GMO | Genetically modified organism |
| ID | Intradermal |
| IV | Intravenous |
| MΦ | Macrophage |
| MFI | Fluorescence Intensity |
| MoDC | Monocyte-derived dendritic cell |
| MoMΦ | Monocyte-derived macrophage |
| <i>Pb</i> | <i>Plasmodium berghei</i> |
| PCR | Polymerase chain reaction |
| <i>Pf</i> | <i>Plasmodium falciparum</i> |
| <i>Pv</i> | <i>Plasmodium vivax</i> |
| <i>Py</i> | <i>Plasmodium yoelii</i> |
| RAS | Radiation attenuated sporozoites |
| Sm | <i>Schistosoma mansoni</i> |
| SPZ | Sporozoites |
| WT | Wild type |

LIST OF PUBLICATIONS

1. **B. Winkel**, L. Pelgrom, R. van Schuijlenburg, E. Baalbergen, M.S. Ganesh, H. Gerritsma, C.M. de Korne, N. Duszenko, M.C.C. Langenberg, S.C. Chevalley-Maurel, H.H. Smits, E.C. de Jong, B. Everts, B. Franke-Fayard, M. Roestenberg. *Plasmodium* sporozoites induce regulatory macrophages. *PLOS pathogens*, 2020
2. M.C.C. Langenberg, M. Hoogerwerf, J.R. Koopman, J.J. Janse, J. Kos-van Oosterhoud, C. Feit, S.P. Jochems, C.J. de Dood, R van Schuijlenburg, A Ozir-Fazalalikhhan, M.D. Manurung, E. Sartono, M.T. van der Beek, **B. Winkel**, P.H. Verbeek-Menken, K.A. Stam, F.W.B. van Leeuwen, P.Meij, A. van Diepen, L. van Lieshout, G.J. van Dam, P.L.A.M. Corstjens, C.H. Hokke, M. Yazdanbakhsh, L.G. Visser, M. Roestenberg. A controlled human *Schistosoma mansoni* infection model to accelerate the development of novel drugs, vaccines and diagnostics. *Nature medicine* 2020
3. N. Duszenko, D. van Willigen, M. Welling, C. de Korne, R van Schuijlenburg, **B. Winkel**, F. van Leeuwen, M. Roestenberg. A supramolecular platform technology for bacterial cell surface modification. (*submitted ACS infectious diseases* 2019)
4. **B. Winkel**, C. de Korne, M. van Oosterom, D. Staphorst, M. Meijhuis, E. Baalbergen, M. Ganesh, K. Dechering, M. Vos, S.Chevalley-Maurel, B. Franke-Fayard, F. van Leeuwen, M. Roestenberg. Quantification of wild-type and radiation attenuated *Plasmodium falciparum* sporozoite motility in human skin. *Scientific Reports* 2019
5. C. de Korne, L. Lageschaar, M. van Oosterom, E. Baalbergen, **B. Winkel**, B. Franke-Fayard, F. van Leeuwen, M. Roestenberg. *Plasmodium* sporozoite motility regulation at the level of nutrient supply. *Malaria Journal* 2019
6. **B. Winkel**, C. de Korne, M. van Oosterom, D. Staphorst, A. Bunschoten, M. Langenberg, S. Chevalley-Maurel, C. Janse, B. Franke-Fayard, F. van Leeuwen, M. Roestenberg. A tracer-based method enables tracking of *falciparum* malaria parasites during human skin infection. *Theranostics* 2019
7. M. Hoogerwerf, L. Coffeng, E. Brienen, J. Janse, M. Langenberg, Y. Kruize, C. Gootjes, M. Manurung, M. Dekker, L. Becker, M. Erkens, M. van der Beek, M. Ganesh, C. Feijt, **B. Winkel**, P. Meij, M. Bauer, D. Diemert, A. Loukas, L. Visser, S. de Vlas, M. Yazdanbakhsh, E. van Lieshout, M. Roestenberg. New insights into the kinetics and variability of egg excretion in controlled human hookworm infections *Journal of Infectious Diseases* 2019

8. **B. Winkel**, M. Dalenberg, C.M. de Korne, C. Feijt, M.C.C. Langenberg, L.R. Pelgrom, M.S. Ganesh, M. Yazdanbakhsh, H.H. Smits, E.C. de Jong, B. Everts, F.W.B. van Leeuwen, C.H. Hokke and M. Roestenberg. Early introduction of human regulatory dermal antigen presenting cells by skin-penetrating *Schistosoma mansoni* cercariae. *Frontiers in Immunology* 2018
9. J. Janse, M.C.C. Langenberg, J. Kos-van-Oosterhoud, A. Ozir-Fazalikhhan, E. Brienen, **B. Winkel**, M. Erkens, M. van der Beek, L. van Lieshout L, H.H. Smits, B. Webster, M. Zandvliet, R. Verbeek, I. Westra, P. Meij, L. Visser, A. van Diepen, C. Hokke, M. Yazdanbakhsh and M. Roestenberg. Establishing the production of male *Schistosoma mansoni* cercariae for a controlled human infection model. *Journal of Infectious Diseases* 2018
10. C. Marin-Mogollon, F. van Pul, S. Miyazaki, T. Imai, J. Ramesar, A. Salman, **B. Winkel**, S. Othman, J. Kroeze, S. Chevalley-Maurel, A. Reyes-Sandoval, Roestenberg, B. Franke-Fayard, C. Janse and S. Khan. Chimeric *P. falciparum* parasites expressing *P. vivax* circumsporozoite protein fail to produce salivary gland sporozoites. *Malaria journal* 2018
11. S. Haeberlein, S. Chevalley-Maurel, A. Ozir-Fazalikhhan, H. Koppejan, **B. Winkel**, J. Ramesar, S. Khan, R. Sauerwein, M. Roestenberg, C. Janse, H. Smits, and B. Franke-Fayard. Protective immunity differs between routes of administration of attenuated malaria parasites, independent of malaria liver load. *Scientific Reports* 2017
12. T. Engelen, **B. Winkel**, D. Rietbergen, N. van den Berg, F. van Leeuwen. The next generation freehandSPECT: localization of the sentinel lymph node using the declipseSPECT system combined with the CrystalCam imaging probe. *American journal of Nuclear Medicine* 2015
13. **B. Winkel**, J. Kuil, D. Rietbergen, R. Valdés Olmos, F. van Leeuwen. Combining radioactivity with fluorescence: the first clinical experiences using hybrid tracers. *Nederlands tijdschrift voor nucleaire geneeskunde* 2014
14. C. Nombela-Arrieta, G. Pivarnik, **B. Winkel**, K.J. Canty, B. Harley, J.E. Mahoney, S.Y. Park, J. Lu, A. Protopopov, L.E. Silberstein. Quantitative imaging of haematopoietic stem and progenitor cell localization and hypoxic status in the bone marrow microenvironment. *Nature Cell Biology* 2013

ACKNOWLEDGMENTS

Science is really a group effort, and this thesis would simply not exist without the help of many. I would like to express my deepest gratitude to everyone who made this work possible.

My first and foremost appreciation goes out to **Meta Roestenberg**. Meta, you have an endless love and enthusiasm for science, but you never lose focus on the wellbeing of “your” people. I am grateful I ended up under your care for the past four years. Thank you not only for your guidance, but also for your personal involvement in everything we set out to do. Secondly, I want to thank **Fijs van Leeuwen**. Fijs, without you my papers would not have so many experimental-setup figures in them. You are a passionate and driven scientist. Sharp minds are a whetstone that should be used to sharpen your own. **Maria Yazdanbakhsh**, you are a role model to look up to. Thank you for your investment in this thesis but also in me personally, as well as for all the good wine during the diving weekends! I felt like I was in good hands at PARA.

I would like to thank all the people in the Leiden Malaria Research Group: Chris, Shahid, Hans, Cathrin, Fiona, Syibly, Jai, Surrendra, Taka, but especially the best French science duo: Blandine and Sev, who performed all the mouse work in this book. French chansons during dissection are the key to success! My appreciation also goes out to everyone in PARA who helped map out experimental designs: Ron, Bart, Hermelijn and Bruno. As well as to the secretariat for their practical support. I also wish to thank my crazy tattooing second team: The Interventional Molecular Imaging Group, for taking science and making it a party.

A special thanks goes out to both of my paranymphs: Marijke and Clarize. Marijke, you were there from beginning till end. I hope to someday be as involved and humane a doctor as you already are. You care so much about people. Never lose focus on that. Clarize, both the (endlessly enthusiastic) best “confocaler” I know, and my buddy on the mountainside, I admire your passion and good spirits! Thank you for all your support.

Without the dedicated hands and brains of Roos, Munisha, Carola, Els, Heleen, Alwin, Jeroen, Yvonne and Arifa none of this would have been possible. Thanks also to “my” students: Kyra, Mirjam and Nikolas who put tremendous effort in and taught me that it is not easy to teach.

Aside from science there was also collegial fun: thanks to my Kunststof pals and my fellow Borrel committee members and all of my buddies of T5: Leonard, Katja, Marijke,

Abena, Alice, Eunice, Mikhael, Maria K, Jan Pieter, Marie-Astrid, Vincent, Mathilde and Dian. From confetti cannons via pizza on the "balcony" to shared publications. It was a lot of fun!

The skin work would not have been possible if not for Esther de Jong and Toni van Capel of the AMC. I would like to thank the participating hospitals (and patients) for skin donation. Especially Truus Venema for coordinating the skin deliveries. And Geert-Jan van Gemert, Robert Sauerwein and Koen Dechering from Nijmegen for their help, knowledge and great parasite lines!

Lastly, I want to thank my family and friends, without whom I would not be the same. Wenda, Sanne B, Marieke, Flo, Sanne V, Paul, Maarten, all of the massagegroep and everyone who entertains my nerdy side by playing games with me. Thank you for being there.

Lieve Jonathan, thank you for being my best friend, my reason and my sanity. You play a lead role in all of my absurdities. Lieve Ira and Einav, your smiles and cuddles put everything in perspective. Mama, a thousand times thank you, for your unending love and devotion to both me as well as your granddaughters. Carlos thanks for being the best and worst brother a sister could wish for; you continue to both haunt and teach me. Chris, thank you for being my dad and a terrific grandfather. And my father Cay, for the winged words "Medicine is a profession, art history is a hobby". Mama, Chris and Gea: you gave me a great gift: time. For which I will always be grateful.

I also want to thank "oma" Debbie and "opa" Sidney, Geraldine, Ryan, Natasha, Edward John, Chita, Joëlle and Bar and all the "kids" for being my second loving family, and Sidney in particular for your wonderful Resúmen na Papiamentu.

